BULLETIN OF RUSSIAN STATE MEDICAL UNIVERSITY

BIOMEDICAL JOURNAL OF PIROGOV RUSSIAN NATIONAL RESEARCH MEDICAL UNIVERSITY

SUBMISSION http://vestnikrgmu.ru/login?lang=en
CORRESPONDENCE editor@vestnikrgmu.ru
COLLABORATION manager@vestnikrgmu.ru
ADDRESS ul. Ostrovityanova, d. 1, Moscow, Russia, 117997

Indexed in Scopus. CiteScore 2018: 0.16

Indexed in WoS. JCR 2018: 0.13

Five-year h-index is 3

Indexed in RSCI. IF 2017: 0.326

Listed in HAC 27.01.2016 (no. 1760)

Open access to archive

Issue DOI: 10.24075/brsmu.2019-04
The mass media registration certificate no. 012769 issued on July 29, 1994
Founder and publisher is Pirogov Russian National Research Medical University (Moscow, Russia)

Approved for print 31.08.2019
Circulation: 100 copies. Printed by Print.Formula
www.print-formula.ru

ВЕСТНИК РОССИЙСКОГО ГОСУДАРСТВЕННОГО МЕДИЦИНСКОГО УНИВЕРСИТЕТА

НАУЧНЫЙ МЕДИЦИНСКИЙ ЖУРНАЛ РНИМУ ИМ. Н. И. ПИРОГОВА

ГЛАВНЫЙ РЕДАКТОР Денис Ребриков, д. б. н., профессор

ЗАМЕСТИТЕЛЬ ГЛАВНОГО РЕДАКТОРА Александр Эттингер, д. м. н., профессор

РЕДАКТОРЫ Валентина Гейдебрехт, Айарпи Ездоглян

ТЕХНИЧЕСКИЙ РЕДАКТОР Нина Тюрина

ПЕРЕВОДЧИКИ Екатерина Третьякова, Вячеслав Витюк

ДИЗАЙН И ВЕРСТКА Марина Доронина

ПОДАЧА РУКОПИСЕЙ http://vestnikrgmu.ru/login
ПЕРЕПИСКА С РЕДАКЦИЕЙ editor@vestnikrgmu.ru
СОТРУДНИЧЕСТВО manager@vestnikrgmu.ru
АДРЕС РЕДАКЦИИ ул. Островитянова, д. 1, г. Москва, 117997

Журнал включен в Scopus. CiteScore 2018: 0,16

Журнал включен в WoS. JCR 2018: 0,13

Индекс Хирша (h^5) журнала по оценке Google Scholar: 3

Журнал включен в РИНЦ. IF 2017: 0,326

Журнал включен в Перечень 27.01.2016 (№ 1760)

Здесь находится открытый архив журнала

DOI выпуска: 10.24075/vrgmu.2019-04
Свидетельство о регистрации средства массовой информации № 012769 от 29 июля 1994 г.
Учредитель и издатель — Российский национальный исследовательский медицинский университет имени Н. И. Пирогова (Москва, Россия)

Подписано в печать 31.08.2019
Тираж 100 экз. Отпечатано в типографии Print.Formula
www.print-formula.ru

BULLETIN OF RSMU **4, 2019**
ВЕСТНИК РГМУ

Contents
Содержание

THE POTENTIAL OF EXOSOMES FOR THE DIAGNOSIS AND TREATMENT OF DUCHENNE MUSCULAR DYSTROPHY

Galkin II[1,2], Egorova TV[1,3] ✉

[1] Marlin Biotech LLC, Moscow, Russia

[2] A. N. Belozersky Institute of Physico-Chemical Biology, Moscow, Russia

[3] Institute of Gene Biology, Russian Academy of Sciences, Moscow, Russia

Duchenne muscular dystrophy is the most common type of muscular dystrophy. There is no effective cure for this disease. Recently, researchers have started to look at the therapeutic potential of exosomes — small (40–100 nm) vesicles secreted by cells into the extracellular environment. They transport a few types of macromolecules, including microRNA and proteins, that can be analyzed to estimate the efficacy of the applied therapy. Besides, exosomes can be harnessed for delivering therapeutic components (microRNA, antisense oligonucleotides) to the target tissue. Below, we analyze the available literature and assess the feasibility of using exosomes in the diagnosis and treatment of Duchenne muscular dystrophy. We conclude that exosomes can have their place in the arsenal of researchers and clinicians once some technical issues are solved.

Keywords: Duchenne muscular dystrophy, exosomes, targeted drug delivery, liquid biopsy, gene therapy

Author contribution: Galkin II, Egorova TV — literature analysis and manuscript preparation.

✉ **Correspondence should be addressed:** Tatiana V. Egorova
Vavilova 34/5, Moscow, 119334; t.dimitrieva@marlinbiotech.com

Received: 21.07.2019 **Accepted:** 05.08.2019 **Published online:** 12.08.2019

DOI: 10.24075/brsmu.2019.049

ВОЗМОЖНОСТИ ПРИМЕНЕНИЯ ЭКЗОСОМ ДЛЯ ДИАГНОСТИКИ И ЛЕЧЕНИЯ МИОДИСТРОФИИ ДЮШЕННА

И. И. Галкин[1,2], Т. В. Егорова[1,3] ✉

[1] ООО «Марлин Биотех», Москва, Россия

[2] Институт физико-химической биологии имени А. Н. Белозерского, Москва, Россия

[3] Институт биологии гена, Москва, Россия

Миодистрофия Дюшенна — наиболее часто встречающаяся форма миодистрофии. Однако эффективного лечения этого заболевания до сих пор не разработано. В настоящее время появляются работы, посвященные использованию экзосом в моделях миодистрофии Дюшенна. Экзосомы, небольшие (40–100 нм) везикулы, секретируемые клетками в межклеточное пространство, переносят некоторые макромолекулы (микроРНК, белки), анализ которых может быть использован для неинвазивной оценки успешности применяемой терапии. Кроме того, они могут обеспечивать адресную доставку активных веществ (например, микроРНК, антисмысловых олигонуклеотидов). Анализируя имеющиеся данные и оценивая возможность диагностики и терапии дистрофии Дюшенна с помощью этих везикул, мы предполагаем, что экзосомы могут занять место в арсенале исследователей и врачей, если удастся решить некоторые технические проблемы.

Ключевые слова: миодистрофия Дюшенна, экзосомы, адресная доставка, жидкостная биопсия, генетическая терапия

Информация о вкладе авторов: И. И. Галкин, Т. В. Егорова — анализ литературы, написание текста статьи.

✉ **Для корреспонденции:** Татьяна Владимировна Егорова
ул. Вавилова, 34/5, г. Москва, 119334; t.dimitrieva@marlinbiotech.com

Статья получена: 21.07.2019 **Статья принята к печати:** 05.08.2019 **Опубликована онлайн:** 12.08.2019

DOI: 10.24075/vrgmu.2019.049

Duchenne muscular dystrophy (DMD) is an X-linked recessive disorder caused by mutations in the *DMD* gene resulting in the deficient or dysfunctional protein known as dystrophin. The disease is characterized by progressive muscle degeneration and fibrosis. Patients lose ambulation at the age of 8 to 12 years and die in their 20s, usually from cardiac or respiratory failure. Those with partially functional dystrophin develop a milder form of the disease called Becker muscular dystrophy.

The majority of currently existing strategies for managing DMD only seek to alleviate its symptoms and include physical therapy and exercise, minor orthotic interventions aimed at preventing contracture, assisted ventilation, and glucocorticoids [1]. These treatments give the affected patients the chance to walk and move independently for longer and increase their life expectancy to 30 years. Obviously, they cannot eliminate the cause of the disease, unlike gene therapies, which can restore dystrophin expression and function. Gene therapies for DMD range from adeno-associated viral vectors (AAV) for the delivery of microdystrophin (a truncated but functional version of the protein) to the muscle [2], to exon skipping (pre-messenger RNA splicing mediated by modified oligonucleotides or CRISPR/Cas systems) [3]. Each of the listed approaches has its own limitations and downsides. AAV-based dystrophin delivery can provoke an unwanted immune response to capsid proteins. Besides, due to the small packaging capacity, the vector can only carry a shortened version of dystrophin inferior to the full-length protein in terms of its function. The efficacy of exon skipping is low. It targets a narrow range of mutations and, therefore, can be beneficial for a small subpopulation of patients [3]. Challenges associated with drug delivery to muscles are the primary hurdle affecting the efficacy of both conventional and innovative DMD treatments. This spurs the development of novel approaches. Recently, exosomes have been receiving increasing attention as promising drug delivery systems [4].

Exosomes are the smallest extracellular vesicles secreted by cells into the extracellular environment, such as blood, lymph, growth media, etc. They are usually reported to be

40 to 100 nm in size; larger exosomes sized up to 150 nm are rarely reported. Unlike other extracellular vesicles, such as apoptotic bodies (50 to 1,000 nm in diameter) or microvesicles (100 to 300 nm in diameter) "blebbed" from the cell membrane, exosomes are secreted after a multivesicular body has fused with the membrane [5]. Initially, exosomes were thought to be "trash bags" responsible for disposing of cellular waste. Later, they were shown to mediate intercellular communication by transporting proteins, RNA and other molecules [5]. On their lipid membrane, exosomes carry a number of surface proteins, including CD9, CD63 and some others, as well as the components of the major histocompatibility complex. On the one hand, these surface proteins prevent exosomes from being eliminated from the bloodstream; on the other hand, they stimulate receptor-mediated endocytosis [6, 7]. One way of modifying exosome surface proteins is click chemistry. Alternatively, cell cultures can be engineered expressing an exosomal surface protein that contains a guide peptide sequence. The guide peptide on the surface of exosomes enhances their affinity for the receptors found on the target cells [6, 8]. Similarly, exosomes can be loaded with useful cargoes — biological macromolecules (nucleic acids, proteins) and low molecular weight compounds (inhibitors and antisense oligonucleotides, ASO) [6]. Compared to liposomes, exosomes seem to be much more effective and appealing candidates for drug delivery because they can be directed precisely into the target tissue once their surface has been modified; they also demonstrate low immunogenicity and high loading potential. There have been attempts to use exosomes for therapeutic applications [9], but generally such therapies are still in development. Most often, exosomes are employed as effective diagnostic markers of cancer, cardiovascular and neurological diseases [9].

Exosomes for Duchenne muscular dystrophy: diagnostics

The diagnosis of Duchenne/Becker muscular dystrophy is based on the results of molecular and genetic tests (PCR, MLPA, sequencing) that can accurately localize and identify the causative mutation. Muscle biopsies are performed in difficult cases to estimate the amount of dystrophin, its distribution in the muscle tissue and the overall condition of muscle fibers. Importantly, patients with DMD should be monitored throughout treatment. However, frequent biopsies are poorly tolerated by patients and provide information about a small area of the affected muscle. A 6-minute walk test is relevant for outpatients only, and its result is largely determined by the ability of a patient to concentrate and their willingness to follow the instructions. This necessitates development of minimally invasive and reliable methods for the assessment of a patient's condition during and after therapy. The solution might be provided by a type of so-called "liquid biopsy": the analysis of microRNA contained in exosomes isolated from a patient's blood. So far, several microRNAs have been explored, including miR-1, miR-21, miR-29, miR-31, miR-29, miR-133, miR-133b, and miR-206, that participate in muscle tissue repair and differentiation. Three main muscle-associated microRNAs (miR-1, miR-133 and miR-206) are elevated in the blood serum of patients with DMD; interestingly, miR-206 levels are increased even in the female carriers of the defective gene [10]. Some authors point to another large group of microRNAs (miR-22, miR-30, miR-95, miR-181, miR-193b, miR-208a, miR-208b, miR-378, and miR-499) that could serve as a DMD marker; however, these data need further confirmation. Still, the dynamics of exosomal muscle-associated microRNA in the course of treatment with such drugs as Eteplirsen (a phosphorodiamidate morpholino oligomer from the class of synthetic ASO used for exon skipping [3]) can provide valuable information about the efficacy of the applied therapy [10].

Exosomes for Duchenne muscular dystrophy: therapy based on native exosomes

Attempts to harness stem cells for therapeutic applications date quite far back. Stem cells tested in DMD models are cardiac progenitor ("cardiosphere-derived") cells [11]. The clinical trials of the drug based on such cells is now in Phase II. The therapeutic effect of stem cells is linked to their ability to stimulate tissue differentiation and regeneration. Recent studies demonstrated that exosomes shed by stem cells mediate signal transfer from stem cells to the target tissue. A study conducted in mdx mice revealed that intracardiac [11] and intravenous [12] administration of exosomes derived from cardiospheres reproduced almost all beneficial effects of exosomes naturally delivered by stem cells. Interestingly, dystrophin was detected in the muscle tissue following the administration of cardiosphere-derived exosomes, but no dystrophin or its mRNA were found inside the exosomes. The analysis of RNA contained in the exosomes revealed that the latter were enriched in miR-148a. Intramuscular injections of miR-148a led to a partial restoration of dystrophin levels, suggesting a possible mechanism of action for cardiosphere-derived exosomes [11]. Similarly, exosomes originating from other sources, such as C2C12 [13, 14] and placental [15] cells, stimulated muscle regeneration, reduced fibrosis and improved the functional state of the muscle. The beneficial effect of exosomes derived from placental cells was determined by microRNA (miR-29). That said, it should be noted that little attention has been paid to the possible treatment-related adverse events. Most often, the side effects of therapeutic exosomes on experimental animals are estimated by measuring animal weight, levels of hepatic enzymes and blood urea; the immune response remains overlooked.

Exosomes for Duchenne muscular dystrophy: exosomes loaded with therapeutic agents. Targeted delivery

Although native exosomes hold promise for DMD treatment, they do not solve the key problem of dystrophin deficiency, similar to existing approaches. Using exosomes as drug delivery platforms may offer the long-awaited solution. The idea of delivering full-length dystrophin, its truncated version (microdystrophin) or the gene itself to the target tissue looks appealing. However, the full-length dystrophin molecule is 150–180 nm in size, which exceeds the maximum possible diameter of an exosome. This means that attempts to load the protein or its coding sequence onto an exosome may fail. However, exosomes can be employed for delivering low molecular weight compounds. Some of DMD treatment options rely on the use of synthetic ASO. In one of the studies, a peptide capable of binding selectively to the exosomal surface protein CD63 was conjugated to ASO. The resulting compound enabled more effective exon skipping, as compared to the unconjugated antisense nucleotide. Moreover, when bound to the M12 muscle-specific peptide, the above-mentioned peptide facilitated targeted delivery of exosomes into the muscle tissue [6]. In another study, exosomes were derived from transfected cells that expressed the chimeric protein Lamp2b (the lysosomal protein appearing also on the surface of exosomes) fused with muscle- or neuron-specific peptides. The modified exosomes

succesfuly delivered effector molecules (short interfering RNA) into the target cells and tissues [8].

CONCLUSIONS

In spite of extensive effort, there is no effective treatment for Duchenne muscular dystrophy. Existing therapies are symptomatic and have serious limitations. Exosomes boast low immunogenicity; in addition, their surface can be modified. Therefore, these vesicles are promising candidates for drug delivery. The analysis of a patient's exosomes can facilitate the diagnosis and help to monitor the response to treatment. However, isolation, standardization and loading of exosomes require further refinement and optimization. Also, the immunogenic properties of exosomes are still understudied. Combining the use of exosomes for muscle regeneration with ASO loading and modification of exosomal surface proteins with muscle-specific peptides looks like a promising approach.

References

1. Birnkrant DJ, Bushby K, Bann CM, Apkon SD, Blackwell A, Brumbaugh D, et al. Diagnosis and management of Duchenne muscular dystrophy, part 1: diagnosis, and neuromuscular, rehabilitation, endocrine, and gastrointestinal and nutritional management. Lancet Neurol. 2018; 17 (3): 251–67. DOI: 10.1016/S1474-4422(18)30024-3. PubMed PMID: 29395989; PMCID: PMC5869704.
2. Duan D. Systemic AAV Micro-dystrophin Gene Therapy for Duchenne Muscular Dystrophy. Mol Ther. 2018; 26 (10): 2337–56. DOI: 10.1016/j.ymthe.2018.07.011. PubMed PMID: 30093306; PMCID: PMC6171037.
3. Lim KR, Maruyama R, Yokota T. Eteplirsen in the treatment of Duchenne muscular dystrophy. Drug Des Devel Ther. 2017; (11): 533–45. DOI: 10.2147/DDDT.S97635. PubMed PMID: 28280301; PMCID: PMC5338848.
4. Bunggulawa EJ, Wang W, Yin T, Wang N, Durkan C, Wang Y, et al. Recent advancements in the use of exosomes as drug delivery systems. J Nanobiotechnology. 2018; 16 (1): 81. DOI: 10.1186/s12951-018-0403-9. PubMed PMID: 30326899; PMCID: PMC6190562.
5. Raposo G, Stoorvogel W. Extracellular vesicles: exosomes, microvesicles, and friends. The Journal of cell biology. 2013; 200 (4): 373–83. DOI: 10.1083/jcb.201211138. PubMed PMID: 23420871; PMCID: PMC3575529.
6. Gao X, Ran N, Dong X, Zuo B, Yang R, Zhou Q, Moulton HM, Seow Y, Yin H. Anchor peptide captures, targets, and loads exosomes of diverse origins for diagnostics and therapy. Sci Transl Med. 2018; 10 (444). DOI: 10.1126/scitranslmed.aat0195. PubMed PMID: 29875202.
7. Kamerkar S, LeBleu VS, Sugimoto H, Yang S, Ruivo CF, Melo SA, et al. Exosomes facilitate therapeutic targeting of oncogenic KRAS in pancreatic cancer. Nature. 2017; 546 (7659): 498–503. DOI: 10.1038/nature22341. PubMed PMID: 28607485; PMCID: PMC5538883.
8. Alvarez-Erviti L, Seow Y, Yin H, Betts C, Lakhal S, Wood MJ. Delivery of siRNA to the mouse brain by systemic injection of targeted exosomes. Nat Biotechnol. 2011; 29 (4): 341–5. DOI: 10.1038/nbt.1807. PubMed PMID: 21423189.
9. Kim YS, Ahn JS, Kim S, Kim HJ, Kim SH, Kang JS. The potential theragnostic (diagnostic + therapeutic) application of exosomes in diverse biomedical fields. Korean J Physiol Pharmacol. 2018; 22 (2): 113–25. DOI: 10.4196/kjpp.2018.22.2.113. PubMed PMID: 29520164; PMCID: PMC5840070.
10. Coenen-Stass AML, Wood MJA, Roberts TC. Biomarker Potential of Extracellular miRNAs in Duchenne Muscular Dystrophy. Trends Mol Med. 2017; 23 (11): 989–1001. DOI: 10.1016/j.molmed.2017.09.002. PubMed PMID: 28988850.
11. Aminzadeh MA, Rogers RG, Fournier M, Tobin RE, Guan X, Childers MK, et al. Exosome-Mediated Benefits of Cell Therapy in Mouse and Human Models of Duchenne Muscular Dystrophy. Stem Cell Reports. 2018; 10 (3): 942–55. DOI: 10.1016/j.stemcr.2018.01.023. PubMed PMID: 29478899; PMCID: PMC5918344.
12. Rogers RG, Fournier M, Sanchez L, Ibrahim AG, Aminzadeh MA, Lewis MI, et al. Disease-modifying bioactivity of intravenous cardiosphere-derived cells and exosomes in mdx mice. JCI Insight. 2019; 4 (7). DOI: 10.1172/jci.insight.125754. PubMed PMID: 30944252; PMCID: PMC6483717.
13. Su X, Shen Y, Jin Y, Jiang M, Weintraub N, Tang Y. Purification and Transplantation of Myogenic Progenitor Cell Derived Exosomes to Improve Cardiac Function in Duchenne Muscular Dystrophic Mice. J Vis Exp. 2019; (146). DOI: 10.3791/59320. PubMed PMID: 31033952.
14. Su X, Jin Y, Shen Y, Ju C, Cai J, Liu Y, et al. Exosome-Derived Dystrophin from Allograft Myogenic Progenitors Improves Cardiac Function in Duchenne Muscular Dystrophic Mice. J Cardiovasc Transl Res. 2018; 11 (5): 412–9. DOI: 10.1007/s12265-018-9826-9. PubMed PMID: 30155598; PMCID: PMC6212302.
15. Bier A, Berenstein P, Kronfeld N, Morgoulis D, Ziv-Av A, Goldstein H, et al. Placenta-derived mesenchymal stromal cells and their exosomes exert therapeutic effects in Duchenne muscular dystrophy. Biomaterials. 2018; (174): 67–78. DOI: 10.1016/j.biomaterials.2018.04.055. PubMed PMID: 29783118.

Литература

1. Birnkrant DJ, Bushby K, Bann CM, Apkon SD, Blackwell A, Brumbaugh D, et al. Diagnosis and management of Duchenne muscular dystrophy, part 1: diagnosis, and neuromuscular, rehabilitation, endocrine, and gastrointestinal and nutritional management. Lancet Neurol. 2018; 17 (3): 251–67. DOI: 10.1016/S1474-4422(18)30024-3. PubMed PMID: 29395989; PMCID: PMC5869704.
2. Duan D. Systemic AAV Micro-dystrophin Gene Therapy for Duchenne Muscular Dystrophy. Mol Ther. 2018; 26 (10): 2337–56. DOI: 10.1016/j.ymthe.2018.07.011. PubMed PMID: 30093306; PMCID: PMC6171037.
3. Lim KR, Maruyama R, Yokota T. Eteplirsen in the treatment of Duchenne muscular dystrophy. Drug Des Devel Ther. 2017; (11): 533–45. DOI: 10.2147/DDDT.S97635. PubMed PMID: 28280301; PMCID: PMC5338848.
4. Bunggulawa EJ, Wang W, Yin T, Wang N, Durkan C, Wang Y, et al. Recent advancements in the use of exosomes as drug delivery systems. J Nanobiotechnology. 2018; 16 (1): 81. DOI: 10.1186/s12951-018-0403-9. PubMed PMID: 30326899; PMCID: PMC6190562.
5. Raposo G, Stoorvogel W. Extracellular vesicles: exosomes, microvesicles, and friends. The Journal of cell biology. 2013; 200 (4): 373–83. DOI: 10.1083/jcb.201211138. PubMed PMID: 23420871; PMCID: PMC3575529.
6. Gao X, Ran N, Dong X, Zuo B, Yang R, Zhou Q, Moulton HM, Seow Y, Yin H. Anchor peptide captures, targets, and loads exosomes of diverse origins for diagnostics and therapy. Sci Transl Med. 2018; 10 (444). DOI: 10.1126/scitranslmed.aat0195. PubMed PMID: 29875202.
7. Kamerkar S, LeBleu VS, Sugimoto H, Yang S, Ruivo CF, Melo SA,

et al. Exosomes facilitate therapeutic targeting of oncogenic KRAS in pancreatic cancer. Nature. 2017; 546 (7659): 498–503. DOI: 10.1038/nature22341. PubMed PMID: 28607485; PMCID: PMC5538883.

8. Alvarez-Erviti L, Seow Y, Yin H, Betts C, Lakhal S, Wood MJ. Delivery of siRNA to the mouse brain by systemic injection of targeted exosomes. Nat Biotechnol. 2011; 29 (4): 341–5. DOI: 10.1038/nbt.1807. PubMed PMID: 21423189.
9. Kim YS, Ahn JS, Kim S, Kim HJ, Kim SH, Kang JS. The potential theragnostic (diagnostic + therapeutic) application of exosomes in diverse biomedical fields. Korean J Physiol Pharmacol. 2018; 22 (2): 113–25. DOI: 10.4196/kjpp.2018.22.2.113. PubMed PMID: 29520164; PMCID: PMC5840070.
10. Coenen-Stass AML, Wood MJA, Roberts TC. Biomarker Potential of Extracellular miRNAs in Duchenne Muscular Dystrophy. Trends Mol Med. 2017; 23 (11): 989–1001. DOI: 10.1016/j.molmed.2017.09.002. PubMed PMID: 28988850.
11. Aminzadeh MA, Rogers RG, Fournier M, Tobin RE, Guan X, Childers MK, et al. Exosome-Mediated Benefits of Cell Therapy in Mouse and Human Models of Duchenne Muscular Dystrophy. Stem Cell Reports. 2018; 10 (3): 942–55. DOI: 10.1016/j.stemcr.2018.01.023. PubMed PMID: 29478899; PMCID: PMC5918344.
12. Rogers RG, Fournier M, Sanchez L, Ibrahim AG, Aminzadeh MA, Lewis MI, et al. Disease-modifying bioactivity of intravenous cardiosphere-derived cells and exosomes in mdx mice. JCI Insight. 2019; 4 (7). DOI: 10.1172/jci.insight.125754. PubMed PMID: 30944252; PMCID: PMC6483717.
13. Su X, Shen Y, Jin Y, Jiang M, Weintraub N, Tang Y. Purification and Transplantation of Myogenic Progenitor Cell Derived Exosomes to Improve Cardiac Function in Duchenne Muscular Dystrophic Mice. J Vis Exp. 2019; (146). DOI: 10.3791/59320. PubMed PMID: 31033952.
14. Su X, Jin Y, Shen Y, Ju C, Cai J, Liu Y, et al. Exosome-Derived Dystrophin from Allograft Myogenic Progenitors Improves Cardiac Function in Duchenne Muscular Dystrophic Mice. J Cardiovasc Transl Res. 2018; 11 (5): 412–9. DOI: 10.1007/s12265-018-9826-9. PubMed PMID: 30155598; PMCID: PMC6212302.
15. Bier A, Berenstein P, Kronfeld N, Morgoulis D, Ziv-Av A, Goldstein H, et al. Placenta-derived mesenchymal stromal cells and their exosomes exert therapeutic effects in Duchenne muscular dystrophy. Biomaterials. 2018; (174): 67–78. DOI: 10.1016/j.biomaterials.2018.04.055. PubMed PMID: 29783118.

MOLECULAR-GENETIC AND PHENOTYPIC CHARACTERISTICS OF DESMOID-TYPE FIBROMATOSIS

Muzaffarova TA[1], Novikova OV[2], Sachkov IYu[3], Kipkeeva FM[1] ✉, Ginter EK[1], Karpukhin AV[1]

[1] Bochkov Research Center for Medical Genetics, Moscow, Russia

[2] Hertsen Moscow Oncology Research Center, Moscow, Russia

[3] Ryzhikh State Research Center for Coloproctology, Moscow, Russia

Desmoid-type fibromatosis (DF) is a rare mesenchymal tumor occurring in only 2 to 4 people per 1,000,000 population a year. Desmoid tumors are either seen sporadically or in individuals with familial adenomatous polyposis (FAP). The etiology of sporadic DF is uncertain. The aim of this study was to estimate the potential significance of germline mutations in the *APC* gene in patients with sporadic DF. *APC* exons were amplified, studied using conformation sensitive gel electrophoresis and then Sanger-sequenced. The obtained data were processed in Statistica 10. Mutations were detected in 6 (12%) of 51 participants with sporadic DF. Those 6 patients shared a typical DF phenotype characterized by early age of onset (5.8 years on average, in contrast to the patients without *APC* mutations, who developed DF at 19 years of age; $p = 0.02$), severe clinical course, multifocal localization on the trunk, and poor prognosis. All of the detected *APC* mutations were localized to the 3'-end of the gene. For the purpose of comparison, we analyzed a sample of 12 patients with FAP-associated DF. Of those patients, 6 carried mutations in the *APC* gene. In the analyzed sample, the patients with FAP and the mutant *APC* gene developed DF at older age (35 years) than the patients with sporadic DF ($p = 0.004$) and their tumors were not multifocal. This means that sporadic and FAP-associated desmoids have different phenotypes in patients with *APC* mutations. Patients with sporadic tumors have mutations at the 3'-end of the *APC* gene more often than individuals with FAP-associated DF. To our knowledge, this is the first study to characterize the subtype of sporadic desmoid fibromatosis phenotypically determined by germline mutations in the *APC* gene.

Keywords: sporadic desmoid-type fibromatosis, *APC* gene, multifocal desmoid tumors, familial adenomatous polyposis

Author contribution: Muzaffarova TA conducted the study, analyzed the literature and wrote the manuscript; Novikova OV, Sachkov IYu provided patients' samples and medical histories; Kipkeeva FM, Ginter EK analyzed the literature and wrote the manuscript; Karpukhin AV organized the study and revised the manuscript.

Compliance with ethical standards: the study was approved by the Ethics committee of Bochkov Research Center for Medical Genetics (Protocol № 3 dated February 09, 2012).

✉ **Correspondence should be addressed:** Fatima M. Kipkeeva
Moskvorechie 1, Moscow, 115522; BRCA1@mail.ru

Received: 25.06.2019 **Accepted:** 13.07.2019 **Published online:** 18.07.2019

DOI: 10.24075/brsmu.2019.045

МОЛЕКУЛЯРНО-ГЕНЕТИЧЕСКИЕ И ФЕНОТИПИЧЕСКИЕ ОСОБЕННОСТИ СЛУЧАЕВ ВОЗНИКНОВЕНИЯ ДЕСМОИДНОГО ФИБРОМАТОЗА

Т. А. Музаффарова[1], О. В. Новикова[2], И. Ю. Сачков[3], Ф. М. Кипкеева[1] ✉, Е. К. Гинтер[1], А. В. Карпухин[1]

[1] Медико-генетический научный центр имени Н. П. Бочкова, Москва, Россия

[2] Московский научно-исследовательский онкологический институт имени П. А. Герцена, Москва, Россия

[3] Государственный научный центр колопроктологии имени А. Н. Рыжих, Москва, Россия

Десмоидные фибромы (ДФ) — редкие мезенхимальные опухоли с частотой возникновения 2–4 случая на 1 млн человек в год. Они могут возникать как спорадически, так и в ассоциации с семейным аденоматозным полипозом (САП). Природа возникновения спорадических ДФ ранее не была выяснена. Целью исследования было определить возможную значимость герминальных мутаций гена *APC* у пациентов со спорадическими ДФ. Экзоны гена *APC* амплифицировали и исследовали с помощью конформационно-чувствительного электрофореза в полиакриламидном геле и последующего секвенирования по Сэнгеру. Статистическую обработку результатов проводили с помощью пакета программ «Statistica 10». При исследовании 51 случая спорадических ДФ мутации выявлены у 6 человек (12%). Пациенты с выявленными мутациями имели характерный фенотип: раннюю манифестацию (в среднем в 5,8 года, в то время как у пациентов без мутаций — в 19 лет ($p = 0,02$)); тяжелое течение заболевания; мультифокальный рост ДФ, локализованных на туловище, и неблагоприятный прогноз. Все выявленные мутации были обнаружены в области 3'-конца гена *APC*. Для сравнения со спорадическими были исследованы ДФ, связанные с САП (12 человек), мутации выявлены у 6 из них. При мутации в гене *APC* у пациентов с САП не было выявлено случаев множественных ДФ, фибромы у пациентов с САП развивались позже (35 лет), чем у пациентов со спорадическими ДФ ($p = 0,004$). Следовательно, при мутациях в одном и том же гене фенотипы спорадических и ДФ, связанных с САП, различны. Для спорадического ДФ характерно более частое расположение мутаций на 3'-конце гена *APC* по сравнению с ДФ при САП. Таким образом, впервые среди спорадических ДФ охарактеризован подтип с фенотипическими особенностями, обусловленными герминальными мутациями в гене *APC*.

Ключевые слова: спорадический десмоидный фиброматоз, ген *APC*, мультифокальные десмоидные опухоли, семейный аденоматозный полипоз

Информация о вкладе авторов: Т. А. Музаффарова — проведение исследования, работа с литературными данными, оформление рукописи; О. В. Новикова, И. Ю. Сачков — предоставление образцов и клинических данных пациентов; Ф. М. Кипкеева, Е. К. Гинтер — работа с литературными данными, участие в оформлении рукописи; А. В. Карпухин — организация исследования, оформление рукописи.

Соблюдение этических стандартов: исследование одобрено комитетом по этике ФГБНУ «МГНЦ имени Бочкова Н. П.» (протокол № 3 от 09 февраля 2012 г.)

✉ **Для корреспонденции:** Фатима Магомедовна Кипкеева
ул. Москворечье, д. 1, г. Москва, 115522; BRCA1@mail.ru

Статья получена: 25.06.2019 **Статья принята к печати:** 13.07.2019 **Опубликована онлайн:** 18.07.2019

DOI: 10.24075/vrgmu.2019.045

Desmoid tumors, also known as desmoid-type fibromatosis (DF), are heterogenous benign neoplasms arising from deep fasciae and aponeuroses. They infiltrate the surrounding soft tissues but do not have the capacity to metastasize. Desmoid tumors are composed of spindle (fibrocyte-like) cells and abundant collagen fibers. A desmoid lacks a capsule and can entrap muscle fibers at the periphery, causing their atrophy. Besides, the tumor can send out long narrow extensions that sometimes reach 20 to 30 cm in length.

DF can occur almost anywhere in the body. Based on the lesion site, DF is categorized into extra-abdominal (the abdominal or chest walls, extremities, neck, or pelvis) and intra-abdominal (the mesentery and the retroperitoneum). Technically, desmoid tumors are benign because they do not metastasize. However, they tend to aggressively proliferate and persistently recur after surgical treatment, bearing similarity to cancer [1].

Desmoid tumors can grow enormously large in size and become a life-threatening condition. DF occurs in 2 to 4 per 1 million people a year [2]. Treatment of desmoid tumors is complicated by their propensity for infiltrative growth and locally aggressive behavior. Usually, surgical resection is the preferred option. However, the postoperative recurrence rate remains high, varying from 45 to 90% [3].

Desmoid tumors either occur sporadically or are associated with familial adenomatous polyposis (FAP), an inherited condition of the colon that eventually transforms into colon cancer. The majority of FAP cases are caused by a mutation in the adenomatous polyposis coli (*APC*) gene. Ten to fifteen percent of patients with FAP also have DF. The risk of developing DF is 2.56 cases per 1,000 FAP patients a year, which is 852 times higher than in the general population [2]. Unlike sporadic DF, 80% of FAP-associated desmoid tumors are intra-abdominal. DF predominantly affects women and can manifest itself at any age although the typical age of onset is between 30 and 40 years. Most FAP-associated desmoids develop within 5 years after surgery [4].

The etiology of sporadic DF is uncertain. Some patients with sporadic DF are reported to carry somatic mutations in the *APC* gene; however, such type of mutations is more commonly found in the *CTNNB1* gene that codes for β-catenin [5–6], a protein involved in the Wnt signaling pathway. Mutations in *CTNNB1* result in the accumulation of β-catenin in fibroblast nuclei, which, in turn, disrupts cell differentiation and communication between the cells [7].

Genetic causes of DF and their association with clinical manifestations of the disease remain understudied. Because DF frequently occurs in FAP-stricken patients, it would be natural to hypothesize that predisposition to sporadic DF is determined by mutations in the *APC* gene. However, the literature on germline mutations in the *APC* gene in patients with sporadic DF is scarce [8, 9].

In this work we attempted to estimate the potential significance of germline mutations in the *APC* gene in a sample of patients with sporadic DF and without a family history of adenomatous polyposis. For the purpose of comparison, we also analyzed molecular characteristics of the *APC* gene in patients with DF and FAP.

METHODS

The study was conducted at the Laboratory of Molecular Genetics (Bochkov Research Center for Medical Genetics) in 2012–2017. Two patient samples were analyzed. The first sample consisted of 51 patients (21 males and 30 females) with DF. The patients' age ranged from 1 month to 60 years (see Fig.); the median age was 16.8 years. Blood samples were provided by Hertsen Moscow Research Oncology Center where the patients had presented at. The following inclusion criteria were applied: a confirmed diagnosis of DF; no gastrointestinal complaints that could be indicative of diffuse polyposis of the colon; no family history of adenomatous polyposis; no family history of DF. All desmoid tumors in the first patient sample were considered sporadic.

The affected sites included the back, chest and abdominal walls, extremities, and the intra-abdominal region. Multifocal DF was observed in 11 patients (see *Results*). In some patients the lesions were recurrent.

The second sample comprised 12 individuals (2 males and 10 females) shortlisted from a group of 65 patients with FAP who had presented at Ryzhikh State Research Center for Coloproctology; blood samples were provided by the Research Center. The age of onset varied from 24 to 57 years and was 32.5 years on average. The following inclusion criteria were applied: a confirmed diagnosis of colonic polyposis and DF. Eight patients had a family history of adenomatous polyposis. Family histories were not available for 4 patients. In the second patient sample, desmoid tumors appeared after surgery and were localized to the anterior abdominal wall or intra-abdominally. The majority of them were solitary.

DNA was isolated from peripheral blood leukocytes using a standard phenol-chloroform extraction technique [10]. The spectrum of mutations in the *APC* gene was analyzed as described in literature [11]. The coding exons of the *APC* gene were amplified using exon-specific primers. The PCR products were studied by conformation-sensitive polyacrylamide gel electrophoresis (silver staining). The gene was Sanger-sequenced in order to identify conformational changes to its primary structure. For sequencing, we used a Big DyeTM Terminator v. 3.1 Cycle Sequencing kit and an ABI Prism 3130x1 genetic analyzer (Applied Biosystems; USA). The obtained chromatograms were analyzed in ChromasPro, NCBI BLAST and Ensembl genome browser 91. The NM_000038.6 sequence of the *APC* gene was used as a reference. Statistical processing was aided by Statistica 10.0 (StatSoft; USA).

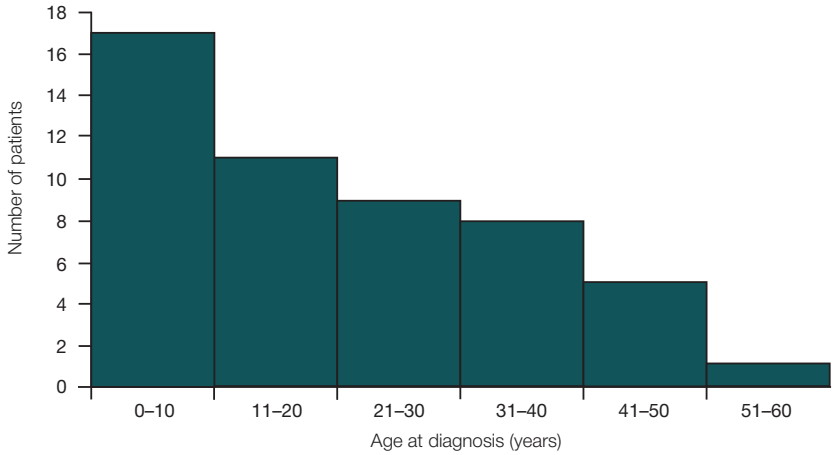

Fig. Age distribution of patients with sporadic DF

RESULTS

The *APC* gene was analyzed in 51 patients with sporadic DF. Six (12%) patients were found to carry germline mutations in this gene. Table 1 lists the mutations we detected, the age of the patients at the time of diagnosis, the number of lesions (single or multiple), and their location in the body.

Of 6 detected mutations, 2 were not described previously, including c.4386-4390 delGAGAG (1462delGAGAG) and c.4575insT (1525insT). Both mutations result in a frame shift and a premature stop codon and are, therefore, deleterious.

The c.4575insT mutation was found in a female patient (patient 1, see Table 1) with severe DF that manifested at 9 years and was multifocal. The endoscopic examination conducted at the age of 19 years revealed no signs of colonic polyposis.

The mutation c.4386-4390 delGAGAG was observed in patient 2 (Table 1). The onset of the disease occurred at the age of 1 month. Since early childhood, the patient had had multiple growing lesions in the chest wall. By the age of 18 years, the patient had gone through 5 surgical interventions, a few chemotherapy courses, hormone treatment, and radiation therapy, to no avail. This case of DF can be classified as extremely severe and resistant to treatment. The mutation found in patient 2 (c.4386-4390 delGAGAG (1462delGAGAG)) was not previously reported in other populations [12–14]. Also, it was not detected in the blood samples of the patient's parents, so it can be considered a *de novo* mutation. The sensitivity of the applied method allows detecting 1 to 5% of mutant alleles, which means that APC mosaicism in the parents is highly unlikely [15].

Three unrelated patients had an identical mutation c.4393-4394 delAG (1465delAG), whose clinical manifestations were, nevertheless, different. One of its carriers, a 28-year-old woman, had multiple lesions in the chest and abdominal walls and the intra-abdominal region. The age of onset was 17 years. At the time of our study, her colonoscopy was negative for colon polyps. Among the two other patients with the same mutations were a boy with multiple desmoids present at birth (the lesions were localized to the chest and the low back) and a girl with a solitary desmoid tumor on the low back developed at the age of 2 years. Interestingly, the age of onset, the number and location of the tumors were different in those 3 patients. Perhaps, DF sites varied between the patients because 2 of them were quite young. So, we cannot rule out the possibility of multifocal growth later in the children's life. It is also possible that the progression of the disease may be affected by environmental factors and differences in the patients' genotypes.

The c.4348C/T; p.R1450X mutation was detected in 1 patient with multifocal DF. The age at onset was 15 years. The patient had undergone multiple surgeries, a few chemotherapy courses and hormone treatment. By the time of our study, the growth of the tumor had been halted.

All patients with *APC* mutations reported an early onset of the disease. Most of them (5 of 6) had multiple desmoids resistant to therapy. In spite of the received treatment, the prognosis was still poor for 3 (50%) of patients. DF was severe in 3 of 6 patients with mutant *APC*, which was more frequent than in the patients who did not carry a germline mutation in this gene (2 of 45). This difference was statistically significant ($p = 0.01$).

The age of onset varied from 1 month to 17 years in the patients with mutant *APC* (Table 1), the median age being 5.8 years. In the patients who did not have mutations in the *APC* gene, the age of onset varied from 1 month to 60 years (Fig. 1), and the median age was 19 years. The difference in the median values was statistically significant ($p = 0.022$; *U*-test).

All *APC* mutations described above were detected in 6 (23%) of 26 patients with desmoid tumors on the trunk. Patients with differently localized DF had no mutations in the *APC* gene (Table 2). Generally, mutations in the *APC* gene occurred more often in the patients with DF lesions localized to the trunk than in the patients with different lesion sites ($p = 0.023$). This phenomenon is not predicated on the accumulation of multiple desmoid tumors on the trunk (which would indicate random accumulation of the lesions in the carriers of *APC* mutations) because the frequency of their occurrence on the trunk was not significantly higher in comparison with other lesion sites (Table 2; $p = 0.17$).

Of 51 patients, 11 had multifocal DF. Five (45%) of those individuals had germline mutations in the *APC* gene (Table 1). In the group of patients with solitary DF (40 individuals) only one carried an *APC* mutation (1/40, or 2.5%). The difference in the incidence of *APC* mutations was statistically significant ($p = 0.001$). The odds ratio value also suggested an association between *APC* mutations and multifocal DF (OR = 32.5; 95% CI: 3.22–326.31). Thus, mutations in the *APC* gene were mainly seen in the patients with multiple desmoid tumors.

Summing up, the mutations in the *APC* gene were linked to the tumor location on the trunk and its multifocal growth (Table 2).

Such significant number of mutations (12%) in the patients with sporadic DF who do not have clinical signs and/or family history of adenomatous polyposis suggest that patients with FAP and patients with sporadic DF can carry different mutations in the *APC* gene. All mutations detected in the patients with sporadic DF were localized 3' of codon 1444.

Bearing that in mind, we decided to study a sample of patients with FAP and co-occurring DF. Of 65 patients with FAP, 12 had DF. Germline mutations in the *APC* gene were observed in 6 out of 12 patients with both FAP and DF (Table 3).

Clinical presentations of fibromatosis did not differ between FAP patients regardless of the presence of *APC* mutations. The age of DF onset in the FAP carriers of *APC* mutations varied from 28 to 57 years (Table 3). The median age in this group of patients was 35.5 years; it did not differ significantly

Table 1. Mutations in the APC gene in patients with sporadic desmoid fibromatosis

№	Lesion site	Name of *APC* mutation	Age at DF onset
1	Multiple lesions; chest and abdominal walls	c.4575insT (1525insT)	9 years
2	Multiple lesions; chest and abdominal walls	c.4386-4390 delGAGAG (1462delGAGAG)	2 months
3	Multiple lesions; chest wall, lower back	R1450X (c.4348C/T)	15 years
4	Multiple lesions; chest and abdominal walls; intra-abdominal location	c.4393-4394 delAG (1465delAG)	17 years
5	Multiple lesions, chest wall, lower back	c.4393-4394 delAG (1465delAG)	1 month
6	Back	c.4393-4394 delAG (1465delAG)	2 years

from the median value (29 years; the range of 24–36 years) for the patients who did not have *APC* mutations.

None of the patients with FAP and co-occurring DF had an *APC* mutation 3' of codon 1444 (Table 3). In patients with sporadic DF, all detected mutations were located 3' of codon 1444 (Table 1). The difference in the sites of *APC* mutations in sporadic and FAP-associated DF was statistically significant (p = 0.0022, OR = 144; 95% CI: 2.43–8517.50), i.e. in the patients with sporadic DF, mutations tended to occur at the 3'-region of the gene more often than in the individuals with FAP-associated desmoid tumors.

The patients with sporadic DF and *APC* mutations tended to develop the condition much earlier in life than carriers of the same mutations with FAP-associated DF (the median age was 5.8 and 35.5 years, respectively; p = 0.004; *U*-test). No statistically significant differences were observed between the patients who did not have APC mutations but had sporadic or FAP-associated DF in terms of DF onset (p = 0.09).

Multifocal DF was more common in the patients with *APC* mutations and sporadic DF (5/6) than in the individuals with *APC* mutations and FAP (0/6): OR = 60; 95% CI: 1.64–2187.79; p = 0.015.

DISCUSSION

In this study, we investigated germline mutations in the *APC* gene using a sample of 51 patients with sporadic desmoid fibromatosis. All patients had no clinical manifestations or family history of FAP. Six patients (12%) were found to have pathogenic mutations, two of which had not been reported previously, including 1525insT and 1462delGAGAG. In previous works, *APC* mutations were studied in patients with sporadic and FAP-associated DF, but detected them only in individuals with FAP but not sporadic DF. This can be explained by specific research objectives or the characteristics of the studied samples. For instance, only 1 case of multifocal DF was included in the sample studied in [16].

It is quite rare that desmoid-type fibromatosis manifests itself in infancy. The available literature presents only several clinical cases of early DF [17, 18]. In our sample of patients with sporadic DF and *APC* mutations there were 3 cases of early DF onset: two patients were diagnosed at 1 and 2 months, respectively, and one patient, at the age of 2 years.

In our study, all *APC* mutations in the patients with sporadic DF were 3' of codon 1444 and associated with the severe clinical course, multifocal growth and early onset. In this group of patients, the median age at onset was 5.8 years, as compared to 19 years for the patients who did not carry *APC* mutations. In the carriers of *APC* mutations, all desmoid tumors were localized to the trunk, although such lesion site was not more frequent than other locations (Table 2; p = 0.17). This is one of the findings that were unknown previously. There are reports of families with hereditary desmoid tumors. For example, the literature describes a case of a family in which 3 generations have been affected by desmoid-type fibromatosis. Their condition is linked to a frameshift mutation in codon 1924 of the *APC* gene. In this family, DF were both extra-abdominal and intra-abdominal and the age of onset varies from birth to 10–20 years. Of 9 members of the family, 3 had polyposis or cancer of the colon. Other known cases of inherited DF are also linked to the mutations at the 3'-end of the *APC* and characterized by multiple lesions and severe course of the disease [19, 20].

It was interesting to compare the features of the detected mutations and DF phenotypes between patients with FAP-associated and those with sporadic desmoid tumors. Research into the association between the patient's genotype and clinical presentations of FAP has yielded controversial results. A study of the association between the site of an *APC* mutation and the risk of DF in patients with FAP found no such association [21]. Another study of a group of 14 patients with FAP and co-occurring DF revealed that only two patients had the mutation 3' of codon 1444 [22], which might be explained by population characteristics of the sample. In our study, we used

Table 2. Associations between the mutations in the *APC* gene and different lesion sites/number of desmoid tumors

Lesion site	Patients with desmoid-type fibromatosis		Patients with multifocal desmoid-type fibromatosis	
	Number of patients	Number of patients with mutant *APC*	Number of patients	Number of patients with mutant *APC*
Chest and/or abdominal wall	26	6	8	5
Intra-abdominal	3	–	–	–
Extremities	14	–	3	–
Other sites	8	–	–	–
Total	51		11	

Table 3. Description of *APC* mutations and clinical data of patients with FAP and co-occurring DF

№	Name of mutations	DF description	Age, years
1	c.3464-3468 delAAGAA (1155del5)	Postoperative DF of the root of the mesentery	57
2	c.3927-3921delAAAGA (1309del5)	DF of the postoperative scar tissue	28
3	c.3930insA (1310insA)	Postoperative DF of the root of the mesentery	34
4	c.3183-3187 delACAAA (1061del5)	Postoperative DF of the root of the mesentery	38
5	c.2274-2278 delAGCCC p.K758Nfs (758-760 delAGCCC)	Postoperative DF of the abdominal wall	30
6	3496delT (1166delT)	DF of the abdominal wall	33
7	–	Postoperative DF of the abdominal wall	33
8	–	Postoperative DF of the root of the mesentery	29
9	–	Postoperative DF of the root of the mesentery	29
10	–	Postoperative DF of the abdominal wall	29
11	–	DF of the abdominal wall	24
12	–	Postoperative DF of the abdominal wall	36

a sample of Russian patients with FAP. Of 65 candidates with FAP, 12 had DF (18%). This figure is close to that obtained by other researchers: some report a value between 3.5 and 32% [23], while others, 10–15% [24]. Half of our patients with FAP and co-occurring DF had mutations in the *APC* gene. All 6 detected mutations were located at the 5' of codon 1444. The difference in the incidence of mutations in the region distal to codon 1444 between sporadic and FAP-associated DF was statistically significant ($p = 0.002$). We compared the values obtained for the patients with FAP-associated DF with the occurrence of similarly located mutations in the pooled international sample of FAP patients [25]. The difference was insignificant ($p = 0.34$). At the same time, our values for sporadic DF differed from those for FAP-associated DF reported by other researchers ($p = 0.0002$) [25]. This leads us to conclude that sporadic desmoid tumors occurring in patients with no signs or family history of FAP are more often caused by mutations 3' of codon 1444 in comparison with FAP-associated DF.

In our sample, all patients with FAP developed desmoid tumors only after surgery; the tumors occurred either intraperitoneally or in the abdominal wall. Other researchers report the same pattern [26, 27].

In our patients with the mutant APC gene, sporadic DF was mainly multifocal and localized to the chest or abdominal walls. Intrabdominal lesions are typical for patients with FAP and less common in sporadic cases of the disease [25]. Most likely, the abdominal location of the tumor in patients with FAP is the result of tissue injury during surgery [28]. No direct association with tissue injury was observed in our study for the patients with sporadic DF and APC mutations.

In our sample, the median age of onset did not differ between the FAP patients with and without mutations, but was significantly lower in the patients with sporadic DF and germline mutations in the *APC* gene. For those who did not carry *APC* mutations, the age at diagnosis did not differ significantly between the patients with sporadic and FAP-associated DF ($p = 0.09$).

These findings suggest that there is a significant difference in the clinical manifestations of sporadic and FAP-associated desmoid tumors in the carriers of *APC* mutations; these differences are (at least to some extent) associated with the position of the mutation in the gene.

Summing up, we have studied a sample of individuals with sporadic DF and identified a subgroup of patients with a specific DF phenotype determined by germline mutations in the *APC* gene. In such patients, DF is severe, multifocal, manifests itself at early age, resists treatment and has a poor prognosis. The causative mutations are localized to the 3'-end of the *APC* gene.

Our findings can help the physician in deciding on the suitable treatment strategy and elaborating approaches to polyposis prevention. They can also be useful in studying mechanisms underlying multifocal DF.

CONCLUSIONS

We have studied a group of patients with DF and no history of FAP and identified a subgroup of individuals with a specific DF phenotype and germline mutations in the *APC* gene. Unlike patients who do not have *APC* mutations, carriers of the mutant gene variant develop multifocal DF on the trunk that manifests itself in infancy. In terms of DF phenotype, patients with sporadic DF and *APC* mutations differ from patients with FAP-associated DF who also have germline mutations in the *APC* gene. In patients with sporadic DF, mutations tend to localize to the 3'-region of the gene. This information should be considered when deciding on the treatment strategy against DF and elaborating approaches to DF and FAP prevention. Our findings provide a basis for the study of molecular mechanisms that trigger primary DF but not FAP.

References

1. Glebovskaja VV. Thermoradiotherapy of patients with primary and recurrent extraabdominal desmoid [dissertation]. M., 2004
2. Eastley N, McCulloch T, Esler C, Hennig I, Fairbairn J, Gronchi A, et al. Extra-abdominal desmoid fibromatosis: A review of management, current guidance and unanswered questions. Eur J Surg Oncol. 2016; 42 (7): 1071–83. DOI: 10.1016/j.ejso.2016.02.012.
3. Tkashev SI, Aliev MD, Glebovskaja VV, et al. The use of thermoradiotherapy in patients with primary and recurrent spastic-dominant desmoid tumors. Sarcomas of bones, soft tissues and skin tumors. 2009; (1): 34–7.
4. DE Marchis ML, Tonelli F, Quaresmini D, Lovero D, Della-Morte D, Silvestris F, et al. Desmoid Tumors in Familial Adenomatous Polyposis. Anticancer Res. 2017 Jul; 37 (7): 3357–66.
5. Mullen JT, DeLaney TF, Rosenberg AE, Le L, Iafrate AJ, Kobayashi W, et al. β-Catenin mutation status and outcomes in sporadic desmoid tumors. Oncologist. 2013; 18 (9): 1043–9. DOI: 10.1634/theoncologist.2012–0449.
6. Alman BA, Li C, Pajerski ME, Diaz-Cano S, Wolfe HJ. Increased beta-catenin protein and somatic APC mutations in sporadic aggressive fibromatoses (desmoid tumors). Am J Pathol. 1997; 151 (2): 329–34. PubMed PMID: 9250146; PubMed Central PMCID: PMC1857985.
7. Nikulin MP, Petrosyan AP, Tsymzhitova NTs, Gubina GI. Retroperitoneal desmoids: analytical review and case report. Clin Experiment Surg. 2015; (4): 103–12.
8. Koskenvuo L, Peltomäki P, Renkonen-Sinisalo L, Gylling A, Nieminen TT, Ristimäki A, et al. Desmoid tumor patients carry an elevated risk of familial adenomatous polyposis. J Surg Oncol. 2016; 113 (2): 209–12. DOI: 10.1002/jso.24117.
9. Brueckl WM, Ballhausen WG, Förtsch T, Günther K, Fiedler W, Gentner B, et al. Genetic testing for germline mutations of the APC gene in patients with apparently sporadic desmoid tumors but a family history of colorectal carcinoma. Dis Colon Rectum. 2005; 48 (6): 1275–81. DOI: 10.1007/s10350-004-0949-5.
10. Sambrook J, Fritsch EF, Maniatis T. Molecular cloning: a laboratory manual, N.Y.: Cold Spring Harbor Laboratory, Cold Spring Harbor, 1989; 1546 p.
11. Muzaffarova TA, Mansorunov DJ, Sachkov IY, Kuzevanova AY, Karpukhin AV, Alimov AA. Molecular genetic aspects of the risk for family adenomatous polyposis. Molecular medicine. 2018; 16 (6): 60–64.
12. The Human Gene Mutation Database (HGMD®). Available from: http://www.hgmd.cf.ac.uk/ac/index.php.
13. Ensembl Genome Browser 96. Available from: http://www.ensembl.org/index.html.
14. LOVD database. Available from: https://www.lovd.nl/.
15. Hes FJ, Nielsen M, Bik EC, Konvalinka D, Wijnen JT, Bakker E, et al. Somatic APC mosaicism: an underestimated cause of polyposis coli. Gut. 2008; 57 (1): 71–6. DOI: 10.1136/gut.2006.117796.
16. Kattentidt Mouravieva AA, Geurts-Giele IR, de Krijger RR, van Noesel MM, van de Ven CP, van den Ouweland, et al. Identification of Familial Adenomatous Polyposis carriers among children with desmoid tumours. Eur J Cancer. 2012 Aug; 48 (12): 1867–74.

DOI: 10.1016/j.ejca.2012.01.004
17. Dalit A, Karen M, Alexander M. Congenital desmoid tumor of the cheek: a clinicopathological case report. Eplasty. 2009 Nov 10; (9): e52. PubMed PMID: 20011031; PubMed Central PMCID: PMC2779781.
18. Roggli VL, Kim HS, Hawkins E. Congenital generalized fibromatosis with visceral involvement. A case report. Cancer. 1980; (45): 954–60.
19. Halling KC, Lazzaro CR, Honchel R, Bufill JA, Powell SM, Arndt CAS, et al. Hereditary Desmoid Disease in a Family with a Germline Alu IRepeat Mutation of the APC Gene. Hum Hered. 1999; (49): 97–102.DOI: 10.1159/000022852.
20. Eccles DM, van der Luijt R, Breukel C, Bullman H, Bunyan D, Fisher A, et al. Hereditary desmoid disease due to a frameshift mutation at codon 1924 of the APC gene. Am J Hum Genet. 1996; 59 (6): 1193–201. PMCID: PMC1914868; PMID: 8940264.
21. Nieuwenhuis MH, De Vos Tot Nederveen Cappel W, Botma A, Nagengast FM, Kleibeuker JH, Mathus-Vliegen EM, et al. Desmoid tumors in a dutch cohort of patients with familial adenomatous polyposis. Clin Gastroenterol Hepatol. 2008; 6 (2): 215–9. DOI: 10.1016/j.cgh.2007.11.011.
22. Torrezan GT, da Silva FC, Santos EM, Krepischi AC, Achatz MI, Aguiar S Jr, et al. Mutational spectrum of the APC and MUTYH genes and genotype-phenotype correlations in Brazilian FAP, AFAP, and MAP patients. Orphanet J Rare Dis. 2013; (8): 54. DOI: 10.1186/1750-1172-8-54.
23. Fallen T, Wilson M, Morlan B, Lindor NM. Desmoid tumors — a characterization of patients seen at Mayo Clinic 1976–1999. Fam Cancer. 2006; 5 (2): 191–4. DOI: 10.1007/s10689-005-5959-5.
24. Lips DJ, Barker N, Clevers H, Hennipman A. The role of APC and beta-catenin in the aetiology of aggressive fibromatosis (desmoid tumors). Eur J Surg Oncol. 2009 Jan; 35 (1): 3–10. DOI: 10.1016/j.ejso.2008.07.003.
25. Nieuwenhuis MH, Lefevre JH, Bülow S, Järvinen H, Bertario L, Kernéis S, et al. Family history, surgery, and APC mutation are risk factors for desmoid tumors in familial adenomatous polyposis: an international cohort study. Dis Colon Rectum. 2011; 54 (10): 1229–34.DOI: 10.1097/DCR.0b013e318227e4e8.
26. Nieuwenhuis MH, Lefevre JH, Bülow S, Järvinen H, Bertario L, Kernéis S, et al. A nation-wide study comparing sporadic and familial adenomatous polyposis-related desmoid-type fibromatoses. Dis Colon Rectum. 2011 Oct; 54 (10): 1229–34. DOI: 10.1002/ijc.25664.
27. Koskenvuo L, Ristimäki A, Lepistö A. Comparison of sporadic and FAP-associated desmoid-type fibromatoses. J Surg Oncol. 2017 Nov; 116 (6): 716–21. DOI: 10.1002/jso.24699.
28. Nieuwenhuis MH, De Vos Tot Nederveen Cappel W, Botma A, Nagengast FM, Kleibeuker JH, Mathus-Vliegen EM, et al. Desmoid tumors in a dutch cohort of patients with familial adenomatous polyposis. Clin Gastroenterol Hepatol. 2008 Feb; 6 (2): 215–9. DOI: 10.1016/j.cgh.2007.11.011.

Литература

1. Глебовская В. В. Терморадиотерапия больных с первичным и рецидивным экстраабдоминальным десмоидом [диссертация]. М., 2004.
2. Eastley N, McCulloch T, Esler C, Hennig I, Fairbairn J, Gronchi A, et al. Extra-abdominal desmoid fibromatosis: A review of management, current guidance and unanswered questions. Eur J Surg Oncol. 2016; 42 (7): 1071–83. DOI: 10.1016/j.ejso.2016.02.012.
3. Ткачев С. И., Алиев М. Д., Глебовская В. В. и др. Применение терморадиотерапии у больных первичными и рецидивными экстраабдоминальными десмоидными опухолями. Саркомы костей, мягких тканей и опухоли кожи. 2009; (1): 34–7.
4. DE Marchis ML, Tonelli F, Quaresmini D, Lovero D, Della-Morte D, Silvestris F, et al. Desmoid Tumors in Familial Adenomatous Polyposis. Anticancer Res. 2017 Jul; 37 (7): 3357–66.
5. Mullen JT, DeLaney TF, Rosenberg AE, Le L, Iafrate AJ, Kobayashi W, et al. β-Catenin mutation status and outcomes in sporadic desmoid tumors. Oncologist. 2013; 18 (9): 1043–9. DOI: 10.1634/theoncologist. 2012–0449.
6. Alman BA, Li C, Pajerski ME, Diaz-Cano S, Wolfe HJ. Increased beta-catenin protein and somatic APC mutations in sporadic aggressive fibromatoses (desmoid tumors). Am J Pathol. 1997; 151 (2): 329–34. PubMed PMID: 9250146; PubMed Central PMCID: PMC1857985.
7. Никулин М. П., Петросян А. П., Цымжитова Н. Ц., Губина Г. И. Забрюшинные десмоиды: аналитический обзор и случай из практики. Клиническая и экспериментальная хирургия. 2015; (4): 103–12.
8. Koskenvuo L, Peltomäki P, Renkonen-Sinisalo L, Gylling A, Nieminen TT, Ristimäki A, et al. Desmoid tumor patients carry an elevated risk of familial adenomatous polyposis. J Surg Oncol. 2016; 113 (2): 209–12. DOI: 10.1002/jso.24117.
9. Brueckl WM, Ballhausen WG, Förtsch T, Günther K, Fiedler W, Gentner B, et al. Genetic testing for germline mutations of the APC gene in patients with apparently sporadic desmoid tumors but a family history of colorectal carcinoma. Dis Colon Rectum. 2005; 48 (6): 1275–81. DOI: 10.1007/s10350-004-0949-5.
10. Sambrook J, Fritsch EF, Maniatis T. Molecular cloning: a laboratory manual, N.Y.: Cold Spring Harbor Laboratory, Cold Spring Harbor, 1989; 1546 p.
11. Музаффарова Т. А., Мансорунов Д. Ж., Сачков И. Ю., Кузеванова А. Ю., Карпухин А. В., Алимов А. А. Молекулярно-генетические аспекты риска семейного аденоматозного полипоза. Молекулярная медицина. 2018; 16 (6): 60–4. DOI: https://doi.org/10.29296/24999490-2018-06-11.
12. The Human Gene Mutation Database (HGMD®). Available from: http://www.hgmd.cf.ac.uk/ac/index.php.
13. Ensembl Genome Browser 96. Available from: http://www.ensembl.org/index.html.
14. LOVD database. Available from: https://www.lovd.nl/.
15. Hes FJ, Nielsen M, Bik EC, Konvalinka D, Wijnen JT, Bakker E, et al. Somatic APC mosaicism: an underestimated cause of polyposis coli. Gut. 2008; 57 (1): 71–6. DOI: 10.1136/gut.2006.117796.
16. Kattentidt Mouravieva AA, Geurts-Giele IR, de Krijger RR, van Noesel MM, van de Ven CP, van den Ouweland, et al. Identification of Familial Adenomatous Polyposis carriers among children with desmoid tumours. Eur J Cancer. 2012 Aug; 48 (12): 1867–74. DOI: 10.1016/j.ejca.2012.01.004
17. Dalit A, Karen M, Alexander M. Congenital desmoid tumor of the cheek: a clinicopathological case report. Eplasty. 2009 Nov 10; (9): e52. PubMed PMID: 20011031; PubMed Central PMCID: PMC2779781.
18. Roggli VL, Kim HS, Hawkins E. Congenital generalized fibromatosis with visceral involvement. A case report. Cancer. 1980; (45): 954–60.
19. Halling KC, Lazzaro CR, Honchel R, Bufill JA, Powell SM, Arndt CAS, et al. Hereditary Desmoid Disease in a Family with a Germline Alu IRepeat Mutation of the APC Gene. Hum Hered. 1999; (49): 97–102.DOI: 10.1159/000022852.
20. Eccles DM, van der Luijt R, Breukel C, Bullman H, Bunyan D, Fisher A, et al. Hereditary desmoid disease due to a frameshift mutation at codon 1924 of the APC gene. Am J Hum Genet. 1996; 59 (6): 1193–201. PMCID: PMC1914868; PMID: 8940264.
21. Nieuwenhuis MH, De Vos Tot Nederveen Cappel W, Botma A, Nagengast FM, Kleibeuker JH, Mathus-Vliegen EM, et al. Desmoid tumors in a dutch cohort of patients with familial adenomatous polyposis. Clin Gastroenterol Hepatol. 2008; 6 (2): 215–9. DOI: 10.1016/j.cgh.2007.11.011.
22. Torrezan GT, da Silva FC, Santos EM, Krepischi AC, Achatz MI, Aguiar S Jr, et al. Mutational spectrum of the APC and MUTYH genes and genotype-phenotype correlations in Brazilian FAP, AFAP, and MAP patients. Orphanet J Rare Dis. 2013; (8): 54. DOI: 10.1186/1750-1172-8-54.
23. Fallen T, Wilson M, Morlan B, Lindor NM. Desmoid tumors — a characterization of patients seen at Mayo Clinic 1976–1999. Fam Cancer. 2006; 5 (2): 191–4. DOI: 10.1007/s10689-005-5959-5.

24. Lips DJ, Barker N, Clevers H, Hennipman A. The role of APC and beta-catenin in the aetiology of aggressive fibromatosis (desmoid tumors). Eur J Surg Oncol. 2009 Jan; 35 (1): 3–10. DOI: 10.1016/j.ejso.2008.07.003.
25. Nieuwenhuis MH, Lefevre JH, Bülow S, Järvinen H, Bertario L, Kernéis S, et al. Family history, surgery, and APC mutation are risk factors for desmoid tumors in familial adenomatous polyposis: an international cohort study. Dis Colon Rectum. 2011; 54 (10): 1229–34.DOI: 10.1097/DCR.0b013e318227e4e8.
26. Nieuwenhuis MH, Lefevre JH, Bülow S, Järvinen H, Bertario L, Kernéis S, et al. A nation-wide study comparing sporadic and familial adenomatous polyposis-related desmoid-type fibromatoses. Dis Colon Rectum. 2011 Oct; 54 (10): 1229–34. DOI: 10.1002/ijc.25664.
27. Koskenvuo L, Ristimäki A, Lepistö A. Comparison of sporadic and FAP-associated desmoid-type fibromatoses. J Surg Oncol. 2017 Nov; 116 (6): 716–21. DOI: 10.1002/jso.24699.
28. Nieuwenhuis MH, De Vos Tot Nederveen Cappel W, Botma A, Nagengast FM, Kleibeuker JH, Mathus-Vliegen EM, et al. Desmoid tumors in a dutch cohort of patients with familial adenomatous polyposis. Clin Gastroenterol Hepatol. 2008 Feb; 6 (2): 215–9. DOI: 10.1016/j.cgh.2007.11.011.

ASSOCIATIONS BETWEEN BLOOD AND CEREBROSPINAL FLUID FLOW IMPAIRMENTS ASSESSED WITH PHASE-CONTRAST MRI AND BRAIN DAMAGE IN PATIENTS WITH AGE-RELATED CEREBRAL SMALL VESSEL DISEASE

Kremneva EI[1] ✉, Akhmetzyanov BM[2], Dobrynina LA[1], Krotenkova MV[1]

[1] Research Center of Neurology, Moscow, Russia

[2] PET-Technology LLC, Ufa, Russia

Hemodynamic parameters of blood and cerebrospinal fluid (CSF) flow can be measured *in vivo* using phase-contrast MRI (PC-MRI). This opens new horizons for studying the mechanisms implicated in the development and progression of age-related cerebral small vessel disease (SVD). In this paper, we analyze associations between cerebral arterial, venous and CSF flow impairments and SVD features visible on MRI. The study was carried out in 96 patients with SVD (aged 60.91 ± 6.57 years) and 23 healthy volunteers (59.13 ± 6.56 years). The protocol of the MRI examination included routine MRI sequences (T2, FLAIR, T1, SWI, and DWI) applied to assess the severity of brain damage according to STRIVE advisory standards and PC-MRI used to quantify blood flow in the major arteries and veins of the neck, the straight and upper sagittal sinuses, and CSF flow at the aqueduct level. We analyzed the associations between linear and volumetric parameters of blood/CSF flow and the degree of brain matter damage using the Fazekas scale. We observed a reduction in tABF, stVBF, sssVBF, aqLF, Saq, and ICC values and a rise in Pi associated with WMH progression, as well as a gradual decline in tABF and an increase in Pi, Saq and ICC associated with a growing number of lacunes ($p < 0.05$). Patients with early (< 5) MB had lower sssVBF and stVBF rates in comparison with patients without MB; aqLF, Saq, and ICC values were elevated in patients with 5 to 10 MB, as compared to patients without MB or early (< 5) MB. The established associations between MRI findings in patients with SVD and blood/CSF flow impairments suggest the important role of mechanisms implicated in the disruption of Monro–Kellie intracranial homeostasis in promoting SVD.

Keywords: phase-contrast MRI, age-related small vessel disease, blood flow, CSF flow

Funding: this work was part of the state assignment for Research Center of Neurology.

Author contribution: Kremneva EI — methodology of the study, data analysis and interpretation, manuscript preparation; Akhmetzyanov BM — data acquisition, statistical processing and interpretation; Dobrynina LA — conception and methodology of the study, data interpretation, clinical data analysis and acquisition; Krotenkova MV — study supervision and methodology, data interpretation.

Compliance with ethical standards: the study was approved by the Ethics Committee of the Research Center of Neurology (Protocol № 2–3/16 dated January 27. 2016). Informed consent was obtained from all study participants.

✉ **Correspondence should be addressed:** Elena I. Kremneva
Volokolamskoe shosse 80, Moscow, 125367; kremneva@neurology.ru

Received: 28.07.2019 **Accepted:** 12.08.2019 **Published online:** 25.08.2019

DOI: 10.24075/brsmu.2019.054

ВЛИЯНИЕ НАРУШЕНИЙ КРОВОТОКА И ЛИКВОРОТОКА ПО ДАННЫМ ФАЗОВО-КОНТРАСТНОЙ МРТ НА СОСТОЯНИЕ ГОЛОВНОГО МОЗГА ПРИ ВОЗРАСТ-ЗАВИСИМОЙ ЦЕРЕБРАЛЬНОЙ МИКРОАНГИОПАТИИ

Е. И. Кремнева[1] ✉, Б. М. Ахметзянов[2], Л. А. Добрынина[1], М. В. Кротенкова[1]

[1] Научный центр неврологии, Москва, Россия

[2] ООО «ПЭТ-Технолоджи», Уфа, Россия

Метод фазово-контрастной МРТ (ФК-МРТ) головного мозга позволяет *in vivo* оценить показатели кровотока и ликворотока, что открывает новые возможности в исследовании механизмов развития и прогрессирования возраст-зависимой церебральной микроангиопатии (ЦМА). Целью работы было провести анализ значимости нарушений церебрального артериального, венозного кровотока и ликворотока в формировании МРТ-признаков ЦМА. Исследовали 96 больных с ЦМА (60,91 ± 6,57 лет) и 23 здоровых добровольца (59,13 ± 6,56 лет). Протокол МРТ включал в себя режимы T2, FLAIR, T1, SWI, ДВИ для оценки поражения головного мозга согласно стандартам STRIVE, а также ФК-МРТ с оценкой кровотока в магистральных артериях и венах шеи, в прямом и верхнем сагиттальном синусах, ликворотока на уровне водопровода мозга. Проводили корреляцию линейных и объемных показателей кровотока и ликворотока с поражением вещества мозга в зависимости от степени тяжести изменений (шкала Фазекас). Отмечно снижение tABF, stVBF, sssVBF, aqLF, Saq, ICC и повышение Pi по мере прогрессирования ГИБВ, постепенное снижение tABF и повышение Pi, Saq и ICC по мере увеличения числа лакун ($p < 0,05$). Значения sssVBF и stVBF также достоверно снижались в группе ранних (< 5) МКР по сравнению с больными без МКР, а aqLF, Saq, ICC увеличивались в группе больных с 5–10 МКР по сравнению с больными без МКР и ранними (< 5) МКР. Установление связи изменений в артериальном, венозном кровотоке и ликворотоке с МРТ-проявлениями у больных ЦМА позволяет предполагать патогенетическую значимость в развитии ЦМА-механизмов, связанных с нарушением гомеостаза Монро–Келли.

Ключевые слова: фазово-контрастная МРТ, возраст-зависимая церебральная микроангиопатия, мозговой кровоток, ликвороток

Финансирование: работа выполнена в рамках государственного задания ФГБНУ НЦН.

Информация о вкладе авторов: Е. И. Кремнева — методика исследования, анализ и интерпретация данных, написание и оформление статьи; Б. М. Ахметзянов — сбор данных; обработка данных и их интерпретация; статистический анализ; Л. А. Добрынина — общая идея и методология исследования, интерпретация данных, сбор и анализ клинической части данных; М. В. Кротенкова — курирование исследования, методология исследования, интерпретация данных.

Соблюдение этических стандартов: исследование одобрено локальным этическим комитетом ФГБНУ Научный центр неврологии (протокол № 2–3/16 от 27 января 2016 г.). Все участники подписали добровольное информированное согласие на участие в исследовании.

✉ **Для корреспонденции:** Елена Игоревна Кремнева
Волоколамское шоссе, д. 80, г. Москва, 125367; kremneva@neurology.ru

Статья получена: 28.07.2019 **Статья принята к печати:** 12.08.2019 **Опубликована онлайн:** 25.08.2019

DOI: 10.24075/vrgmu.2019.054

MR neuroimaging has enabled visualization of the tiniest anatomical structures of the brain and provided new insights into its functions, metabolism, blood supply and cerebrospinal fluid (CSF) circulation. Phase contrast MRI (PC-MRI) is a method of functional MR neuroimaging that yields information about arterial, venous and CSF flows. In conventional PC-MRI, two data sets are acquired and subtracted from each other following the application of bipolar gradients with the same magnitude but opposite directions. The net phase gain will be 0 for stationary spins. However, moving spins will undergo a non-zero phase shift proportional to their velocity. This happens in flowing media, where traveling protons experience a stronger or weaker magnetic field following the application of the second gradient, as compared to the first. Since the amount of phase shift depends on the velocity of protons, PC-MRI can be used to measure hemodynamic parameters of the flow, including velocity [1]. When synchronized with the cardiac cycle, the pulse sequence generates a series of images containing flow velocity data that represent a particular cardiac cycle phase. Thus, a single scan can yield both phase and magnitude images, facilitating flow quantification and brain anatomy visualization.

PC-MRI is mainly used to quantify cerebral fluid flow and assess the efficacy of surgical treatment in patients with hydrocephalus [2]. PC-MRI is a rapid, noninvasive and objective technique for measuring the amount and velocity of arterial, venous and CSF flows and their temporal relationship to cardiac cycle phases; it also provides valuable information about arteries, veins, sinuses and perivascular spaces that determine cerebral compliance [3]. This makes PC-MRI an optimal tool for studying central nervous system disorders arising from the dysfunction of the mentioned intracranial components, including cerebral microangiopathy, also known as small vessel disease (SVD). SVE is essentially a combination of neuroimaging features, morphological and clinical symptoms associated with damage to small arteries, arterioles, capillaries and venules [4]. In Russia SVD is considered to be part of a broader concept referred to as dyscirculatory encephalopathy (DE) [5]. The social impact of SVD should not be underestimated: it accounts for at least 20% of all strokes and 45% of dementia cases worldwide [6]. Although the leading risk factors for SVD are hypertension and age [4], the disease is often diagnosed in non-hypertensive elderly patients; in many cases, its etiology is uncertain [7]. This has inspired research into the pathophysiology of SVD and the role of other risk factors [6], including early endothelial dysfunction accompanied by increased permeability of the blood brain barrier (BBB), vasogenic cerebral edema, and white matter damage that impair venous blood flow and affect CSF circulation [8]. Studies elucidating the role of blood or CSF flow impairments in brain damage in patients with SVD are scarce. However, once their role is clarified, the new knowledge can pave the way to novel therapeutic approaches for patients with SVD. Since PC-MRI is a perfect tool for this task, we decided to exploit it in our study. Below, we attempt to investigate the associations between cerebral arterial, venous and CSF flow impairments and SVD features visible on MRI.

METHODS

The main group consisted of 96 patients with SVD (31 men and 65 women aged 60.91 ± 6.57 years) referred to the Research Center of Neurology. The following inclusion criteria were applied: complaints of cognitive decline; MRI findings suggestive of SVD (according to STRIVE neuroimaging guidelines, those are recent small subcortical infarcts, lacunes, white matter hyperintensities (WMH), dilated perivascular spaces (PVS), cerebral microbleeds (MB), and brain atrophy) [9]. Patients with dementia that prevented the examination, stroke or brain damage caused by reasons other than SVD, aphasia, contraindications for MRI, severe pathology, atherosclerosis of major arteries of the head and neck (50% stenosis) were excluded from the study. The control group comprised 23 healthy volunteers (8 men and 15 women aged 59.13 ± 6.56 years) with no clinical symptoms and MRI findings suggesting vascular or degenerative brain disease. All patients and all controls underwent a standard neurological examination and did standard neuropsychological tests; their ability to function independently in daily life was also assessed. All participants underwent an MRI scan.

Brain scans were performed using a 3.0 T Magnetom Verio scanner (Siemens AG; Erlangen, Germany) with a 12-channel head coil. Routine MR sequences were used to investigate imaging features of the disease; PC-MRI was carried out to quantify blood and CSF flows.

The protocol for routine MRI included the following sequences: T2-spin-echo, 3D T1mpr, FLAIR, DWI, and SWI. The acquired images were analyzed in RadiAnt DICOM Viewer, version 3.0.2 (Medixant; Poznań, Poland) in compliance with STRIVE neuroimaging standards. Diffusion-weighted imaging revealed the absence of acute or subacute lacunar infarcts; therefore, we will not discuss them in this work. Fig. 1 shows the basic MR sequences applied in the study and the corresponding findings, including the location and extent of the lesion. The patients were distributed into a few groups based on the total severity of white matter lesions, which was assessed using the Fazekas scale: F1 represented single punctate lesions; F2, beginning confluency of lesions; F3, confluent lesions [12, 13].

Cerebral circulation and CSF flow were assessed with PC-MRI synchronized with a peripheral pulse sensor. The frame rate was 32 frames per cardiac cycle. The following scan parameters were applied: TR = 28.7 ms, TE = 8 ms, section thickness = 5.0 mm, field of view =101 × 135 mm, matrix = 256 × 192 pixels; Venc (velocity encoding value) was 5–20 cm/s for CSF flow and 60–80 cm/s for blood flow. The slice plane was orientated strictly perpendicular to the direction of blood flow in the internal carotid (ICA) and vertebral (VA) arteries at the C2/C3 level, to the direction of CSF flow at the cerebral aqueduct level and was also perpendicular to blood flow in the straight and superior sagittal sinuses (Fig. 2). The images were processed in Bio Flow Image, Flow Analysis Software, Version 04.12.16 (France). We calculated the amount of blood flow in ICA and VA, the rates of total arterial blood flow (tABF, ml/min), superior sagittal sinus venous blood flow (sssVBF, ml/min), straight sinus venous blood flow (stVBF, ml/min), aqueduct CSF flow (aqLF, mm^3/s) and the area occupied by the cerebral aqueduct (Saq, mm^2).

Resistance and elasticity (stiffness) of the arterial wall were measured using the pulsatility index (Pi) calculated by the formula: $Pi = (V_{max}–V_{min})/V_{mean}$, where V_{mean} is the mean blood flow velocity during one cardiac cycle, V_{max} and V_{min} are peak and minimal values of blood flow velocity, respectively; the index of intracranial compliance (ICC) = the amount of CSF flow (mm/s) at the cerebral aqueduct level divided by the amount of blood flowing through an artery (mm^3/s); the latter is an area under the arterial flow curve that lies above the mean value of blood flow during the cardiac cycle. Elevated ICC means a deterioration in the ability of the intracranial system, which includes brain tissue, CSF and blood flowing in the vessels, to adapt to an increased volume of any of its components or a

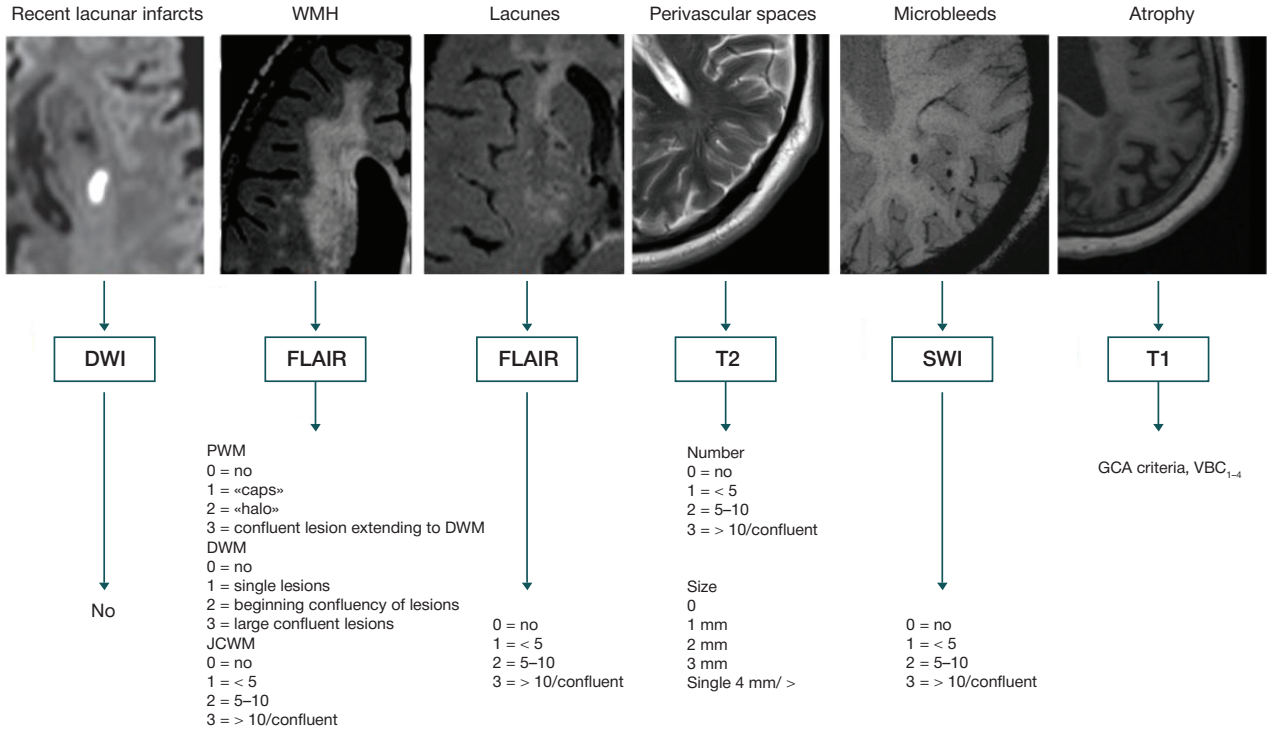

Fig. 1. An algorithm used to assess MRI features of SVD. PWM — periventricular white matter; DWM — deep white matter; JCWM — juxtacortical white matter [10]; PS — perivascular space; VBC — ventricle to brain coefficient; GCA — global cortical atrophy [11]

lesion, such as a hematoma or a tumor, without inducing a rise in cerebral pressure.

The acquired data were postprocessed in IBM SPSS Statistics 23.0 (IBM Company; USA). The effect of independent quantitative variables on dependent qualitative variables was assessed by one-way ANOVA followed by pairwise comparison and the least significant difference (LSD) test.

RESULTS

Basic characteristics of MRI features for SVD are provided in Table. PVP > 10 were observed in the semioval centers of 94 (97.9%) patients and in the subcortical structures of all patients; therefore, we analyzed the degree of their expansion only.

Associations between cerebral arterial blood flow parameters and MRI features of SVD

The measured hemodynamic parameters of arterial blood flow differed significantly ($p < 0.05$) between the patients with different degrees of severity of WMH, lacunar cavities, PVS dilation, and atrophy in the parietal, temporal and occipital cortex. No associations were established between the severity of MB or atrophy in other cortical regions and the values of tABF and Pi. The LSD test revealed that the patients with a Fazekas score of 3 had a significantly lower tABF rate and a higher Pi than the controls or the patients with a Fazekas score of 1 and 2. A gradual decline in tABF and elevated Pi were observed in almost all patients with lacunes, as compared to the patients who did not have lacunar cavities (Fig. 3).

Associations between cerebral venous blood flow parameters and MRI features of SVD

One-way ANOVA revealed that the hemodynamic parameters of cerebral venous flow in the upper sagittal and straight sinuses (stVBF, sssVBF) differed significantly between the controls and the patients with varying severity of WMH. Further post hoc comparison of the mean values aided by the LSD test revealed a statistically significant decline in stVBF and sssVBF rates in the patients with Fazekas 3, as compared with the controls; in such patients, the stVBF value was also lower than in the patients with a Fazekas score of 2 (Fig. 4).

Using the same statistical tools, we found significant differences in the hemodynamic parameters of cerebral venous flow between the controls and the patients with varying numbers of white matter and subcortical lacunes. A statistically significant decline in stVBF and sssVBF values was observed in the patients with 5 to 10 and > 10 white matter lacunes in comparison with the patients without lacunes. Low stVBF and sssVBF rates were seen in the patients with 5–10 and > 10 lacunes and in the patients with > 10 and < 5 lacunes in the subcortical ganglia, respectively, in comparison with the patients who did not have lacunar cavities (Fig. 4).

The measured hemodynamic parameters of cerebral venous blood flow differed significantly between the controls and the patients with juxtacortical MB in different brain regions. The post hoc analysis aided by the LSD test revealed a statistically significant correlation between lower sssVBF/stVBF rates and early MB (< 5) in the juxtacortical white matter of the parietal lobe in comparison with patients without MB. We also observed a decline in sssVBF values in the patients with early MB (< 5) in the deep white matter of the posterior frontal lobe in comparison with the patients without MB.

One-way ANOVA revealed statistically significant differences in sssVBF rates between the controls and the patients with dilated PVS and an association between stVBF/sssVBF rates and atrophy of the parietal and temporal lobes.

Associations between blood flow parameters, intracranial compliance and MRI features of SVD

The values of aqLF, Saq and the ICC index differed significantly between the controls and the patients with WMH. The patients

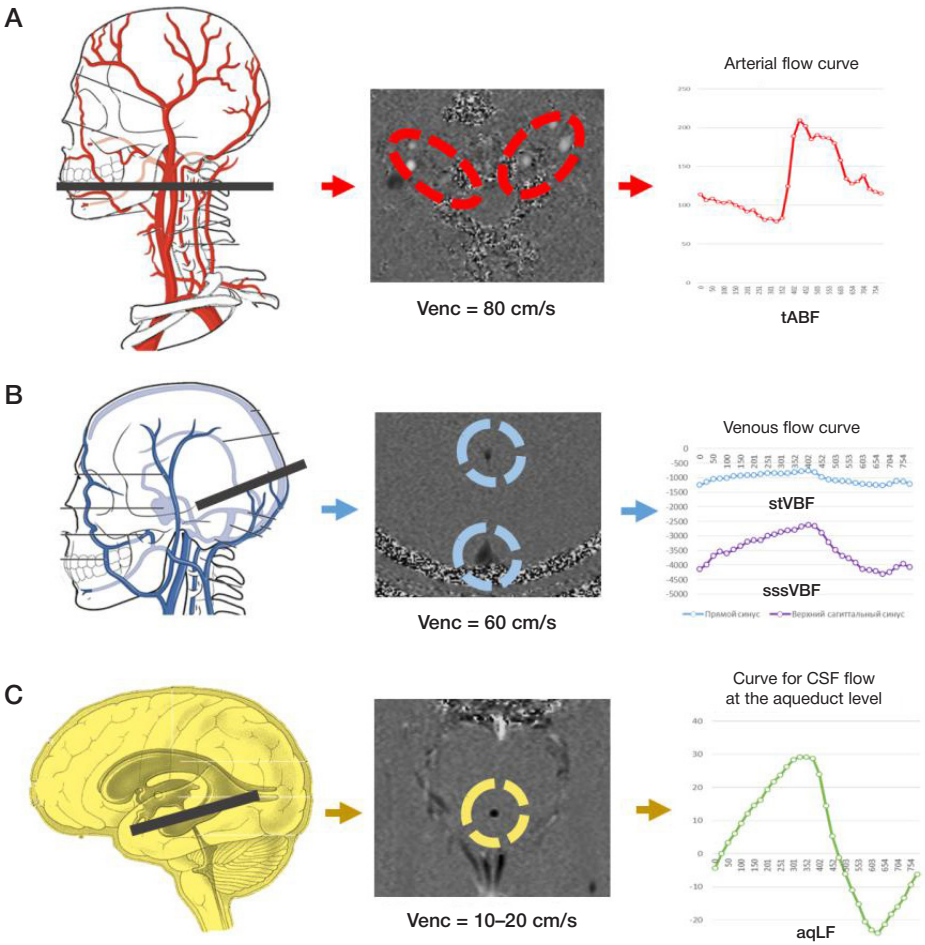

Fig. 2. A schematic representation of the PC-MRI procedure. **A**. Blood flow in the internal carotid and vertebral arteries. **B**. Blood flow in the straight and sagittal sinuses. **C**. CSF flow at the cerebral aqueduct level

with Fazekas 3 had lower aqLF, Saq and ICC than the controls or patients with other Fazekas scores. Increased Saq and elevated ICC were observed in the patients with over 10 white matter lacunes, as compared to the patients who did not have lacunar cavities (Fig. 5). aqLF, Saq, and ICC were increased in the patients with 5 to 10 MB in the juxtacortical white matter of the parietal and temporal lobes in comparison with the patients with a smaller number of MB (< 5) or their total absence.

DISCUSSION

In this study, we attempted to investigate the associations between vascular and CSF flow changes measured with PC-MRI and SVD features visible on MRI. The analysis of the generated images was guided by STRIVE neuroimaging standards [9]. Previous research works studied the associations between cerebral vascular changes and leukoaraiosis (WMH) or lacunes [14]. Numerous combinations of MRI features seen

Table. MRI findings in patients with SVD. WMH — white matter hyperintensities; MB — cerebral microbleeds; PVS — perivascular spaces; WM — white matter

Parameter	*n* (%)
WMH on the Fazekas scale: Fazekas 1 / Fazekas 2 / Fazekas 3	26 (27.1%) / 31 (32.3%) / 39 (40.6%)
Lacunes (number of) in WM of brain hemispheres: no / < 5 / 5–10 / > 10 in subcortical structures: no / < 5 / 5–10 / > 10	42 (43.8%) / 16 (16.7%) / 9 (9.4%) / 17 (17.7%) 32 (33.3%) / 11 (11.5%) / 9 (9.4%) / 12 (12.5%)
MB (number of) in WM of brain hemispheres: no / < 5 / 5–10 / > 10 in subcortical structures: no / < 5 / 5–10 / > 10	28 (29.2%) / 12 (12.5%) / 5 (5.2%) / 11 (11.5%) 28 (29.2%) / 13 (13.5%) / 4 (4.2%) / 11 (11.5%)
Brain atrophy: no / mild / moderate / severe	57 (59.4%) / 51 (53.1%) / 6 (6.3%) / 0 (0%)
PVS in semioval centers: 1–2 mm / 3 mm / 4 mm in subcortical structures: 1–2 mm / 3 mm / 4 mm	90 (93.8%) / 4 (4.2%) / 2 (2%) 68 (70.8%) / 21 (21.9%) / 7 (7.3%)

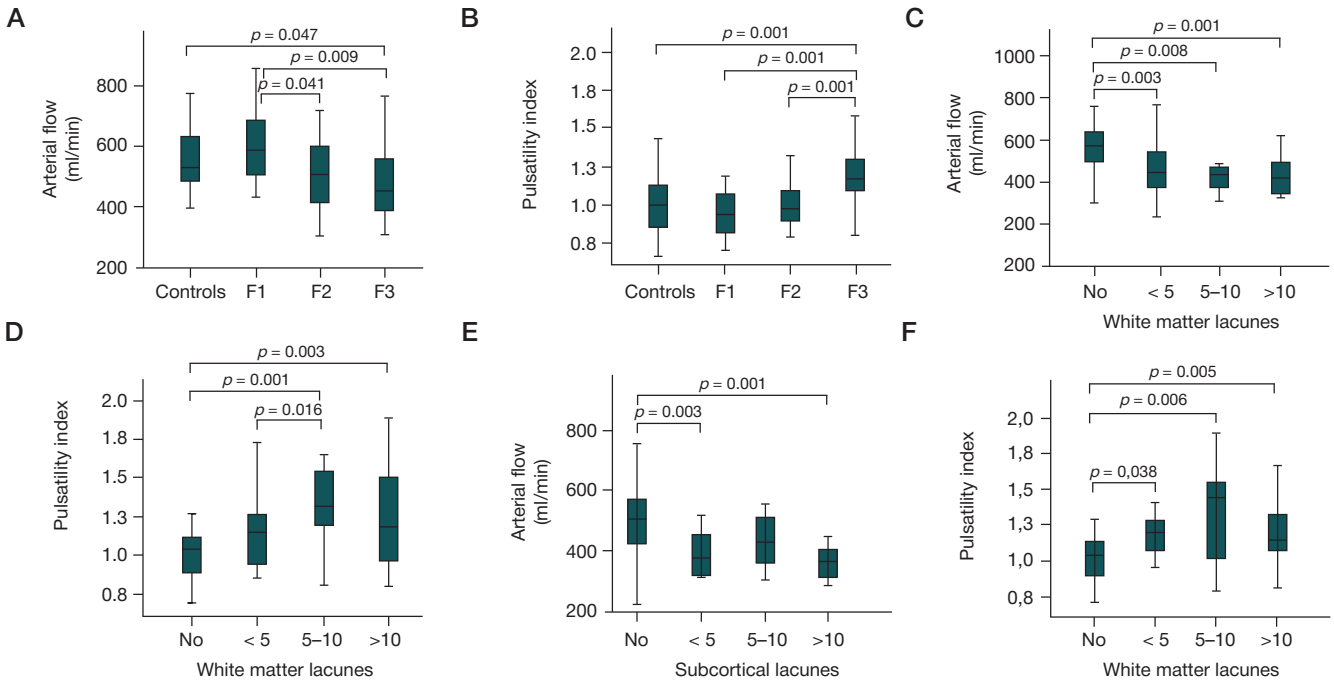

Fig. 3. Comparison of the tABF rate and Pi between the patients with WMH assessed using the Fazekas scale and the controls (**A** and **B**, respectively), between the groups of patients with different number of lacunes and without lacunes in the white matter (**C**, **D**) and subcortical structures (**E**, **F**)

in patients with age-related SVD coupled with the absence of a clear association between the severity of WMH, as well as other MRI findings, and the severity of clinical manifestations of the disease led us to hypothesize that neuroimaging features of SVD could be determined by a combination of abnormalities in the intracranial system homeostasis described by the Monro–Kellie doctrine, with one of such abnormalities prevailing.

Our study discovered that a gradual change in the hemodynamic parameters of arterial, venous and CSF flow was accompanied by WMH exacerbation measured on the Fazekas scale. However, we were able to establish a statistically significant association only between Fazekas 3 (as compared to the control group) and the measured hemodynamic parameters, including low tABF, elevated Pi, low stVBF/sssVBF, increased aqLF, Saq and ICC, and Fazekas 3. The cooccurrence of blood and CSF flow impairments in patients with severe WMH, which is the main MRI feature for SVD, suggests the complexity of mechanisms underlying the disruption of intracranial homeostasis. Our findings are consistent with the results of studies of SVD morphology that reported vascular changes associated with atherosclerosis-induced ischemia and venous collagenosis leading to vascular congestion and cerebral edema in hypertensive patients [15].

It should be noted that reports of arterial flow dynamics in patients with progressing WMH are controversial: some authors reveal a decline in the arterial flow rate [16], whereas others point to the lack of association between leukoaraiosis and impaired cerebral circulation [14]. Research into the association between WMH and cerebral circulation [17] demonstrated that patients with initially more severe WMH developed serious impairments of cerebral blood flow and not the other way around: impaired cerebral circulation did not precede the progression of WMH. It was concluded that a reduction in the brain tissue volume causes a decline in the cerebral blood flow rate. The association between increased arterial flow and Fazekas 1 established by our study and the lack of significant differences in blood flow rates between patients with Fazekas 2 and the controls confirm the role of non-ischemic mechanisms in the development of early WMH and a possible reduction in blood flow in response to brain matter damage in patients with pronounced WMH [3].

Our study demonstrates that a gradual reduction in blood flow leads to an increase in the number of lacunes. These findings are consistent with the results of other studies [18] and confirm that ischemia does play a role in the formation of lacunar cavities. Our study also reveals a correlation between reduced blood flow in the upper sagittal and straight sinuses, as well as increased CSF flow and the elevated intracranial compliance index, and the formation of multiple lacunes, which possibly reflects the severity of brain damage in patients with multiple lacunes [19].

Importantly, we observed an association between the elevated pulsatility index and an increase in the number of lacunar cavities, as well as in WHM severity, which is again consistent with other research works [18]; another association between the increased pulsatility index and the dilation of PVS was not discussed in the literature previously. Elevated Pi is a sign of reduced elasticity of arterial walls associated with their high permeability and swelling that eventually lead to arteriolosclerosis in hypertensive and non-hypertensive patients with SVD [20]. Increased pulsatile pressure cannot be attenuated by the windkessel mechanism; therefore, more pulsation is “absorbed” by veins [21]. This obstructs drainage of the interstitial fluid from PVS and promotes accumulation of toxic waste products, leading to PVS dilation and WMH [22]. The latter has been actively discussed in the literature in the context of a recently described glymphatic system (a waste clearance system of the brain) [23] and could explain the associations between Pi and PVS size; also, it is possibly another contributor to WMH. At present, there is ongoing debate in the literature over the associations between the cerebral venous collagenosis and venous ischemia, increased vascular resistance, disrupted interstitial fluid circulation and damage to BBB accompanied by a vasogenic edema, which, in turn, provides another explanation for WMH [22]. It is still not known whether damage to the venules is caused by a pressure surge or develops independently. Interestingly, WMH (leukoaraiosis) are commonly found in the regions where deep veins perform their drainage function and are less pronounced in the regions

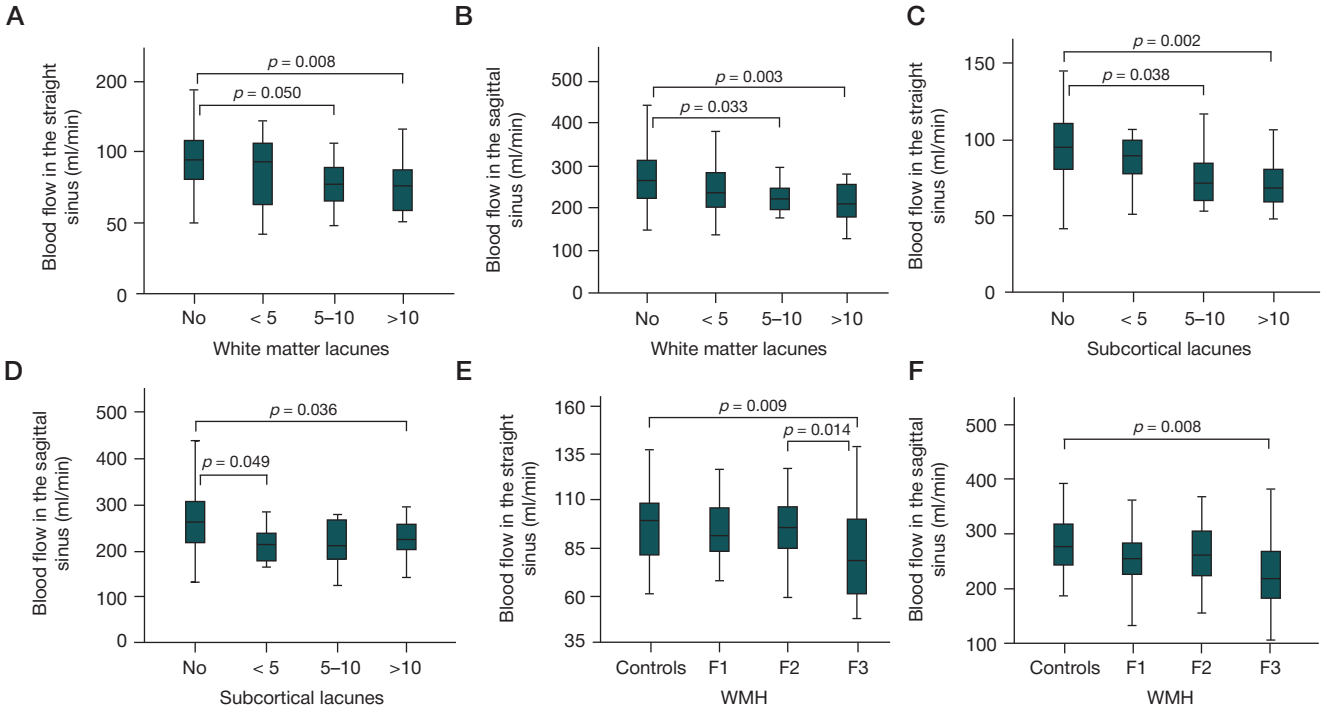

Fig. 4. Comparison of venous blood flow parameters between the controls and the patients with lacunes (**A**–**D**) and WMH assessed using the Fazekas scale (**E**–**F**)

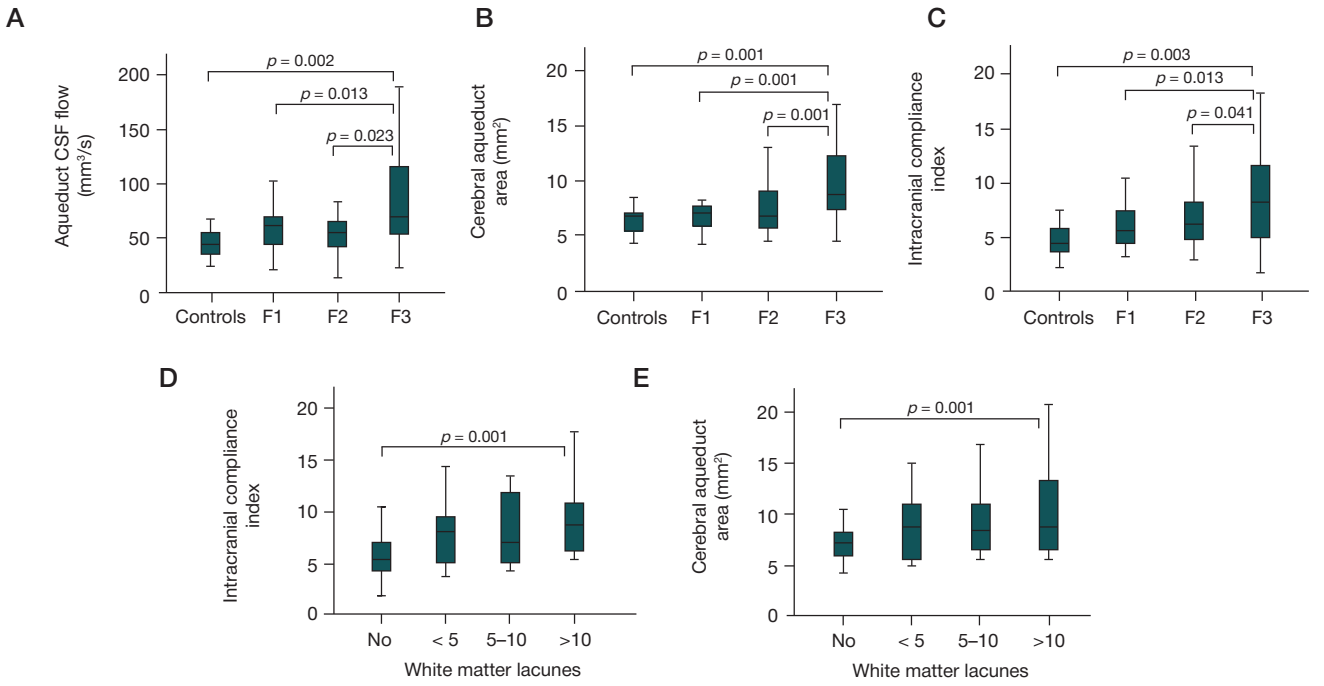

Fig. 5. Comparison of CSF flow parameters and the intracranial compliance index between the controls and the patients with WMH measured on the Fazekas scale (**A**–**C**) and lacunes (**D**–**E**)

of superficial veins. However, we found statistically significant associations between reduced venous flow in the upper and straight sagittal sinuses and early (< 5) microbleeds, which confirms the important role of cortical veins in maintaining intracranial compliance [24] and the link between their damage or rupture and broken autoregulation mechanism.

In our opinion, microbleeds and their association with blood or CSF flow impairments should be discussed at length. Single and multiple MB were observed in more than one-third of patients. The majority of the lesions were localized to either subcortical or juxtacortical structures; both localizations were observed in 56.8% of patients [25]. Some authors point to an association between MB localizations and the nature of the pathology: MB found in the subcortical ganglia are associated with hypertension, whereas those localized to juxtacortical or cortical structures, with cerebral amyloid angiopathy [26]. Because patients from our sample did not have lobar and superficial MB, which signal cerebral amyloid angiopathy (CAA) and are used as a criterion for its diagnosis *in vivo*, we cannot rule out early CAA in some of the participants, given the upper age limit applied in our study. At the same time, MB were the most pronounced in the Fazekas 3 group characterized by multiple lacunes that are not typical of CAA [27]. A recent comparison of data yielded by MRI and Pittsburg compound

PET showed that the presence of MB/hemorrhages in both subcortical and juxtacortical structures were more typical for hypertensive patients with SVD than for those with CAA [28]. Our previous findings showed a correlation between juxtacortical/deep MB and the volume of superficial veins and another correlation between deep/periventricular MB and the volume of deep veins [29], so we drew a conclusion about a possible role of venous congestion in the corresponding regions in the formation of variously localized MB, similarly to how it occurs in cerebral venous sinus thrombosis. The proposed mechanism could explain the cooccurrence of MB in subcortical structures and the subcortical white matter. Prospective observation of these patients will help us to investigate the prognostic value of MB localization and its combination with other MRI features as markers of early SVD. This is particularly important, because the overuse of antiplatelets is one of the leading factors for lobar hemorrhage in elderly patients.

CONCLUSIONS

The established associations between MRI findings and arterial, venous and CSF flow impairments in patients with SVD suggest the important role of mechanisms implicated in the disruption of Monro–Kellie intracranial homeostasis in promoting SVD. Most likely, the initial contribution is done by increased arterial pulsatility, as suggested by the universal association between this parameter and other clinical manifestations (cognitive decline and gait disturbances), as well as diagnostic features of SVD visible on MRI. This determines the clinical relevance of interpreting the acquired MR images using STRIVE advisory standards and analyzing the hemodynamic parameters of blood and CSF flow based on PC-MRI data in patients with SVD in order to assess the efficacy of the applied treatment or prevention measures.

References

1. Dumoulin CL, Yucel EK, Vock P, et al. Two- and three-dimensional phase contrast MR angiography of the abdomen. J Comput Assist Tomogr. 1990; (14): 779–84.
2. Halperin JJ, Kurlan R, Schwalb JM, Cusimano MD, Gronseth G, Gloss D. Practice guideline. Idiopathic normal pressure hydrocephalus: Response to shunting and predictors of response. Report of the Guideline Development, Dissemination, and Implementation Subcommittee of the American Academy of Neurology. Neurology. 2015; (85): 2063–71.
3. Ahmetzyanov BM, Kremneva EI, Morozova SN, Dobrynina LA, Krotenkova MV. Vozmozhnosti magnitno-rezonansnoj tomografii v ocenke likvornoj sistemy v norme i pri razlichnyh zabolevanijah nervnoj sistemy. Russian electronic journal of radiology. 2018; 8 (1): 145–66. Russian.
4. Pantoni L. Cerebral small vessel disease: from pathogenesis and clinical characteristics to therapeutic challenges. Lancet Neurol. 2010; (9): 689–701.
5. Shahparonova NV, Kadykov AS. Hronicheskie sosudistye zabolevanija golovnogo mozga: algoritm diagnostiki i lechenija. Consilium Medicum. 2017; 19 (2): 104–9.
6. Wardlaw JM, Smith C, Dichgans M. Mechanisms of sporadic cerebral small vessel disease: insights from neuroimaging. Lancet Neurol. 2013; (12): 483–97.
7. Rost NS, Rahman RM, Biffi A, et al. White matter hyperintensity volume is increased in small vessel stroke subtypes. Neurology. 2010; (75): 1670–7.
8. Gulevskaya TS. Patologija belogo veshhestva polusharij golovnogo mozga pri arterial'noj gipertonii s narushenijami mozgovogo krovoobrashhenija [dissertacija]. M., 1994.
9. Wardlaw JM, Smith EE, Biessels GJ, et al. Neuroimaging standards for research into small vessel disease and its contribution to ageing and neurodegeneration. Lancet Neurol. 2013; (12): 822–38.
10. Kim KW, MacFall JR, Payne ME. Classification of white matter lesions on magnetic resonance imaging in elderly persons. Biol Psychiatry. 2008; (64): 273–80.
11. Harper L, Barkhof F, Fox NC, Schott JM. Using visual rating to diagnose dementia: a critical evaluation of MRI atrophy scales. J Neurol Neurosurg Psychiatry. 2015; 86 (11): 1225–33. DOI: 10.1136/jnnp-2014-310090.
12. Fazekas F, Chawluk JB, Alavi A, et al. MR signal abnormalities at 1.5 T in Alzheimer's dementia and normal aging. AJR Am J Roentgenol. 1987; 149 (2): 351–6.
13. Pantoni L, Basile AM, Pracucci G, Asplund K, Bogousslavsky J, Chabriat H. et al. Impact of age-related cerebral white matter changes on the transition to disability: the LADIS study: rationale, design and methodology. Neuroepidemiology. 2005; 24: 51–62.
14. Henry-Feugeas MC, Roy C, Baron G, Schouman-Claeys E. Leukoaraiosis and pulse-wave encephalopathy: observations with phase contrast MRI in mild cognitive impairment. J Neuroradiol. 2009; (36): 212–8.
15. Schmidt R, Schmidt H, Haybaeck J, et al. Heterogeneity in age-related white matter changes. Acta Neuropathol. 2011; (122): 171–85.
16. Shi Y, Wardlaw J. Update on cerebral small vessel disease: a dynamic whole-brain disease. Stroke and Vascular Neurology. 2016; (2): 83–92.
17. Van der Veen PH, Muller M, Vincken KL, et al. Longitudinal relationship between cerebral small-vessel disease and cerebral blood flow: the second manifestations of arterial disease-magnetic resonance study. Stroke. 2015; (46): 1233–8.
18. Poels MM, Zaccai K, Verwoert GC, et al Arterial stiffness and cerebral small vessel disease: the Rotterdam Scan Study. Stroke. 2012; (43): 2637–42.
19. Kremneva EI, Akhmetzyanov BM, Gadzhieva ZSh, Sergeeva AN, Zabitova MR, Morozova SN, et al. Assessment of different pathogenetic mechanisms and disease progression in sporadic cerebral small vessel disease patients based on MRI STRIVE criteria. Neuroradiology. 2018; 60 (suppl 2): S430–S430.
20. Shi Y, Thrippleton MJ, Marshall I, Wardlaw JM. Intracranial pulsatility in patients with cerebral small vessel disease: a systematic review. Clinical Science (London). 2018; 32 (1): 157–71.
21. Bateman GA, Levi CR, Schofield P, et al. The venous manifestations of pulse wave encephalopathy: windkessel dysfunction in normal aging and senile dementia. Neuroradiology. 2008; (50): 491–7.
22. Potter GM, Doubal N, Jackson CA, et al. Enlarged perivascular spaces and cerebral small vessel disease. Int J Stroke. 2015; (10): 376–81.
23. Mestre H, Kostrikov S, Mehta RI, Nedergaard M. Perivascular spaces, glymphatic dysfunction, and small vessel disease. Clinical science. 2017; (131): 2257–74.
24. Vignes JR, Dagain A, Guerin J, Liguoro D. A hypothesis of cerebral venous system regulation based on a study of the junction between the cortical bridging veins and the superior sagittal sinus. Laboratory investigation. J Neurosurg. 2007; (107): 1205–10.
25. Zabitova MR, Shabalina AA, Dobrynina LA, Kostyreva MV, Ahmetzyanov BM, Gadzhieva ZSh, i dr. Tkanevoj aktivator plazminogena i MRT-priznaki cerebral'noj mikroangiopatii. Annaly klinicheskoj i jeksperimental'noj nevrologii. 2018; 12 (4): 30–6.
26. Charidimou A, Pantoni L, Love S. The concept of sporadic cerebral small vessel disease: A road map on key definitions and current concepts. Int J Stroke. 2016; 11 (1): 6–18.
27. Greenberg SM, Vernooij MW, Cordonnier C. Cerebral microbleeds: a guide to detection and interpretation. Lancet Neurol. 2009; (8): 165–74.
28. Tsai HH, Pasi M, Tsai LK, et al. Microangiopathy underlying mixed-location intracerebral hemorrhages / microbleeds: A PiB-

PET study. Neurology. 2019; 92 (8): e774–e781. DOI: 10.1212/WNL.0000000000006953.
29. Ahmetzyanov BM. Rol' narushenij krovotoka i likvorotoka v porazhenii golovnogo mozga pri cerebral'noj mikroangiopatii [dissertacija]. M., 2019.

Литература

1. Dumoulin CL, Yucel EK, Vock P, et al. Two- and three-dimensional phase contrast MR angiography of the abdomen. J Comput Assist Tomogr. 1990; (14): 779–84.
2. Halperin JJ, Kurlan R, Schwalb JM, Cusimano MD, Gronseth G, Gloss D. Practice guideline. Idiopathic normal pressure hydrocephalus: Response to shunting and predictors of response. Report of the Guideline Development, Dissemination, and Implementation Subcommittee of the American Academy of Neurology. Neurology. 2015; (85): 2063–71.
3. Ахметзянов Б. М., Кремнева Е. И., Морозова С. Н., Добрынина Л. А., Кротенкова М. В. Возможности магнитно-резонансной томографии в оценке ликворной системы в норме и при различных заболеваниях нервной системы. Russian electronic journal of radiology. 2018; 8 (1): 145–66.
4. Pantoni L. Cerebral small vessel disease: from pathogenesis and clinical characteristics to therapeutic challenges. Lancet Neurol. 2010; (9): 689–701.
5. Шахпаронова Н. В., Кадыков А. С. Хронические сосудистые заболевания головного мозга: алгоритм диагностики и лечения. Consilium Medicum. 2017; 19 (2): 104–9.
6. Wardlaw JM, Smith C, Dichgans M. Mechanisms of sporadic cerebral small vessel disease: insights from neuroimaging. Lancet Neurol. 2013; (12): 483–97.
7. Rost NS, Rahman RM, Biffi A, et al. White matter hyperintensity volume is increased in small vessel stroke subtypes. Neurology. 2010; (75): 1670–7.
8. Гулевская Т. С. Патология белого вещества полушарий головного мозга при артериальной гипертонии с нарушениями мозгового кровообращения [диссертация]. М., 1994.
9. Wardlaw JM, Smith EE, Biessels GJ, et al. Neuroimaging standards for research into small vessel disease and its contribution to ageing and neurodegeneration. Lancet Neurol. 2013; (12): 822–38.
10. Kim KW, MacFall JR, Payne ME. Classification of white matter lesions on magnetic resonance imaging in elderly persons. Biol Psychiatry. 2008; (64): 273–80.
11. Harper L, Barkhof F, Fox NC, Schott JM. Using visual rating to diagnose dementia: a critical evaluation of MRI atrophy scales. J Neurol Neurosurg Psychiatry. 2015; 86 (11): 1225–33. DOI: 10.1136/jnnp-2014-310090.
12. Fazekas F, Chawluk JB, Alavi A, et al. MR signal abnormalities at 1.5 T in Alzheimer's dementia and normal aging. AJR Am J Roentgenol. 1987; 149 (2): 351–6.
13. Pantoni L, Basile AM, Pracucci G, Asplund K, Bogousslavsky J, Chabriat H. et al. Impact of age-related cerebral white matter changes on the transition to disability: the LADIS study: rationale, design and methodology. Neuroepidemiology. 2005; 24: 51–62.
14. Henry-Feugeas MC, Roy C, Baron G, Schouman-Claeys E. Leukoaraiosis and pulse-wave encephalopathy: observations with phase contrast MRI in mild cognitive impairment. J Neuroradiol. 2009; (36): 212–8.
15. Schmidt R, Schmidt H, Haybaeck J, et al. Heterogeneity in age-related white matter changes. Acta Neuropathol. 2011; (122): 171–85.
16. Shi Y, Wardlaw J. Update on cerebral small vessel disease: a dynamic whole-brain disease. Stroke and Vascular Neurology. 2016; (2): 83–92.
17. Van der Veen PH, Muller M, Vincken KL, et al. Longitudinal relationship between cerebral small-vessel disease and cerebral blood flow: the second manifestations of arterial disease-magnetic resonance study. Stroke. 2015; (46): 1233–8.
18. Poels MM, Zaccai K, Verwoert GC, et al Arterial stiffness and cerebral small vessel disease: the Rotterdam Scan Study. Stroke. 2012; (43): 2637–42.
19. Kremneva EI, Akhmetzyanov BM, Gadzhieva ZSh, Sergeeva AN, Zabitova MR, Morozova SN, et al. Assessment of different pathogenetic mechanisms and disease progression in sporadic cerebral small vessel disease patients based on MRI STRIVE criteria. Neuroradiology. 2018; 60 (suppl 2): S430–S430.
20. Shi Y, Thrippleton MJ, Marshall I, Wardlaw JM. Intracranial pulsatility in patients with cerebral small vessel disease: a systematic review. Clinical Science (London). 2018; 32 (1): 157–71.
21. Bateman GA, Levi CR, Schofield P, et al. The venous manifestations of pulse wave encephalopathy: windkessel dysfunction in normal aging and senile dementia. Neuroradiology. 2008; (50): 491–7.
22. Potter GM, Doubal N, Jackson CA, et al. Enlarged perivascular spaces and cerebral small vessel disease. Int J Stroke. 2015; (10): 376–81.
23. Mestre H, Kostrikov S, Mehta RI, Nedergaard M. Perivascular spaces, glymphatic dysfunction, and small vessel disease. Clinical science. 2017; (131): 2257–74.
24. Vignes JR, Dagain A, Guerin J, Liguoro D. A hypothesis of cerebral venous system regulation based on a study of the junction between the cortical bridging veins and the superior sagittal sinus. Laboratory investigation. J Neurosurg. 2007; (107): 1205–10.
25. Забитова М. Р., Шабалина А. А., Добрынина Л. А., Костырева М. В., Ахметзянов Б. М., Гаджиева З. Ш. и др. Тканевой активатор плазминогена и МРТ-признаки церебральной микроангиопатии. Анналы клинической и экспериментальной неврологии. 2018; 12 (4): 30–6.
26. Charidimou A, Pantoni L, Love S. The concept of sporadic cerebral small vessel disease: A road map on key definitions and current concepts. Int J Stroke. 2016; 11 (1): 6–18.
27. Greenberg SM, Vernooij MW, Cordonnier C. Cerebral microbleeds: a guide to detection and interpretation. Lancet Neurol. 2009; (8): 165–74.
28. Tsai HH, Pasi M, Tsai LK, et al. Microangiopathy underlying mixed-location intracerebral hemorrhages / microbleeds: A PiB-PET study. Neurology. 2019; 92 (8): e774–e781. DOI: 10.1212/WNL.0000000000006953.
29. Ахметзянов Б. М. Роль нарушений кровотока и ликворотока в поражении головного мозга при церебральной микроангиопатии [диссертация]. М., 2019.

CONTRAST-ENHANCED ULTRASONOGRAPHY FOR ASSESSING NEOVASCULARIZATION OF CAROTID ATHEROSCLEROTIC PLAQUE

Evdokimenko AN ✉, Chechetkin AO, Druina LD, Tanashyan MM

Research Center of Neurology, Moscow, Russia

Neovascularization of a carotid atherosclerotic plaque (AP) is associated with an increased risk of stroke. Contrast-enhanced ultrasonography (CEUS) is a widely used method for imaging intraplaque neovascularization *in vivo*. Unfortunately, there are no standardized guidelines for CEUS interpretation. The aim of this study was to identify the most reliable method for CEUS-based assessment of AP neovascularization. Seventy-eight AP were removed during carotid endarterectomy in 73 patients, of whom 5 had AP on both sides, and examined morphologically. All patients underwent preoperative duplex scanning and CEUS; Sonovue was used as a contrast agent. AP neovascularization was assessed on a 4-grade visual scale and with 3 different quantitative methods using QLAB software. On the visual scale (method 1), poorly (37%) and moderately (51%) vascularized plaques were the most common. Quantitative analysis (data were presented as Me (Q1; Q3)) revealed that the number of blood vessels per 1 cm^2 of the plaque (method 2) was 16 (10; 26), the ratio of the total vessel area to the plaque area (method 3) was 6% (3; 9), and AP ROI (method 4) was 2.6 dB (1.8; 4.1). Significant correlations were demonstrated between the results produced by method 2 and method 3 ($p < 0.0001$), method 3 and method 2 ($p = 0.0006$), and between pathomorphological findings and the results produced by methods 1–3, especially method 2 ($p < 0.004$). AP ROI brightness did not correlate with other results. The presence of hyperechoic components (calcifications) in AP dramatically reduced the reliability of US-based intraplaque neovascularization assessment. The most accurate CEUS-based quantitative method for assessing intraplaque neovascularization is estimation of blood vessel number per 1 cm^2 of the plaque.

Keywords: atherosclerosis, carotid artery, intraplaque neovascularization, contrast-enhanced ultrasonography, Sonovue, visual scale, quantitative analysis, histopathological examination

Funding: this study was supported by Research Center of Neurology Government funding.

Acknowledgment: the authors thank Skrylev SI, Shchipakin VL and Koshcheev AYu (Vascular and Endovascular Surgery Unit, Research Center of Neurology) for providing biopsy specimens.

Author contribution: Evdokimenko AN — literature analysis, study design, data acquisition and interpretation, manuscript preparation; Chechetkin AO — literature analysis, study design, data acquisition and interpretation, manuscript revision; Druina LD — data acquisition; Tanashyan MM — study design, manuscript revision.

Compliance with ethical standards: the study was approved by the Ethics Committee of the Research Center of Neurology (Protocol № 4/15 dated April 22, 2015). Informed consent was obtained from all study participants.

✉ **Correspondence should be addressed:** Anna N. Evdokimenko
Volokolamskoe shosse 80, Moscow, 125367; evdokimenko@neurology.ru

Received: 15.08.2019 **Accepted:** 30.08.2019 **Published online:** 31.08.2019

DOI: 10.24075/brsmu.2019.057

ОЦЕНКА НЕОВАСКУЛЯРИЗАЦИИ АТЕРОСКЛЕРОТИЧЕСКОЙ БЛЯШКИ КАРОТИДНОГО СИНУСА С ПОМОЩЬЮ КОНТРАСТ-УСИЛЕННОГО УЗИ

А. Н. Евдокименко ✉, А. О. Чечеткин, Л. Д. Друина, М. М. Танашян

Научный центр неврологии, Москва, Россия

Степень неоваскуляризации атеросклеротической бляшки (АСБ) каротидного синуса связывают с повышенным риском развития инсульта. Для выявления новообразованных сосудов в структуре бляшки *in vivo* широко применяют контраст-усиленное ультразвуковое исследование (КУУЗИ), однако до настоящего времени отсутствует единый подход к интерпретации результатов. Целью работы было установить наиболее надежный метод оценки неоваскуляризации АСБ каротидного синуса по данным КУУЗИ. У 73 пациентов удалено при каротидной эндартерэктомии, проанализировано, и морфологически исследовано 78 АСБ. Всем пациентам проводили стандартное дуплексное сканирование сонных артерий и КУУЗИ с введением эхоконтрастного препарата «Соновью». Неоваскуляризацию АСБ оценивали с использованием 4-балльной визуальной шкалы и трех методов количественной оценки в программе QLAB. По данным визуальной шкалы (метод 1), преобладали слабо и умеренно васкуляризированные бляшки (37% и 51% соответственно). Результаты количественной оценки (Me (Q1; Q3)): количество сосудов на 1 $см^2$ бляшки (метод 2) составило 16 (10; 26); соотношение площадей сосудов и бляшки (метод 3) — 6% (3; 9); значение ROI АСБ (метод 4) — 2,6 дБ (1,8; 4,1). Значимая корреляция отмечена: между результатами оценки по методам 2 и 3 ($p < 0,0001$); по методам 3 и 1 ($p = 0,0006$); морфологическими данными и результатами оценки по методам 1–3, особенно по методу 2 ($p < 0,004$). Значение ROI АСБ с данными других методов не коррелировало. Продемонстрировано резкое снижение надежности УЗ-оценки неоваскуляризации с увеличением объема гиперэхогенного компонента (кальцификатов) в АСБ. Наиболее точным способом количественной оценки неоваскуляризации АСБ при КУУЗИ является подсчет количества сосудов на 1 $см^2$ бляшки.

Ключевые слова: атеросклероз, сонная артерия, неоваскуляризация атеросклеротической бляшки, контраст-усиленное ультразвуковое исследование, препарат «Соновью», визуальная шкала, количественный анализ, морфологическое исследование

Финансирование: работа выполнена в рамках государственного задания ФГБНУ НЦН.

Благодарности: сотрудникам группы сосудистой и эндоваскулярной хирургии Научного центра неврологии С. И. Скрылеву, В. Л. Щипакину и А. Ю. Кощееву за предоставленный биопсийный материал.

Информация о вкладе авторов: А. Н. Евдокименко — анализ литературы, разработка дизайна исследования, сбор, анализ и интерпретация данных, написание рукописи; А. О. Чечеткин — анализ литературы, разработка дизайна исследования, сбор и интерпретация данных, редактирование рукописи; Л. Д. Друина — сбор данных; М. М. Танашян — разработка дизайна исследования, редактирование рукописи.

Соблюдение этических стандартов: исследование одобрено этическим комитетом Научного центра неврологии (протокол № 4/15 от 22 апреля 2015 г.); все пациенты подписали добровольное информированное согласие на его проведение.

✉ **Для корреспонденции:** Анна Николаевна Евдокименко
Волоколамское шоссе, д. 80, г. Москва, 125367; evdokimenko@neurology.ru

Статья получена: 15.08.2019 **Статья принята к печати:** 30.08.2019 **Опубликована онлайн:** 31.08.2019

DOI: 10.24075/vrgmu.2019.057

Carotid sinus (CS) atherosclerosis accounts for up to one-third of all ischemic strokes. The most common causes of stroke in these cases are atherothrombosis, thromboembolism or atheroembolism of cerebral arteries, associated with unstable atherosclerotic plaque (AP) [1, 2]. Pathologic studies have demonstrated that unstable AP are usually characterized by a large atheromatous core, thin or ulcerated fibrous cap, hemorrhage and pronounced inflammation [2, 3]. Recently, neovascularization has been increasingly recognized as the key factor in promoting AP instability and atherosclerosis progression [1, 3–6].

Contrast-enhanced ultrasonography (CEUS) is one of the most widely used techniques for assessing the degree of neovascularization *in vivo*. Since CEUS was first applied to visualize carotid plaque neovascularization in 2003 [7], its accuracy and reliability have been confirmed by multiple animal and human studies that demonstrated a high correlation between ultrasonography findings and histopathologic data [8–9].

Although CEUS has been exploited as an AP neovascularization imaging technique for over 15 years, there is still no consensus as to what approaches should be used to interpret the acquired data. The majority of CEUS-based studies employ qualitative or semi-quantitative scoring systems; however, there is broad agreement that such scoring approach is somewhat biased and unsuitable for the dynamic assessment of atherosclerosis progression. This indicates the need for a uniform, precise and validated scoring system [6, 10]. Methods used for quantitative assessment of CEUS findings are still a matter of ongoing debate [9–11]. Besides, studies comparing CEUS findings and histopathologic data are rare and their results often require further validation.

There is a pressing need for a uniform, accurate and reliable approach to the assessment of CEUS findings in light of emerging ultrasound contrast agents for *in vivo* molecular imaging of vascular phenotypes and targeted drug delivery that are currently in preclinical trials [12, 13]. Novel ultrasound contrast agents and drug delivery systems open new horizons for effective personalized strategies of prevention, diagnosis and treatment of carotid artery disease. Their adoption into clinical practice may be complicated by the absence of a uniform approach to CEUS data analysis.

This study aimed to identify a reliable, informative and clinically friendly method for CEUS-based assessment of carotid AP neovascularization.

METHODS

Studied population

The study was conducted at the Research Center of Neurology in 2015–2018. Eligible patients had atherosclerotic lesions of the carotid sinus and indications for carotid endarterectomy described in the Russian National guidelines for the management of patients with brachiocephalic artery disease [14]. The following exclusion criterion was applied: heavily calcified plaques detected on ultrasonography (> 50% of the total plaque area) casting an acoustic shadow that prevented accurate estimates of AP neovascularization. The study recruited a total of 73 patients (50 men and 23 women aged 40 to 79 years; the mean age was 63 ± 8 years) with ≥ 50% atherosclerotic carotid stenosis (50–90%, the mean value was 70 ± 16%) according to NASCET criteria [15]. All patients underwent carotid endarterectomy at the Research Center of Neurology between January 1, 2015 and December 31, 2017; the intervention was bilateral in 5 patients. The removed plaques were examined histopathologically. A total of 78 plaques were analyzed. Stenosis was symptomatic in 25 (32%) and asymptomatic in 53 (68%) patients.

Conventional and contracts-enhanced ultrasonography examinations

Preoperatively, the patients underwent duplex ultrasound scanning of the carotid arteries and CEUS of the identified carotid atherosclerotic plaques in the longitudinal projection. Examinations were performed using an iU22 scanner (Philips Healthcare NV; Netherlands) equipped with an L9-3 linear array probe.

Duplex ultrasound scanning was performed in order to determine plaque echogenicity, the degree of carotid stenosis and the best visible plaque aspect for the subsequent CEUS examination. Plaques were stratified into 4 groups based on their echogenicity as proposed by A. Gray-Weale [16]: group 1, uniformly hypoechoic; group 2, heterogeneous, predominantly hypoechoic; group 3, heterogeneous, predominantly hyperechoic, and group 4, uniformly hyperechoic.

For CEUS, 2.4 ml of SonoVue contrast agent (Bracco; Italy) dissolved in 5 ml of 0.9% normal saline were administered into a patient's peripheral vein via a bolus injection; 5 ml of normal saline were subsequently injected intravenously through the same catheter. The scan was performed in the Contrast General mode, at a low mechanic index (0.06) and 85% signal enhancement. The probe was held in a fixed position until the arterial lumen was well contrasted; then the angle of the probe was slowly changed to facilitate visualization of the entire plaque. Video clips were recorded for 2 minutes from the moment the patient received the SonoVue injection.

The clips were analyzed off-line using QLAB software (Philips Healthcare NV; Netherlands). Plaque neovascularization was inferred from time-variant dynamic signal enhancement (dynamic hyperechoic signals, DHS) in the plaque caused by nonlinear responses from the microbubbles; hyperechoic signals that did not change over time were interpreted as calcifications. The degree of plaque neovascularization was assessed in QLAB using the following methods.

1. Method 1: semiquantitative assessment on the 4-grade scale: 0 — no DHS; 1 — single DHS; 2 — a moderate number of DHS; 3 — a substantial number of DHS.

2. Three quantitative methods (see the Figure): a still frame showing the maximal number of blood vessels was selected from the CEUS cine loop. The frame was analyzed as described below.

a) method 2: the number of DHS per 1 cm^2 of the plaque was counted. The contours of the plaque were delineated manually and DHS were counted within the circled area. The obtained number was divided by the automatically computed area of the plaque;

b) method 3: the ratio of the total DHS area to the plaque area was calculated and expressed as %. The contours of the plaque and all DHS were manually delineated on the selected still frame. The total DHS area was divided by the plaque area and multiplied by 100%;

c) method 4: plaque ROI (signal intensity) was determined. The area of interest, i.e. the entire plaque, was circled manually on the selected still frame; hyperechoic signals that did not change over time (calcifications) were excluded where possible, and the software automatically computed ROI brightness expressed in dB units.

Histopathological examination

A total of 13 atherosclerotic plaques fragmented during surgery were excluded from the histopathological analysis. The

rest 65 removed plaques were fixed in 10% neutral buffered formalin (pH 7.4), cut into 4 to 9 (depending on the plaque size) transverse 0.3 cm-thick blocks and embedded in paraffin. Five-µm sections of each block were stained with hematoxylin-eosin and van Gieson's stain and then scanned using Aperio AT2 (Leica Biosystems; Germany) at ×400 magnification.

Plaque neovascularization was analyzed in Aperio ImageScope ver. 11.2.0.780 (Leica Biosystems; Germany). Blood vessels were defined as structures that had an endothelial lining and a lumen. To calculate the total vessel density per 1 cm^2 of the plaque, we divided the total number of blood vessels contained in all studied slides by the total area of those slides. Additionally blood vessel density was analyzed for the vessels of certain diameter (< 20, ≥ 20, ≥ 30, ≥ 40, ≥ 50 µm) due to the limitations of CEUS spatial resolution. In noncircular sections, the diameter of the blood vessel was inferred from its transverse size at its widest site.

Statistical analysis

Statistical analysis was done in Statistica 10.0 (StatSoft; USA). Statistical differences and correlations were calculated using nonparametric Mann–Whitney U test and Spearman's correlation coefficient. Differences were considered significant at $p = 0.05$. In this work the data are presented as a median (Me) (quartile Q1; quartile Q3).

RESULTS

On the duplex ultrasound scans, the majority of plaques were heterogenous (81%) and predominantly hypoechoic (51%) (Table 1). Small or medium-sized calcifications were observed in 67% of the plaques. Blood vessels were detected in all studied plaques; none of the applied methods revealed any significant differences between different groups of AP (classification by Gray-Weale [16]) in terms of plaque neovascularization (see Table 1).

Semiquantitative analysis (method 1) demonstrated that the general group of plaques was dominated by AP with a moderate or low DHS number (2 points and 1 point on the visual scale, respectively) that amounted to 51% and 37% of all studied AP, respectively. Plaques with a substantial number of DHS (3 points on the applied scale) were seen > 3 times as rare, making 12% of all AP. When comparing ultrasonography findings and morphological data, we noticed that the more points the plaque scored on the applied scale, the more blood vessels it contained per 1 cm^2 of its area. However, the difference in the degree of AP neovascularization was significant only for the plaques characterized by a low number of hyperechoic signals (Table 2).

All of the applied quantitative methods revealed considerable variability in the degree of AP vascularization: the number of DHS per 1 cm^2 of the plaque (method 2) was 16 signals/cm^2 (10; 26); the ratio of the total DHS area to the plaque area (method 3) was 6% (3; 9); AP ROI (method 4) was 2.6 dB (1.8; 4.1). A direct correlation was established between the results produced by methods 2 and 3 ($R = 0.45$; $p = 0.000034$), and between the results of methods 3 and 1 ($R = 0.38$; $p = 0.0006$). ROI values were not correlated with the results produced by other assessment methods.

We have discovered a significant correlation between the histopathologic data and the results of CEUS-based AP neovascularization assessment aided by the applied methods 1, 2 and 3; the correlation was especially high for method 2 (DHS number per 1 cm^2 of the plaque) (Table 3). Method 2 allowed us to directly compare ultrasonography and histopathologic findings and determine the mean diameter of blood vessels that were visible on CEUS — 30 µm (22; 37).

In order to assess the impact of hyperechoic AP components on CEUS results, we attempted to correlate CEUS and histopathologic data in 3 groups of plaques with different echogenicity (Table 4). We found that the greater was the degree of the hyperechoic component, the weaker was

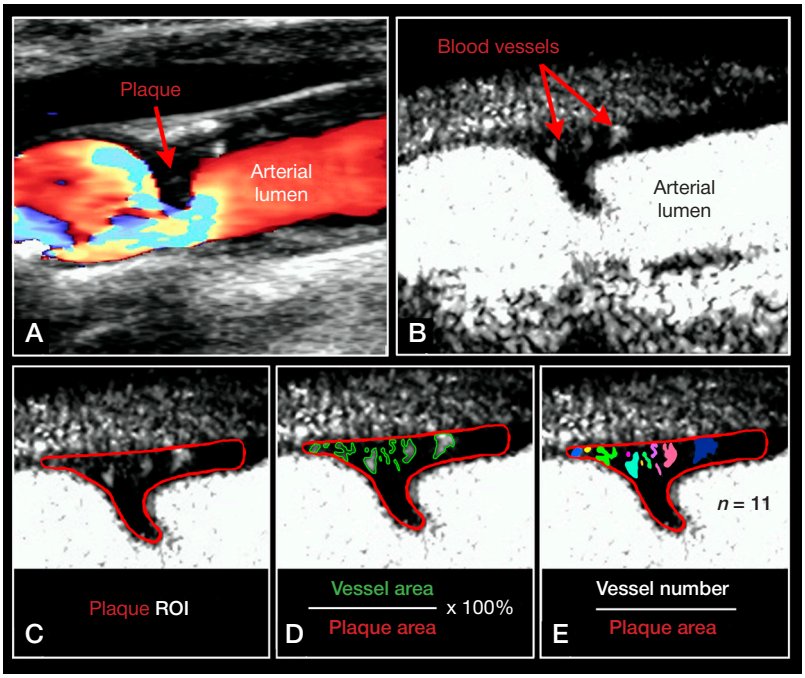

Fig. Quantitative methods for the assessment of carotid atherosclerotic plaque neovascularization from contrast-enhanced ultrasonography data. **A**. A heterogeneous, predominantly hypoechoic atherosclerotic plaque on a conventional Color Doppler Image. **B**. Contrast-enhanced ultrasonography: a predominantly hypoechoic atherosclerotic plaque with single hyperechoic echogenic components (blood vessels, shown by arrows), hyperechoic arterial lumen and surrounding tissue. **C**–**E**. Quantitative analysis of intraplaque neovascularization on a still frame showing the max number of blood vessels (the contour of the plaque is shown in red): ultrasound signal intensity (ROI) (**C**); the ratio of the total vessel area to the plaque area (blood vessels are shown in green) (**D**); blood vessel number per 1 cm^2 of the plaque (blood vessels are shown in different colors) (**E**)

the correlation between CEUS findings and vessel density (histopathologic examination) and the lower was the reliability of US-based assessment of AP neovascularization. For example, the DHS number per 1 cm^2 of the plaque (CEUS, method 2) that had the highest correlation with the results of the histopathologic examination in the general group of plaques demonstrated an even higher correlation in the group of predominantly hypoechoic plaques, whereas for other plaque groups the correlation analysis produced dubious results (see Table 4). The ratio of the total DHS area to the plaque area (method 3) was correlated with the histopathologic findings only for predominantly hypoechoic plaques (Table 4). The correlation analysis between semiquantative scores and histopathologic data in different groups of plaques produced controversial results (Table 4).

DISCUSSION

Visual scales for CEUS data interpretation have received a lot of attention in the literature because they are simple, time-saving, do not require any software for quantitative analysis, and, therefore, can be used in the clinical setting. So far, over 10 different approaches to semiquantitative assessment of AP neovascularization have been described based on visual 2- to 5-grade scales. The majority of such scales take into account both the number and location of dynamic hyperechoic signals [8, 17–22]; scales that rely solely on the number of DHS are rare [17, 23, 24]. The problem with type 1 scales is that an increase in the number of DHS is expected to be directly dependent on signal propagation from the adventitial side of the plaque to its surface. This complicated the choice of an adequate scale for our study, because the identified patterns of AP neovascularization did not fit into any of the considered scales. Therefore, we decided to use a simple one-parameter 4-grade scale for DHS count that was similar to the one described in the literature [24]. Its author proposed that plaques with large artery-like vessels should be classified as having pronounced vascularization (grade 3) with no elaboration on the acoustic characteristics of those artery-like vessels. In our study, the results produced by CEUS and histopathologic examinations revealed the presence of poorly vascularized AP with large artery-like vessels and abundantly vascularized AP that did not contain large artery-like vessels; therefore, we decided to ignore blood vessel size when conducting semiquantitative assessment.

Vessel density in AP was measured during the histopathologic examination and then compared between 3 groups of plaques with different degree of neovascularization assessed on a 4-grade visual scale. The difference was significant only between the group of poorly vascularized plaques with single DHS and the groups of plaques with a moderate or high number of DHS. At the same time, CEUS data assessed on the applied 4-grade visual scale were correlated significantly with histopathologic data, as was the case with other visual scales described in the literature [8, 20, 23, 24]. However, the correlation analysis of plaque groups characterized by different echogenicity produced controversial results, which rendered the applied method of semiquantitative assessment unreliable. This could be explained by a small sample size, a subjective approach to establishing the degree of neovascularization in the absence of clear grading criteria, or frequently occurring calcifications in AP leading to under- or overestimation of the neovascularization degree [25]. Duplex scanning detected the presence of small and medium-sized calcifications in 67% of AP that may have been mistaken for blood vessels on CEUS. The difficulty in discriminating between blood vessels and small calcifications was associated with similarity between their visualization patterns first discovered in this study. The majority

Table 1. Neovascularization of carotid plaques of different types (classification by Gray-Weale)

	Plaque structure			
	Group 1	**Group 2**	**Group 3**	**Group 4**
Number of plaques	3	40	23	12
Of them, morphologically studied	2	33	20	10
Neovascularization, Me (Q1; Q3)				
Contrast-enhanced ultrasonography				
Method 1 (scored points)	1	1 (1; 2)	1 (1; 2)	2 (1; 2)
Method 2 (signal/cm^2)	9 (5; 13)	13 (10.5; 25)	20 (11; 29)	20.5 (9.5; 33.5)
Method 3 (%)	3 (0.4; 5)	6 (3; 7)	7 (3; 11)	8.5 (5; 15)
Method 4 (dB)	2.8 (2.2; 3.1)	2.7 (1.6; 4.2)	2.4 (1.9; 5.5)	2.7 (2.1; 3.4)
Histopathological examination, number of vessels per 1 cm^2 of the plaque	62. 111	161 (96; 253)	90 (61; 305)	230 (125; 300)

Table 2. Results of the semiquantitative analysis of contrast-enhanced ultrasonography data compared to the vessel density determined during the histopathologic examination (* — $p \leq 0.03$)

	AP neovascularization score on the semiquantitative scale (contrast-enhanced ultrasonography)		
Number of blood vessels of a specific diameter per 1 cm^2 of the plaque, Me (Q1; Q3)	1 point	2 points	3 points
	(n = 40)	(n = 29)	(n = 9)
All blood vessels	**108.6 (55.3; 182.4)***	168.6 (125; 356.8)	370 (229; 485)
Blood vessels < 20 μm in diameter	**66.5 (40.8; 111.4)***	117.4 (70.8; 216.8)	277.3 (174.5; 332)
Blood vessels ≥ 20 μm in diameter	**30.5 (9.6; 54.7)***	55.8 (38; 90.2)	90.2 (38.4; 131.8)
Blood vessels ≥ 30 μm in diameter	**13.2 (2.4; 26.1)***	25.5 (12.8; 46.7)	41.4 (13.4; 50.3)
Blood vessels ≥ 40 μm in diameter	**5.5 (1.2; 13.9)***	11.9 (6.2; 23.1)	17.5 (5.8; 25.4)
Blood vessels ≥ 50 μm in diameter	**2.2 (0; 7.6)***	5.9 (3.4; 12.6)	8.8 (2.9; 15.2)

of small and medium-sized calcifications became visible on CEUS only when the contrast agent reached the plaque vasculature, which might be associated with a change in tissue reflectance in those areas [26]. Besides, our histopathologic examination revealed that blood vessels were often located in close proximity to calcifications, which also complicated their identification on CEUS due to a limited resolution capacity of the scanner.

The literature describes 3 principally different approaches to quantitative analysis of CEUS data, all of which were applied in this study. The most common approach relies on the assessment of signal intensity in the region of interest (a contrasted plaque); other include the ratio of the total DHS area to the plaque area and DHS number per 1 cm^2 of the plaque. We did not find any correlation between plaque ROI brightness and vessel density. ROI was not correlated with the results of other CEUS-based neovascularization assessment methods. Some authors have reported a correlation between ROI-based plaque neovascularization assessment and vessel density verified by a histopathologic examination [20, 27, 28]. However, those studies had limitations, such as a small sample size, or employed a less accurate semiquantitative approach to the assessment of plaque neovascularization during a histopathologic examination. Other researchers have established a correlation between the intensity of the signal during CEUS and the results of a histopathologic examination for stable plaques only [8]. The intensity of the US signal is affected by a variety of factors, including tissue reflectance, the degree of plaque calcification (specifically, the presence of small or powdery calcifications that cannot be excluded from the analyzed site), predominant location of the plaque on the anterior or posterior artery wall; brightness and contrast properties of the image that cannot be standardized, etc. [2, 25, 26]. All those factors may have contributed to the outcome we got. Besides, the authors of all articles cited above used a corrected (but not absolute) value of US signal intensity: the ratio of plaque ROI to the arterial lumen [8, 17] or to the intact adjacent vascular wall [27]; the difference between plaque ROI values before and after the injection of a contrast agent [18, 20]; complex algorithms that took into account a number of factors

Table 3. The correlation analysis of data on plaque neovascularization obtained from contrast-enhanced ultrasonography and the histopathologic examination (n = 65)

Histopathologic examination — density of blood vessels of a specified diameter	Contrast-enhanced ultrasonography — the degree of AP neovascularization assessed with different methods							
	Method 1		Method 2		Method 3		Method 4	
	R	*p*	*R*	*p*	*R*	*p*	*R*	*p*
All blood vessels	**0.45**	**0.00019**	**0.41**	**0.00069**	0.23	0.06545	–0.04	0.75
< 20 μm	**0.43**	**0.00033**	**0.36**	**0.0034**	0.18	0.15532	–0.07	0.6
≥ 20 μm	**0.45**	**0.00017**	**0.52**	**0.00001**	**0.37**	**0.00257**	0	0.99
≥ 30 μm	**0.41**	**0.00068**	**0.57**	**0**	**0.36**	**0.00338**	0.03	0.82
≥ 40 μm	**0.41**	**0.00074**	**0.6**	**0**	**0.35**	**0.00438**	0.02	0.89
≥ 50 μm	**0.4**	**0.00102**	**0.6**	**0**	**0.32**	**0.01103**	0.03	0.81

Table 4. The correlation analysis of data on neovascularization in different types of plaques obtained from contrast-enhanced ultrasonography and the histopathologic examination (classification by Gray-Weale)

Histopathological examination — density of blood vessels of a specified diameter	Contrast-enhanced ultrasonography — the degree of AP neovascularization assessed with different methods					
	Method 1		Method 2		Method 3	
	R	*p*	*R*	*p*	*R*	*p*
Heterogeneous, predominantly hypoechoic plaques, group 2 (n = 33)						
All blood vessels	0.34	0.05493	**0.43**	**0.01164**	0.06	0.73935
< 20 μm	0.3	0.08642	**0.35**	**0.04485**	-0.01	0.96716
≥ 20 μm	**0.41**	**0.01825**	**0.67**	**0.00002**	0.33	0.06705
≥ 30 μm	0.34	0.05633	**0.72**	**0**	0.3	0.0897
≥ 40 μm	**0.4**	**0.02162**	**0.74**	**0**	**0.43**	**0.01507**
≥ 50 μm	**0.45**	**0.00857**	**0.79**	**0**	**0.47**	**0.00718**
Heterogeneous, predominantly hyperechoic plaques, group 3 (n = 20)						
All blood vessels	**0.5**	**0.02512**	0.41	0.07403	0.14	0.5446
< 20 μm	**0.47**	**0.03701**	**0.45**	**0.04716**	0.21	0.38029
≥ 20 μm	**0.52**	**0.01815**	0.41	0.07345	0.22	0.35255
≥ 30 μm	**0.51**	**0.02294**	0.43	0.06146	0.15	0.52769
≥ 40 μm	0.38	0.10226	0.41	0.07068	0.12	0.60956
≥ 50 μm	0.34	0.1424	0.4	0.0782	0.15	0.51773
Uniformly hyperechoic plaques, group 4 (n = 10)						
All blood vessels	0.62	0.05444	0.21	0.5667	0.41	0.23349
< 20 μm	**0.71**	**0.02047**	0.06	0.86751	0.27	0.44295
≥ 20 μm	0.43	0.21702	0.36	0.3088	0.43	0.21862
≥ 30 μm	0.13	0.7209	0.46	0.17886	0.3	0.4017
≥ 40 μm	0.25	0.49232	**0.67**	**0.03451**	0.21	0.55384
≥ 50 μm	0.22	0.53903	0.61	0.06125	0.18	0.61791

[12, 22], etc. [28]. We intentionally used the absolute ROI value that can be determined during scanning without additional calculations because it was deemed comparable to the visual scale in terms of time and convenience and at the same time allowed performing dynamic assessment of atherosclerosis progression. However, the obtained results suggest that in order to use ROI as a quantitative method for assessing AP neovascularization, one need to take into account a variety of factors and apply correction coefficients.

The ratio of the total DHS area to the plaque area (method 3) did not provide information on the total vessel density in the plaque or the density of small 20 μm vessels that amounted to 96% of all intraplaque vessels [29]. However, CEUS data were correlated with the density of larger vessels (≥ 20 μm and ≥ 40 μm, respectively) determined during the histopathologic analysis in the general group of plaques and the subgroup of predominantly hypoechoic plaques. The analysis of plaques characterized by different echogenicity demonstrated that this assessment method should not be recommended for hyperechoic plaques because there was no correlation between CEUS and histopathologic data for groups 3 and 4 (classification by Gray-Weale). This can be explained by over- or underestimation of neovascularization degree from CEUS data in the plaques that contained calcifications, as described above. The authors of the method reported a high correlation of CEUS data with the total plaque vessel density assessed during a morphological examination [10]. We did not observe such correlation in our study, which is probably because we used a commercial QLAB package and delineated the area of DHS manually whereas A. Hoogi et al. used a specially developed automated algorithm based on Matlab software (Mathworks). Besides, the accuracy of manual DHS delineation can decrease significantly as the signal area (the vessel size) becomes lower. However, considering the reports of a high correlation been the density of AP blood vessels of different diameters [29] and our data supporting the possibility of reliable CEUS-based identification of vessels over 30 μm in diameter, the applied method can be used for quantitative assessment of AP neovascularization in the absence of a pronounced hyperechoic component. We recommend using an automated algorithm in order to improve the accuracy of measurements.

DHS number per 1 cm^2 of the plaque was well correlated with histopathologic findings both in the general group of plaques and the subgroup with predominantly hypoechoic component. Similar to other quantitative approaches, the results of this method for the group of hyperechoic plaques were not convincing, suggesting a need for developing a complex automated algorithm for accurate assessment of neovascularization in type 3 and type 4 plaques. There are no reports on the comparison of histopathologic data and CEUS findings assessed using this approach. A similar method was used to assess neovascularization from CEUS data [12], but the authors of that work did not verify CEUS results by histology and used an automated MevisLab-based algorithm. They compared the results of semiquantitative and quantitative analyses of plaque neovascularization based on ROI, the area and number of DHS in the plaque and showed a correlation between the ratio of total DHS area to plaque area, DHS number per 1 cm^2 of the plaque and the results of visual assessment; the correlation turned out to be even higher when hyperechoic AP were excluded from the analysis.

CONCLUSIONS

CEUS is an effective, rapid and reliable technique for assessing the degree of neovascularization of carotid AP that do not contain hyperechoic components. The analysis can be performed in standard QLAB software. The most reliable and convenient method for quantitative assessment of AP neovascularization is DHS number per 1 cm^2 of the plaque on a still frame that contains the maximal number of visible signals. Its results were well correlated with the histopathologic findings. The ratio of the total DHS area to the plaque area can also be an option, but this method is more time-consuming and less reliable. We do not recommend using absolute ROI brightness of the plaque for assessing intraplaque neovascularization. Semiquantitative assessment on a 2–3 grade visual scale should be used as a qualitative express method for detecting the presence of blood vessels in the plaque. Hyperechoic AP components have a significant impact on CEUS results. This indicates a need for an algorithm that can automatically detect and exclude from the analysis not only large but also small and medium-sized calcifications.

References

1. Dunmore BJ, McCarthy MJ, Naylor AR, Brindle NPJ. Carotid plaque instability and ischemic symptoms are linked to immaturity of microvessels within plaques. J Vasc Surg. 2007; 45 (1): 155–9. DOI:10.1016/j.jvs.2006.08.072.
2. Filis K, Toufektzian L, Galyfos G, et al. Assessment of the vulnerable carotid atherosclerotic plaque using contrast-enhanced ultrasonography. Vascular. 2017; 25 (3): 316–25. DOI:10.1177/1708538116665734.
3. Gulevskaya TS, Morgunov VA, Anufriev PL. Struktura aterosklerоticheskih blyashek karotidnogo sinusa i narusheniya mozgovogo krovoobrashcheniya. Annals of Clinical and Experimental Neurology. 2010; 4 (1): 13–9. Russian.
4. Tuhbatullin MG, Bayazova NI, Zakirzhanov NR, i dr. Primenenie kontrastnogo usileniya pri ul'trazvukovom issledovanii aterosklerоticheskoj blyashki v sonnyh arteriyah u pacientov s narusheniem mozgovogo krovoobrashcheniya. Prakticheskaya medicina. 2017; 103 (2): 124–9. Russian.
5. Jeziorska M, Woolley DE. Local neovascularization and cellular composition within vulnerable regions of atherosclerotic plaques of human carotid arteries. J Pathol. 1999; 188 (2): 189–96.
6. Saha SA, Gourineni V, Feinstein SB. The Use of Contrast-enhanced Ultrasonography for Imaging of Carotid Atherosclerotic Plaques: Current Evidence, Future Directions. Neuroimaging Clin N Am. 2016; 26 (1): 81–96. DOI:10.1016/j.nic.2015.09.007.
7. Feinstein SB. The powerful microbubble: from bench to bedside, from intravascular indicator to therapeutic delivery system, and beyond. Am J Physiol Circ Physiol. 2004; 287 (2): H450–7. DOI:10.1152/ajpheart.00134.2004.
8. Coli S, Magnoni M, Sangiorgi G, et al. Contrast-enhanced ultrasound imaging of intraplaque neovascularization in carotid arteries: correlation with histology and plaque echogenicity. J Am Coll Cardiol. 2008; 52 (3): 223–30. DOI:10.1016/j.jacc.2008.02.082.
9. Hoogi A, Adam D, Hoffman A, Kerner H, Reisner S, Gaitini D. Carotid plaque vulnerability: quantification of neovascularization on contrast-enhanced ultrasound with histopathologic correlation. AJR Am J Roentgenol. 2011; 196 (2): 431–6. DOI:10.2214/AJR.10.4522.
10. Varetto G, Gibello L, Castagno C, et al. Use of Contrast-Enhanced Ultrasound in Carotid Atherosclerotic Disease: Limits and Perspectives. Biomed Res Int [Internet]. 2015; 2015 (Article ID 293163): [about 7 p.]. Available from: https://DOI.

org/10.1155/2015/293163.
11. van den Oord S, Akkus Z, Bosch J, et al. Quantitative Contrast-Enhanced Ultrasound of Intraplaque Neovascularization in Patients with Carotid Atherosclerosis. Ultraschall der Medizin — Eur J Ultrasound. 2014; 36 (02): 154–61. DOI:10.1055/s-0034-1366410.
12. Feinstein SB. The Evolution of Contrast Ultrasound: From Diagnosis to Therapy. J Am Coll Cardiol. 2016; 67 (21): 2516–8. DOI:10.1016/j.jacc.2016.04.004.
13. Moccetti F, Weinkauf CC, Davidson BP, et al. Ultrasound Molecular Imaging of Atherosclerosis Using Small-Peptide Targeting Ligands Against Endothelial Markers of Inflammation and Oxidative Stress. Ultrasound Med Biol. 2018; 44 (6): 1155–63. DOI:10.1016/j.ultrasmedbio.2018.01.001.
14. Nacionalnye rekomendacii po vedeniyu pacientov s zabolevaniyami brahiocefal'nyh arterij. Angiology and vascular surgery. 2013; 19 (2) (suppl.): 1–72. Russian.
15. von Reutern G-M, Goertler M-W, Bornstein NM, et al. Grading Carotid Stenosis Using Ultrasonic Methods. Stroke. 2012; 43 (3): 916–21. DOI:10.1161/STROKEAHA.111.636084.
16. Gray-Weale AC, Graham JC, Burnett JR, Byrne K, Lusby RJ. Carotid artery atheroma: comparison of preoperative B-mode ultrasound appearance with carotid endarterectomy specimen pathology. J Cardiovasc Surg (Torino). 1988; 29 (6): 676–81.
17. Cattaneo M, Staub D, Porretta AP, et al. Contrast-enhanced ultrasound imaging of intraplaque neovascularization and its correlation to plaque echogenicity in human carotid arteries atherosclerosis. Int J Cardiol. 2016; 223: 917–22. DOI:10.1016/j.ijcard.2016.08.261.
18. Huang PT, Chen CC, Aronow WS, et al. Assessment of neovascularization within carotid plaques in patients with ischemic stroke. World J Cardiol. 2010; 2 (4): 89–97. DOI:10.4330/wjc.v2.i4.89.
19. Iezzi R, Petrone G, Ferrante A, et al. The role of contrast-enhanced ultrasound (CEUS) in visualizing atherosclerotic carotid plaque vulnerability: which injection protocol? Which scanning technique? Eur J Radiol. 2015; 84 (5): 865–71. DOI:10.1016/j.ejrad.2015.01.024.
20. Li C, He W, Guo D, et al. Quantification of carotid plaque neovascularization using contrast-enhanced ultrasound with histopathologic validation. Ultrasound Med Biol. 2014; 40 (8): 1827–33. DOI:10.1016/j.ultrasmedbio.2014.02.010.
21. Staub D, Patel MB, Tibrewala A, et al. Vasa vasorum and plaque neovascularization on contrast-enhanced carotid ultrasound imaging correlates with cardiovascular disease and past cardiovascular events. Stroke. 2010; 41 (1): 41–7. DOI:10.1161/STROKEAHA.109.560342.
22. Xiong L, Deng Y-B, Zhu Y, Liu Y-N, Bi X-J. Correlation of Carotid Plaque Neovascularization Detected by Using Contrast-enhanced US with Clinical Symptoms. Radiology. 2009; 251 (2): 583–9. DOI:10.1148/radiol.2512081829.
23. Müller HFG, Viaccoz A, Kuzmanovic I, et al. Contrast-enhanced ultrasound imaging of carotid plaque neo-vascularization: accuracy of visual analysis. Ultrasound Med Biol. 2014; 40 (1): 18–24. DOI:10.1016/j.ultrasmedbio.2013.08.012.
24. Shah F, Balan P, Weinberg M, et al. Contrast-enhanced ultrasound imaging of atherosclerotic carotid plaque neovascularization: a new surrogate marker of atherosclerosis? Vasc Med. 2007; 12 (4): 291–7. DOI:10.1177/1358863X07083363.
25. Huang R, Abdelmoneim SS, Ball CA, et al. Detection of Carotid Atherosclerotic Plaque Neovascularization Using Contrast Enhanced Ultrasound: A Systematic Review and Meta-Analysis of Diagnostic Accuracy Studies. J Am Soc Echocardiogr. 2016; 29 (6): 491–502. DOI:10.1016/j.echo.2016.02.012.
26. Thapar A, Shalhoub J, Averkiou M, Mannaris C, Davies AH, Leen ELS. Dose-Dependent Artifact in the Far Wall of the Carotid Artery at Dynamic Contrast-enhanced US. Radiology. 2011; 262 (2): 672–9. DOI:10.1148/radiol.11110968.
27. Leo NDi, Venturini L, De Soccio V, et al. Multiparametric ultrasound evaluation with CEUS and shear wave elastography for carotid plaque risk stratification. J Ultrasound. 2018; 21 (4): 293–300. DOI:10.1007/s40477-018-0320-7.
28. Meshcheryakova OM, Katrich AN, Vinogradov RA, i dr. Sravnitel'naya ocenka re-zul'tatov kolichestvennogo analiza ul'trazvukovogo issledovaniya s kontrastnym usileniem i patomorfologii v opredelenii stepeni neoangiogeneza v ateroskleroticheskih blyashkah. Ul'trazvukovaya i funkcional'naya diagnostika. 2018; (1): 43–59. Russian.
29. Evdokimenko AN, Anufriev PL, Kulichenkova KN, Gulevskaya TS, Tanashyan MM. Morphometric characteristics of neovascularization of carotid atherosclerotic plaques. Arkh Patol. 2018; 80 (2): 24–9. DOI:10.17116/patol201880224-29. Russian.

Литература

1. Dunmore BJ, McCarthy MJ, Naylor AR, Brindle NPJ. Carotid plaque instability and ischemic symptoms are linked to immaturity of microvessels within plaques. J Vasc Surg. 2007; 45 (1): 155–9. DOI:10.1016/j.jvs.2006.08.072.
2. Filis K, Toufektzian L, Galyfos G, et al. Assessment of the vulnerable carotid atherosclerotic plaque using contrast-enhanced ultrasonography. Vascular. 2017; 25 (3): 316–25. DOI:10.1177/1708538116665734.
3. Гулевская Т. С., Моргунов В. А., Ануфриев П. Л. Структура атеросклеротических бляшек каротидного синуса и нарушения мозгового кровообращения. Анналы клинической и экспериментальной неврологии. 2010; 4 (1): 13–19.
4. Тухбатуллин М. Г., Баязова Н. И., Закиржанов Н. Р., и др. Применение контрастного усиления при ультразвуковом исследовании атеросклеротической бляшки в сонных артериях у пациентов с нарушением мозгового кровообращения. Практическая медицина. 2017; 103 (2): 124–9.
5. Jeziorska M, Woolley DE. Local neovascularization and cellular composition within vulnerable regions of atherosclerotic plaques of human carotid arteries. J Pathol. 1999; 188 (2): 189–96.
6. Saha SA, Gourineni V, Feinstein SB. The Use of Contrast-enhanced Ultrasonography for Imaging of Carotid Atherosclerotic Plaques: Current Evidence, Future Directions. Neuroimaging Clin N Am. 2016; 26 (1): 81–96. DOI:10.1016/j.nic.2015.09.007.
7. Feinstein SB. The powerful microbubble: from bench to bedside, from intravascular indicator to therapeutic delivery system, and beyond. Am J Physiol Circ Physiol. 2004; 287 (2): H450–7. DOI:10.1152/ajpheart.00134.2004.
8. Coli S, Magnoni M, Sangiorgi G, et al. Contrast-enhanced ultrasound imaging of intraplaque neovascularization in carotid arteries: correlation with histology and plaque echogenicity. J Am Coll Cardiol. 2008; 52 (3): 223–30. DOI:10.1016/j.jacc.2008.02.082.
9. Hoogi A, Adam D, Hoffman A, Kerner H, Reisner S, Gaitini D. Carotid plaque vulnerability: quantification of neovascularization on contrast-enhanced ultrasound with histopathologic correlation. AJR Am J Roentgenol. 2011; 196 (2): 431–6. DOI:10.2214/AJR.10.4522.
10. Varetto G, Gibello L, Castagno C, et al. Use of Contrast-Enhanced Ultrasound in Carotid Atherosclerotic Disease: Limits and Perspectives. Biomed Res Int [Internet]. 2015; 2015 (Article ID 293163): [about 7 p.]. Available from: https://DOI.org/10.1155/2015/293163.
11. van den Oord S, Akkus Z, Bosch J, et al. Quantitative Contrast-Enhanced Ultrasound of Intraplaque Neovascularization in Patients with Carotid Atherosclerosis. Ultraschall der Medizin — Eur J Ultrasound. 2014; 36 (02): 154–61. DOI:10.1055/s-0034-1366410.
12. Feinstein SB. The Evolution of Contrast Ultrasound: From Diagnosis to Therapy. J Am Coll Cardiol. 2016; 67 (21): 2516–8. DOI:10.1016/j.jacc.2016.04.004.
13. Moccetti F, Weinkauf CC, Davidson BP, et al. Ultrasound Molecular Imaging of Atherosclerosis Using Small-Peptide Targeting Ligands Against Endothelial Markers of Inflammation and Oxidative Stress. Ultrasound Med Biol. 2018; 44 (6): 1155–63. DOI:10.1016/j.

ultrasmedbio.2018.01.001.
14. Национальные рекомендации по ведению пациентов с заболеваниями брахиоцефальных артерий. Ангиология и сосудистая хирургия. 2013; 19 (2) (приложение): 1–72.
15. von Reutern G-M, Goertler M-W, Bornstein NM, et al. Grading Carotid Stenosis Using Ultrasonic Methods. Stroke. 2012; 43 (3): 916–21. DOI:10.1161/STROKEAHA.111.636084.
16. Gray-Weale AC, Graham JC, Burnett JR, Byrne K, Lusby RJ. Carotid artery atheroma: comparison of preoperative B-mode ultrasound appearance with carotid endarterectomy specimen pathology. J Cardiovasc Surg (Torino). 1988; 29 (6): 676–81.
17. Cattaneo M, Staub D, Porretta AP, et al. Contrast-enhanced ultrasound imaging of intraplaque neovascularization and its correlation to plaque echogenicity in human carotid arteries atherosclerosis. Int J Cardiol. 2016; 223: 917–22. DOI:10.1016/j.ijcard.2016.08.261.
18. Huang PT, Chen CC, Aronow WS, et al. Assessment of neovascularization within carotid plaques in patients with ischemic stroke. World J Cardiol. 2010; 2 (4): 89–97. DOI:10.4330/wjc.v2.i4.89.
19. Iezzi R, Petrone G, Ferrante A, et al. The role of contrast-enhanced ultrasound (CEUS) in visualizing atherosclerotic carotid plaque vulnerability: which injection protocol? Which scanning technique? Eur J Radiol. 2015; 84 (5): 865–71. DOI:10.1016/j.ejrad.2015.01.024.
20. Li C, He W, Guo D, et al. Quantification of carotid plaque neovascularization using contrast-enhanced ultrasound with histopathologic validation. Ultrasound Med Biol. 2014; 40 (8): 1827–33. DOI:10.1016/j.ultrasmedbio.2014.02.010.
21. Staub D, Patel MB, Tibrewala A, et al. Vasa vasorum and plaque neovascularization on contrast-enhanced carotid ultrasound imaging correlates with cardiovascular disease and past cardiovascular events. Stroke. 2010; 41 (1): 41–7. DOI:10.1161/STROKEAHA.109.560342.
22. Xiong L, Deng Y-B, Zhu Y, Liu Y-N, Bi X-J. Correlation of Carotid Plaque Neovascularization Detected by Using Contrast-enhanced US with Clinical Symptoms. Radiology. 2009; 251 (2): 583–9. DOI:10.1148/radiol.2512081829.
23. Müller HFG, Viaccoz A, Kuzmanovic I, et al. Contrast-enhanced ultrasound imaging of carotid plaque neo-vascularization: accuracy of visual analysis. Ultrasound Med Biol. 2014; 40 (1): 18–24. DOI:10.1016/j.ultrasmedbio.2013.08.012.
24. Shah F, Balan P, Weinberg M, et al. Contrast-enhanced ultrasound imaging of atherosclerotic carotid plaque neovascularization: a new surrogate marker of atherosclerosis? Vasc Med. 2007; 12 (4): 291–7. DOI:10.1177/1358863X07083363.
25. Huang R, Abdelmoneim SS, Ball CA, et al. Detection of Carotid Atherosclerotic Plaque Neovascularization Using Contrast Enhanced Ultrasound: A Systematic Review and Meta-Analysis of Diagnostic Accuracy Studies. J Am Soc Echocardiogr. 2016; 29 (6): 491–502. DOI:10.1016/j.echo.2016.02.012.
26. Thapar A, Shalhoub J, Averkiou M, Mannaris C, Davies AH, Leen ELS. Dose-Dependent Artifact in the Far Wall of the Carotid Artery at Dynamic Contrast-enhanced US. Radiology. 2011; 262 (2): 672–9. DOI:10.1148/radiol.11110968.
27. Leo NDi, Venturini L, De Soccio V, et al. Multiparametric ultrasound evaluation with CEUS and shear wave elastography for carotid plaque risk stratification. J Ultrasound. 2018; 21 (4): 293–300. DOI:10.1007/s40477-018-0320-7.
28. Мещерякова О. М., Катрич А. Н., Виноградов Р. А. и др. Сравнительная оценка результатов количественного анализа ультразвукового исследования с контрастным усилением и патоморфологии в определении степени неоангиогенеза в атеросклеротических бляшках. Ультразвуковая и функциональная диагностика. 2018; (1): 43–59.
29. Евдокименко А. Н., Ануфриев П. Л., Куличенкова К. Н., Гулевская Т. С., Танашян М. М. Морфометрическая характеристика неоваскуляризации атеросклеротических бляшек каротидного синуса. Архив патологии. 2018; 80 (2): 24–9. DOI:10.17116/patol201880224-29.

DYNAMICS OF POST-STROKE HAND PARESIS KINEMATIC PATTERN DURING REHABILITATION

Khizhnikova AE ✉, Klochkov AS, Kotov–Smolenskiy AM, Suponeva NA, Piradov MA

Research Center of Neurology, Moscow, Russia

According to the literature data, only 5–20% of post-stroke patients are able to restore the hand motor function completely. Correct goal setting and individual approach to the patient's functional recovery are important. Our study aimed to develop an algorithm of impaired hand motor functioning assessment for post-stroke patients and to determine the principles of the rehabilitation tactics choosing based on the biomechanical analysis. Twenty five patients with hemispheric stroke and 10 healthy volunteers participated in the study. Formal clinical observation scales (Fugl–Meyer Assessment, Ashworth Scale, ARAT) and video motion analysis were used for evaluation of the hand motor function. Patients were divided into 2 groups according to the hand paresis severity (mild/moderate and pronounced/severe). Rehabilitation was carried out in both groups, including mechanotherapy, massage and physical therapy. It was revealed that in the 1st group of patients the motor function recovery in the paretic hand was due to movement performance recovery: biomechanical parameters restoration directly correlated with a decrease in the paresis degree according to the Fugl–Meyer Assessment Scale (r = 0.94; p = 0.01). In the 2nd group of patients, the motor function recovery in the paretic hand was due to motor deficit compensation: according to biomechanical analysis, the pathological motor synergies inversely correlated with a decrease in the paresis degree (r = –0.9; p = 0.03). As a result of the study, an algorithm for selecting the patient management tactics based on the baseline clinical indicators was developed.

Keywords: stroke, hand paresis, neurorehabilitation, adaptation, motor relearning, movement biomechanics, motion capture, abnormal synergy

Funding: the study was performed as a part of the public contract № 0512-2014-0036.

Author contribution: Khizhnikova AE — research planning, literature analysis, data acquisition, analysis and interpretation, manuscript draft writing; Klochkov AS — research planning, literature analysis, data interpretation, manuscript writing; Kotov–Smolenskiy AM — training of surveyed patients, patients examination using clinical scales; Suponeva NA — research planning, data interpretation, manuscript writing; Piradov MA — manuscript writing.

Compliance with ethical standards: the study was approved by the Ethics Committee of Research Center of Neurology (protocol № 5/16 dated January 27, 2016). All enrolled patients signed informed consent to participation in the study.

✉ **Correspondence should be addressed:** Anastasia E. Khizhnikova
Volokolamskoye Shosse 80, Moscow, 125367; nastushkapal@gmail.com

Received: 16.08.2019 **Accepted:** 30.08.2019 **Published online:** 31.08.2019

DOI: 10.24075/brsmu.2019.056

ДИНАМИКА КИНЕМАТИЧЕСКОГО ПОРТРЕТА ПОСТИНСУЛЬТНОГО ПАРЕЗА РУКИ НА ФОНЕ РЕАБИЛИТАЦИИ

А. Е. Хижникова ✉, А. С. Клочков, А. М. Котов–Смоленский, Н. А. Супонева, М. А. Пирадов

Научный центр неврологии, Москва, Россия

По данным литературы, только 5–20% пациентов после инсульта могут полностью восстановить двигательную функцию руки. Важны корректная постановка целей и индивидуальный подход, направленный на восстановление функционального статуса пациента. Целью исследования было на основании клинико-биомеханического анализа разработать алгоритм оценки нарушения двигательной функции руки у пациентов после инсульта и определить принципы выбора тактики реабилитации. В исследование были включены 25 пациентов с инсультом полушарной локализации и 10 здоровых добровольцев. Для оценки двигательной функции руки применяли формализованные клинические шкалы (шкала Фугл–Мейера, Эшворта, тест ARAT) и видеоанализ движений. Пациенты были разделены на 2 группы по степени тяжести пареза руки (легкий/умеренный и грубый/выраженный). В обеих группах проводили курс реабилитации, включавший механотерапию, массаж, ЛФК. Выявлено, что у пациентов 1-й группы восстановление двигательной функции в паретичной руке происходит по пути нормализации паттерна движения: нормализация биомеханических параметров, прямо коррелирующая с уменьшением клинической выраженности степени пареза по шкале Фугл–Мейера (r = 0,94; p = 0,01). У пациентов 2-й группы восстановление двигательной функции в паретичной руке происходит по пути компенсации двигательного дефицита: сохранение патологической синергии по данным биомеханического анализа, обратно коррелирующее с уменьшением клинической выраженности степени пареза (r = –0,9; p = 0,03). В результате проведенного исследования сформирован алгоритм выбора тактики ведения пациентов, основанный на исходных клинических показателях.

Ключевые слова: инсульт, парез в руке, нейрореабилитация, адаптация, двигательное переобучение, биомеханика движений, видеоанализ движений, патологическая синергия

Финансирование: работа выполнена в рамках государственного заказа № 0512-2014-0036.

Информация о вкладе авторов: А. Е. Хижникова — планирование исследования, анализ литературы, сбор, анализ и интерпретация данных, подготовка черновика рукописи; А. С. Клочков — планирование исследования, анализ литературы, интерпретация данных, подготовка рукописи; А. М. Котов–Смоленский — проведение тренировок с пациентами, включенными в исследование, осмотр пациентов по клиническим шкалам; Н. А. Супонева — планирование исследования, интерпретация данных, подготовка рукописи; М. А. Пирадов — подготовка рукописи.

Соблюдение этических стандартов: исследование одобрено этическим комитетом ФГБНУ НЦН (протокол № 1–5/16 от 27 января 2016 г.). Все пациенты подписали добровольное информированное согласие на участие в исследовании.

✉ **Для корреспонденции:** Анастасия Евгеньевна Хижникова
Волоколамское шоссе, д. 80, г. Москва, 125367; nastushkapal@gmail.com

Статья получена: 16.08.2019 **Статья принята к печати:** 30.08.2019 **Опубликована онлайн:** 31.08.2019

DOI: 10.24075/vrgmu.2019.056

According to a number of authors, in the acute phase of a stroke, the hand paresis occurs in 48–77% of patients [1, 2]. At the same time, only 5–20% of patients are able to restore the motor function of the paretic arm completely by the end of the early recovery period [3, 4].

Restoration of the upper limb motor function consists of six consecutive stages (from flaccid paralysis to the ability to perform complex coordinated movements). However, the improvement can be completed at any stage, and the patient remains partially or completely lost self-care capabilities [5]. In

this regard, an important condition for effective motor function restoration is to determine the tactics of patient rehabilitation to achieve the maximum effect, depending on the current stage.

It is known that in post-stroke patients with severe paresis and increased muscle tone the physiological movement pattern is impossible. As a consequence, prerequisites arise for the development of new motor synergies, which are inherently a compensatory mechanism. As a result, the body uses the remaining motor functions of the limb, or active movements in adjacent joints and functionally related kinematic chains to provide motion. The use of movements with a lower level of regulation as a part of compensatory synergies leads to a decrease in the adaptability to changing environmental conditions. Subsequently, compensatory synergies become pathological [6], which leads to a decrease in the patient's functional capabilities and a slowdown of further rehabilitation.

Nevertheless, it is worth noting that, according to some authors, compensation mechanisms are necessary for patients with severe paresis and the presence of these is important for the successful movement performance in post-stroke patients [7]. During the recovery process, the motor synergies manifest more comprehensively and become associated with spasticity and related reactions. Currently, the generally accepted view is that for better functional motor recovery it is necessary to conduct training within the existing pathological stereotype with the subsequent expansion of the active movement zone [8]. Thus, the restructuring of pathological synergy due to an increase in the number of "beneficial" motion components usually occurs during the training [9].

Correct goal setting and individual approach are important in developing a rehabilitation program aimed primarily at restoring the functional status of the patient. Video analysis of the paretic arm and shoulder girdle movements with a complex evaluation of inter-articular relationships and kinematic characteristics during rehabilitation can be invaluable in retrospective assessment of the recovery process. The study aimed to develop the principles of choosing the hand motor function restoration tactics in patients after a cerebrovascular accident on the basis of clinical and biomechanical analysis.

METHODS

The study was conducted on the basis of the Department of Neurorehabilitation and Physiotherapy of the Research Center of Neurology (2017–2018). Inclusion criteria: male and female patients aged 18–80; confirmed cerebrovascular accident of ischemic or hemorrhagic type; single lesion site of hemispheric localization which arose from 3 months to 2 years ago; post-stroke hand paresis (grade 2–4 according to MRC Scale for Muscle Strength) [10]. Exclusion criteria: hand paresis grade according to MRC Scale for Muscle Strength less than 2; severe defect of deep sensitivity; neglect syndrome; muscle tone increase score exceeding 2 according to the Ashworth scale (score 0 corresponds to normal muscle tone); severe vision impairment not allowing to distinguish the image on the computer monitor; severe cognitive impairment which makes it difficult to execute the instructions; severe sensory or motor aphasia; left-handedness according to Edinburgh Handedness Inventory [11]. Twenty five patients with hemispheric cerebrovascular accident participated in the study. Among them, there were 17 men and 8 women aged 30–80 (median age 55 [45; 61]). The prescription of stroke was 3–23 months (median prescription of stroke was 7 months [4; 12]). Nine patients (36%) were observed in the early recovery period, 9 patients (36%) were observed in the late recovery period and 7 patients (28%) were observed in the residual period. The study did not include patients with severe spasticity, gross speech and cognitive impairment, limiting the possibility of communication and following the instructions of the physical therapist.

To determine the normal kinematic pattern of hand movement, 10 healthy volunteers aged 24–42 (4 women and 6 men, right-handed, without pathologies of the musculoskeletal and nervous systems) were selected. For each subject, an analysis of movements was performed in both the dominant (right) and non-dominant (left) hands.

For clinical assessment of motor deficit, pathological synergies severity, reflex activity, surface and deep sensitivity, passive movement volume and pain sensation in the affected hands the Fugl–Meyer Assessment Scale was used [12]: the section for hand function evaluation (the maximum score for this section is normally 126). The Ashworth Scale was used for spasticity assessment in the paretic arm [13]. The wrist motor skills and functional movement were assessed using the ARAT test [14].

The 3D analysis of movements in patients was performed using the Biosoft-Videomotion 3D system (Biosoft; Russia). Since hand movements are very diverse and variable, the least variable parameter was chosen for the evaluation of biomechanical parameters: reaching an object (reaching test). Patients were seated at the table on a chair without a back, with armrests for both hands. Hands were placed on the armrests palms down (wrists were on the table). Within reach of each patient, a glass with a 10 g weigh was placed on the table. The patient was asked to reach the glass, take it, bring it to his mouth simulating the drinking process, then put the glass back and return the hand to its original position. If it was not possible to grasp the glass (severe hand paresis), the patient was asked to attempt to grasp it. To ensure the most automated movement, the patients were informed that the main objective of the study was to observe a drinking simulation movement. Thus, the reaching movement was performed with a minimum focus of attention, which made it possible to obtain automated action. Only the first part of the movement was measured (reaching a remotely located object).

To study intra-joint and inter-joint synergies in the sagittal and frontal planes, the following synergy coefficients (C) were introduced: C_1 — shoulder joint (SJ) flexion to SJ abduction ratio; C_2 — elbow joint extension (EJ) to the SJ flexion ratio; C_3 — EJ extension to SJ abduction ratio.

During rehabilitation, the paretic hand functional skills training was performed using the mechanotherapeutic exoskeleton arm weight support Armeo Spring system (Hocoma; Switzerland), as well as training of bimanual and coordination movements controlled by the physical therapist and paretic hand massage. Rehabilitation was successful in all patients.

Statistical processing of the results was carried out using the Mann–Whitney test (independent samples), Wilcoxon signed ranks test (dependent samples), and Spearman's rank correlation coefficient on the personal computer using the Statsoft Statistica v. 7.0 software (StatSoft; USA). Data were presented as the median and 25% and 75% quartiles of the median. The differences were considered statistically significant at $p < 0.05$.

RESULTS

Clinical assessment

During the comparative analysis of data according to the Fugl–Meyer Assessment Scale, a statistically significant increase in

active movements in the shoulder, forearm, wrist and hand was observed in all patients after rehabilitation. A significant increase in the volume of passive movements in the elbow and wrist joints was also noted. It is important, that according to the Fugl–Meyer Assessment Scale, the pathological flexion synergy severity was significantly reduced (the higher the Fugl–Meyer Assessment score, the lower the degree of severity) (Table 1).

Statistical analysis of the Ashworth Scale score revealed that after rehabilitation the degree of spasticity in the elbow flexor muscles ($p = 0.00008$), wrist flexor muscles ($p = 0.00098$) and superficial flexor muscles of fingers ($p = 0.0022$) was significantly reduced. A decrease in spasticity in the studied muscle groups was observed in patients with a slight and mild muscle tone increase (1; 1+) and in patients with a more pronounced muscle tone increase (2).

Clinical data analysis using the Fugl–Meyer Assessment Scale revealed a close relationship between the severity of pathological flexion synergy in the hand and the overall motor deficiency degree ($r = 0.81$; $p = 0.000000$). According to the Fugl–Meyer Assessment score patients with severe paresis whose motor deficit was less than 50% of maximum active movement score (less than 33), patients with pronounced paresis — 50–70% (34–46), patients with moderate paresis — 71–89% (47–56) and patients with mild paresis — 90–99% (57–65) were identified. For further analysis, patients were divided into 2 groups: group 1 — patients with mild/moderate paresis, group 2 — patients with pronounced/severe paresis.

A comparative analysis using some subsections of the Fugl-Meyer Assessment Scale showed that a significant improvement in the hand motor function occurred both in the proximal and distal parts of the hand in both subgroups (Table 2).

Video analysis of the paretic hand movements while performing a reach test

Analysis of the reach test time characteristics demonstrated that patients of both groups needed significantly more time to complete the target movement than a healthy person. In case of severe/pronounced paresis reaching a remotely located object needed significantly more time compared to normal ($p = 0.001$). The time difference between the group of healthy volunteers and the group of patients with mild/moderate paresis was less significant, it was only 0.55 s (Fig. 1).

Analysis of the reach test time characteristics after rehabilitation demonstrated that in the 1st group of patients (mild/moderate hand paresis) there was a statistically significant decrease in the time needed to reach the object ($p = 0.04$). In the 2nd group of patients (severe paresis) the time needed to complete the test, on the contrary, significantly increased ($p = 0.043$). It exceeded the corresponding normal indicator by more than 2 times.

Biomechanical research results analysis revealed that in patients with mild/moderate paresis the maximum angular amplitude of the shoulder joint flexion significantly reduced and the maximum angular amplitude of the shoulder joint abduction significantly increased while performing the reach test (Fig. 2A).

In addition to decreasing the maximum angle of movement of some joints in patients with mild/moderate paresis, the time needed to establish the maximum angular amplitude for all movements was increased compared to normal (Fig. 3A, C).

Kinematic pattern in the group of patients with severe/pronounced paresis was different: when performing the movement, the maximum abduction angle of the shoulder joint was greater than normal (Fig. 2B). At the same time, the maximum extension angle of the elbow joint was significantly below normal (Fig. 3B, C).

Table 1. Median indicators (Me [25%; 75%]) of the hand motor impairment according to the Fugl–Meyer Assessment Scale subsections

Scale section	Group ($n = 25$)	
	Before treatment	After treatment
Total score	103 [91; 109]	109 [99; 120]
		$p = 0.000025$
Shoulder and forearm movements	29 [24; 34]	32 [24; 38]
		$p = 0.000821$
Wrist and hand movements	18 [13; 21]	20 [9; 23.5]
		$p = 0.000168$
Synergies	9 [6; 10]	9.5 [5; 11]
		$p = 0.000049$
Passive movement amount	21 [20; 22]	23 [22; 24]
		$p = 0.000327$

Table 2. Median indicators (Me [25%; 75%]) of the hand motor impairment according to the Fugl–Meyer Assessment Scale in patients before and after the rehabilitation

Shoulder and forearm movements, score ($n = 25$)		
	Mild/moderate ($n = 13$)	Severe/pronounced ($n = 12$)
Before treatment	34 [32; 37]	24 [21.5; 27]
After treatment	38 [34; 41]	30.5 [25.5; 33.5]
p-level	**$p = 0.041$**	**$p = 0.0068$**
Wrist and hand movements, score ($n = 25$)		
	Mild/moderate ($n = 13$)	Severe/pronounced ($n = 12$)
Before treatment	21 [19; 21]	12 [8; 14.5]
After treatment	23 [22; 24]	14 [10; 19.5]
p-level	**$p = 0.0044$**	**$p = 0.012$**

In addition to some joints maximum angle reducing in patients with severe/pronounced paresis, the time needed to establish the maximum angular amplitude for all movements significantly increased compared to normal. In patients of this group, attention should be drawn to the change of time needed to reach the peak amplitude of the joint while moving. If in the group of patients with mild/moderate paresis the order of reaching maximum amplitudes of the joints remained the same, then in the group of patients with severe/pronounced paresis it was different. Thus, the abduction of the shoulder joint, which was the first of all joints to reach its peak both in healthy people and in patients with mild/moderate paresis, in patients with severe/pronounced paresis appeared only in the middle of the movement, after the extension of the wrist joint.

When comparing the maximum angular amplitudes of joints in the 1st group of patients before and after rehabilitation, no statistically significant differences were observed. At the same time, analysis of changes in the range of joint motion after training revealed significant changes in biomechanical parameters of the shoulder joint: the flexion amount increased ($p = 0.04$) and the abduction amount decreased ($p = 0.01$).

Analysis of the movement velocity parameters changes demonstrated a significant increase in the angular velocity of the shoulder joint flexion ($p = 0.01$), the elbow joint extension ($p = 0.02$), as well as a decrease in the angular velocity of the shoulder joint abduction ($p = 0.02$). When studying synergy coefficients reflecting inter-joint interactions in the 1st group of patients, significant differences after rehabilitation were revealed only by the C_2 coefficient ($p = 0.04$) reflecting the interaction between the shoulder joint flexion and the elbow joint extension during the reach test execution.

When comparing the maximum angular amplitudes of the joints in the 2nd group of patients (severe/pronounced paresis) before and after rehabilitation, a significant decrease in the maximum extension angle of the elbow joint was revealed ($p = 0.01$). No significant changes in other joints were noted.

When analyzing the range of motion of the joints in the second group of patients, changes were observed that were opposite to those obtained in patients of the first group. During rehabilitation the shoulder joint flexion significantly reduced ($p = 0.02$), a significant increase of the shoulder joint abduction was also observed ($p = 0.04$). No significant differences were found in the elbow joint before and after rehabilitation. It is also worth noting that, despite a decrease in the shoulder joint flexion, statistically significant differences in this indicator from normal values were not found.

Significant differences in the amount of movements from the normal motor stereotype persisted in other indicators: shoulder joint abduction amount ($p = 0.04$), elbow joint extension amount ($p = 0.007$), wrist joint extension amount ($p = 0.02$). In addition, the opposite changes in the movement velocity characteristics in the 2nd group patients were revealed compared to changes in patients of the first group. Thus, after rehabilitation, a significant increase in the angular velocity of the shoulder joint abduction was noted ($p = 0.02$), at the same time, a significant decrease in the angular velocity ($p = 0.02$) occurred in the elbow joint while reducing the extension and maximum angular amplitude. When studying synergy coefficients reflecting inter-articular interactions in patients of the second group, the significant differences after rehabilitation were observed only by the C_2 coefficient, which significantly decreased ($p = 0.04$) after training.

Analysis of the shoulder girdle movement biomechanics while performing the reach test

Despite the fact that the study results demonstrated that there was no effect of training on the severity of pathological synergy

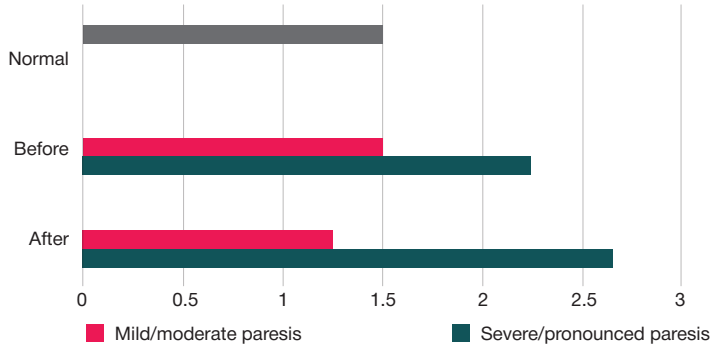

Fig. 1. Time (s) needed to complete the reach movement n patients with varying degrees of hand paresis

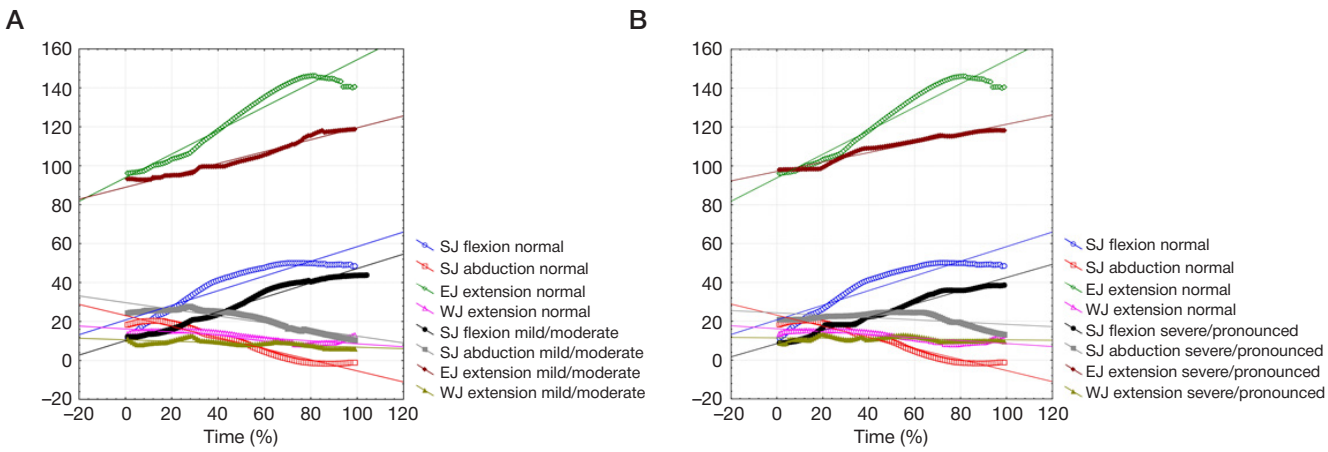

Fig. 2. The paretic hand inter-articular interactions in patients with mild/moderate (**A**) and severe/pronounced (**B**) paresis

in patients with severe/pronounced hand paresis, the clinical assessment showed an improvement of functional capabilities in the paretic hand, which was expressed as a significant improvement of fine motor skills confirmed by the ARAT test. In some studies, a decrease in the displacement of the body and shoulder girdle was observed during the video analysis of movements in patients with moderate paresis having the improved functionality according to clinical scales [15, 16]. To confirm the hypothesis of the shoulder girdle compensatory movement in patients with severe/pronounced hand paresis the additional movement analysis was carried while performing the reach test. For this purpose, the displacement of two markers located on the acromion of the healthy and paretic shoulders in the frontal plane was evaluated.

The results demonstrated a shoulder girdle displacement towards the object in patients with severe/pronounced paresis when performing the reach test before training (23 [19.8; 57.4] — healthy shoulder; 169 [88.0; 178.0] — paretic shoulder) as well as after training (66 [49.0; 81.0] — healthy shoulder; 215 [162.0; 229.0] — paretic shoulder) with significantly greater prevalence of paretic shoulder displacement. In addition, the analysis revealed a significant (p = 0.04) increase in the shoulder girdle forward displacement when performing a reach movement during rehabilitation.

DISCUSSION

After rehabilitation, the data was obtained that both groups of patients not only differ significantly in their kinematic pattern, but also have different ways of motor function recovery.

Thus, in patients with mild/moderate paresis, the motor function restoration in the paretic hand was due to movement performance recovery which was evidenced by an increase in the C_2 coefficient, reflecting the inter-articular interaction in the shoulder and elbow joints. The latter directly correlated with a decrease in the paresis degree according to the Fugl–Meyer Assessment Scale (r = 0.94; p = 0.01). In patients with severe/pronounced hand paresis the motor function recovery in the paretic hand was due to motor deficit compensation which was evidenced by decrease in the C_2 coefficient. The latter inversely correlated with a decrease in the paresis degree according to the Fugl–Meyer Assessment Scale (r = –0.9; p = 0.03), i.e. in said patients the functional hand movement improved while maintaining a pathological pattern of movement. Further analysis showed that in patients with severe/pronounced paresis the shoulder girdle forward shift significantly increased after rehabilitation while performing the reaching test. During the correlation analysis, a negative relationship between the marker displacement in the paretic shoulder and the C_2 value was found (r = –0.9; p = 0.03). Relationship between the trunk and paretic limb movements is also noted in a number of studies [17]. These data indicate the presence of a compensatory mechanism in patients with severe/pronounced paresis and explain the decrease in this coefficient after rehabilitation since the larger is the body displacement, the less are the range of motion and maximum angles of the joints. It can be assumed that in patients with severe/pronounced paresis the motor skills recovery is due to compensation, therefore, it is impossible to return to the normal pattern of movements for patients with fully developed pathological hand synergy. According to our data, the training carried out by a rehabilitation specialist should not always be aimed at overcoming pathological synergies, since it is advisable to use compensatory mechanisms as efficiently as possible to adapt and train patients with severe/pronounced paresis. This conclusion was also confirmed by clinical examination data analysis, since after rehabilitation a significant improvement in the functionality of the paretic arm was noted

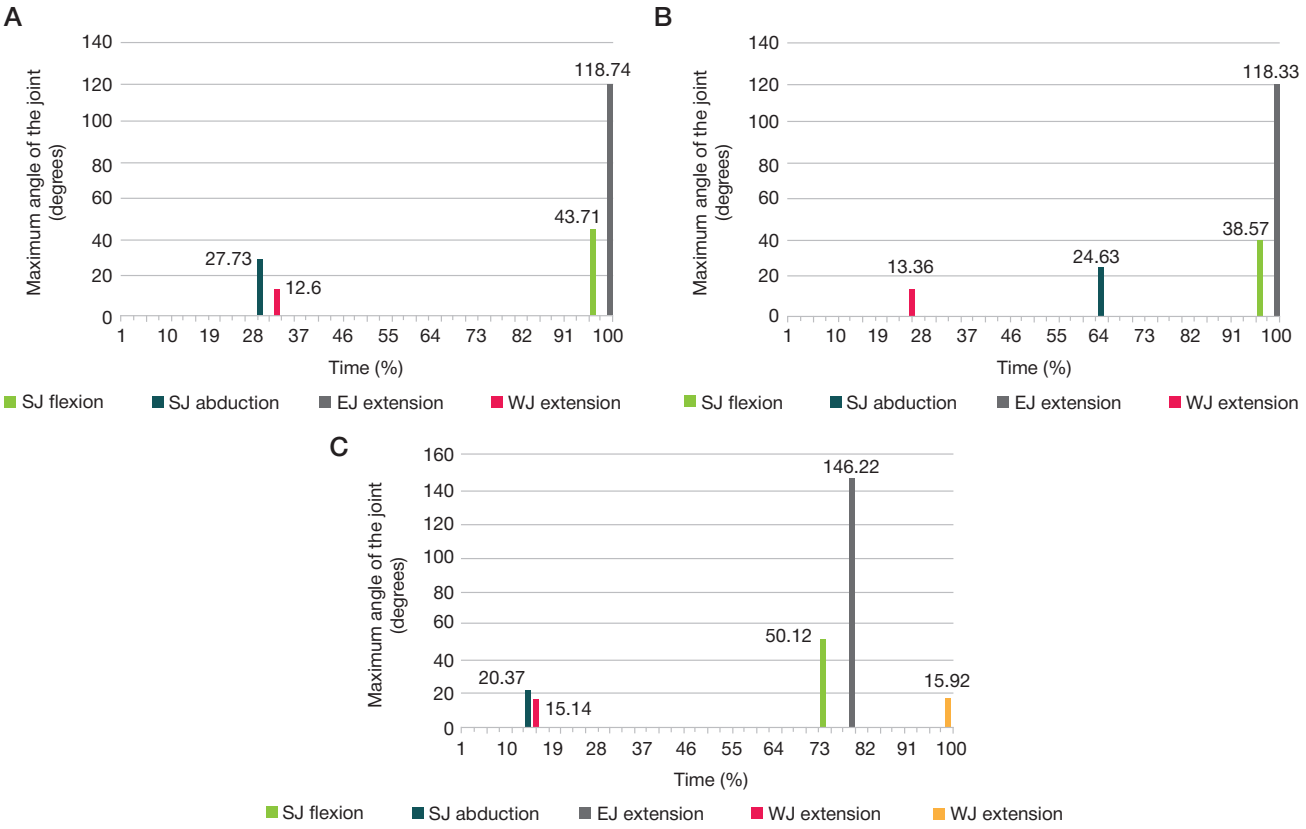

Fig. 3. The maximum angular amplitude of different joints while performing the reach test in healthy people (**A**) and in patients with mild/moderate paresis (**B**) compared to normal (**C**)

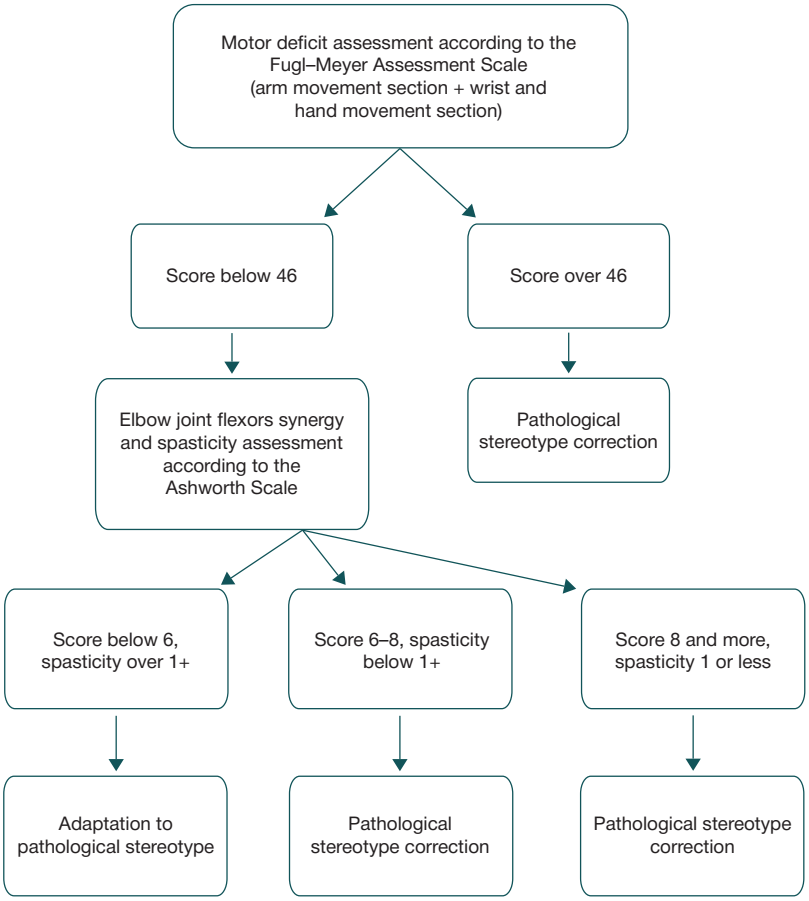

Fig. 4. Algorithm for choosing tactics of rehabilitation in patients with post-stroke hand paresis

in both groups of patients, in particular, their fine motor skills improved. We assume, and this is comparable with the data of many studies [18–21], that this effect may be associated with the restriction absence of axis in the paretic limb during training, as the patients are trained to act within their stereotype and overcome it arbitrarily if necessary.

Based on the obtained clinical biomechanical data for the groups of patients with different spasticity degree and hand paresis severity, the algorithm of rehabilitation tactics choosing was determined for patients with post-stroke hand paresis (Fig. 4). In this case, an assessment before the start of the rehabilitation and the rehabilitation strategy development should be carried out according to the subsection of the Fugl–Meyer Assessment Scale for the upper limb. It is worth noting that an assessment according to the Ashworth Scale is also necessary and should be carried out in three muscle groups: elbow and wrist joints flexors and flexors of the fingers. The spasticity degree which affects the patient management tactics choice in two or more muscle groups is 1+.

CONCLUSIONS

The detailed clinical biomechanical study of the kinematic pattern change dynamics for one of the most functionally significant human movements (reach test) during rehabilitation demonstrated that the baseline lesion severity and spasticity degree are crucial for the most effective and successful restoration of the paretic hand function. These are responsible for the formation of pathological motor synergies in patients with post-stroke hand paresis and for activation of various mechanisms of the motor stereotype transformation during the recovery process. The data obtained made it possible to determine an algorithm for choosing the rehabilitation tactics based primarily on clinical indicators: in patients with mild/moderate paresis it is useful to conduct training within the physiological movement pattern aimed at correcting the pathological stereotype together with the suppression of compensatory mechanisms; on the contrary, patients with severe/pronounced hand paresis need training with the promotion of compensation mechanisms and an increase in the functionality of the paretic hand within the previously formed pathological stereotype.

References

1. Lawrence ES, Coshall C, Dundas R, et al. Estimates of the prevalence of acute stroke impairments and disability in a multiethnic population. J Stroke. 2001; (32): 1279–84.
2. Persson HC, Parziali M, Danielsson A, Sunnerhagen KS. Outcome and upper extremity function within 72 hours after first occasion of stroke in an unselected population at a stroke unit. A part of the SALGOT study. J BMC Neurol. 2012; (12): 162.
3. Langhorne P, Coupar F, Pollock A. Motor recovery after stroke: a systematic review. Lancet Neurol. 2009; 8 (8): 741–54.
4. Veerbeek JM, Kwakkel G, van Wegen EE, Ket JC, Heymans MW. Early prediction of outcome of activities of daily living after stroke: a systematic review. Stroke. 2011; 42 (5): 1482–8.
5. Brunnstrom S. Movement Therapy in Hemiplegia: A Neurophysiological Approach. Facts and Comparisons. NewYork: Harper and Row, 1970.

6. Santello M, Lang CE. Are movement disorders and sensorimotor injuries pathologic synergies? When normal multi-joint movement synergies become pathologic. J Front Hum Neurosci. 2015; (8): 1050.
7. van Kordelaar J, van Wegen EE, Kwakkel G. Unraveling the interaction between pathological upper limb synergies and compensatory trunk movements during reach-to-grasp after stroke: a cross-sectional study. J Exp Brain Res. 2012; 221 (3): 251–62.
8. Van Vliet PM, Sheridan MR. Coordination between reaching and grasping in patients with hemiparesis and healthy subjects. J Arch Phys Med Rehabil. 2007; (88): 1325–31.
9. Hogan L, Dipietro HI, Krebs SE, et al. Changing Motor Synergies in Chronic Stroke. J Neurophysiol. 2007; (98): 757–68.
10. Compston A. Aids to the investigation of peripheral nerve injuries. Medical Research Council: Nerve Injuries Research Committee. His Majesty's Stationery Office: 1942; pp. 48 (iii) and 74 figures and 7 diagrams; with aids to the examination of the peripheral nervous system. By Michael O'Brien for the Guarantors of Brain. Saunders Elsevier. Brain. 2010; 133 (10): 2838–44.
11. Oldfield RC. The assessment and analysis of handedness: the Edinburgh inventory. Neuropsychologia. 1971; (9): 97–113.
12. Sanford J, Moreland J, Swanson LR, Stratford PW. Reliability of the Fugl-Meyer assessment for testing motor performance in patients following stroke. J Gowland C Phys Ther. 1993; 73 (7): 447–54.
13. Bohannon RW, Smith MB. Interrater reliability of a modified Ashworth scale of muscle spasticity. J Phys Ther. 1987; 67 (2): 206–7.
14. Doussoulin SA, Rivas SR, Campos SV. Validation of «Action Research Arm Test» (ARAT) in Chilean patients with a paretic upper limb after a stroke. Rev Med Chil. 2012; 140 (1): 59–65.
15. Alt Murphy M, Willén C, Sunnerhagen KS. Movement kinematics during a drinking task are associated with the activity capacity level after stroke. J Neurorehabil Neural Repair. 2012; 26 (9): 1106–15.
16. Valdés BA, Glegg SMN, Van der Loos HFM. Trunk Compensation During Bimanual Reaching at Different Heights by Healthy and Hemiparetic Adults. J Mot Behav. 2017; 49 (5): 580–92.
17. van Kordelaar J, van Wegen EE, Kwakkel G. Unraveling the interaction between pathological upper limb synergies and compensatory trunk movements during reach-to-grasp after stroke: a cross-sectional study. J Exp Brain Res. 2012; 221 (3): 251–62.
18. Roh J, Rymer WZ, Perreault EJ, et al. Saturated muscle activation contributes to compensatory reaching strategies after stroke. J Neurophysiol. 2013; 109 (3): 768–81.
19. Basteris A, Nijenhuis SM, Stienen AH, et al. Training modalities in robot-mediated upper limb rehabilitation in stroke: a framework for classification based on a systematic review. J Neuroeng Rehabil. 2014; 10 (11): 111.
20. Daunoraviciene K, Adomaviciene A, Grigonyte A, Griškevičius J, Juocevicius A. Effects of robot-assisted training on upper limb functional recovery during the rehabilitation of poststroke patients. J Technol Health Care. 2018; 26 (2): 533–42.
21. Ustinova KI, Chernikova LA, Khizhnikova AE, Poydasheva AG, Suponeva NA, Piradov MA. Theoretical basis for classical methods of motor rehabilitation in neurology. Annals of clinical and experimental neurology. 2018; 12 (3): 54–60.

Литература

1. Lawrence ES, Coshall C, Dundas R, et al. Estimates of the prevalence of acute stroke impairments and disability in a multiethnic population. J Stroke. 2001; (32): 1279–84.
2. Persson HC, Parziali M, Danielsson A, Sunnerhagen KS. Outcome and upper extremity function within 72 hours after first occasion of stroke in an unselected population at a stroke unit. A part of the SALGOT study. J BMC Neurol. 2012; (12): 162.
3. Langhorne P, Coupar F, Pollock A. Motor recovery after stroke: a systematic review. Lancet Neurol. 2009; 8 (8): 741–54.
4. Veerbeek JM, Kwakkel G, van Wegen EE, Ket JC, Heymans MW. Early prediction of outcome of activities of daily living after stroke: a systematic review. Stroke. 2011; 42 (5): 1482–8.
5. Brunnstrom S. Movement Therapy in Hemiplegia: A Neurophysiological Approach. Facts and Comparisons. NewYork: Harper and Row, 1970.
6. Santello M, Lang CE. Are movement disorders and sensorimotor injuries pathologic synergies? When normal multi-joint movement synergies become pathologic. J Front Hum Neurosci. 2015; (8): 1050.
7. van Kordelaar J, van Wegen EE, Kwakkel G. Unraveling the interaction between pathological upper limb synergies and compensatory trunk movements during reach-to-grasp after stroke: a cross-sectional study. J Exp Brain Res. 2012; 221 (3): 251–62.
8. Van Vliet PM, Sheridan MR. Coordination between reaching and grasping in patients with hemiparesis and healthy subjects. J Arch Phys Med Rehabil. 2007; (88): 1325–31.
9. Hogan L, Dipietro HI, Krebs SE, et al. Changing Motor Synergies in Chronic Stroke. J Neurophysiol. 2007; (98): 757–68.
10. Compston A. Aids to the investigation of peripheral nerve injuries. Medical Research Council: Nerve Injuries Research Committee. His Majesty's Stationery Office: 1942; pp. 48 (iii) and 74 figures and 7 diagrams; with aids to the examination of the peripheral nervous system. By Michael O'Brien for the Guarantors of Brain. Saunders Elsevier. Brain. 2010; 133 (10): 2838–44.
11. Oldfield RC. The assessment and analysis of handedness: the Edinburgh inventory. Neuropsychologia. 1971; (9): 97–113.
12. Sanford J, Moreland J, Swanson LR, Stratford PW. Reliability of the Fugl-Meyer assessment for testing motor performance in patients following stroke. J Gowland C Phys Ther. 1993; 73 (7): 447–54.
13. Bohannon RW, Smith MB. Interrater reliability of a modified Ashworth scale of muscle spasticity. J Phys Ther. 1987; 67 (2): 206–7.
14. Doussoulin SA, Rivas SR, Campos SV. Validation of «Action Research Arm Test» (ARAT) in Chilean patients with a paretic upper limb after a stroke. Rev Med Chil. 2012; 140 (1): 59–65.
15. Alt Murphy M, Willén C, Sunnerhagen KS. Movement kinematics during a drinking task are associated with the activity capacity level after stroke. J Neurorehabil Neural Repair. 2012; 26 (9): 1106–15.
16. Valdés BA, Glegg SMN, Van der Loos HFM. Trunk Compensation During Bimanual Reaching at Different Heights by Healthy and Hemiparetic Adults. J Mot Behav. 2017; 49 (5): 580–92.
17. van Kordelaar J, van Wegen EE, Kwakkel G. Unraveling the interaction between pathological upper limb synergies and compensatory trunk movements during reach-to-grasp after stroke: a cross-sectional study. J Exp Brain Res. 2012; 221 (3): 251–62.
18. Roh J, Rymer WZ, Perreault EJ, et al. Saturated muscle activation contributes to compensatory reaching strategies after stroke. J Neurophysiol. 2013; 109 (3): 768–81.
19. Basteris A, Nijenhuis SM, Stienen AH, et al. Training modalities in robot-mediated upper limb rehabilitation in stroke: a framework for classification based on a systematic review. J Neuroeng Rehabil. 2014; 10 (11): 111.
20. Daunoraviciene K, Adomaviciene A, Grigonyte A, Griškevičius J, Juocevicius A. Effects of robot-assisted training on upper limb functional recovery during the rehabilitation of poststroke patients. J Technol Health Care. 2018; 26 (2): 533–42.
21. Устинова К. И., Черникова Л. А., Хижникова А. Е., Пойдашева А. Г., Супонева Н. А., Пирадов М. А. Теоретическое обоснование классических методов двигательной реабилитации в неврологии. Анналы клинической и экспериментальной неврологии. 2018; 12 (3): 54–60.

EFFICIENCY OF IMAGE VISUALIZATION SIMULATOR TECHNOLOGY FOR PHYSICAL REHABILITATION OF CHILDREN WITH CEREBRAL PALSY THROUGH PLAY

Gorelik VV[1]✉, Filippova SN[2], Belyaev VS[3], Karlova EV[4]

[1] Togliatti State University, Togliatti, Russia

[2] Russian State Social University, Klin, Russia

[3] Moscow City Pedagogical University, Moscow, Russia

[4] FGBUZ MRTs Sergievsky Mineral Waters of FMBA, Samara Region, Russia

The number of children born with cerebral palsy (CP) remains stably high. Novel approaches for rehabilitation of such patients are being sought. This study aimed to define the efficiency of the image visualization technologies in play activity for the physical rehabilitation of children with cerebral palsy. Sixteen boys with spastic diplegia aged 7–9 participated in the study. They were divided into treatment group (TG) and control group (CG), 8 children each. The TG patients were trained using the virtual reality based Krisaf training simulator twice a week for 40 minutes during 8 months. The child was suspended in the horizontal position and looked at the monitor through the specialised eyeglasses. Under the conditions of the marine environment immersion simulation with reduced gravity children performed motor tasks through play: searched for treasures, competed with dolphins etc. The CG patients attended the physical therapy lessons. Rehabilitation lessons using the virtual reality based Krisaf training simulator for children affected with spastic cerebral palsy led to a significant improvement of motor skills. Various motion tests showed an improvement over baseline, the average indicators increased 1.30–1.48 times. The difference between TG and CG results was statistically significant. In the CG referred to physical therapy the indicators increase was less than 10%, in the TG the increase reached 30–40%. It was concluded that the use of virtual reality based technologies promotes the optimization of neurophysiological processes in the motor analyzer cortical areas and better adaptation to motor loads.

Keywords: cerebral palsy, game situations, virtual reality technologies, motor actions, adaptation

Author contribution: Gorelik VV — study concept and design; Filippova SN — text writing and editing, statistical analysis; Belyaev VS — manuscript editing; Karlova EV — data acquisition and processing, statistical analysis.

Compliance with ethical standards: this study was approved by the Ethics Committee of Togliatti State University (protocol № 3 dated September 10, 2018). Parents of the children submitted the informed consent forms allowing their children to participate in the study.

✉ **Correspondence should be addressed:** Viktor V. Gorelik
Belorusskaya 14, Togliatti, 445020; lecgoy@list.ru

Received: 19.07.2019 **Accepted:** 04.08.2019 **Published online:** 17.08.2019

DOI: 10.24075/brsmu.2019.051

ЭФФЕКТИВНОСТЬ ТРЕНАЖЕРНОЙ ТЕХНОЛОГИИ ВИЗУАЛИЗАЦИИ ОБРАЗОВ В ИГРОВОЙ ДЕЯТЕЛЬНОСТИ ДЛЯ ДВИГАТЕЛЬНОЙ РЕАБИЛИТАЦИИ ДЕТЕЙ С ДЕТСКИМ ЦЕРЕБРАЛЬНЫМ ПАРАЛИЧОМ

В. В. Горелик[1]✉, С. Н. Филиппова[2], В. С. Беляев[3], Е. В. Карлова[4]

[1] Тольяттинский государственный университет, Тольятти, Россия

[2] Российский государственный социальный университет, Клин, Россия

[3] Московский городской педагогический университет, Москва, Россия

[4] Медицинский реабилитационный центр Сергиевские минеральные воды Федерального медико-биологического агентства, Самарская область, Россия

Число детей, рождающихся с диагнозом «детский церебральный паралич» (ДЦП), остается стабильно высоким. Ведется поиск новых подходов к реабилитации таких пациентов. Целью исследования было определить эффективность использования технологии игровой деятельности на основе визуализации образов в процессе физической реабилитации детей с ДЦП. В исследовании участвовали 16 мальчиков со спастической диплегией в возрасте 7–9 лет, разделенные на две группы: экспериментальную (ЭГ) и контрольную (КГ) — по 8 детей в каждой. В ЭГ занятия проводили на тренажере виртуальной реальности «Крисаф» 2 раза в неделю по 40 мин в течение 8 месяцев. Ребенок при этом находится в подвешенном горизонтальном положении и, используя специальные очки, смотрит на экран. В условиях имитации состояния погружения в морскую среду, при понижении гравитационных воздействий дети выполняют двигательные задания в игровой форме: ищут сокровища, соревнуются с дельфинами и т. д. Дети КГ посещали занятия ЛФК. Реабилитационные занятия детей со спастической формой ДЦП на тренажере «Крисаф» с элементами технологии виртуальной реальности приводили к значительному возрастанию двигательных возможностей. В ЭГ наблюдали рост показателей при проведении разных двигательных тестов, средние тестовые значения улучшились в 1,30–1,48 раза по сравнению с исходными данными. Улучшение результатов в ЭГ статистически достоверно отличалось от результатов КГ. У детей КГ результаты в среднем улучшились менее чем на 10% под влиянием ЛФК, в ЭГ — на 30–40%. Сделан вывод, что применение технологий виртуальной реальности способствует оптимизации нейрофизиологических процессов в корковых зонах двигательного анализатора, повышению адаптации к двигательным нагрузкам.

Ключевые слова: ДЦП, игровая деятельность, технологии виртуальной реальности, двигательные упражнения, адаптация

Информация о вкладе авторов: В. В. Горелик — концепция и дизайн исследования; С. Н. Филиппова — написание текста, редактирование, статистическая обработка; В. С. Беляев — редактирование рукописи; Е. В. Карлова — сбор и обработка материала, статистическая обработка.

Соблюдение этических стандартов: исследование одобрено локальным этическим комитетом Тольяттинского государственного университета (протокол № 3 от 10 сентября 2018 г.). На участие в эксперименте для всех детей получено добровольное информированное согласие от их родителей.

✉ **Для корреспонденции:** Виктор Владимирович Горелик
ул. Белорусская, 14, г. Тольятти, Самарская обл., 445020; lecgoy@list.ru

Статья получена: 19.07.2019 **Статья принята к печати:** 04.08.2019 **Опубликована онлайн:** 17.08.2019

DOI: 10.24075/vrgmu.2019.051

According to statistics, the overall incidence of newborns is increasing in Russia, against the background of an unstable birth rate in the regions. In 2018, in Russia, cerebral palsy (CP) was diagnosed in ~8 of 1000 newborns. The incidence growth trends were previously recorded by the WHO specialists [1, 2].

Cerebral palsy is a polyetiologic disease, it belongs to the group of neurological diseases and is characterized by a variety of pathogenetic forms. The disease appears as neurological symptoms resulting from lesions of the cortical areas as well as of the the brain cerebellar area. Early onset and ineffective diagnosis lead to the predominance of severe forms of musculoskeletal system structural and functional impairment (upright posture maintenance, balance and muscle tone) [3–6]. Muscle tone (MT) and its regulation are considered the main factors of voluntary motor activity in humans. Various muscle disorders are observed in patients with cerebral palsy: spasticity, muscle hypertonia, rigidity, hypotonia, dystonia, atonia [7–9].

Manifesting as a MT increase the spastic cerebral palsy prevails among the different disease forms. Due to impairment of the pyramidal pathways the muscles of the patients are excessively tense. Together with an increase in MT, limb deformities and flexion contractures (a decrease in the volume of passive movements in the joints) can be observed. Spasticity is characteristic for spastic diplegia and hemiplegic cerebral palsy [10–14]. Despite the morbidity of the cerebral palsy as a severe disease that violates the psychophysical and social adaptation of patients, there is a shortage of methods based on the age-related psychophysical features of an affected patient for the rehabilitation of primary school age children [15–18]. Novel comprehensive and integrative approaches to the rehabilitation of patients are being sought, including treatment of comorbidity (epilepsy, somatic diseases), pharmaceutical and surgical treatment of spasticity and organic muscle damage. Development of methods for influencing the adaptive mechanisms and body reserves of infants and children, activating the psychophysiological regulatory mechanisms of the motor analyzer, optimizing emotional processes taking into account the age-related needs in game activity and motivating motor activity seem promising to us.

To achieve the correction and developmental results, physical rehabilitation of children with cerebral palsy should be based on the effective instruments choice which could influence the affected child [19–21]. It is extremely important to take into account the age-related psychophysical features of the patients in order to create optimal conditions for the formation of motor skills in children with disabilities and to increase the efficiency of their rehabilitation [22, 23].

During ontogenesis in children with cerebral palsy the individual, fundamentally different from normal, hierarchical regulatory systems of the motor analyzer are formed, which ensure the performance of involuntary and voluntary movements [10–17].

It is well known that motor activity is one of the main physiological components of the formation and development of the child's organism. A decrease in motor activity leads to the functional status of the musculoskeletal system impairment, causing changes in the functional status of the vascular and respiratory systems, metabolic disturbances, and decreased performance [8, 18].

Every movement depends on the spatial sense. Brain processes information coming through the sensory system and uses it for the locomotor movement formation. Children with cerebral palsy demonstrate the abnormal sensory system development pattern, which causes the inadequate responce to the incoming information and leads to the locomotor movement development delay [16].

The cerebral palsy associated motor development impairment is a result of the motor analyzer cortical areas regulatory effects disorder. Motor analyzer is the main control center of the entire human body muscle system (MS). In speech activity, the motor component is responsible for the speech and motor acts, therefore patients with cerebral palsy often demonstrate the impaired speech [19].

For patients with musculoskeletal disorders and neurological diseases the formation of altered motor stereotypes and pathologically incorrect movements is typical. These are formed due to the desire of patients to reduce pain or compensate the incorrect work of hypotonic muscles [20]. The altered motor stereotypes lead to the gravity center shift and to improper gait, which enhance the disease severity. Therefore, the main task is to correct the pathological motor stereotypes during rehabilitation. The Krisaf training simulator registers the body pressure force over the entire area (in prone position) and allows one to detect these problems at an early stage and successfully eliminate them. To identify its rehabilitation capability, a pedagogical experiment (PE) was carried out using the Krisaf training simulator at the forming stage.

This study aimed to define the rehabilitation capability of the play methods using the image visualization based Krisaf training simulator during the complex physical rehabilitation of the 7–9 years old children suffering from spastic cerebral palsy.

The goals were: 1) to assess the baseline indicators of motor functions in children with spastic cerebral palsy aged 7–9; 2) to determine the effectiveness of the virtual reality based Krisaf training simulator for the motor functions development in children with spastic cerebral palsy aged 7–9; 3) to evaluate the virtual reality technology rehabilitating capabilities during the play activity and their possible impact on the various types of motor skills in children with cerebral palsy.

METHODS

Study management and methods for diagnosing the functional status of muscle system in 7–9 years old children with cerebral palsy

The study lasted 8 months (September 2018 through April 2019). It was conducted at FGBUZ MRTs Sergievsky Mineral Waters of FMBA, Russia. Sixteen boys with cerebral palsy aged 7–9 participated in the study. Inclusion criteria: children with cerebral palsy (spastic diplegia); children of the same gender; children of a similar age with the same height-weight relationship. The participants were divided into two groups (8 children each): treatment group (TG) and control group (CG). In the TG training was performed using the Krisaf virtual reality based training simulator 2 times a week for 40 minutes during 8 months, the children also practiced physical therapy excercises twice a week. Children of the CG only performed the physical therapy excercises 2 times a week.

Exclusion criteria: acute infectious diseases and other medical contraindications to physical therapy. Physical features of the TG and CG children were similar.

Pedagogical experiment (PE)

The pedagogical experiment lasted September 2018 through April 2019. It included benchmarking, formation and control stages.

1. *Benchmarking stage*: registration of the muscular system functional status baseline indicators in children with cerebral palsy aged 7–9.

2. *Formation stage*: the TG children were trained using the Krisaf virtual reality based training simulator, they also practiced physical therapy excercises twice a week. The CG children were trained by the instructor according to the standard exercise therapy program for the rehabilitation of children with cerebral palsy.

3. *Control stage*: registration of the resulting indicators using the methods applied in the beginning of the pedagogical experiment.

Motion tests

Assessment of motor skills in children with cerebral palsy was performed using the number of motion tests allowing us to evaluate the functional status of the children's musculoskeletal system.

1. Assessment of the back muscles static endurance capability

Head lifting from the back position.

Starting position: lying flat on the back. The trainer takes the child by the wrists and lifts him. The child should raise his head and hold it in this position. Results are measured in seconds.

Head lifting from the stomach position.

Starting position: lying on the stomach, the arms bent at the elbow joints remain at the shoulder level. The child straightens his arms and lifts his head. Results are measured in seconds.

2. Assessment of the abdominal muscles endurance capability

Trunk lifting from the back position.

Starting position: lying flat on the back; the trainer holds the child's legs bent at the knee joints. The child raises the body from the starting position on his own touching the knees by his chest. The result is registered as the number of repeats.

3. Assessment of the hand muscles endurance capability

Wrist flexion and extension.

Starting position: sitting on the chair. The child's wrists are hanging from the armrests. The patient should bend and strengthten the left and right wrists alternately 10 times in a row. Results are measured in seconds. Normally, the result should be within 12–15 s.

Finger flexion.

Starting position: sitting on the chair. The child should alternately touch the thumb with each of the other fingers tips making his fingers to form a ring. Results are measured in seconds.

4. Assessment of the leg muscles endurance capability

Leg raise.

Starting position: lying flat on the back. The child raises his legs alternately and bends them at the knee joints. Results are measured in seconds.

Statistical analysis

The following mathematical statistics methods were applied when processing the data obtained: Kolmogorov–Smirnov test (nonparametric test of the equality of continuous, onedimensional probability distributions) and parametric Student's *t*-test. The differences were considered statistically significant at $p < 0.05$.

Kolmogorov–Smirnov test revealed that the studied variables fall within the limits of normality, which allowed applying the Student's *t*-test for interrelated and independent samples.

The SPSS 17.0 software for Windows was used to process the experimental data.

Forming method based on using the Krisaf training simulator for children with cerebral palsy aged 7–9

During the PE the Krisaf training simulator (Krisaf; Russia) was used to provide the forming effect. Simulator helps to imitate

Table 1. Musculoskeletal system functional status assessment results for children with cerebral palsy aged 7–9 obtained at the benchmarking stage of the PE

№	Tests	TG M ± *m*	CG M ± *m*	Student's *t*-test
1	Head lifting from the back position (s)	19.7 ± 2.7	20.6 ± 2.6	0.7
2	Head lifting from the stomach position (s)	17.4 ± 2.1	16.9 ± 2.04	0.34
3	Trunk lifting from the back position (number of repeats)	7.6 ± 1.4	7.3 ± 1.8	0.13
4	Wrist flexion and extension (s)	18.7 ± 2.8	19.9 ± 2.65	0.4
5	Finger flexion (s)	20.2 ± 3.1	19.6 ± 2.9	0.32
6	Leg raises (s)	15.5 ± 2.4	15.5 ± 2.4	0.12

Note: M — average; *m* — standard error of the mean; *p* — significance of differences between the TG and CG results; no statistically significant differences between the groups ($p > 0.05$).

Table 2. Musculoskeletal system functional status re-assessment results for children with cerebral palsy aged 7–9 obtained at the control stage of the PE

№	Tests	TG M ± *m*	CG M ± *m*	Student's *t*-test
1	Head lifting from the back position (s)	28.7 ± 3.8*	21.4 ± 3.6	2.4
2	Head lifting from the stomach position (s)	25.9 ± 2.76*	18.9 ± 2.5	2.54
3	Trunk lifting from the back position (number of repeats)	14.6 ± 2.1*	8.4 ± 1.5	3.13
4	Wrist flexion and extension (s)	12.4 ± 1.32*	17.7 ± 1.7	3.1
5	Finger flexion (s)	14.4 ± 2.9*	18.6 ± 3.1	2.5
6	Leg raises (s)	22.9 ± 2.36*	16.7 ± 2.4	3.03

Note: M — average; *m* — standard error of the mean; TG — treatment group; CG — control group; * — significant differences between the TG and CG results, $p < 0.05$.

the movements of the affected child in the aquatic environment [4, 21].

The Krisaf training simulator dispays images on the monitor. Audio signals transmitted through headphones help the patient to adjust his motor activity. Thus, the correct execution of excercises can be achieved and the new, close to normal, motor stereotypes can be formed.

Physical rehabilitation of children with cerebral palsy is a labour-intensive and complex process that requires significant efforts of medical personnel and physical therapy trainers. Virtual reality modeling takes place simulating immersion of the child in the gaming aquatic environment. The game situation encourages the child to move more actively. This helps to simulate movements in the aquatic environment, balancing the child's weight by a special pneumatic system, which helps to establish the conditions of reduced gravity. The child with weakened muscle strength and lack of sufficient coordination due to cerebral palsy can perform the movements more accurately. The patient's training using the simulator is based on the execution of wave-like movements that look like the dolphin's movements [22, 23]. Play elements are important, because play activity is essential for little patients. In children

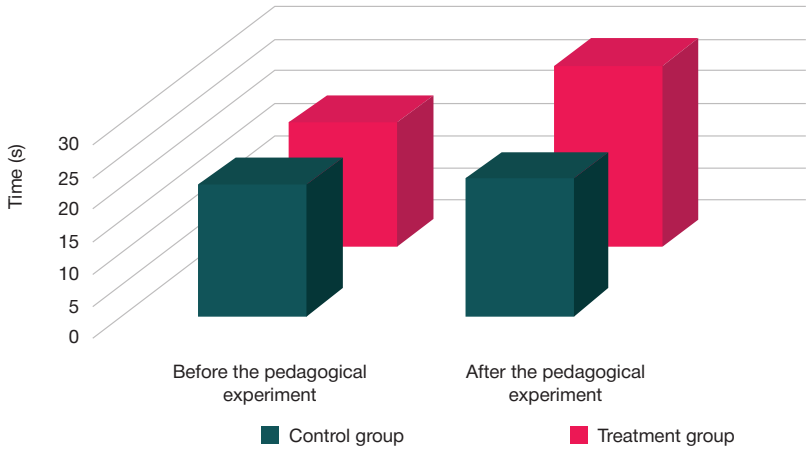

Fig. 1. Comparative data of the "Head lifting from the back position" motion test for children with cerebral palsy aged 7–9 from CG and TG obtained at the control stage of the PE

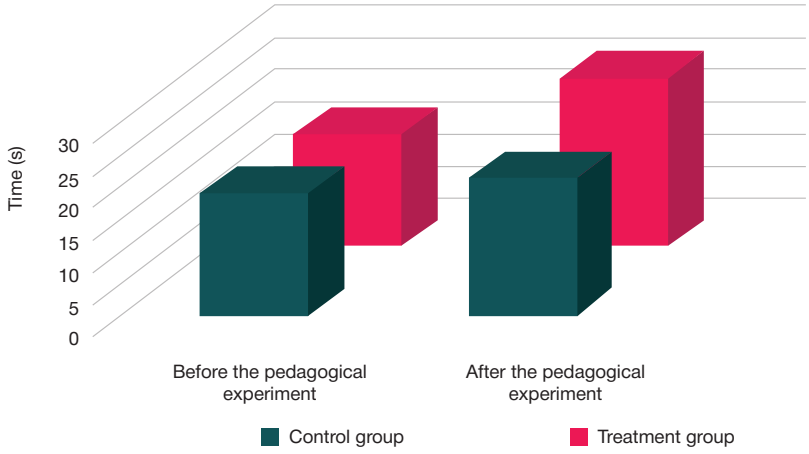

Fig. 2. Comparative data of the "Head lifting from the stomach position" motion test for children with cerebral palsy aged 7–9 from CG and TG obtained at the control stage of the PE

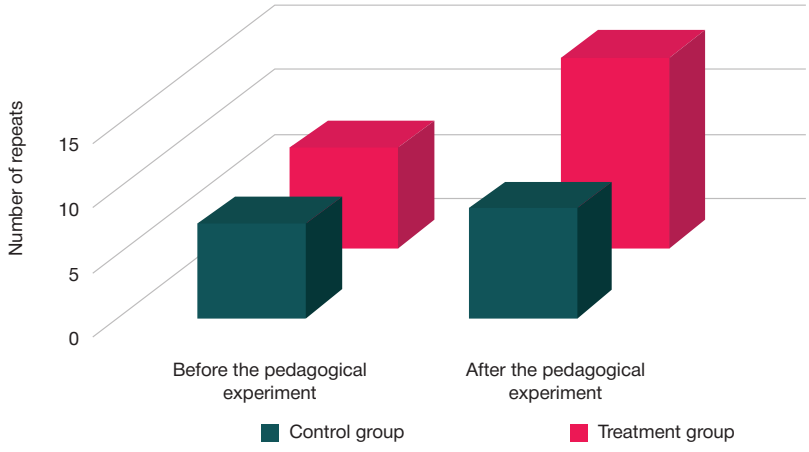

Fig. 3. Results of the "Trunk lifting from the back position" motion test for children with cerebral palsy aged 7–9 from CG and TG obtained at the control stage of the PE

with cerebral palsy the Krisaf training simulator: a) improves the information perception and the quality of the arbitrary movements performance through image visualization; b) activates the right hemisphere by the virtual reality elements and facilitates the movements execution due to the gravity decrease.

RESULTS

At the benchmarking stage of the study preliminary testing was performed to define the baseline of the motor skills development in children with cerebral palsy (Table 1).

According to the results of initial testing, we can conclude that there are no significant differences in the indicators of motor characteristics in children with cerebral palsy of both groups.

After a course of lessons using the virtual reality based Khrisaf training simulator, a control test was conducted in both groups to identify the effectiveness of the method for physical rehabilitation of children with cerebral palsy (Table 2).

Re-examination using the motion tests at the PE control stage revealed a pronounced positive dynamics in the TG and slight changes in the indicators in the CG. Significant differences in the results were found between the control and treatment groups. Figs. 1 and 2 show the "Head lifting from the back position" and "Head lifting from the stomach position" tests results obtained for the CG and TG before and after the experiment.

Head holding time in children in the TG increased by 9 s (back position) and 8.5 s (stomach position), which corresponds to the 32% increase of strength and endurance of the limb girdle muscles in children with cerebral palsy.

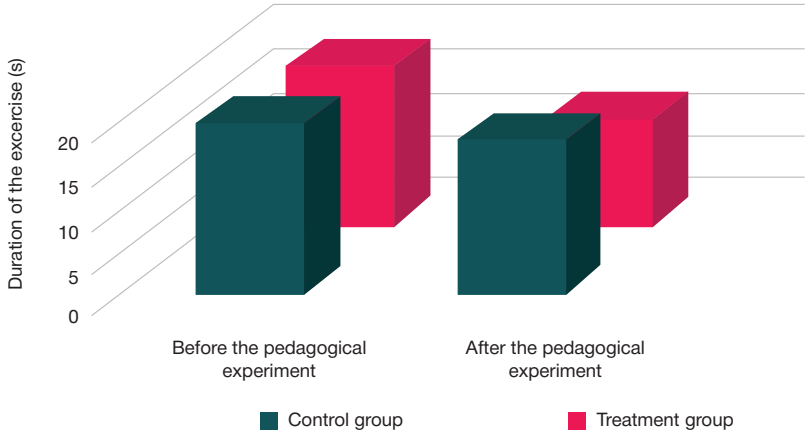

Fig. 4. Results of the "Wrist flexion and extension" motion test for children with cerebral palsy aged 7–9 from CG and TG obtained at the control stage of the PE

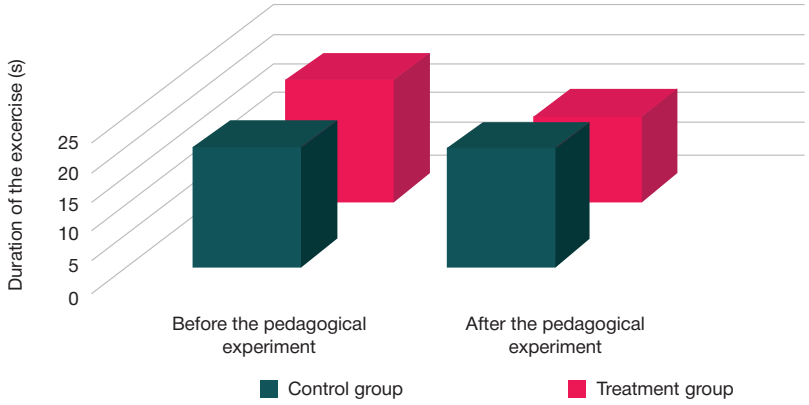

Fig. 5. Results of the "Finger flexion" motion test for children with cerebral palsy aged 7–9 from CG and TG obtained at the control stage of the PE

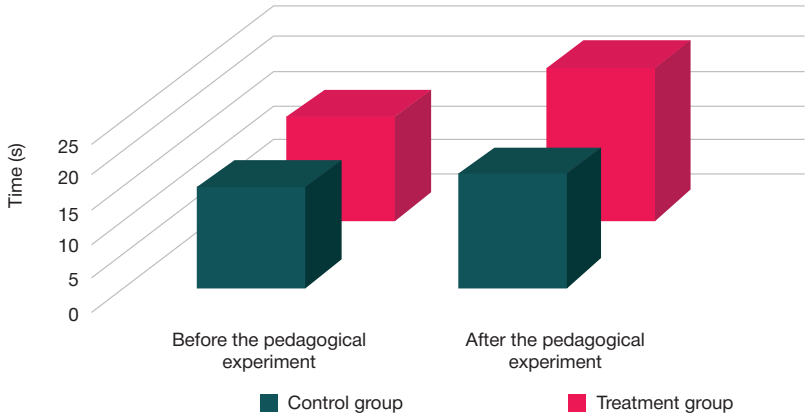

Fig. 6. Results of the "Legs lifting" motion test for children with cerebral palsy aged 7–9 from CG and TG obtained at the control stage of the PE

This is important for the normalization of the upper limbs function, in addition, an increase in the activity of these muscle groups helps to improve the brain blood supply. In the CG, the increase in the muscle strength was 3.8% (back position) and 7% (stomach position), the increase over values was not statistically significant. Thus, it can be said that the use of virtual reality base simulator technologies is effective for rehabilitation of 7–9 years old children with spastic cerebral palsy. The effectiveness of lessons is associated with the activation of the right hemisphere neurophysiological mechanisms and with the increase of the body's adaptive capabilities [14, 17].

Fig. 3 shows the "Trunk lifting from the back position" motion test results.

The "Trunk lifting from the back position" test results demonstrate that after the simulator lessons the back and abdomenal muscle strength significantly increased in the TG children (1.9 times compared to the baseline, i.e. from 7.6 to 14.6 repeats). In the CG the muscle strength remained almost the same. These data serve as an indirect proof of the improvement of motor skills and adaptive mechanisms in children aged 7–9 with spastic cerebral palsy, testify to the good rehabilitation effect of the Krisaf virtual reality based training simulator.

Figs. 4 and 5 show the "Wrist flexion and extension" and "Finger flexion" motion tests results.

The speed qualities of the limb girdle muscles, the flexor-extensors of the upper limbs, as well as the finger muscles of fine motor skills increased in the TG after a series of lessons using the Khrisaf training simulator. For the limb girdle muscles the test execution time was reduced by 6.3 s (35%), and in the CG it was reduced by 2.2 s (11%). In the TG the fine motor skills also improved: test execution time was reduced by 5.8 s (29%). In the CG it was reduced by 0.3 s (1.5%). This suggests that image visualisation during the training lessons helped to establish a friendly environment for children aged 7–9 with delayed verbal function development due to impaired speech and motor functions as compared with the verbal commands and instructions of the physical therapy trainers. Improvement of the fine motor skills in children with cerebral palsy after rehabilitation using the visualization elements was associated with the motor analyzer cortical areas activation. The speed of the small differentiated movements of the fingers also increased.

Fig. 6 shows the "Legs lifting" motion test results for children aged 7–9 with cerebral palsy.

When determining the speed-strength characteristics of the lower limbs muscles, it was clear that the average result improved. In the TG it increased by 7.4 s (33%), and in the CG by 1.2 s (6%). These data indicated the effectiveness of rehabilitation in children with spastic cerebral palsy using the image visualization technology based Krisaf training simulator. An increase in the motor and strength capabilities of the lower extremities in such patients indicated a trend towards the motor analyzer cortical areas neurophysiological processes improvement together with adaptation to motor loads due to the increase in the balance of the right hemisphere functions while using the image visualization method.

Thus, when comparing the TG and CG indicators at the control stage of PE, the significant improvements in the TG indicators were found, which exceeded the results of the CG. These differences arose due to the fact that virtual reality technologies were introduced in the TG, while in the CG the standard exercise therapy program was used.

DISCUSSION

Our study has shown that the virtual reality technologies influence on both the control and executive centers of the motor analyzer is not well understood. It can be assumed that immersion of children in the reduced gravity conditions and in the aquatic environment virtual reality promotes involuntary relaxation of all muscles, as it happens in case of real water immersion. With the help of the simulator complex neurophysiological and sensory effects, muscles start working and somatic and sensory integration improves. This increases the efficiency of lessons and makes the rehabilitation of children with cerebral palsy more effective.

Stimulation of the right hemisphere by visual information facilitates execution of physical exercises. For children with cerebral palsy aged 7–9 the visual information is easier to understand than the trainer's verbal instructions [19]. In addition, the right hemisphere associated adaptive mechanisms of the body can be activated [17]. Positive emotions from training through play promote relaxation of constricted muscles [3]. Thus, the virtual reality based Khrisaf training simulator affecting a number of neurophysiological and sensory mechanisms has an integrative rehabilitative effect on the psychophysical state of 7–9 years old children with spastic cerebral palsy. This indicates that image visualization helps to establish friendly environment for the children with cerebral palsy as compared with the exercise therapy trainer's verbal instructions. Since children with cerebral palsy aged 7–9 often demonstrate the speech development delay and it is difficult for them to understand the meaning of verbal constructions, communication between patient and trainer may be impaired. Image visualization helps to restore mutual understanding and interaction.

Currently the simulator-based methods attract close attention of researchers even in the field of rehabilitation of children with various forms of cerebral palsy. Novel types of simulators are being developed taking into account the latest advances in the understanding of the pathogenesis of diseases, including cerebral palsy. At the same time, application and research using simulator methods provide valuable data for understanding the mechanisms of correction and rehabilitation of the affected person.

Image visualization and virtual reality based training simulator meets the need of a 7–9 years old child in playing. The simulator has an impact both on the regulatory neuropathological, psychopathological, and executive links of the motor analyzer as well as the psychological processes and the quality of life of rehabilitated children.

Improvement in the functional status of the children's musculoskeletal system obtained in this study with the use of virtual reality based technology opens up the prospect of the further research of regulatory mechanisms and recovery processes in children with cerebral palsy.

CONCLUSIONS

1. Rehabilitation using the virtual reality based Krisaf training simulator led to significant (1.3–1.5 times) improvement of the motor capabilities in children with spastic cerebral palsy aged 7–9. 2. Significant increase in the strength and endurance of the limb girdle and lower limbs muscles indicated the effectiveness of rehabilitation using the image visualization technology based Krisaf training simulator. The endurance of the back and abdomen muscles in the TG increased 1.9 times, the adaptation to motor loads improved. In the CG minor changes took place. 3. After training using the image

visualization based training simulator the speed of movements in the upper limbs increased, the fine motor skills of the hands improved. Improvement of the fine motor skills in children with cerebral palsy testified to the better balance of the cortical areas of the motor analyzer neurophysiological processes.

4. The positive dynamics of the motor capabilities in children with cerebral palsy when using novel virtual reality technologies for rehabilitation purposes testified to the optimization of neurophysiological processes in the cortical areas of the motor analyzer and better adaptation to motor loads.

References

1. Golovach MV. Modern trends in the growth of cerebral palsy. Materials of the First International Congress "Problems of complex rehabilitation of children suffering from cerebral palsy". March 2–3, 2006. M., 2006; 37–8.
2. Shalina OS, Zhuravleva OS. Study of somatosensory integration in children with cerebral palsy. VIII interdisciplinary scientific and practical Congress with international participation "Cerebral palsy and other movement disorders in children". The proceedings of the Congress. M., 2018; p. 128–9.
3. Malkova EE. the Problem of improving the effectiveness of the system of medical,psychological and social rehabilitation of children with cerebral palsy. VIII interdisciplinary scientific and practical Congress with international participation "Cerebral palsy and other movement disorders in children". The proceedings of the Congress. M., 2018; p. 96–7.
4. Mikadze YuV. Neuropsychology of childhood: textbook. St. Petersburg: Peter, 2013; 288.
5. Ivanova EV, Nikitina DN. Basic principles and aspects of the use of therapeutic physical culture in the comprehensive rehabilitation of children and adolescents with cerebral palsy. In the collection: the Study of various areas of psychology and pedagogy. Collection of articles of the International scientific-practical conference. M., 2018; p. 69–72.
6. Blum EE, Blum NE, Antonov AR. To the issue of rehabilitation of children suffering from cerebral palsy (cerebral palsy). Bulletin of the peoples' friendship University of Russia. Series: Medicine. 2004; (1): 96–9.
7. Baranov AA, Klochkova OA, Kurenkov AL, et al. The Role of brain plasticity in the functional adaptation of the body in cerebral palsy with hand injury. Pediatric pharmacology. 2013; (9): 6–11.
8. Bykova OV, Platonova AN, Balkanskaya SV, Batysheva TT. Children's cerebral palsy and epilepsy: approaches to treatment and rehabilitation. Journal of neurology and psychiatry. 2014; (7): 25–34.
9. Vlasenko SV, Golubova TF. Features of correction of spastic contractures, combined with changes in limb muscles in patients with cerebral palsy. In the collection: VIII interdisciplinary scientific and practical Congress with international participation "Cerebral palsy and other movement disorders in children." The proceedings of the Congress. M., 2018; p. 52–3.
10. Badalyan LO. Children's cerebral palsy. M.: Media, 2015; 983.
11. Bundy A, Lane S, Murray E. Sensory integration. Theory and practice. M.: Terevinf, 2018; 768.
12. Khlynov DYu, Filippova SN. Stretching: prospects of application for improvement and rehabilitation of the population, monograph. M.: Teler, 2019; 139.
13. Novikova TV. Physical rehabilitation of children 8–12 years with cerebral palsy in the form of spastic diplegia. In the collection: Medical physical culture: achievements and prospects of development. Proceedings of the VI all-Russian scientific-practical conference with international participation. M., 2017; p. 162–6.
14. Fedina RG, Filippova SN. Neurophysiological and hormonal-regulatory determinants of adaptation of the Russian population in extreme and sub-extreme climatic regions. In the collection: XIV international Interdisciplinary Congress "Neuroscience for medicine and psychology. The proceedings of the Congress. 30 may — 10 June 2018. Sudak: Crimea, 2018; 471.
15. Voronin DM, Chaychenko MV. Technology, the use of physical rehabilitation in the recovery of children with cerebral palsy. Problems of modern pedagogical education. 2019; 63 (2): 95–9.
16. Korsakov EA. the Role of verticalization and orthopedic correction in medical rehabilitation of children with cerebral palsy. Bulletin of physiotherapy and balneology. 2015; 21 (2): 133a–133.
17. Filippova SN, Egoshina VI, Matveev YuA. Physical rehabilitation of children with cerebral palsy on the basis of determining the rate of formation of the cerebral motor programs. Physical culture and health. 2017; (1): 7–11.
18. Abasov RG, Gorelik VV. Features of coordination abilities of children of cerebral palsy at the age of 10–12 years at occupation by mini football. Collector. Problems and prospects of physical education, sports training and adaptive physical culture materials of the all-Russian conference with international participation. VOLGA region state Academy of physical culture, sports and tourism. Kazan, 2018; 788–92.
19. Lobastova IV. Influence of physical rehabilitation on the development of cognitive sphere in children with cerebral palsy. Siberian psychological journal. 2010; (36): 59–61.
20. Galieva GYu, Panchenko TN, Valueva IV, et al. Modern approaches and methods of physical therapy in rehabilitation of children with cerebral palsy in a clinical psychoneurological sanatorium. 2018; (17): 72–5.
21. Baranov AA, Namazova-Baranova LS, Kuzenkova LM, et al. Children's cerebral palsy in children. Clinical guidelines. Ministry of health of the Russian Federation, Union of pediatricians of Russia. M., 2016; 478.
22. Dobrynina EA. Physical rehabilitation of children with cerebral palsy. Bulletin of science and education. 2018; 1, 4 (40): 109–10.
23. Troska ZA, Shershnev OA. Improvement of professional rehabilitation of children with cerebral palsy. Scientific notes of the Russian state social University. 2015; 14 (3): 156–67.

Литература

1. Головач М. В. Современные тенденции роста детского церебрального паралича. Материалы Первого Международного конгресса «Проблемы комплексной реабилитации детей, страдающих детским церебральным параличем» 2–3 марта 2006. М.: 2006; 37–8.
2. Шалина О. С., Журавлева О. С. Исследование особенностей соматосенсорной интеграции у детей с детским церебральным параличем. VIII междисциплинарный научно-практический конгресс с международным участием «Детский церебральный паралич и другие нарушения движения у детей». Материалы конгресса. М., 2018; 128–9.
3. Малкова Е. Е. Проблема повышения эффективности системы медико-психолого-социальной реабилитации детей с ДЦП. VIII междисциплинарный научно-практический конгресс с международным участием «Детский церебральный паралич и другие нарушения движения у детей». Материалы конгресса. М., 2018; 96–7.
4. Микадзе Ю. В. Нейропсихология детского возраста: учебное пособие. СПб.: Питер, 2013; 288 с.
5. Иванова Е. В., Никитина Д. Н. Основные принципы и аспекты использования лечебной физической культуры в комплексной реабилитации детей и подростков с ДЦП. В сборнике: Исследование различных направлений психологии и педагогики. Сборник статей Международной научно-

практической конференции. М., 2018; 69–72.
6. Блюм Е. Э., Блюм Н. Э., Антонов А. Р. К вопросу реабилитации детей, страдающих детским церебральным параличом (ДЦП). Вестник Российского университета дружбы народов. Серия: Медицина. 2004; (1): 96–9.
7. Баранов А. А., Клочкова О. А., Куренков А. Л. и др. Роль пластичности головного мозга в функциональной адаптации организма при церебральном параличе с поражением рук. Педиатрическая фармакология. 2013; (9): 6–11.
8. Быкова О. В., Платонова А. Н., Балканская С. В., Батышева Т. Т. Детский церебральный паралич и эпилепсия: подходы к лечению и реабилитации. Журнал неврологии и психиатрии. 2014; (7): 25–34.
9. Власенко С. В., Голубова Т. Ф. Особенности коррекции спастических контрактур, сочетающихся с изменением мышц конечностей у больных ДЦП. В сборнике: VIII междисциплинарный научно-практический конгресс с международным участием «Детский церебральный паралич и другие нарушения движения у детей». Материалы конгресса. М., 2018; 52–3.
10. Бадалян Л. О. Детские церебральные параличи. М.: Медиа, 2015; 983 с.
11. Банди А., Лейн Ш., Мюррей Э. Сенсорная интеграция. Теория и практика. М.: Теревинф, 2018; 768 с.
12. Хлынов Д. Ю., Филиппова С. Н. Стретчинг: перспективы применения для оздоровления и реабилитации населения. М.: Телер, 2019; 139 с.
13. Новикова Т. В. Физическая реабилитация детей 8–12 лет с ДЦП в форме спастической диплегии. В сборнике: Лечебная физическая культура: достижения и перспективы развития. Материалы VI Всероссийской научно-практической конференции с международным участием. М., 2017; 162–6.
14. Федина Р. Г., Филиппова С. Н. Нейрофизиологические и гормонально-регуляторные детерминанты адаптации населения РФ в экстремальных и субъэкстремальных климатических регионах. В сборнике: XIV Международный Междисциплинарный Конгресс «Нейронаука для медицины и психологии. Материалы конгресса 30 мая — 10 июня 2018. Судак: Крым, 2018; 471.
15. Воронин Д. М., Чайченко М. В. Технологии использования физической реабилитации при восстановлении детей с ДЦП. Проблемы современного педагогического образования. 2019; 63 (2): 95–9.
16. Корсакова Е. А. Роль веритикализации и ортопедической коррекции в медицинской реабилитации детей с ДЦП. Вестник физиотерапии и курортологии. 2015; 21 (2): 133а–133.
17. Филиппова С. Н., Егозина В. И., Матвеев Ю. А. Физическая реабилитация детей с диагнозом ДЦП на основе определения скорости формирования церебральных моторных программ. Культура физическая и здоровье. 2017; (1): 7–11.
18. Абасов Р. Г., Горелик В. В. Особенности координационных способностей детей ДЦП в возрасте 10–12 лет при занятии мини футболом. Сборник. Проблемы и перспективы физического воспитания, спортивной тренировки и адаптивной физической культуры материалы Всероссийской с международным участием научно-практической конференции. Казань: ФГБОУ ВО «Поволжская государственная академия физической культуры, спорта и туризма», 2018; 788–92.
19. Лобастова И. В. Влияние физической реабилитации на развитие когнитивной сферы у детей с ДЦП. Сибирский психологический журнал. 2010; (36): 59–61.
20. Галиева Г. Ю., Панченко Т. Н., Валуева И. В. и др. Современные подходы и методы физической терапии в реабилитации детей с ДЦП в условиях клинического психоневралогического санатория. 2018; (17): 72–5.
21. Баранов А. А., Намазова-Баранова Л. С., Кузенкова Л. М. и др. Детский церебральный паралич у детей. Клинические рекомендации. Министерство здравоохранения РФ, Союз педиатров России. М., 2016; 478 с.
22. Добрынина Е. А. Физическая реабилитация детей с ДЦП. Вестник науки и образования. 2018; 1; 4 (40): 109–10.
23. Троска З. А., Шерншнева О. А. Совершенствование профессиональной реабилитации детей, больных ДЦП. Ученые записки Российского государственного социального университета. 2015; 14 (3): 156–67.

EFFECTIVENESS OF INTRAOSSEOUS INFILTRATION OF AUTOLOGOUS PLATELET-RICH PLASMA IN THE AREA OF THE BONE MARROW EDEMA IN OSTEOARTHRITIS OF THE KNEE JOINT

Lychagin AV, Garkavi AV, Islaieh OI ✉, Katunyan PI, Bobrov DS, Yavlieva RH, Tselisheva EYu

I.M. Sechenov First Moscow State Medical University, Moscow, Russia

Osteoarthritis (OA) affects both elderly people, for whom it is one of the main causes of disability, and people of active working age and is an urgent clinical and social problem of resistance of pain syndrome to therapy. The disease is characterized by both destruction of intra-articular and paraarticular structures, such as subchondral bone. While OA is an important sign of pathological changes believe the bone marrow edema (BME). This work examines the effect of BME on development osteoarthritis, and therapeutic approaches to the management of patients with OA. The aim of the study was to develop a method of treatment of BME in OA of the knee joint by locally intraosseous injection of autologous thrombotic-rich plasma (PRP) into the edema zone. In this study 17 patients with the diagnosis: Osteoarthritis II-IV Grade. according to the classification of Kellgren–Lawrence, in which areas of local inflammation in the form of BME were detected on MRI in the subchondral zone in accordance with the international classification of WORMS (Whole Organ Magnetic Resonance Imaging Score). The mean age of patients was 41,7 ± 14,3 years, 10 of them were women and 7 men. Patients were treated with autological platelet-rich plasma under x-ray control injected from extra-articular intraosseous access in the area of BME. Evaluation of effectiveness of treatment performed by VAS, WOMAC and KOOS scales, before the introduction of autoplasma, after 1 and 3 months after the start of treatment. Three months after the manipulation, there was a statistically significant decrease in the intensity of inflammatory syndrome: for WOMAC by 17.5%, for KOOS by 19.4% and for VAS by 33,1% ($p < 0,01$). Thus, the efficiency of intraosseous Infiltration of autologous platelet-rich plasma in the treatment of patients with OA, accompanied by edema of the bone marrow in the subchondral zone, was proved.

Keywords: bone marrow edema, osteoarthritis, autologous platelet-rich plasma, intraosseous Infiltration, quality of life

Author contribution: Lychagin AV and Islaieh OI — research planning, literature collection and analysis, data interpretation, draft preparation; Garkavi AV — research planning, data interpretation; Katunyan PI — research planning, draft preparation; Bobrov DS, Yavlieva RH and Tselisheva EYu — research planning.

Compliance with ethical standards: the study was approved by the local ethics committee of the Sechenov University (protocol № 06–18 dated June 06, 2018). All patients agreed to participate in the study in writing.

✉ **Correspondence should be addressed:** Osama I. Islaieh
Bolshoi Tishinsky Pereulok 26/15, Moscow, 123557; osaibso@yahoo.com

Received: 12.07.2019 **Accepted:** 26.07.2019 **Published online:** 20.08.2019

DOI: 10.24075/brsmu.2019.053

ЭФФЕКТИВНОСТЬ ВНУТРИКОСТНОГО ВВЕДЕНИЯ АУТОЛОГИЧНОЙ ОБОГАЩЕННОЙ ТРОМБОЦИТАМИ ПЛАЗМЫ В ЗОНУ ОТЕКА КОСТНОГО МОЗГА ПРИ ОСТЕОАРТРОЗЕ КОЛЕННОГО СУСТАВА

А. В. Лычагин, А. В. Гаркави, О. И. Ислейих ✉, П. И. Катунян, Д. С. Бобров, Р. Х. Явлиева, Е. Ю. Целищева

Первый Московский государственный медицинский университет имени И. М. Сеченова (Сеченовский Университет), Москва, Россия

Остеоартроз (ОА) поражает как пожилых людей, для которых он одна из основных причин инвалидности, так и лиц трудоспособного возраста и является актуальной клинической и социальной проблемой ввиду устойчивости болевого синдрома к проводимой терапии. Заболеванию характерна деструкция внутрисуставных и параартикулярных структур, таких как субхондральная кость. При ОА важным признаком патологических изменений служит отек костного мозга (ОКМ). В работе рассмотрены вопросы влияния ОКМ на развитие гонартроза, а также терапевтические подходы к ведению пациентов с ОА. Целью исследования была разработка методики лечения ОКМ при ОА коленного сустава путем локального внутрикостного введения в зону отека аутологичной обогащенной тромбоцитами плазмы (PRP). Исследовали 17 пациентов с диагнозом «Остеоартроз II–IV ст.» по классификации Kellgren–Lawrence, у которых на МРТ в субхондральной зоне выявлены области локального воспаления в виде ОКМ в соответствии с международной классификацией WORMS. Средний возраст пациентов составил 41,7 ± 14,3 лет. Пациентам внутрикостно из внесуставного доступа в зону ОКМ вводили аутологичную обогащенную тромбоцитами плазму под рентгеноскопическим контролем. Оценку эффективности лечения проводили по шкалам ВАШ, WOMAC и KOOS до введения аутоплазмы, через 1 и 3 месяца после начала лечения. Через 3 месяца после манипуляции отмечалось статистически значимое снижение показателей интенсивности воспалительного синдрома: по WOMAC на 17,5%, KOOS на 19,4% и по ВАШ на 33,1% ($p < 0,01$). Таким образом, доказана эффективность внутрикостного введения аутологичной обогащенной тромбоцитами плазмы в лечении пациентов с ОА, сопровождающимся ОКМ в субхондральной зоне.

Ключевые слова: отек костного мозга, остеоартроз, аутологичная обогащенная тромбоцитами плазма, внутрикостное введение, качество жизни

Информация о вкладе авторов: А. В. Лычагин и О. И. Ислейих — планирование исследования, подбор литературы, интерпретация данных, подготовка черновика рукописи; А. В. Гаркави — планирование исследования, интерпретация данных; П. И. Катунян — планирование исследования, подготовка черновика рукописи; Д. С. Бобров, Р. Х. Явлиева и Е. Ю. Целищева — планирование исследования.

Соблюдение этических стандартов: исследование одобрено локальным комитетом по этике ФГАОУ ВО Первый МГМУ имени И. М. Сеченова (протокол № 06–18 от 06 июня 2018 г.). Все пациенты подписали добровольное информированное согласие.

✉ **Для корреспонденции:** Осама Ибрахим Ислейих
ул. Большой Тишинский переулок, д. 26/15, г. Москва, 123557; osaibso@yahoo.com

Статья получена: 12.07.2019 **Статья принята к печати:** 26.07.2019 **Опубликована онлайн:** 20.08.2019

DOI: 10.24075/vrgmu.2019.053

According to the WHO, 11 to 13% of the world's population suffer from osteoarthritis (OA). OA affects both the elderly, for whom it is one of the main causes of disability, and the working age people [1–4]. Peculiar to the disease are chronic pain, destruction and loss of articular cartilage, remodeling of subchondral bone, formation of osteophytes, inflammation of the synovial membrane of varying degree, involvement of both intraarticular and paraarticular structures in the pathological process [5].

For a long time, it was the articular cartilage that was believed to be the driver of OA development. However, in the last decade the role of the subchondral bone (SB) has been attracting attention both from the point of view of etiopathogenesis and

that of its clinical significance in the processes [6]. It was proved that SC remodeling plays an important part in OA pathogenesis [7]. The changes therein can come first and trigger OA of they can be a consequence of the developing degenerative dystrophic processes [8–10].

An important sign of pathological changes in SC with OA in the background is the MRI-detected bone marrow edema (BME). This term was first registered in 1988; it is increasingly used to describe an MR signal alerting of an OA-associated pathology [11, 12]. BME is usually found in the subchondral sclerosis zone, aggravated by the increased share of the bone tissue volume and trabecular layer compaction [13]. As OA advances, BME tends to grow, which is considered an important risk factor in the subsequent progressive destruction of articular structures [2, 14, 15]. BME and joint deformation were shown to be the predictors of OA transition to the rapid progression stage [4]. Moreover, focal cartilage lesions often develop next to BME, and the MR signal intensity typically reflects the degree of cartilage tissue destruction [16, 17]. a number of researchers consider BME one of the reasons behind the associated severe pain. OA patients complaining about intense pain around the affected joint had a BME measuring over 1 sq cm (as detected by MRI) more often than those who did not report pain as severe [14, 18]. Patients with BME were showing significant progression of cartilage destruction accompanied by pain [19]. Thus, BME can be considered a predictor of the onset of cartilage degradation and pain even before manifestation of all typical clinical symptoms of OA. At the same time, some researchers believe that BME can also be a sign of osteonecrosis, which causes pain at rest [20, 21].

Despite the increasing attention paid to the BME's influence on OA lately, a consensus has not yet been reached. Treating subchondral bone pathology in the context of a complex OA therapy is one of the most-discussed topics. When the nature of articular cartilage and subchondral bone interrelation was understood, the importance of changes in this bone became more apparent. The interrelation was called the osteochondral (functional) unit. It was shown that BME is closely associated with the progression of intraarticular structures degeneration and joint pains intensification. Thus, the likelihood of arthroplasty as the optimal therapy grows together with the expansion of BME [22, 23].

Genetic and histological analysis of the bone marrow samples taken from the affected zone revealed that pain linearly correlates not only with the OA progression status but also with changes in the subchondral BME microenvironment [24]. BME zones have shown to host intense metabolic activity that implies expression of genes involved in the inflammatory processes [24]. Thus, it is assumed that bone metabolism rate in a BME is high, as is the accumulation of cytokines and angiogenic factors, which drives growth of new vessels and nerve endings in this region [25].

There is a subchondroplasty technique applied to treat OA-associated bone and cartilage pathology that implies introducing calcium phosphate to the affected subchondral bone under arthroscopic control. a trial on 133 gonarthrosis patients that also had BME has proven the technique effective, although 2.5 years after the procedure 25% of them reported no improvements and agreed to joint replacement [23]. Another paper describes a trial of the same technique on 164 gonarthrosis patients that were recommended to have their joint replaced. After subchondroplasty, 70% of them reported significant improvement and decided to refuse the replacement [26].

Currently, a growing number of practitioners turn their attention to a group of techniques implying intraosseous administration of autologous platelet-rich plasma [27–29]. The mechanisms behind the good results registered after injection of autologous platelet-rich plasma (PRP) are still being investigated, however, its anti-inflammatory and regenerative effects are no longer called into question. in this connection, it seems promising to seek development of an OA therapy that would revolve around administering PRP to the BME locus.

This study aimed to develop a PRP therapy against OA-associated BME that implies local intraosseous injections into the edema zone.

METHODS

The study involved 17 patients (41,7 ± 14,3 years), 15 of them with grade II–IV knee OA (Kellgren–Lawrence classification) concomitant with MRI-detected BME primarily located in the medial (inner) parts of the knee joint [30]. Inclusion criteria: patients of both sexes in age from 40 to 80 years; predominance of the knee joint arthrosis, joint pain score more than 3 points on VAS; radiological 2 and 4 degrees of the disease severity according to I. Kellgren and I. Lawrence classifications with bone marrow edema in the subchondral zone; body mass index 20–33; opportunity for observation during the entire study period; mental adequacy, ability and willingness to cooperate and implement the doctor's recommendations. Exclusion criteria: bilateral arthrosis of the knee joints with synovitis; body mass index > 33; polyarthritis; severe limb deformation — varus curvature of the diaphysis more than 4 °C and valgus — more than 16 °C; arthroscopy less than 1 year before treatment; intraarticular injections of hyaluronic acid over the past 6 months; systemic autoimmune diseases; poorly controlled diabetes mellitus (glycosylated hemoglobin above 9%); blood diseases (coagulopathy, anemia with HB < 90); ongoing immunosuppressive therapy, treatment with warfarin or other anticoagulants; treatment with corticosteroids for 6 months before inclusion in the study; patient refusal from further participation in the study; identification of objective contraindications to surgery; lack of the possibility of dynamic monitoring and control during the established period.

The duration of the disease ranged from 1 to 9 years (5,2 ± 4,5). The patients were diagnosed with OA based on their complaints, history and clinical-radiological examination. All patients had their knee joints x-rayed in two projections, anteroposterior and lateral, with tibia flexed at 30 (Table1).

MRI provided the data needed to evaluate the condition of the subchondral zone and BME in all patients. We used WORMS (Whole Organ Magnetic Resonance Imaging Score) to describe the bone marrow edema. The Score is designed to assess signal intensity on T2-weighted images [2]. The lesions were evaluated in points; we measured the maximum diameter of the edemas using RadiAnt DICOM Viewer 4.6.9 (64-bit) software (Medixant; France). Table 2 contains the diagnosis criteria. Figures 1 and 2 are tomograms depicting severe BME in some of the patients participating in the study.

Upon admission, all patients had their pain level evaluated with the help of VAS and filled the WOMAC and KOOS questionnaires [31–33]. The values of the same indicators were registered further on, in 1 and 3 months after the studied procedure.

PRP preparation and method description

We used a Regenlab PRP kit (REGEN ACR technology, 2011, Switzerland) to prepare PRP injections. The kit allows making a preparation that persists for a specific period of time after intraosseous administration. We distributed 30 ml of

autologous venous blood into three tubes: two REGEN BCT tubes to prepare autologous platelet-rich plasma and one REGEN ATS tube to obtain autologous thrombin serum used to activate the preparation (step 1). All tubes were centrifuged for 5 minutes at 3100 rpm (step 2). Then, under sterile conditions, we mixed PRP from REGEN BCT and autologous thrombin serum from REGEN ATS in a syringe at 10:1 ratio (step 3) (Fig. 2). The PRP was injected into the BME zone as identified on the T2-weighted images, i.e. in the medial or lateral condyle of femur or tibia. For the manipulation, the patients were put on to the operating table, supine, under the influence of intravenous anesthesia (step 4) (Fig. 2).

The preparation was administered through a stylet with a 13 gauge mandrin (Stryker, USA); the process was monitored with the help of an electron-optical converter (EOC). The lesion received 5 ml of the preparation through the needle that reached it (Fig. 3).

For the days following the procedure, the patients were recommended to apply cold locally, limit loads for up to 1 week, restrain from increased loads for up to 2 weeks, take 4 g of paracetamol a day (orally) if in pain. No selective non-steroidal anti-inflammatory drugs were used.

Statistica 13.3 software (StatSoft; USA) enabled statistical analysis of the data.

RESULTS

According to MRI, 2 patients had minimal BME, in 7 patients the edema was moderate and in 8 it was qualified as severe (Fig. 4).

After PRP administration, the pain, as measured with VAS, subsided significantly over time. Before the treatment, it was identified as "severe" (51.4 ± 6.9 points); 1 month after, the score decreased by 36.4 points, which corresponds to "minor" (15.0 ± 8.3, $p < 0$, 01), and 3 months later the value was 18.3 ± 11.6 points, ($p < 0.01$), which is also within the "minor" range (Fig. 5).

WOMAC figures also reflect significant improvement of the indicators. The average score (summed) at admission was 57.38 ± 12.85 points, 1 month after drug administration — 76.45 ± 5.91 points ($p < 0.01$), and after 3 months it reached 75.33 ± 8.41 ($p < 0.01$) (Fig. 5).

KOOS figures followed the same pattern: the average score at admission was 52.78 ± 13.38 points, a month after PRP injection — 72.00 ± 7.35 points ($p < 0.01$), and 3 months later it reached 72.13 ± 8.50 points ($p < 0.01$) (Fig. 5).

Since KOOS includes 5 subscales that consider various aspects of the knee joint condition, it is of interest to evaluate them individually (Table 3). Relative to the beginning of the

Table 1. The patients

Gender (number of patients)	Female	10 (58.8%)
	Male	7 (41.2%)
Average age (years)		41.7 ± 14.3
Knee joint disease duration (years)		5.2 ± 4.5
Average time under medical supervision (months)		5.5 ± 2.5
Affected joint (amount)	One side	17 (100%)
Kellgren–Lawrence grade based on x-ray	I	0
	II	5 (29.4%)
	III	10 (58.8%)
	IV	2 (11.8%)

Table 2. WORMS diagnosis criteria

BME degree	Lesion diameter (mm)	WORMS score
None		0
Minimal	< 5	1
Moderate	5–20	2
Severe	> 20	3

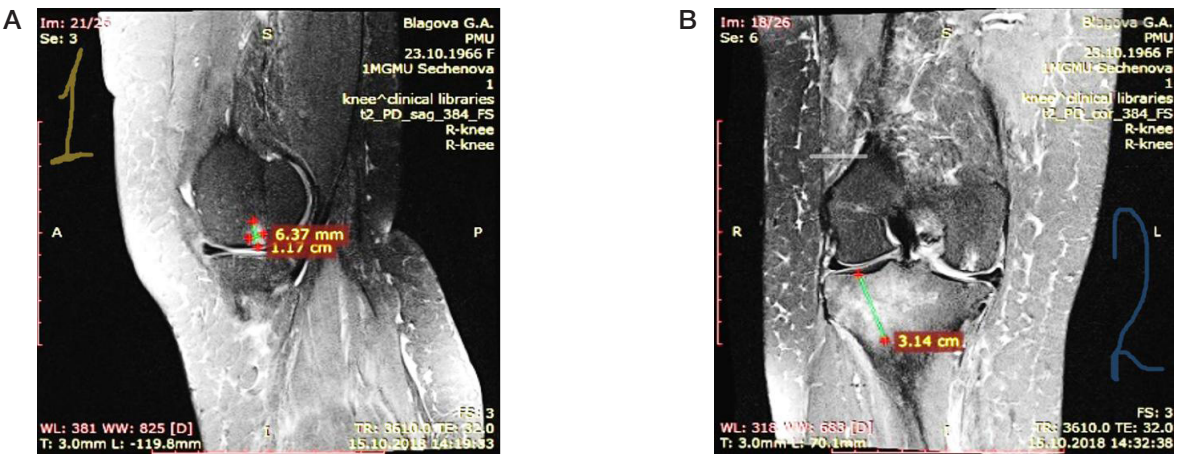

Fig. 1. Measuring the BME with the help of RadiAnt DICOM Viewer 4.6.9 (64-bit), WORMS. **A**. BME in the lateral condyle of the femur, size 1.17 cm. **B**. BME in the medial condyle of the tibia, size 3.14 cm

treatment, all indicators have shown significant positive dynamics. It should be noted that the most pronounced improvement in the average values was recorded in the Sport and Recreation Function (from 25.83 ± 21 to 53.33 ± 28.86) and the Quality of Life (from 24.08 18.39 to 54.18 21.48) subscales by the third month. The pain subsided by the first month and then increased slightly by the third months but still remained significantly less intense.

It is important to note that the majority of KOOS subscales, as well as VAS and WOMAC, revealed that the improvement peaks 1 month after administration of the preparation, and by the third month the average values deteriorate slightly, although the change was not always significant.

DISCUSSION

The intraosseous subchondral PRP injection technique we developed is a minimally invasive and affordable modality to treat gonarthrosis with BME. The PRP preparation made with the Regenlab PRP kit offers a prolonged therapeutic effect. Previously, it was shown that BME is a zone of high bone metabolism and accumulation of cytokines and angiogenic factors, which is essentially translates into local inflammation [24, 25]. The improvement of the patients' condition after administration of PRP supports the theory that such plasma produces a pronounced anti-inflammatory effect when applied topically. Despite the fact that PRP contains angiogenic and

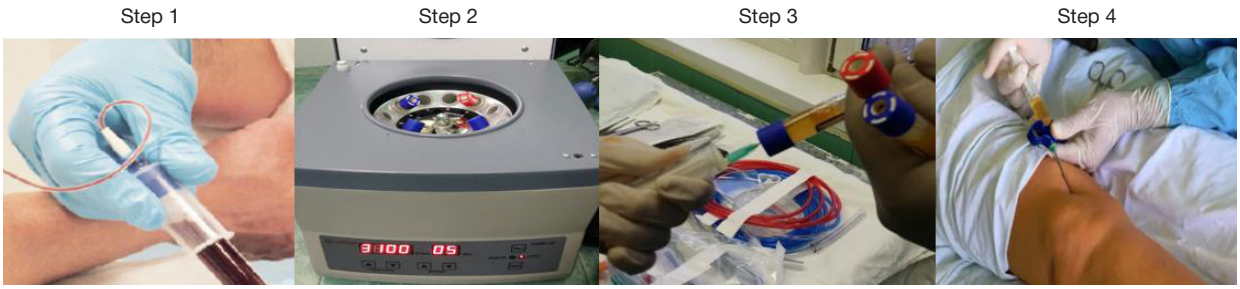

Fig. 2. Preparation of PRP. 1: Blood collection. 2: Centrifugation. 3: Mixing (10 : 1 ratio). 4: Injection

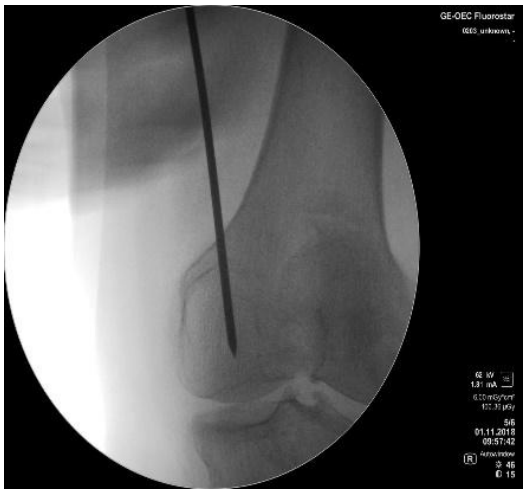

Fig. 3. EOC-controlled administration of PRP into the BME zone, medial condyle of the femur. EOC image: needle in the femur's medial condyle

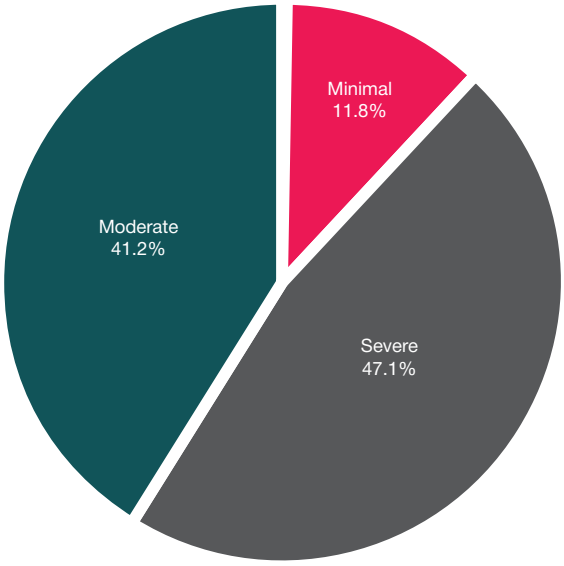

Fig. 4. Patients by BME severity, WORMS

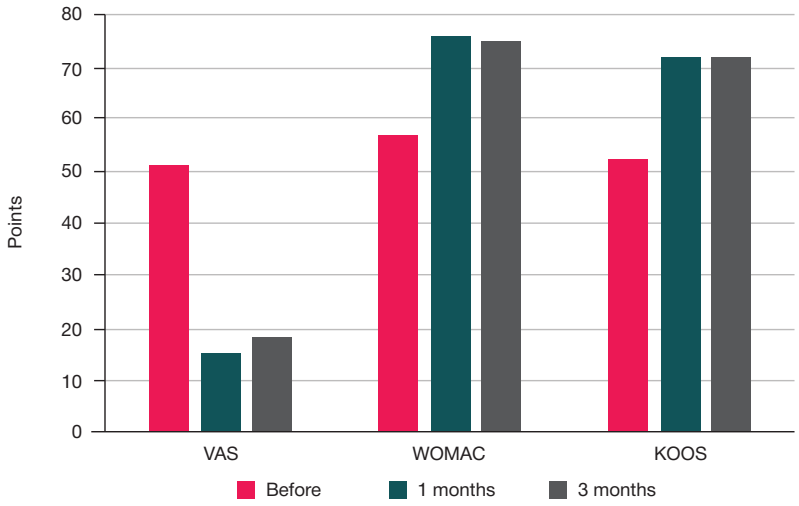

Fig. 5. Dynamics of the average values, VAS, WOMAC and KOOS. 17 knee OA patients were injected PRP in the BME zone. Their condition was assessed before injection and 1 and 3 months after treatment.

Table 3. Functional scale, KOOS subscales

	Before	1 month after treatment	3 months after treatment
Symptoms	62.85 ± 10.28	74.28 ± 10.53*	71.43 ± 6.18*
Pain	53.70 ± 7.18	74.40 ± 11.87*	70.36 ± 12.52*
Activites of Daily Living	53.36 ± 15.41	73.04 ± 10.21	74.51 ± 4.24*
Sports and Recreation	25.83 ± 21	58.33 ± 19.66 *	53.33 ± 28.86 *
Quality of Life	24.08 ± 18.39	40.62 ± 23.30 *	54.18 ± 21.48*
Final index	52.78 ± 13.38	72.00 ± 7.35*	72.13 ± 8.50 *

Note: * — statistically significant change of the value compared to the initial measurements, $p < 0.01$.

profibrotic growth factors, there was not reported a single case of aggravation.

The data we obtained in the context of this research effort are largely consistent with those of other authors who injected PRP intraosseously to treat gonarthrosis [27–29]. One of the papers describes treating 14 gonarthrosis patients (severe condition) with three intraarticular injections of 8 ml of PRP in combination with subchondral intraosseous injections of 5 ml of PRP (delivered to the medial tibial condyle and the medial condyle of the femur); after 6 months, all patients reported less pain and improved KOOS scores, which echoes our results [29]. In our case, the drug was administered intraosseously, once, and the clinical improvement was recorded 3 months earlier.

Nevertheless, it must be recognized that by the third month the achieved effect fades, although clinical tests still show that the improvement is significant.

The most pronounced improvements, which were recorded in the Sport and Recreation Function and the Quality of Life subscales, probably result from the emotional state of the patients who felt the positive effect of the treatment; thus, it should be monitored individually and with other measurement techniques.

CONCLUSIONS

II–IV grade OA, as defined by the Kellgren–Lawrence system, is aggravated by an MRI-detectable subchondral BME lesions, which are part of the disease pathogenesis contributing to its further progression and causing pain. Autologous platelet-rich plasma injected into the BME lesion produces a pronounced and persistent positive effect, alleviating pain and improving function of the affected joint; the effect lasts for at least 3 months.

Further investigation of the gonarthrosis-associated BME treatment method that implies use of PRP is an important task for modern orthopedics with considerable promise in the view of improvements registered in patients and the data on the role played by the osteochondral functional unit in the pathological process.

References

1. Felson DT, McLaughlin S, Goggins J, LaValley MP, Gale ME, Totterman S, et al. Bone marrow edema and its relation to progression of knee osteoarthritis. Ann Intern Med. 2003; (139): 330–6.
2. Kazakia GJ, Kuo D, Schooler J, Siddiqui S, Shanbhag S, Bernstein G et al. Arthritis Research & Therapy. 2013; (15): 11–2.
3. Meizer R, Radda C, Stolz G, Kotsaris S, Petje G, Krasny C, et al. MRI-controlled analysis of 104 patients with painful bone marrow edema in different joint localizations treated with the prostacyclin analogue iloprost. Wien Klin Wochenschr. 2005; (117): 278–86.
4. Zajceva EM, Smirnov AV, Alekseeva I. Ocenka mineral'noj plotnosti kostnoj tkani subhondral'nyh otdelov bedrennoj i bol'shebercovoj kostej pri gonartroze. Nauchno-prakticheskaja revmatologija. 2005; (1): 27–30.
5. Felson DT. An update on the pathogenesis and epidemiology of osteoarthritis. Radiol Clin North Am. 2004; (42): 1–9.
6. Alekseeva LI, Zajceva EM. Rol' subhondral'noj kosti pri osteoartroze.

NII revmatologii RAMN, Moskva. Nauchno-prakticheskaja revmatologija. 2009; (4): 43–8.
7. Delgado D, Garate A, Vincent H, Bilbao AM, Patel R, Fiz N, at al. Current concepts in intraosseous Platelet-Rich Plasma injections for knee osteoarthritis. Journal of Clinical Orthopaedics and Trauma. 2019; (10): 36–4.
8. Roemer FW, Frobell R, Hunter DJ, Crema MD, Fischer W, Bohndorf K, et al. MRI-detected subchondral bone marrow signal alterations of the knee joint: terminology, imaging appearance, relevance and radiological differential diagnosis. Osteoarthritis Cartilage. 2009; (17): 1115–31.
9. Roemer FW, Neogix T, Nevittk MC, Felsonx DT, Zhux Y, Zhangx Y, et al. Subchondral bone marrow lesions are highly associated with and predict subchondral bone attrition longitudinally. the MOST study Osteoarthritis and Cartilage. 2010; (18): 47–53.
10. Sowers MF, Hayes C, Jamadar D, Capul D, Lachance L, Jannausch M, et al. Magnetic resonance-detected subchondral bone marrow and cartilage defect characteristics associated with pain and X-ray-defined knee osteoarthritis. Osteoarthritis and Cartilage. 2003; (6): 387–393.
11. Wilson AJ, Murphy WA, Hardy DC, Totty WG. Transient osteoporosis: transient bone marrow edema? Radiology. 1988; (167): 757–760.
12. Lecouvet FE, van de Berg BC, Maldague BE, Lebon CJ, Jamart J, Saleh M, et al. Early irreversible osteonecrosis versus transient lesions of the femoral condyles: prognostic value of subchondral bone and marrow changes on MR imaging. AJR Am J Roentgenol. 1998; (170): 71–7.
13. Hunter DJ, Gerstenfeld L, Bishop G, Davis AD, Mason ZD, Einhorn TA, et al. Bone marrow lesions from osteoarthritis knees are characterized by sclerotic bone that is less well mineralized. Arthritis Res Ther. 2009; (11): 11.
14. Manicourt DH, Brasseur JP, Boutsen Y, Depreseux G, Devogelaer JP. Role of alendronate in therapy for posttraumatic complex regional pain syndrome type I of the lower extremity. Arthritis Rheum. 2004; (50): 3690–97.
15. Pelletier JP, Raynauld JP, Berthiaume MJ, Abram F, Choquette D, Haraoui B, et al. Risk factors associated with the loss of cartilage volume on weight-bearing areas in knee osteoarthritis patients assessed by quantitative magnetic resonance imaging: a longitudinal study. Arthritis Research and Therapy. 2007; (4): 74.
16. Zhao J, Li X, Bolbos RI, Link TM, Majumdar S. Longitudinal assessment of bone marrow edema-like lesions and cartilage degeneration in osteoarthritis using 3 T MR T1rho quantification. Skeletal Radiol. 2010: (39): 523–31.
17. Carrino JA, Blum J, Parellada JA, Schweitzer ME, Morrison WB. MRI of bone marrow edema-like signal in the pathogenesis of subchondral cysts. Osteoarthritis Cartilage. 2006; (14): 1081–15.
18. Peterfy CG, Guermazi A, Zaim S, Tirman PF, Miaux Y, White D, et al. Whole-Organ Magnetic Resonance Imaging Score (WORMS) of the knee in osteoarthritis. Osteoarthritis and Cartilage. 2004; 12 (3): 177–90.
19. Wluka AE, Hanna F, Davies-Tuck M, Wang Y, Bell RJ, Davis SR, et al. Bone marrow lesions predict increase in knee cartilage defects and loss of cartilage volume in middle-aged women without knee pain over 2 years. Ann Rheum Dis. 2009; (68): 850–5.
20. Iida S, et al. Correlation between bone marrow edema and collapse of the femoral head in steroid-induced osteonecrosis. AJR. American Journal of Roentgenology. 2000; 174 (3): 735–43.
21. Ito H, Matsuno T, Minami A. Relationship between bone marrow edema and development of symptoms in patients with osteonecrosis of the femoral head. AJR. American Journal of Roentgenology. 2006; 186 (6): 1761–70.
22. Perry T, O'Neill T, Parkes M, Felson DT, Hodgson R, Arden NK. Bone marrow lesion type and pain in knee osteoarthritis. Ann Rheum Dis. 2018; (77): 1145.
23. Tanamas SK, Wluka AE, Pelletier JP, Pelletier JM, Abram F, Berry PA, et al. Bone marrow lesions in people with knee osteoarthritis predict progression of disease and joint replacement. A longitudinal study Rheumatology. 2010; (49): 2413–19.
24. Berger CE, Kroner AH, Minai-Pour MB, Ogris E, Engel A. Biochemical markers of bone metabolism in bone marrow edema syndrome of the hip. Bone. 2003; (33): 346–51.
25. Kuttapitiya A, Assi L, Laing K, Hing C, Mitchell P, Whitley G, et al. Microarray analysis of bone marrow lesions in osteoarthritis demonstrates upregulation of genes implicated in osteochondral turnover, neurogenesis and inflammation. Ann Rheum Dis. 2017; 76 (10): 1764–73.
26. Astur DC, de Freitas EV, Cabral PB, Morais CC, Pavei BS, Kaleka CC, et al. Evaluation and management of subchondral calcium phosphate injection technique to treat bone marrow lesion Cartilage. 2018; (10): 1177.
27. Su K, Bai Y, Wang J, Zhang H, Liu H, Ma S. Comparison of hyaluronic acid and PRP intra-articular injection with combined intra-articular and intraosseous PRP injections to treat patients with knee osteoarthritis. 2018; (37): 1341–50.
28. Fiz N, Pérez JC, Guadilla J, Garate A, Sánchez P, Padilla S, et al. Intraosseous Infiltration of Platelet-Rich Plasma for Severe Hip Osteoarthritis. 2017; 19 (6): 821–5.
29. Sánchez M, Anitua E, Delgado D, Sanchez P, Prado R, Goiriena JJ, et al. A new strategy to tackle severe knee osteoarthritis: Combination of intra-articular and intraosseous injections of Platelet Rich Plasma. Expert Opinion on Biological Therapy. 2016; (10): 15–7.
30. Kellgren JH, JeVrey M, Ball J. Atlas of standard radiographs. Vol 2. Oxford: Blackwell Scientific, 1963.
31. Roos E, Lohmander L. The Knee injury and Osteoarthritis Outcome Score (KOOS): from joint injury to osteoarthritis. Health and Quality of Life Outcomes. 2003; 1 (1): 64–72.
32. Marot V, Murgier J, Carrozzo A, Reina N, Monaco E, Chiron P et al. Determination of normal KOOS and WOMAC values in a healthy population. Knee Surgery, Sports Traumatology, Arthroscopy. 2018; 27 (2): 541–8.
33. Hawker G, Mian S, Kendzerska T, French M. Measures of adult pain: Visual Analog Scale for Pain (VAS Pain), Numeric Rating Scale for Pain (NRS Pain), McGill Pain Questionnaire (MPQ), Short-Form McGill Pain Questionnaire (SF-MPQ), Chronic Pain Grade Scale (CPGS), Short Form-36 Bodily Pain Scale (SF. Arthritis Care & Research. 2011; 63 (S11): S240-52.

Литература

1. Felson DT, McLaughlin S, Goggins J, LaValley MP, Gale ME, Totterman S, et al. Bone marrow edema and its relation to progression of knee osteoarthritis. Ann Intern Med. 2003; (139): 330–6.
2. Kazakia GJ, Kuo D, Schooler J, Siddiqui S, Shanbhag S, Bernstein G et al. Arthritis Research & Therapy. 2013; (15): 11–2.
3. Meizer R, Radda C, Stolz G, Kotsaris S, Petje G, Krasny C, et al. MRI-controlled analysis of 104 patients with painful bone marrow edema in different joint localizations treated with the prostacyclin analogue iloprost. Wien Klin Wochenschr. 2005; (117): 278–86.
4. Зайцева Е. М. Оценка минеральной плотности костной ткани субхондральных отделов бедренной и большеберцовой костей при гонартрозе. Научно-практическая ревматология. 2005; (1): 27–30.
5. Felson DT. An update on the pathogenesis and epidemiology of osteoarthritis. Radiol Clin North Am. 2004; (42): 1–9.
6. Алексеева Л. И., Зайцева Е. М. Роль субхондральной кости при остеоартрозе. НИИ ревматологии РАМН. Научно-практическая ревматология. М., 2009; (4): 43–8.
7. Delgado D, Garate A, Vincent H, Bilbao AM, Patel R, Fiz N, at al. Current concepts in intraosseous Platelet-Rich Plasma injections for knee osteoarthritis. Journal of Clinical Orthopaedics and Trauma. 2019; (10): 36–4.
8. Roemer FW, Frobell R, Hunter DJ, Crema MD, Fischer W, Bohndorf K, et al. MRI-detected subchondral bone marrow signal alterations of the knee joint: terminology, imaging appearance, relevance and radiological differential diagnosis. Osteoarthritis Cartilage. 2009; (17): 1115–31.
9. Roemer FW, Neogix T, Nevittk MC, Felsonx DT, Zhux Y, Zhangx Y,

et al. Subchondral bone marrow lesions are highly associated with and predict subchondral bone attrition longitudinally. The MOST study Osteoarthritis and Cartilage. 2010; (18): 47–53.
10. Sowers MF, Hayes C, Jamadar D, Capul D, Lachance L, Jannausch M, et al. Magnetic resonance-detected subchondral bone marrow and cartilage defect characteristics associated with pain and X-ray-defined knee osteoarthritis. Osteoarthritis and Cartilage. 2003; (6): 387–393.
11. Wilson AJ, Murphy WA, Hardy DC, Totty WG. Transient osteoporosis: transient bone marrow edema? Radiology. 1988; (167): 757–760.
12. Lecouvet FE, van de Berg BC, Maldague BE, Lebon CJ, Jamart J, Saleh M, et al. Early irreversible osteonecrosis versus transient lesions of the femoral condyles: prognostic value of subchondral bone and marrow changes on MR imaging. AJR Am J Roentgenol. 1998; (170): 71–7.
13. Hunter DJ, Gerstenfeld L, Bishop G, Davis AD, Mason ZD, Einhorn TA, et al. Bone marrow lesions from osteoarthritis knees are characterized by sclerotic bone that is less well mineralized. Arthritis Res Ther. 2009; (11): 11.
14. Manicourt DH, Brasseur JP, Boutsen Y, Depreseux G, Devogelaer JP. Role of alendronate in therapy for posttraumatic complex regional pain syndrome type I of the lower extremity. Arthritis Rheum. 2004; (50): 3690–97.
15. Pelletier JP, Raynauld JP, Berthiaume MJ, Abram F, Choquette D, Haraoui B, et al. Risk factors associated with the loss of cartilage volume on weight-bearing areas in knee osteoarthritis patients assessed by quantitative magnetic resonance imaging: a longitudinal study. Arthritis Research and Therapy. 2007; (4): 74.
16. Zhao J, Li X, Bolbos RI, Link TM, Majumdar S. Longitudinal assessment of bone marrow edema-like lesions and cartilage degeneration in osteoarthritis using 3 T MR T1rho quantification. Skeletal Radiol. 2010: (39): 523–31.
17. Carrino JA, Blum J, Parellada JA, Schweitzer ME, Morrison WB. MRI of bone marrow edema-like signal in the pathogenesis of subchondral cysts. Osteoarthritis Cartilage. 2006; (14): 1081–15.
18. Peterfy CG, Guermazi A, Zaim S, Tirman PF, Miaux Y, White D, et al. Whole-Organ Magnetic Resonance Imaging Score (WORMS) of the knee in osteoarthritis. Osteoarthritis and Cartilage. 2004; 12 (3): 177–90.
19. Wluka AE, Hanna F, Davies-Tuck M, Wang Y, Bell RJ, Davis SR, et al. Bone marrow lesions predict increase in knee cartilage defects and loss of cartilage volume in middle-aged women without knee pain over 2 years. Ann Rheum Dis. 2009; (68): 850–5.
20. Iida S, et al. Correlation between bone marrow edema and collapse of the femoral head in steroid-induced osteonecrosis. AJR. American Journal of Roentgenology. 2000; 174 (3): 735–43.
21. Ito H, Matsuno T, Minami A. Relationship between bone marrow edema and development of symptoms in patients with osteonecrosis of the femoral head. AJR. American Journal of Roentgenology. 2006; 186 (6): 1761–70.
22. Perry T, O'Neill T, Parkes M, Felson DT, Hodgson R, Arden NK. Bone marrow lesion type and pain in knee osteoarthritis. Ann Rheum Dis. 2018; (77): 1145.
23. Tanamas SK, Wluka AE, Pelletier JP, Pelletier JM, Abram F, Berry PA, et al. Bone marrow lesions in people with knee osteoarthritis predict progression of disease and joint replacement. A longitudinal study Rheumatology. 2010; (49): 2413–19.
24. Berger CE, Kroner AH, Minai-Pour MB, Ogris E, Engel A. Biochemical markers of bone metabolism in bone marrow edema syndrome of the hip. Bone. 2003; (33): 346–51.
25. Kuttapitiya A, Assi L, Laing K, Hing C, Mitchell P, Whitley G, et al. Microarray analysis of bone marrow lesions in osteoarthritis demonstrates upregulation of genes implicated in osteochondral turnover, neurogenesis and inflammation. Ann Rheum Dis. 2017; 76 (10): 1764–73.
26. Astur DC, de Freitas EV, Cabral PB, Morais CC, Pavei BS, Kaleka CC, et al. Evaluation and management of subchondral calcium phosphate injection technique to treat bone marrow lesion Cartilage. 2018; (10): 1177.
27. Su K, Bai Y, Wang J, Zhang H, Liu H, Ma S. Comparison of hyaluronic acid and PRP intra-articular injection with combined intra-articular and intraosseous PRP injections to treat patients with knee osteoarthritis. 2018; (37): 1341–50.
28. Fiz N, Pérez JC, Guadilla J, Garate A, Sánchez P, Padilla S, et al. Intraosseous Infiltration of Platelet-Rich Plasma for Severe Hip Osteoarthritis. 2017; 19 (6): 821–5.
29. Sánchez M, Anitua E, Delgado D, Sanchez P, Prado R, Goiriena JJ, et al. A new strategy to tackle severe knee osteoarthritis: Combination of intra-articular and intraosseous injections of Platelet Rich Plasma. Expert Opinion on Biological Therapy. 2016; (10): 15–7.
30. Kellgren JH, JeVrey M, Ball J. Atlas of standard radiographs. Vol 2. Oxford: Blackwell Scientific, 1963.
31. Roos E, Lohmander L. The Knee injury and Osteoarthritis Outcome Score (KOOS): from joint injury to osteoarthritis. Health and Quality of Life Outcomes. 2003; 1 (1): 64–72.
32. Marot V, Murgier J, Carrozzo A, Reina N, Monaco E, Chiron P et al. Determination of normal KOOS and WOMAC values in a healthy population. Knee Surgery, Sports Traumatology, Arthroscopy. 2018; 27 (2): 541–8.
33. Hawker G, Mian S, Kendzerska T, French M. Measures of adult pain: Visual Analog Scale for Pain (VAS Pain), Numeric Rating Scale for Pain (NRS Pain), McGill Pain Questionnaire (MPQ), Short-Form McGill Pain Questionnaire (SF-MPQ), Chronic Pain Grade Scale (CPGS), Short Form-36 Bodily Pain Scale (SF. Arthritis Care & Research. 2011; 63 (S11): S240-52.

APPLICATION OF CULTURE-BASED, MASS SPECTROMETRY AND MOLECULAR METHODS TO THE STUDY OF GUT MICROBIOTA IN CHILDREN

Efimov BA ✉, Chaplin AV, Sokolova SR, Chernaia ZA, Pikina AP, Savilova AM, Kafarskaya LI

Pirogov Russian National Research Medical University, Moscow, Russia

In recent decades, nucleic acid sequencing technologies used for metagenomic analysis have become the main methods for assessing the composition of microbiota. At the same time, the use of novel methods of cultivation and identification of microorganisms in microbiological research led to the renaissance of culture-based technologies, because facilitated the discovery and isolation of both new strains of well-known microorganisms as well as uncultivated and unexplored bacterial taxa. The aim of this study was to evaluate the potential of using the culture-based method for the assessment of the qualitative and quantitative composition of the intestinal microbiota in healthy children. Eleven growth media were inoculated with serial dilutions of stool samples in order to analyze the profile of dominant anaerobic bacteria, as well as aerobic bacteria and fungi in 20 healthy children aged 2–4 years. The identification of microorganisms was performed using MALDI TOF MS and 16S rRNA gene fragment sequencing were used. 1,819 isolated and identified strains belong to 7 phyla, 13 classes, 18 orders, 33 families, 77 genera and 149 species in the *Bacteria* domain. The *Bacteroidetes*, *Firmicutes*, *Actinobacteria* and *Proteobacteria* phyla were most abundant and frequent. The greatest species diversity (more than 85 species) was found in the *Firmicutes* phylum. Ten new previously uncharacterized bacterial strains were isolated.

Keywords: gastrointestinal tract microbiota, children, isolation and purification of bacteria, biodiversity, microbiological techniques/methods, DNA sequencing, mass spectrometry, Matrix-Assisted Laser Desorption-Ionization

Funding: the study was supported by Russian Science Foundation (research grant № 17-15-01488).

Author contribution: Efimov BA — research planning, literature analysis, screening children, specimen collection, microbiological research, mass spectrometry research, analysis and interpretation of data, preparing a draft manuscript; Chaplin AV — research planning, literature analysis, isolation of bacterial DNA, carrying out PCR, amplicons purification for sequencing, data analysis and interpretation, preparing a draft manuscript; Sokolova SR — research planning, literature analysis, specimen collection, microbiological research, isolation of bacterial DNA, carrying out PCR, amplicons purification for sequencing, data analysis and interpretation preparing a draft manuscript; Chernaia ZA — research planning, literature analysis, microbiological research, mass spectrometry research, data analysis and interpretation, preparing a draft manuscript; Pikina AP — research planning, literature analysis, microbiological research, mass spectrometry research, data analysis and interpretation, preparing a draft manuscript; Savilova AM — literature analysis, microbiological research, preparing a draft manuscript; Kafarskaya LI — research planning, literature analysis, screening children, microbiological research, analysis and interpretation of data, preparing a draft manuscript.

Compliance with ethical standards: the study was approved by the Ethics Committee of Pirogov Russian National Research Medical University (protocol № 165 of May 22, 2017). The parents of children participants signed a voluntary informed consent to participate in the study.

✉ **Correspondence should be addressed:** Boris A. Efimov
Ostrovityanova 1, Moscow, 117997; efimov_ba@mail.ru

Received: 27.06.2019 **Accepted:** 12.07.2019 **Published online:** 09.08.2019

DOI: 10.24075/brsmu.2019.048

ОПЫТ ПРИМЕНЕНИЯ КУЛЬТУРАЛЬНОГО, МАСС-СПЕКТРОМЕТРИЧЕСКОГО И МОЛЕКУЛЯРНОГО МЕТОДОВ В ИССЛЕДОВАНИИ КИШЕЧНОЙ МИКРОБИОТЫ У ДЕТЕЙ

Б. А. Ефимов ✉, А. В. Чаплин, С. Р. Соколова, З. А. Черная, А. П. Пикина, А. М. Савилова, Л. И. Кафарская

Российский национальный исследовательский медицинский университет имени Н. И. Пирогова, Москва, Россия

В последние десятилетия основными методами оценки состава микробиоты стали технологии секвенирования нуклеиновых кислот, используемые для метагеномного анализа. В то же время внедрение в практику микробиологических исследований новых методов культивирования и идентификации микроорганизмов привело к ренессансу культуральных технологий, поскольку позволило решить задачи по поиску и выделению новых штаммов как уже известных микроорганизмов, так и ранее некультивируемых и неизученных бактериальных таксонов. Целью работы было оценить потенциал использования культурального метода для оценки качественного и количественного состава кишечной микробиоты здоровых детей. Анализ состава доминирующих групп анаэробных бактерий, а также аэробных бактерий и грибов у 20 здоровых детей в возрасте 2–4 лет проводили путем высева серийных разведений фекалий на 11 питательных сред. Для идентификации микроорганизмов использовали метод MALDI TOF MS и секвенирование фрагмента гена 16S рРНК. Идентификация 1819 выделенных штаммов микроорганизмов показала, что они принадлежали к 7 типам, 13 классам, 18 порядкам, 33 семействам, 77 родам и 149 видам домена бактерий. По количеству и частоте встречаемости доминировали бактерии типов *Bacteroidetes*, *Firmicutes*, *Actinobacteria* и *Proteobacteria*. Наибольшее видовое разнообразие (более 85 видов) обнаружено среди бактерий типа *Firmicutes*. Выделено 10 штаммов новых, пока не охарактеризованных бактериальных видов.

Ключевые слова: микробиота кишечника, дети, выделение бактерий, биоразнообразие, микробиологические методы, секвенирование ДНК, масс-спектрометрия, MALDI TOF MS

Финансирование: работа поддержана грантом Российского научного фонда (№ 17-15-01488).

Информация о вкладе авторов: Б. А. Ефимов — планирование исследования, анализ литературы, отбор обследуемых детей, сбор биоматериала, микробиологическое исследование, спектрометрическое исследование, анализ и интерпретация данных, подготовка черновика рукописи; А. В. Чаплин — планирование исследования, анализ литературы, выделение бактериальной ДНК, проведение ПЦР, очистка ампликонов для секвенирования, анализ и интерпретация данных, подготовка черновика рукописи; С. Р. Соколова — планирование исследования, анализ литературы, сбор биоматериала, микробиологическое исследование, выделение бактериальной ДНК, проведение ПЦР, очистка ампликонов для секвенирования, анализ и интерпретация данных, подготовка черновика рукописи; З. А. Черная — планирование исследования, анализ литературы, микробиологическое исследование, спектрометрическое исследование, анализ и интерпретация данных, подготовка черновика рукописи; А. П. Пикина — планирование исследования, анализ литературы, микробиологическое исследование, спектрометрическое исследование, анализ и интерпретация данных, подготовка черновика рукописи; А. М. Савилова — анализ литературы, микробиологическое исследование, подготовка черновика рукописи; Л. И. Кафарская — планирование исследования, анализ литературы, отбор обследуемых детей, микробиологическое исследование, анализ и интерпретация данных, подготовка черновика рукописи.

Соблюдение этических стандартов: исследование было одобрено этическим комитетом РНИМУ имени Н. И. Пирогова (протокол № 165 от 22 мая 2017 г.). Родители каждого ребенка подписали добровольное информированное согласие на участие в исследовании.

✉ **Для корреспонденции:** Борис Алексеевич Ефимов
ул. Островитянова, д. 1, г. Москва, 117997; efimov_ba@mail.ru

Статья получена: 27.06.2019 **Статья принята к печати:** 12.07.2019 **Опубликована онлайн:** 09.08.2019

DOI: 10.24075/vrgmu.2019.048

Most representatives of human and animal intestinal microbiome are classified as difficult-to-cultivate or nonculturable groups of microorganisms. Currently, massive parallel sequencing of DNA samples is used predominantly for the assessment of the composition of gut microbiota, for example, sequencing of the fragments of genes encoding 16S rRNA or sequencing of genomic DNA fragments [1, 2]. However, it is often difficult to interpret the obtained data, since the analyzed nucleotide sequences sometimes cannot be correlated with known bacteria or bacteriophages [3–5]. These approaches also have a disadvantage: only the relative ratio of the dominant groups of bacteria can be characterized efficiently, while the exact number of dominant or minor taxa remains beyond such studies [6, 7]. Real-time PCR with species-specific or group-specific primers and subsequent normalization of the results using recombinant plasmid DNA containing the cloned regions of amplified gene fragments are used for more accurate quantitative determination of bacteria [8]. However, this method makes it possible to determine the total number of copies of amplified DNA regions in the sample rather than the number of viable bacterial cells. In addition, due to the complexity of the method, especially in the studies aimed at quantification of the wide range of microorganisms, this approach is mainly used to analyze the composition of large taxonomic clusters of microorganisms (genera, families, groups) rather than certain known species. Thus, along with the development of technologies based on the sequencing of the genetic material of microorganisms, it is still important to improve cultural methods, since it allows us to solve the problem of searching for, isolating, determining the number and studying the biological properties of new strains in well-known bacteria, as well as in unexplored bacterial taxa [9].

The aim of the study was to evaluate the potential of using the culture-based method to assess the qualitative and quantitative composition of the intestinal microbiota of healthy children by stool samples inoculation of growth media widely used in laboratory practice for fastidious bacteria.

METHODS

The study of the parameters of colon microbial colonization was carried out in a group of 20 healthy children of both sexes living in Moscow. 17 of them regularly attended preschool institutions, and three children were in home schooling. Children were selected by the authors of the study. The age of the subjects ranged from 2 years 11 months to 4 years 10 months (average age 3 years 5 months), of which there were 12 boys and 8 girls. Inclusion criteria: children of both genders; children's age 2.5–4 years; parental consent presence. Exclusion criteria: children of other age; the presence of any chronic disease, such as diabetes mellitus, bronchial asthma, gastrointestinal diseases (celiac disease, functional constipation, short bowel syndrome, or inflammatory bowel disease); the presence of food allergies or parental belief in lactose intolerance in a child; pronounced selectivity in food consumption; use of antibiotics, immunomodulatory, steroid or probiotic drugs for 6 months before the study; infectious gastroenteritis in the last 6 months before the study, confirmed by laboratory tests; history of gastrointestinal surgery.

The material for the study was the feces of children which were collected by the parents with a sterile spatula and placed in a sterile container for transportation. The study was carried out under the condition that the amount of material placed in a container was not less than 15 g, and the time of its delivery to the laboratory did not exceed 2 hours from the moment of collection. In the laboratory immediately after receiving the feces were homogenized, their tenfold serial dilutions (from 10 to 10^9 times) were prepared in test tubes with sterile Schaedler Anaerobe Broth liquid medium (Oxoid, Basingstoke; UK), and aliquots in a volume of 0.1 ml of the corresponding dilutions were inoculated on Petri plates with growth media. The isolation of strictly anaerobic bacteria was performed on the Schaedler Anaerobe Agar (Oxoid, Basingstoke; UK) with the addition of 5% (v/v) defibrinated sheep blood, Anaerobe Basal Agar (Oxoid, Basingstoke; UK) with the addition of sheep blood, Columbia Agar (bioMérieux, Marcy l'Etoile; France) with the addition of sheep blood. Inoculation of growth media was carried out from the 10^7, 10^8, and 10^9 fold dilutions of the sample. Bifidobacteria and sulfate-reducing bacteria were also isolated on the Bifidobacterium Agar (Himedia Labs Inc.; India) and Perfringens Agar Base (Himedia Labs Inc.; India) respectively from the specimen 10^5, 10^7 and 10^8 fold dilutions. The Petri dishes were incubated in the anaerobic jars (Schutt Labortechnik GmbH; Germany) filled with a gas mixture (85% N_2, 10% H_2, 5% CO_2) in the presence of platinum catalysts at 37 °C for 72 hours. Lactic acid bacteria were cultured on Lactobacillus MRS Agar medium (Himedia Labs Inc.; India) from the specimen 10^3 and 10^5 fold dilutions, the plates were incubated in the anaerobic jars (GasPak; USA) with the 7% CO_2 atmosphere for 48 hours. Aerobic bacteria were isolated from the sample 10, 10^3, 10^5 and 10^7 fold dilutions on the following media: Endo Agar (Becton Dickinson and Company, USA), Salmonella–Shigella-Agar (bioMerieux Marcy l'Etoile; France), Gelatin Mannitol Salt Agar (Staphylococcus Agar # 110, Himedia Labs Inc.; India), m-Enterococcus Agar (Difco Laboratories, Franklin Lakes; USA), Columbia Agar (bioMérieux, Marcy l'Etoile; France) with the addition of 5% (v/v) sheep blood. The Sabouraud Chloramphenicol 2 Agar medium (bioMérieux, Marcy l'Etoile; France) was used to isolate the fungi.

After incubation the culture properties of bacteria were described, morphological types were counted separately for each colony type. In addition, bacteria from each type of colonies were stained by Gram method, subcultured on plates with the same medium and incubated under anaerobic or aerobic conditions to obtain the stock of bacteria for identification and preservation. Partially, the isolated microorganism strains were lyophilized after freezing in a 10% sucrose/1% gelatin (w/v) solution in the Freeze Dryer SB1 (Chemlab; UK). Test tubes with lyophilized strains of microorganisms were stored at a temperature of –80 °C.

The primary identification of bacteria and fungi was performed using the MALDI TOF mass spectrometry on the Vitek MS Plus unit (bioMérieux; France) with the Saramis Premium v. 4.10 software according to the manufacturer's recommendations [10, 11]. The strains of bacteria, the species identity of which could not be established using MALDI-TOF mass spectrometry, were identified by 16S rRNA gene sequencing [12, 13]. In addition, 16S rRNA gene sequencing was used for some strains to confirm the results of species identification by mass spectrometry. The polymerase chain reaction (PCR) amplified a portion of the 16S rRNA gene using the universal bacterial primers 27F (5'-AGAGTTTGATCCTGGCTCAG-3') and 1492R (5'-ACGGYTACCTTGTTACGACTT-3') for 35 cycles with the following program: denaturation 20 s at 94 °C; primer annealing 20 s at 58 °C; elongation 90 s at 72 °C. The obtained PCR product was purified using the Cleanup Standard kit (Evrogen; Russia). The Sanger sequencing of the amplified DNA fragment from the UF1 primer was carried out at Evrogen (Evrogen; Russia). The determination of the cut-off boundaries

of the sequences by the quality of electrophoregrams was carried out visually using the Chromas Lite software (version 2.6.6, Technelysium Pty. Ltd.; Australia). The species of bacteria was determined on the basis of a search for the nucleotide sequences obtained in the GenBank database using the Megablast algorithm. The result of the comparison was considered to correspond to the level of the species in the case when its partially sequenced 16S rRNA gene sequence resembled ≥ 98.7% of the sequence of the closest known bacterial species in the GenBank database [14].

The number of bacteria was expressed in $\log_{10}$ colony forming units in 1 g of the test material ($\log_{10}$ CFU/g). The CFU/g of the test material was calculated using the following formula: CFU/g = the number of colonies of the corresponding type of microorganisms grown on the plate (or the average number of colonies of the corresponding type of microorganisms, in cases when bacteria of one type gave growth on different media or gave growth only on one of growth media, but were determined at more than one dilution) × 10 × dilution ratio. The total number of cultured microorganisms per sample was calculated by adding the quantitative values of individual species.

Statistical data processing was performed using the Mann–Whitney test and Fisher's exact test, multiple comparisons were corrected using the Bonferroni method. The tendency to form clusters was checked using the VAT algorithm [15] and the principal component analysis.

RESULTS

In total, 1,819 strains of microorganisms were isolated from 20 healthy children. The species identification of most strains was carried out using the MALDI TOF MS. To establish the taxonomic identity of 140 bacterial strains that could not be identified by mass spectrometry 16S rRNA gene sequencing was performed. Comparative analysis of the obtained nucleotide sequences with the GenBank database showed that 130 bacterial strains belonged to 88 known species, and 10 belonged to new, not yet studied bacterial taxa. The number of identified microorganism species per sample varied from 21 to 48 and averaged 34 ± 8. The total number of viable bacteria per 1 g of faeces varied from 10.0 to 11.1 $\log_{10}$ CFU/g and averaged 10.6 ± 0.4 $\log_{10}$ CFU/g.

In general, it was found that the isolated strains belonged to 7 phyla, 13 classes, 18 orders, 33 families, 77 genera, and 149 species of the Bacteria domain. Also 3 species of fungi from 2 families of the *Saccharomycetales* order were identified.

The reduction in the dimension by principal component analysis, as well as the use of the VAT algorithm, did not reveal a tendency to form clusters from the microbiocenoses of the examined children on the basis of the obtained data on the quantitative and qualitative composition, which does not allow classifying the microbiocenoses in this study into enterotypes or their analogs. There were no statistically significant differences in the microbial composition of the gut tract microbiota, depending on the age and gender of children, which may be due to the small size and homogeneity of the sample.

Generic assignment, frequency of occurrence and the quantitative level of microorganisms isolated from feces of 20 healthy children are presented in tables 1–5. It was revealed that dominant by the number and frequency of occurrence bacteria belonged to the *Firmicutes* (9.8 ± 0.4 $\log_{10}$ CFU/g), *Bacteroidetes* (10.3 ± 0.4 $\log_{10}$ CFU/g), *Actinobacteria* (10.0 ± 0.5 $\log_{10}$ CFU/g), and *Proteobacteria* (8.5 ± 1.1 $\log_{10}$ CFU/g) phyla. Representatives of each of these groups of bacteria were found in all children. In addition, in 25% of children (an average of 9.1 ± 0.4 $\log_{10}$ CFU/g) the bacteria of the *Akkermansia muciniphila* species were obtained in pure culture, which belong to the *Verrucomicrobia* phylum, in two children the *Fusobacterium mortiferum* (8.8 and 8.6 $\log_{10}$ CFU/g) were isolated which represent the *Fusobacteria* phylum. From one child the strain of the *Victivallis vadensis* bacteria belonging to the *Lentisphaerae* phylum was isolated, its concentration was 10^9 $\log_{10}$ CFU/g.

The phylum *Actinobacteria* consisted of the two classes of bacteria: *Actinobacteria* and *Coriobacteriia* (Table 1). Bacteria of *Actinobacteria* class belonged to 4 orders and 4 families, the representatives of the *Bifidobacteriaceae* and *Propionibacteriaceae* families prevailed. *Bifidobacteria* (occurred in 100% of children), were the dominant microorganisms in the gut microbiota of healthy children. A total of 6 species of bifidobacteria were isolated, among them *B. longum*, *B. bifidum*, *B. adolescentis*, and bifidobacteria of the *B. catenulatum/pseudocatenulatum* group.

The *Coriobacteria* class was represented mostly by the families *Coriobacteriaceae* and *Eggerthellaceae*, the dominant species were *Collinsella aerofaciens* and *Eggerthella lenta*.

The phylum *Bacteroidetes* consisted of 5 bacteria families belonging to order *Bacteroidales* (Table 2). The *Bacteroidaceae* family was represented by single genus *Bacteroides*, to which the 14 identified species belong. The bacteroids were isolated in 100% of cases in average number 10.1 ± 0.4 $\log_{10}$ CFU/g of feces. Among bacteroids the *B. dorei/vulgatus* and *B. ovatus/xylanisolvens* species dominated in healthy children, as well as *B. uniformis*, *B. fragilis* and *B. thetaiotaomicron*.

The *Rikenellaceae* family was also represented by only one genus *Alistipes* and 9 isolated species. *Alistipes* occurred in 90% of healthy children. The average number of bacteria was 9.5 ± 0.4 $\log_{10}$ CFU/g, the dominating species were *A. onderdonkii*, *A. putredinis* and *A. finegoldii*.

The *Porphyromonadaceae* family bacteria were isolated from 75% of children, they belonged to the *Parabacteroides*, *Barnesiella* and *Coprobacter* genera. The dominant species of these taxa were *P.distasonis*, *P. merdae* and *B. intestinihominis* observed in 45%, 35% and 40% of children respectively. Moreover, in almost all cases when bacteria of these taxonomic groups were detected, their concentration in the specimen was equal to or was close to 10^9 CFU/g.

Bacteria of the *Prevotellaceae* family turned out to be the rarest representatives of the order *Bacteroidales* at the used threshold for the detection of anaerobic bacteria, which was at least 10^8 microbial cells per 1 g of feces. In total from three children (15%) 5 strains of bacteria belonging to the *Prevotella copri*, *P. melaninogenica*, *P. rara* and *Paraprevotella clara* species were isolated.

The phylum *Firmicutes* demonstrated the greatest diversity of taxa, it was represented by 4 classes of bacteria, including 7 orders, 17 families, 45 genera, and 93 species of microorganisms, including new bacterial taxa found in this study (Table 3). Class *Clostridia* was represented only by the order *Clostridiales*, which included 47 species of bacteria belonging to 30 genera and 6 families. Representatives of the *Lachnospiraceae* family were found in 85% of children in average concentration of 9.0 ± 1.0 $\log_{10}$ CFU/g and were the most common taxon of this class. Among the bacteria species belonging to this family and found more often than others, was *Clostridium clostridioforme*, observed in 55% of children at an average concentration of 8.2 ± 1.0 $\log_{10}$ CFU/g. The other common genera of the family *Lachnospiraceae* were *Blautia* (in 65% of children, average concentration 8.9 ± 0.9 $\log_{10}$ CFU/g), as well as bacteria belonging to the

Table 1. Species identity of the *Actinobacteria* phylum cultured bacteria of the gastrointestinal tract microflora isolated from healthy children (*n* = 20)

Phylum *Actinobacteria*			
Class *Actinobacteria*			
Taxa	Observed number (%)[a]	Mean ± SD $\log_{10}$ CFU/g[b]	Growth media[e]
Order *Bifidobacteriales*, family *Bifidobacteriaceae*, genus *Bifidoibacterium*	**20 (100)**	**9.8 ± 0.6**	
Bifidobacterium longum	20 (100)	9.3 ± 0.5	SAA; ABA; CA; BA
Bifidobacterium adolescentis	8 (40)	9.5 ± 0.6	SAA; ABA; CA; BA
Bifidobacterium catenulatum/pseudocatenulatum[c]	11 (55)	9.1 ± 0.7	SAA; ABA; CA; BA
Bifidobacterium bifidum	8 (40)	9.5 ± 0.6	SAA; ABA; CA; BA
Bifidobacterium animalis	6 (30)	9.3 ± 0.7	SAA; ABA; CA; BA
Bifidobacterium breve	2 (10)	9 – 10.2[d]	SAA; ABA; BA
Order *Propionibacteriales*, family *Propionibacteriaceae*, genus *Cutibacterium*	**7 (35)**	**9.1 ± 0.6**	
Cutibacterium acnes	5 (25)	8.9 ± 0.7	SAA; ABA; BA
Cutibacterium granulosum	2 (10)	9 – 9.8	ABA; CA
Class *Coriobacteriia*			
Order *Coriobacteriales*, family *Coriobacteriaceae*			
Collinsella aerofaciens	11 (55)	9.2 ± 0.7	SAA; ABA; CA; BA
Genus *Eggerthellales*, family *Eggerthellaceae*			
Eggerthella lenta	17 (85)	8.8 ± 0.7	SAA; ABA; CA
Gordonibacter pamelae	3 (15)	8.5 ± 0.9	ABA; CA; PAB
Raoultibacter massiliensis	1 (5)	9	CA
Slackia isoflavoniconvertens	1 (5)	9.3	CA
Adlercreutzia equolifaciens	1 (5)	9	CA

Note (used in this table and tables 2–5): [a] Frequency of occurrence (absolute number of subjects/percentage of subjects); [b] Mean ± standard deviation $\log_{10}$ of the number of viable microorganisms in 1 g of feces (CFU/g — colony forming units in 1 g of feces); [c] */* — A group of phylogenetically related microorganisms, identity was established using the MALDI TOF MS method on the Vitek MS Plus unit with the Saramis Premium V. 4.10 software; [d] Smaller and larger value of the $\log_{10}$ index of the number of viable microorganisms, if they were found only in two examined children in the group; [e] Names of the growth media used for isolation and registration of the relevant microorganisms types. SAA — Schaedler Anaerobe Agar; ABA — Anaerobe Basal Agar; CA — Columbia Agar; BA — Bifidobacterium Agar; PAB — Perfringens Agar Base; MRS — Lactobacillus MRS Agar; EA — Endo Agar; SSA — Salmonella–Shigella-Agar; GMSA — Gelatin Mannitol Salt Agar (Staphylococcus Agar # 110); mEA — mEnterococcus Agar; CAa — Columbia Agar, plates with which were incubated aerobically; SC2A — Sabouraud Chloramphenicol 2 Agar.

genus *Anaerostipes* (in 40% of children, concentration 8.2 ± 1.0 $\log_{10}$ CFU/g). Another common family of bacteria in the *Clostridia* class were the *Ruminococcaceae* representatives (in 65% of children, average concentration 8.8 ± 0.5 $\log_{10}$ CFU/g) mostly represented by the species *Flavonifractor plautii*, *Ruthenibacterium lactatiformans* and *Anaerotruncus colihominis*. It is worth noting that the bacteria of such species of the *Ruminococcaceae* family as *Faecalibacterium prausnitzii* and *Gemmiger formicilis*, which, according to the results of sequencing of the libraries of 16S rRNA genes, constitute the dominant part of the normal human gastrointestinal tract microflora [16], were isolated only from one child. Such results indicate that it is necessary to use selective growth media and exclude the specimen contact with atmospheric oxygen, due to the extremely high sensitivity of these bacterial taxa to the latter. Another frequently detected taxon of the *Firmicutes* phylum were members of the *Erysipelotrichaceae* family (class *Erysipelotrichia*, order *Erysipelotrichales*), which were found in 55% of healthy children at an average concentration of 8.5 ± 1.0 $\log_{10}$ CFU/g. Among 6 genera and 9 species of bacteria of this family, *Clostridium innocuum* and *Clostridium ramosum* dominated. They were detected with frequency equal to 40% in concentration exceeding 10^8 CFU/g.

Bacteria belonging to the *Negativicutes* class were present in 100% of children, the average concentration was 8.9 ± 0.7 $\log_{10}$ CFU/g. The dominant taxa of this group were representatives of the *Veillonellaceae* family, which included the bacteria of the genera *Veillonella* and *Dialister* (in 35% and 45% of children respectively), as well as the family *Acidaminococcaceae* mainly represented by the *Phascolarctobacterium faecium* species, isolated in high concentrations from 40% of children.

Among colon bacteria belonging to the phylum *Proteobacteria*, representatives of the *Betaproteobacteria*, *Deltaproteobacteria* and *Gammaproteobacteria* classes were identified (Table 4). The *Betaproteobacteria* class included different bacteria species of the *Sutterellaceae* family (isolated from 60% of children, the average concentration 8.8 ± 0.4 $\log_{10}$ CFU/g). The *Deltaproteobacteria* was mainly represented by the hydrogen sulfide forming bacteria of the *Bilophila wadsworthia* species (isolated from 55% of children, the average concentration 8.0 ± 0.8 $\log_{10}$ CFU/g). Finally, the *Gammaproteobacteria* class was represented by only one family *Enterobacteriaceae*. *Escherichia coli* were determined in 100% of children at the average concentration of 7.2 ± 0.4 $\log_{10}$ CFU/g. Other relatively frequently observed members of the family were bacterial species *Enterobacter cloacae* (30%), *Citrobacter freundii* (20%) and *Klebsiella pneumoniae* (20%), their concentrations usually didn't exceed 10^6 CFU/g.

Fungi were found in 45% of healthy children in the amount of 3.4 ± 1.4 $\log_{10}$ CFU/g, all of the isolated strains belonged to the order *Saccharomycetales* (Table 5). In the feces of 35% of the children, fungi of the genus *Candida* of the family *Debaryomycetaceae* were identified. They belong mainly to the *C. albicans* species. In addition, in two children fungi of the *Clavispora lusitaniae* species belonging to the *Metschnikowiaceae* family were present.

The taxonomic properties of 10 strains of bacteria which were isolated during this study and the species identity of

Table 2. Species identity of the *Firmicutes* phylum cultured bacteria of the gastrointestinal tract microflora isolated from healthy children (*n* = 20)

Phylum *Firmicutes*			
Taxa	Observed number (%)	Mean ± SD $\log_{10}$ CFU/g	Growth media
Class *Erysipelotrichia*, order *Erysipelotrichales*			
Family *Erysipelotrichaceae*	**11 (55)**	**8.5 ± 1.0**	
Genus *Erysipelatoclostridium*	11 (55)	8.4 ± 0.9	
Clostridium ramosum	8 (40)	8.2 ± 0.9	SAA; ABA; CA; PAB
Clostridium innocuum	8 (40)	8.1 ± 0.43	SAA; ABA; CA; PAB
Clostridium saccharogumia	1 (5)	8.7	ABA
Clostridium spiroforme	1 (5)	9	SAA
Holdemanella biformis	1 (5)	9.4	SAA
Dielma fastidiosa	1 (5)	8	SAA; ABA; CA
Coprobacillus cateniformis	1 (5)	9	ABA
Absiella dolichum	1 (5)	8	CA
Turicibacter sanguinis	1 (5)	8	SAA
Class *Clostridia*, order *Clostridiales*			
Family *Clostridiaceae*	**10 (50)**	**8.5 ± 1.1**	
Genus *Clostridium*	4 (20)	8.1 ± 1.4	
Clostridium perfringens	3 (15)	8.5 ± 0.7	SAA; CA; PAB
Clostridium paraputrificum	2 (10)	6.3 – 9.4	SAA; ABA; PAB
Clostridium ventriculi	1 (5)	10.4	ABA
Clostridium barattii	1(5)	6	PAB
Hungatella hathewayi	7 (35)	7.8 ± 0.8	SAA; PAB
Mordavella sp.	1 (5)	9	ABA
Lactonifactor sp. ASD3451	1 (5)	8	PAB
Family *Lachnospiraceae*	**17 (85)**	**9.0 ± 1.0**	
Genus *Lachnoclostridium*	**13 (65)**	**8.4 ± 1.0**	
Clostridium clostridioforme	11 (55)	8.2 ± 1.0	SAA; ABA; PAB
Clostridium scindens	3 (15)	8.0 ± 0.0	SAA; PAB
Clostridium symbiosum	2 (10)	6.0 – 8.0	SAA; PAB
Lachnoclostridium sp. ASD2032	1 (5)	9	SAA
Clostridium lavalense	1 (5)	6	PAB
Clostridium hylemonae	1 (5)	9	SAA
Lachnoclostridium sp. ASD3950	1 (5)	9.3	ABA
Anaerostipes sp.	8 (40)	8.2 ± 1.0	SAA; ABA; CA
Eisenbergiella tayi	2 (10)	8.0 – 9.0	ABA; CA
Genus *Blautia*	**13/65**	**8.9 ± 0.9**	
Blautia torques	7 (35)	8.8 ± 0.5	SAA; ABA; CA
Blautia coccoides	6 (30)	7.5 ± 0.8	ABA; PAB
Blautia gnavus	6 (30)	8.7 ± 0.6	SAA; ABA; CA
Blautia luti	5 (25)	8.5 ± 0.7	SAA; ABA
Blautia faecis	5 (25)	8.6 ± 0.6	SAA; CA
Blautia obeum	3 (15)	8.5 ± 0.5	SAA; ABA
Blautia wexlerae	2 (10)	8.0 – 9.0	ABA; PAB
Blautia sp. ASD2945	1 (5)	8	ABA
Blautia caecimuris	1(5)	9.6	ABA; CA
Family *Ruminococcaceae*	**13/65**	**8.8 ± 0.5**	
Flavonifractor plautii	7 (35)	8.7 ± 0.5	SAA; ABA; PAB
Ruthenibacterium lactatiformans	5 (25)	8.5 ± 0.5	ABA; CA
Anaerotruncus colihominis	4 (20)	8.3 ± 0.5	ABA; PAB
Flavonifractor sp. ASD20665	1 (5)	7.3	PAB
Monoglobus pectinilyticus	1 (5)	8.3	SAA
Ruminiclostridium leptum	1 (5)	8	ABA

Faecalibacterium prausnitzii	1 (5)	8.3	ABA
Gemmiger formicilis	1 (5)	8	ABA
Agathobaculum sp. ASD2948	1 (5)	8	ABA
Ruminococcaceae ASD2818	1 (5)	8	SAA
Genus *Dorea*	**4 (20)**	**8.6 ± 0.6**	
Dorea *longicatena*	3 (15)	**8.2 ± 0.3**	SAA; ABA; PAB
Dorea *formicirans*	1 (5)	8	PAB
Dorea sp.	1 (5)	9.3	ABA
Sellimonas intestinalis	7 (35)	8.8 ± 0.5	SAA; ABA;
Fusicatenibacter saccharivorans	3 (15)	**8.4 ± 0.5**	ABA; CA
Coprococcus comes	1 (5)	8.8	ABA
Family *Eubacteriaceae*	4 (20)	7.8 ± 0.39	ABA; PAB
Eubacterium limosum			
Family *Christensenellaceae*	1 (5)	9	CA
Christensenella minuta			
Family *Peptostreptococcaceae*			
Terrisporobacter sp.	1 (5)	8	PAB
Paeniclostridium sordellii	1 (5)	9	SAA
Genera with uncertain taxonomic position			
Intestinimonas sp.	1 (5)	9	ABA
Lawsonibacter asaccharolyticus	1 (5)	9	CA
Class *Bacilli*			
Order *Lactobacillales*			
Family *Lactobacillaceae*			
Genus *Lactobacillus*	13/65	6.3 ± 1.6	
Lactobacillus casei/paracasei	6 (30)	6.3 ± 1.9	MRS
Lactobacillus gasseri/acidophilus	5 (20)	7.0 ± 1.2	MRS
Lactobacillus rhamnosus	3 (15)	4.5 ± 0.2	MRS
Lactobacillus salivarius/delbruekii	2 (10)	5.5 – 6.3	MRS
Lactobacillus fermentum	1 (5)	4	MRS
Lactobacillus brevis	1 (5)	4	MRS
Family *Leuconostocaceae*	1 (5)	6.3	MRS
Leuconostoc lactis			
Family *Enterococcaceae*			
Genus *Enterococcus*	16/80	6.1 ± 1.3	
Enterococcus faecalis	8 (40)	5.8 ± 1.0	mEA
Enterococcus faecium	9 (45)	4.9 ± 0.7	mEA
Enterococcus durans	3 (15)	4.3; 4.8; 9.5	mEA
Enterococcus avium/raffinosus	7 (35)	6.5 ± 0.8	mEA
Enterococcus casseliflavus	1 (5)	6	mEA
Enterococcus gallinarum	1 (5)	4	mEA
Family *Streptococcaceae*			
Genus *Streptococcus*	19/95	7.5 ± 1.2	
Streptococcus salivarius	17/85	6.9 ± 1.2	mEA. MRS
Streptococcus parasanguinis	9 (45)	6.6 ± 1.0	mEA. MRS
Streptococcus oralis/pneumoniae/mitis	5 (45)	7.1 ± 2.6	mEA. MRS
Streptococcus anginosus	2 (10)	5.0 – 5.7	mEA. MRS
Streptococcus mutans	2 (10)	6.1 – 6.3	mEA. MRS
Streptococcus constellatus	1 (5)	6	MRS
Streptococcus infantarius	1 (5)	8.4	MRS
Streptococcus disgalactiae	1 (5)	8.9	CA
Genus *Lactococcus*	1 (5)	6.1	MRS
Lactococcus lactis			

Family *Aerococcaceae*	1 (5)	6	SAA
Aerococcus viridans			
Order *Bacillales*			
Family *Staphylococcaceae*	18/90	5.0 ± 1.7	
Staphylococcus aureus	14/70	3.9 ± 0.8	GMSA
Staphylococcus epidermidis	6 (30)	4.3 ± 1.4	GMSA
Staphylococcus hominis	3 (15)	4.6 ± 0.8	GMSA
Staphylococcus haemolyticus	3 (15)	2.5 – 5.2	GMSA
Staphylococcus sacharolyticus	2 (10)	9	ABA
Staphylococcus warneri	2 (10)	5.2 – 8.8	GMSA; CA
Staphylococcus capitis	1 (5)	4.3	GMSA
Staphylococcus gallinarum	1 (5)	3.2	GMSA
Family *Bacillaceae*	6 (30)	3.4 ± 0.3	GMSA
Bacillus sp.			
Class *Negativicutes*			
Order *Veillonellales*	**12 (60)**	**8.8 ± 0.9**	
Family *Veillonellaceae*			
Veilonella sp.	7 (35)	8.0 ± 0.9	SAA; ABA; CA
Allisonella histaminiformans	1 (5)	8	ABA
Genus *Dialister*	**9 (45)**	**9.0 ± 0.5**	
Dialister invisus	8 (40)	9.1 ± 0.4	SAA; ABA
Dialister succinatiphilus	1 (5)	8	CA
Order *Selenomonadales*, family *Selenomonadacea*			
Megamonas sp.	2 (10)	8.8 – 9.0	ABA; CA
Order *Acidaminococcales,* family *Acidaminococcaceae*			
Phascolarctobacterium faecium	8 (40)	9.0 ± 0.4	SAA; ABA; CA
Phascolarctobacterium succinatutens	1 (5)	8	SAA

which could not be established are listed in the Table 6. Most of them (7 of 10 strains) belonged to the phylum *Firmicutes*. Four of them had a phylogenetic relationship with species from the genera *Blautia*, *Flintibacter* and *Lachnoclostridium* of the family *Lachnospiraceae*. Two clones were close to different species of the family *Ruminococcaceae*, and another clone was phylogenetically similar to members of the genus *Lactonifractor* of the family *Clostridiaceae*. In addition, one clone of the new bacterial taxon was associated with a typical strain belonging to the family *Sutterellaceae*, included in the *Proteobacteria* phylum, and one clone belonged to the genera *Parabacteroides* and *Bacteroides* (families *Porphyromonadaceae* and *Bacteroidaceae* respectively, phylum *Bacteroidetes*).

DISCUSSION

This age group of children was chosen for the study because earlier it was shown that the qualitative and quantitative parameters of the gut microbiota by the age of three years become close to the typical adults values [17]. By this age, the gut microbiota acquires relative compositional stability and does not change significantly over time [18].

The main problems regarding the culture-based methods are associated with the selection of growth media, which provide the growth of fastidious strictly anaerobic bacteria, and with the further identification of numerous strains of microorganisms growing on these media. In our study we used well-known growth media including media for the strictly anaerobic bacteria. After inoculation of media Petri dishes were incubated at 37 °C in the anaerobic jars.

It was previously shown that increase the number of growth media and the number of samples leads to isolation of a large number of bacterial species, which indicates significant individual differences in the composition of the human gut microbiota [3]. This is confirmed by the results of metagenomic sequencing, which revealed a very high variability in abundance (12–2,200 times) for the 57 most common human bacterial species [19]. In our study, though an average of 34 ± 8 species of microorganisms was isolated from each child, in total, 159 species of bacteria were found in all children, including new taxa.

The greatest species diversity (more than 90 species of bacteria) was found in the phylum *Firmicutes*, with more than half of them belonging to the class *Clostridia* of the order *Clostridiales*. The dominating by frequency of occurrence and quantitative content families of this class were *Lachnospiraceae* and *Ruminococcaceae*. The obtained data characterizing the composition of this part of microbiota in Russian children correspond with the results of previous studies, in which both culture-based methods and the analysis of the nucleotide sequences of the libraries of 16S rDNA genes established the dominance of these taxa in human gut microbiota [6, 20].

Among the representatives of intestinal endosymbionts, which belong to the classes *Erysipelotrichia* and *Clostridia* isolated in pure culture from feces of healthy children the bacteria associated with various infectious diseases were also present. Therefore, the improvement of the culture methods and species identification for the bacteria of these taxa has not only ecological but also clinical significance. For example, *Clostridium innocuum* is often associated with bacteriemia in

Table 3. Species identity of the *Bacteroidetes* phylum cultured bacteria of the gastrointestinal tract microflora isolated from healthy children (n = 20)

Phylum *Bacteroidetes*, class *Bacteroidia*, order *Bacteroidales*			
Taxa	Observed number (%)	Mean ± SD $\log_{10}$ CFU/g	Growth media
Family *Bacteroidaceae*	**20 (100)**	**10.1 ± 0.4**	
Bacteroides dorei/vulgatus	19 (95)	9.5 ± 0.5	SAA; ABA; CA
Bacteroides ovatus/xylanisolvens	16 (80)	9.2 ± 0.5	SAA; ABA; CA
Bacteroides uniformis	17 (85)	9.4 ± 0.5	SAA; ABA; CA
Bacteroides fragilis	9 (45)	9.1 ± 0.6	SAA; ABA; CA
Bacteroides thetaiotaomicron	9 (45)	9.1 ± 0.5	SAA; ABA; CA
Bacteroides caccae	8 (40)	9.0 ± 0.7	SAA; ABA; CA
Bacteroides eggerthii	6 (30)	9.2 ± 0.5	SAA; ABA; CA
Bacteroides stercoris	4 (20)	9.0 ± 0.2	SAA; ABA; CA
Bacteroides intestinalis	3 (15)	9.2 ± 0.3	SAA; ABA; CA
Bacteroides clarus	2 (10)	9.0 – 10.3	ABA
Bacteroides massiliensis	2 (10)	9.3 – 9.5	SAA; ABA; CA
Bacteroides plebeius	1 (5)	9.6	SAA; ABA; CA
Bacteroides coprocola	1 (5)	8	ABA
Bacteroides salyersiae	1 (5)	8	CA
Bacteroides sp. ASD2038	1 (5)	9.7	SAA
Family *Rikenellaceae*	**18/90**	**9.5 ± 0.4**	
Alistipes onderdonkii	11 (55)	9.1 ± 0.5	SAA; ABA; CA
Alistipes putredinis	10 (50)	9.5 ± 0.5	SAA; ABA; CA
Alistipes finigoldii	8 (40)	8.8 ± 0.7	SAA; ABA; CA
Alistipes shachii	5 (25)	9.2 ± 0.3	SAA; ABA; CA
Alistipes indistinctus	2 (10)	8.0 – 9.0	CA
Alistipes obessii	3 (15)	9.1 ± 0.2	ABA
Alistipes inops	3 (15)	8.8 ± 0.7	SAA; ABA
Alistipes massiliensis	1 (5)	8.8	ABA; CA
Alistipes ihumii	1 (5)	9.4	SAA; ABA
Family *Porphyromonadaceae*	**15 (75)**	**9.4 ± 0.5**	
Genus *Parabacteroides*	13 (65)	9.2 ± 0.7	
Parabacteroides distasonis	9 (45)	9.1 ± 0.8	SAA; ABA; CA
Parabacteroides merdae	7 (35)	8.9 ± 0.7	SAA; ABA; CA
Parabacteroides sp. ASD2049	1 (5)	9	SAA
Barnesiella intestinihominis	8 (40)	9.2 ± 0.3	SAA; ABA; CA
Coprobacter fastidiosus	3 (15)	9.1 ± 0.1	SAA; ABA; CA
Family *Odoribacteraceae*	**8 (40)**	**9.3 ± 0.3**	
Odoribacter splanchnicus	5 (25)	9.3 ± 0.3	SAA; ABA; CA
Butyricimonas sp.	4 (20)	9.3 ± 0.4	ABA; CA
Family *Prevotellaceae*	**3 (15)**	**8.8 ± 0.9**	
Prevotella copri	2 (10)	8.5 – 9.0	SAA; ABA; CA
Prevotella melaninogenica	1 (5)	8	ABA
Prevotella rara	1 (5)	9	ABA; CA
Paraprevotella clara	1 (5)	9.6	ABA; CA

patients with immunodeficiency. It is resistant to antibacterial drugs used for treatment of anaerobic infections. *C. ramosum*, which were also isolated, are considered the second most common bacteria from the clostridium group after *C. perfringens*, causing abscesses, peritonitis, bacteriemia and chronic otitis media in children, and the third most common type of clostridia causing bacteriemia in adults [21, 22].

The *Bacteroidetes* phylum made up the second group by the number of identified taxa after *Firmicutes* and was represented by 33 species of bacteria belonging, however, to only one order *Bacteroidales*.

It is known that *Bacteroidales* includes the main part of anaerobic nonsporeforming gram-negative rod-shaped bacteria that colonize the human gastrointestinal tract [23]. We found, that in the group of children under study representatives of the *Bacteroidaceae*, *Rikenellaceae* and *Porphyromonadaceae* families dominated and were isolated from 100%, 90% and 75% of children respectively. In our previous study, to assess

Table 4. Species identity of the *Proteobacteria* phylum cultured bacteria of the gastrointestinal tract microflora isolated from healthy children (*n* = 20)

Phylum *Proteobacteria*			
Class *Gammaproteobacteria*			
Taxa	Observed number (%)	Mean ± SD log_{10} CFU/g	Growth media
Order *Enterobacteriales*, family *Enterobacteriaceae*			
Escherichia coli	20 (100)	7.2 ± 1.4	EA; CAa
Enterobacter cloacae	6 (30)	6.0 ± 1.5	EA; SSA; CAa
Citrobacter freundii	4 (20)	5.8 ± 0.68	EA; SSA; CAa
Klebsiella pneumonia	4 (20)	6.5 ± 1.7	EA; CAa
Leclercia adecarboxylata	1 (5)	6.5	CAa
Proteus mirabilis	1 (5)	6	SSA; CAa
Class *Betaproteobacteria*, order *Burkholderiales*			
Family *Sutterellaceae*	12 (60)	8.8 ± 0.4	
Parasutterella excrementihominis	4 (20)	8.6 ± 0.4	ABA; CA
Sutterella wadsworthensis	5 (25)	8.9 ± 0.1	ABA
Sutterella massiliensis	1 (5)	9.5	CA
Sutterella sp. ASD3426	1 (5)	8	CA
Duodenibacillus massiliensis	1 (5)	9.1	SAA
Family *Oxalobacteraceae*	1 (5)	8	CA
Massilia timonae			
Class *Deltaproteobacteria*			
Order *Desulfovibrionales*, family *Desulfovibrionaceae*			
Bilophila wadsworthia	11 (55)	8.0 ± 0.8	SAA; CA; PAB
Desulfovibrio piger	1 (5)	8.1	PAB

the composition of the dominant groups of intestinal bacteria belonging to the *Bacteroidales* order in 6 years old children, we inoculated serial dilutions of feces only on Columbia Blood Agar with the addition of sheep blood followed by determining the species of anaerobic gram-negative rod-shaped bacteria using the restriction analysis of amplified fragments of the 16S rRNA gene (ARDRA), as well as their sequencing.

In that study, we isolated only 38 strains of bacteria belonging to 13 species of *Bacteroidales* from 8 children [12]. In the present study, we used 3 different growth media to identify the same group of bacteria, with preliminary identification of all the grown bacteria using mass spectrometry and additional 16S rDNA gene sequencing for strains with an unclear taxonomic position. This approach allowed us to distinguish 33 species of bacteria belonging to 9 genera and 5 families of the order *Bacteroidales* in addition to bacteria belonging to other taxonomic groups.

Bacteria of *Prevotellaceae* family, also belonging to the order *Bacteroidales*, were found only in three children (15%). In spite of the fact that about 30 prevotella's species are known to date, as bacteria colonizing mainly the human oral cavity, until recently only 2 species *P. copri* and *P. stercorea* were considered commensals of the gastrointestinal tract. In our study in addition to *P. copri* the bacteria from species *P. melaninogenica*, which are rarely isolated from the intestine, and recently described new species *P. rara* were isolated from a child for the first time [24].

As predominant groups of intestinal bacteria, prevotella is most often determined in people whose diet is based on the products of plant origin, which is associated with the ability of these bacteria to degrade plant polysaccharides in the distal intestinal tract [20]. On the other hand, the prevalence in the gut microbiota the bacteria of the *Bacteroides* genus and the *Clostridiales* order, as shown in our study, had been previously associated with a mixed diet characterized by the inclusion in diet both animal and vegetable products along with easily digestible carbohydrates [25, 26].

CONCLUSIONS

The approach we used, based on the use of a wide range of growth media for the isolation of difficult-to-cultivate groups of intestinal endosymbionts, both under aerobic and anaerobic conditions, followed by the bacteria species identification by the MALDI TOF mass spectrometry and the 16S rRNA gene sequencing, allowed us to analyze the qualitative and quantitative composition of the dominant cultivated groups of gut microbiota in children. In general, the results describing the taxonomic composition of the fecal microbiota of children obtained by the culture-based method do not contradict the data obtained by molecular methods based on the sequencing of bacterial DNA. In addition, we have isolated in pure culture the numerous strains of difficult-to-cultivate bacteria and 10 strains of new bacteria with not yet studied biological properties. The data obtained allow us to expand our understanding of the spectrum of cultivated taxonomic groups of colon bacteria and their quantitative content in children. The strains we isolated, both belonging to known and new taxa, can be used to study a wide repertoire of their properties, including their biotherapeutic potential for creating the new probiotic medications. At the same time, many well-known taxa of gut microbiota, including representatives of such dominant genera as *Faecalibacterium* and *Roseburia*, we were unable to isolate, which indicates the need to use

Table 5. Species identity of the *Saccharomycetales* order fungi isolated from healthy children (*n* = 20)

Fungi taxa	Observed number (%)	Mean ± SD log_{10} CFU/g	Growth media
Order *Saccharomycetales*	**9 (45)**	**3.4 ± 1.4**	
Family *Debaryomycetaceae*	**7 (35)**	**3.5 ± 1.4**	
Candida albicans	5 (25)	3.7 ± 1.4	SC2A
Candida parapsilosis	1 (5)	2.5	SC2A
Candida sp.	1 (5)	2.5	SC2A
Family *Metschnikowiaceae*	2 (10)	2.0 – 5.0	SC2A
Clavispora lusitaniae			

Table 6. New gastrointestinal tract bacteria phylotypes isolated from healthy children and the values of the nucleotide sequences of their 16S rDNA levels of homology with the same sequences of typical strains of the most closely related validated species in accordance with the International Code of Nomenclature of Bacteria (Bacteriological Code)

№	Strain number	Phylum/family	№ of sequencing in the GenBank database	Related strains with high level of sequence similarity (megablast algorithm) in the GenBank database	Homology (%)
1	ASD 3426	*Proteobacteria Sutterellaceae*	MK615133.1	*Sutterella wadsworthensis* WAL9799	97.93
2	ASD2049	*Bacteroidetes Porphyromonadaceae*	MG321612.1	*Parabacteroides merdae* JCM9497	96.63
3	ASD2038	*Bacteroidetes Bacteroidaceae*	MK615124.1	*Bacteroides ovatus* ATCC 8483	98.19
4	ASD2032	*Firmicutes Lachnospiraceae*	MK615123.1	[Clostridium] *amygdalinum* BR-10	95.72
5	ASD2945	*Firmicutes Lachnospiraceae*	MK615128.1	*Blautia faecis* KB1	96.03
6	ASD3950	*Firmicutes Lachnospiraceae*	MK615131.1	[Clostridium] *glycyrrhizinilyticum* ZM35	95.73
7	ASD3451	*Firmicutes Clostridiaceae*	MK615130.1	*Lactonifactor longoviformis* ED-Mt61/PYG-s6	94.61
8	ASD20665	*Firmicutes Ruminococcaceae*	MK615126.1	*Flintibacter butyricus* BLS21	97.33
9	ASD2818	*Firmicutes Ruminococcaceae*	MH043116.1	*Caproiciproducens galactitolivorans* BS-1	93.76
10	ASD2948	*Firmicutes Ruminococcaceae*	MK615129.1	*Agathobaculum desmolans* ATCC43058	97.01

more advanced anaerobic technologies in such studies, in particular, anaerobic glove box at the stages of sample preparation, inoculation and grown culture counting. The complexity and labor input of the culture-based method do not allow recommend it for the routine use in clinical practice, even assuming that in the future all stages of the study would be fully automated. However, the development of methods of isolation and identification of strictly anaerobic colon bacteria is necessary, since these bacteria can have pathobiotic potential and occur in clinical material (wound discharge, biopsy specimens, blood, liquor, etc.), in which the usual quantitative content of the species of bacteria is not so great.

References

1. Mailhe M, Ricaboni D, Vitton V, Gonzalez JM, Bachar D, Dubourg G, et al. Repertoire of the gut microbiota from stomach to colon using culturomics and next-generation sequencing. BMC Microbiol. 2018; (18): 157.
2. Atanu A, Mojibur RK. An insight into gut microbiota and its functionalities. Cellular and Molecular Life Sciences. 2019; (76): 473–93.
3. Hayashi H, Sakamoto M, Benno Y. Phylogenetic analysis of the human gut microbiota using 16S rDNA clone libraries and strictly anaerobic culture-based methods. Microbiol Immunol. 2002; 46 (8): 535–48.
4. Lagier J-C, Khelaifia S, Alou MT, Ndongo S, Dione N, Hugon P, et al. Culture of previously uncultured members of the human gut microbiota by culturomics. Nature Microbiology. 2016; (1): 16203.
5. Shkoporov AN, Hill C. Bacteriophages of the Human Gut: The "Known Unknown" of the Microbiome. Cell Host Microbe. 2019; 25 (2): 195–209.
6. Vandeputte D, Kathagen G, D'hoe K, Vieira-Silva S, Valles-Colomer M, Sabino J, et al. Quantitative microbiome profiling links gut community variation to microbial load. Nature. 2017; (551): 507–11.
7. Tanoue T, Morita S, Plichta DR. A defined commensal consortium elicits CD8 T cells and anti-cancer immunity. Nature. 2019; (565): 600–05.
8. Shkoporov AN, Efimov BA, Khokhlova EV, Chernaia ZA, Postnikova EA, Belkova MD. Effect of probiotic *Lactobacillus* and *Bifidobacterium* cultures on intestinal microbiota composition in healthy adults. Tekhnika i Tekhnologiya Pishchevykh Proizvodstv. 2014; (1): 126–30. Russian.
9. Lagier JC, Dubourg G, Million M, Cadoret F, Bilen M, Fenollar F, et al. Culturing the human microbiota and culturomics. Nat Rev Microbiol. 2018; (1): 540–50.
10. Rychert J, Burnham CA, Bythrow M, Garner OB, Ginocchio CC, Jennemann R, et al. Multicenter evaluation of the Vitek MS matrix-assisted laser desorption ionization-time of flight mass spectrometry system for identification of Gram-positive aerobic

bacteria. J Clin Microbiol. 2013; 51 (7): 2225–31.
11. McMullen AR, Wallace MA, Pincus DH, Wilkey K, Burnham CA. Evaluation of the Vitek MS matrix-assisted laser desorption ionization–time of flight mass spectrometry system for identification of clinically relevant filamentous fungi. J Clin Microbiol. 2016; (54): 2068–73.
12. Shkoporov AN, Khokhlova EV, Kulagina EV, Smeianov VV, Kafarskaia LI, Efimov BA. Application of several molecular techniques to study numerically predominant Bifidobacterium spp. and Bacteroidales order strains in the feces of healthy children. Biosci Biotechnol Biochem. 2008; 72 (3): 742–8.
13. Chaplin AV, Brzhozovskii AG, Parfenova TV, Kafarskaia LI, Volodin NN, Shkoporov AN, et al. Species Diversity of *Bifidobacteria* in the Intestinal Microbiota Studied Using MALDI-TOF Mass-Spectrometry. Vestn Ross Akad Med Nauk. 2015; 70 (4): 435–40. Russian.
14. Stackebrandt E, Ebers J. Taxonomic parameters revisited: tarnished gold standards. Microbiol Today. 2006; (8): 6–9.
15. Bezdek JC, Hathaway RJ. VAT: A Tool for Visual Assessment of Cluster Tendency. In: Proceedings of the 2002 International Joint Conference Neural Networks. 2002; (3): 2225–30.
16. Fitzgerald CB, Shkoporov AN, Sutton TDS, Chaplin AV, Velayudhan V, Ross RP, et al. Comparative analysis of *Faecalibacterium prausnitzii* genomes shows a high level of genome plasticity and warrants separation into new species-level taxa. BMC Genomics. 2018; 19 (1): 931.
17. Yatsunenko T, Rey FE, Manary MJ, Trehan I, Dominguez-Bello MG, Contreras M, et al. Human gut microbiome viewed across age and geography. Nature. 2012; 486 (7402): 222–7.
18. De Meij TGJ, Budding AE, De Groot EFJ, Jansen FM, Kneepkens CMF, Benninga MA, et al. Composition and stability of intestinal microbiota of healthy children within a Dutch population. FASEB J. 2016; 30 (4): 1512–22.
19. Qin J, Li R, Raes J, Arumugam M, Burgdorf KS, Manichanh C, et al. MetaHIT Consortium A human gut microbial gene catalogue established by metagenomic sequencing. Nature. 2010; (464): 59–65.
20. Browne HP, Forster SC, Anonye BO. Culturing of 'unculturable' human microbiota reveals novel taxa and extensive sporulation. Nature. 2016; 533 (7604): 543–6.
21. Brook I. Clostridial Infections in Children: Spectrum and Management. Curr Infect Dis Rep. 2015; (17): 47.
22. Chia JH, Feng Y, Su LH, Wu TL, Chen CL, Liang YH, et al. Clostridium innocuum is a significant vancomycin-resistant pathogen for extraintestinal clostridial infection Clinical Microbiology and Infection. 2017; (23): 560–6.
23. The Human Microbiome Project Consortium. Structure, function and diversity of the healthy human microbiome. Nature. 2012; 486 (7402): 207–14.
24. Efimov BA, Chaplin AV, Shcherbakova VA, Suzina NE, Podoprigora IV, Shkoporov AN. Prevotella rara sp. nov., isolated from human faeces. Int J Syst Evol Microbiol. 2018; 68 (12): 3818–25.
25. Shankar V, Gouda M, Moncivaiz J, Gordon A, Reo NV, Hussein L, et al. Differences in Gut Metabolites and Microbial Composition and Functions between Egyptian and U.S. Children Are Consistent with Their Diets. mSystems. 2017; 2 (1): e00169–16.
26. Arumugam M, Raes J, Pelletier E, Le Paslier D, Yamada T, Mende DR, et al. Enterotypes of the human gut microbiome. Nature. 2011; 473 (7346): 174–80.

Литература

1. Mailhe M, Ricaboni D, Vitton V, Gonzalez JM, Bachar D, Dubourg G, et al. Repertoire of the gut microbiota from stomach to colon using culturomics and next-generation sequencing. BMC Microbiol. 2018; (18): 157.
2. Atanu A, Mojibur RK. An insight into gut microbiota and its functionalities. Cellular and Molecular Life Sciences. 2019; (76): 473–93.
3. Hayashi H, Sakamoto M, Benno Y. Phylogenetic analysis of the human gut microbiota using 16S rDNA clone libraries and strictly anaerobic culture-based methods. Microbiol Immunol. 2002; 46 (8): 535–48.
4. Lagier J-C, Khelaifia S, Alou MT, Ndongo S, Dione N, Hugon P, et al. Culture of previously uncultured members of the human gut microbiota by culturomics. Nature Microbiology. 2016; (1): 16203.
5. Shkoporov AN, Hill C. Bacteriophages of the Human Gut: The "Known Unknown" of the Microbiome. Cell Host Microbe. 2019; 25 (2): 195–209.
6. Vandeputte D, Kathagen G, D'hoe K, Vieira-Silva S, Valles-Colomer M, Sabino J, et al. Quantitative microbiome profiling links gut community variation to microbial load. Nature. 2017; (551): 507–11.
7. Tanoue T, Morita S, Plichta DR. A defined commensal consortium elicits CD8 T cells and anti-cancer immunity. Nature. 2019; (565): 600–05.
8. Шкопоров А. Н., Ефимов Б. А., Хохлова Е. В., Черная З. А., Постникова Е. А., Белкова М. Д. Влияние приема пробиотических бактерий рода *Lactobacillus* и *Bifidobacterium* на состав микрофлоры кишечника у здоровых людей. Техника и технология пищевых производств. 2014; (1): 126–30.
9. Lagier JC, Dubourg G, Million M, Cadoret F, Bilen M, Fenollar F, et al. Culturing the human microbiota and culturomics. Nat Rev Microbiol. 2018; (1): 540–50.
10. Rychert J, Burnham CA, Bythrow M, Garner OB, Ginocchio CC, Jennemann R, et al. Multicenter evaluation of the Vitek MS matrix-assisted laser desorption ionization-time of flight mass spectrometry system for identification of Gram-positive aerobic bacteria. J Clin Microbiol. 2013; 51 (7): 2225–31.
11. McMullen AR, Wallace MA, Pincus DH, Wilkey K, Burnham CA. Evaluation of the Vitek MS matrix-assisted laser desorption ionization–time of flight mass spectrometry system for identification of clinically relevant filamentous fungi. J Clin Microbiol. 2016; (54): 2068–73.
12. Shkoporov AN, Khokhlova EV, Kulagina EV, Smeianov VV, Kafarskaia LI, Efimov BA. Application of several molecular techniques to study numerically predominant Bifidobacterium spp. and Bacteroidales order strains in the feces of healthy children. Biosci Biotechnol Biochem. 2008; 72 (3): 742–8.
13. Чаплин А. В., Бржозовский А. Г., Парфёнова Т. В., Кафарская Л. И., Володин Н. Н., Шкопоров А. Н. и др. Изучение видового разнообразия бактерий рода *Bifidobacterium* кишечной микрофлоры с использованием метода MALDI-TOF масс-спектрометрии. Вестник РАМН. 2015; 70 (4): 435–40.
14. Stackebrandt E, Ebers J. Taxonomic parameters revisited: tarnished gold standards. Microbiol Today. 2006; (8): 6–9.
15. Bezdek JC, Hathaway RJ. VAT: A Tool for Visual Assessment of Cluster Tendency. In: Proceedings of the 2002 International Joint Conference Neural Networks. 2002; (3): 2225–30.
16. Fitzgerald CB, Shkoporov AN, Sutton TDS, Chaplin AV, Velayudhan V, Ross RP, et al. Comparative analysis of *Faecalibacterium prausnitzii* genomes shows a high level of genome plasticity and warrants separation into new species-level taxa. BMC Genomics. 2018; 19 (1): 931.
17. Yatsunenko T, Rey FE, Manary MJ, Trehan I, Dominguez-Bello MG, Contreras M, et al. Human gut microbiome viewed across age and geography. Nature. 2012; 486 (7402): 222–7.
18. De Meij TGJ, Budding AE, De Groot EFJ, Jansen FM, Kneepkens CMF, Benninga MA, et al. Composition and stability of intestinal microbiota of healthy children within a Dutch population. FASEB J. 2016; 30 (4): 1512–22.
19. Qin J, Li R, Raes J, Arumugam M, Burgdorf KS, Manichanh C, et al. MetaHIT Consortium A human gut microbial gene catalogue established by metagenomic sequencing. Nature. 2010; (464): 59–65.
20. Browne HP, Forster SC, Anonye BO. Culturing of 'unculturable' human microbiota reveals novel taxa and extensive sporulation. Nature. 2016; 533 (7604): 543–6.
21. Brook I. Clostridial Infections in Children: Spectrum and Management. Curr Infect Dis Rep. 2015; (17): 47.
22. Chia JH, Feng Y, Su LH, Wu TL, Chen CL, Liang Y-H, et al. Clostridium innocuum is a significant vancomycin-resistant pathogen for extraintestinal clostridial infection Clinical Microbiology and Infection.

2017; (23): 560–6.
23. The Human Microbiome Project Consortium. Structure, function and diversity of the healthy human microbiome. Nature. 2012; 486 (7402): 207–14.
24. Efimov BA, Chaplin AV, Shcherbakova VA, Suzina NE, Podoprigora IV, Shkoporov AN. Prevotella rara sp. nov., isolated from human faeces. Int J Syst Evol Microbiol. 2018; 68 (12): 3818–25.
25. Shankar V, Gouda M, Moncivaiz J, Gordon A, Reo NV, Hussein L, et al. Differences in Gut Metabolites and Microbial Composition and Functions between Egyptian and U.S. Children Are Consistent with Their Diets. mSystems. 2017; 2 (1): e00169–16.
26. Arumugam M, Raes J, Pelletier E, Le Paslier D, Yamada T, Mende DR, et al. Enterotypes of the human gut microbiome. Nature. 2011; 473 (7346): 174–80.

THE FEASIBILITY OF USING COMPUTER-BASED MODELS FOR REDUCING THE RISKS OF COMPLICATIONS ASSOCIATED WITH TEMPORARY DENTURES

Bagryantseva NV[1,2] ✉, Gazhva SI[1], Baranov AA[2], Shubin LB[2], Bagryantsev VA[2], Bagryantseva OV[2]

[1] Privolzhsky Research Medical University, Nizhny Novgorod, Russia

[2] Yaroslavl State Medical University, Yaroslavl, Russia

Contemporary prosthetic dentistry has a vast arsenal of solutions for completely edentulous patients. However, it is crucial to consider a variety of factors that can cause complications in patients wearing temporary dentures in the osseointegration period. The aim of this study was to retrospectively analyze the medical records of completely edentulous patients wearing temporary removable or fixed dentures in the osseointegration period, to identify the risk factors for complications and to calculate the odds of adverse events. We performed a multivariate analysis and developed a computerized algorithm that could be used to facilitate selection of the proper denture type and material. The algorithm demonstrates high sensitivity and specificity: 94.37 (76.2 : 98.7) and 92.56 (79.8 : 97.6), respectively; the AUC value is 0.921 (0.843 : 0.963). We are planning to develop a software based on the proposed algorithm that would help the dentist to make a more objective decision when selecting the type of temporary denture and its material.

Keywords: dental implants, osseointegration, temporary prosthesis, risks, odds, computer-based model

Author contribution: Bagryantseva NV — study design, data acquisition, analysis and interpretation, manuscript editing; Gazhva SI — study planning and manuscript editing; Baranov AA — manuscript editing; Shubin LB — data analysis and interpretation; Bagryantsev VA, Bagryantseva OV — data acquisition and preparing the manuscript draft.

Compliance with ethical standards: the study was approved by the Ethics Committee of Privolzhsky Research Medical University (Protocol No.10 dated December 25, 2017)

✉ **Correspondence should be addressed:** Natalia V. Bagryantseva
March 8, d. 1, kor. 2, kv. 71, Yaroslavl, 150002; nbogryanceva@mail.ru

Received: 25.07.2019 **Accepted:** 09.08.2019 **Published online:** 16.08.2019

DOI: 10.24075/brsmu.2019.050

ВОЗМОЖНОСТИ ИСПОЛЬЗОВАНИЯ КОМПЬЮТЕРНЫХ МОДЕЛЕЙ ДЛЯ СНИЖЕНИЯ РИСКОВ ПРИ ВРЕМЕННОМ ПРОТЕЗИРОВАНИИ

Н. В. Багрянцева[1,2] ✉, С. И. Гажва[1], А. А. Баранов[2], Л. Б. Шубин[2], В. А. Багрянцев[2], О. В. Багрянцева[2]

[1] Приволжский исследовательский медицинский университет, Нижний Новгород, Россия

[2] Ярославский государственный медицинский университет, Ярославль, Россия

Современная ортопедическая стоматология обладает большим арсеналом решений для оказания помощи пациентам с полной вторичной адентией, что, однако, может вызывать ряд проблем. При выборе вида временного протеза на момент остеоинтеграции дентальных имплантатов необходимо учитывать большое количество факторов, возникающих при различных клинических ситуациях. Целью работы было в ходе ретроспективного анализа медицинской документации пациентов с полной вторичной адентией и установленными временными протезами (покрывными съемными и условно-съемными) на момент остеоинтеграции дентальных имплантатов оценить факторы риска и отношение шансов их реализации в развитии осложнений на этот период. Осуществлено многомерное математико-статистическое моделирование с построением компьютерного алгоритма принятия решений в выборе типа протеза и материала для его изготовления. Алгоритм (модель) обладает высокими значениями чувствительности и специфичности — 94,37 (76,2 : 98,7) и 92,56 (79,8 : 97,6), при площади под характеристической кривой, равной 0,921 (0,843 : 0,963). Используя автоматизацию поэтапного алгоритма, планируется создать компьютерную программу для повышения степени объективности при выборе способа временного протезирования и материала протеза.

Ключевые слова: дентальная имплантация, остеоинтеграция, временное протезирование, риски, шансы, компьютерная модель

Информация о вкладе авторов: Н. В. Багрянцева — разработка дизайна исследования, получение данных, анализ и интерпретация данных, редактирование рукописи; С. И. Гажва — планирование исследования, редактирование рукописи; А. А. Баранов — редактирование рукописи; Л. Б. Шубин — анализ и интерпретация данных; В. А. Багрянцев, О. В. Багрянцева — сбор данных, подготовка черновика рукописи.

Соблюдение этических стандартов: исследование одобрено этическим комитетом ФГБОУ ВО НижГМА Минздрава России (протокол № 10 от 25 декабря 2017 г.)

✉ **Для корреспонденции:** Наталья Владимировна Багрянцева
ул. 8 марта, д. 1, кор. 2, кв. 71, г. Ярославль, 150002; nbogryanceva@mail.ru

Статья получена: 25.07.2019 **Статья принята к печати:** 09.08.2019 **Опубликована онлайн:** 16.08.2019

DOI: 10.24075/vrgmu.2019.050

To date, dental implant surgery has become a routine practice that boasts good long-term outcomes [1, 2]. Its results can be predicted even before treatment commences. Once an implant is placed in the jawbone, the patient can be offered temporary dentures, either removable or fixed, available in a variety of materials [3].

However, approaches to temporary tooth restoration during osseointegration in completely edentulous patients are controversial [4]. The analysis of the literature reveals the need for an adequate algorithm that would facilitate the right choice of a provisional denture and stresses the importance of a mathematically accurate approach to the rehabilitation of edentulous patients [2] that will minimize the risks of poor outcomes or complications and improve the quality of life for such parents.

METHODS

We conducted a retrospective analysis of medical records obtained from Yaroslavl regional dental clinic (Yaroslavl, Russia). Specifically, we studied the dental histories of patients (form 043/u) and reports of oral surgeons (form 039-4/u) dating back

to 2015 to 2019. The following inclusion criteria were applied: any sex or age and acquired absence of teeth. Patients with decompensated conditions, buccal exostosis, cancer, or blood clotting disorders were excluded from the study. Information about the causes of teeth loss, patients' complaints, treatment planning, and the type of temporary dental prostheses was retrieved from the records. Implant materials were analyzed separately. The obtained data were saved into cross-tables, and the necessary codes were submitted. In total, we analyzed the medical records of 102 patients and reports of 1 oral surgeon. Of those patients, 34 were completely edentulous and 68 retained either loose teeth or healthy roots, which were removed in the course of treatment. All 102 patients received dental implants and temporary dentures. Considering the objective of this work, the patients were distributed into two groups. Group 1 included patients with successful osseointegration (n = 73); group 2 comprised patients who developed complications (n = 29). All patients underwent panoramic radiography aimed to evaluate the bone around the implant and the quality of osseointegration. The examination was performed three times using a Strato 2000d OPG machine (Villa Sistemi Medicali; Italy). Besides, intraoral periapical radiographs were taken using an EzSensor radiovisiography imaging system (Vatech; South Korea). An MRI scan was also ordered for some patients (a Brilliance 64 MRI scanner; Philips; Netherlands).

Jawbone atrophy and quality were assessed using the classification developed by Lekholm and Zarb [5] based on jaw density and structure. The condition of oral mucosa was assessed using the conventional classification proposed by Supple (Table 1). Comorbidities and health compromising behaviors were also noted.

Statistical analysis was performed in Statistica ver. 12, 2014 (StatSoft Inc.; USA) and MedCalc Statistical Software ver. 18.2.1, 2018 (MedCalc Software bvba; Ostend, Belgium). We identified risk factors, calculated their odds and the 95% CI. Variables characterized by a high probability of occurrence served as a basis for our multivariate statistical models that were built using logistic regression. ROC-curve analysis was applied to assess the quality of the models.

RESULTS

The initial analysis revealed that in the osseointegration period, the patients developed a variety of complications associated with temporary dentures. The total number of complications was 29, occurring in 28% of the studied patients. The most common (34%) problem was difficulty adapting to overdentures. Oral mucositis (20%) and denture fractures or breakages (20%) ranked second. Peri-implantitis and allergy to denture materials (plastic monomers) were the third most common problem, accounting for 10% of complications each. Bad breath and implant instability occurred in 3% of the complicated cases.

Comparison of Groups 1 and 2 allowed us to draw a mathematically accurate profile of statistically significant risk factors. When analyzing the risk of a particular event (a complication) in the patients with acquired edentulism who were wearing provisional dentures in the osseointegration period, we calculated its odds. The risk was understood as an exposure that increased the likelihood of a particular complication. Relative risks were calculated as a ratio of frequency of the complication in the group at risk for this event to the frequency of this event in the control group. Six statistically significant risk factors were identified, including the severity of jawbone atrophy (grades C, D, or E, according to Lekholm and Zarb's classification), the density of cortical and cancellous bones (same classification, types III and IV), the condition of oral mucosa (types 3 and 4, Supple's classification), allergy to monomer components of the denture, poor mouth hygiene and health compromising behaviors (Table 2).

In order to characterize the relationship between the complication and the corresponding risk factor, we calculated the odds ratio (the ratio of the odds of the event occurring to the

Table 1. Supple's classification of oral mucosa

Grade 1	Ideal mouth	Well-defined alveolar bones covered with a slightly supple pale pink mucous membrane, showing no signs of pathology
Grade 2	Hard mouth	Atrophied thickened dry mucosa, attaches to the alveolar ridge closer than in Grade 1
Grade 3	Soft mouth	A hypertrophic lax mucous membrane, low alveolar bones
Grade 4	Flabby ridge	Excessive flabby tissue, easily displaced by applying slight pressure, can get pinched between the denture and the alveolar ridge

Table 2. Relative risks for complications associated with temporary dentures

Risk factor	Relative risk	"–" 95% CI	"+" 95% CI
Severity of bone atrophy, grades C, D, or E	1.7997	0.5518	2.1929
Bone quality, classes III and IV	0.9858	0.4542	2.2258
Oral mucosa condition, types 3 and 4	1.3947	0.5566	2.2588
Allergy +	0.8716	0.3044	2.2069
Poor mouth hygiene +	0.7891	0.2391	1.9864
Smoking +	0.5333	0.2593	2.6781

Table 3. Odds ratios for complications associated with temporary dentures

Risk factor	Odds ratio	"–" 95% CI	"+" 95% CI
Bone atrophy, grade C	1.8879	0.1518	2.2854
Bone atrophy, grade D	1.5858	0.1542	2.2546
Bone atrophy, grade E	1.2845	0.1566	2.2588
Oral mucosa condition, type 3	1.2143	0.2044	2.2608
Oral mucosa condition, type 4	1.1947	0.2721	1.9864
Allergy +	0.8333	0.2593	2.6781
Poor mouth hygiene +	0.6891	0.2694	1.8871
Smoking +	0.4222	0.2443	2.5398

odds of the event not occurring). We found that 6 identified risk factors had a high probability of occurrence. However, because some factors, including jaw bone atrophy and the condition of oral mucosa, could be further graded into different degrees of severity and types, the likelihood of their occurrence varied. For example, bone atrophy was represented by 3 probabilistic states corresponding to grades C, D, or E of the applied classification; the condition of oral mucosa was represented by types 3 and 4 of the same classification [2, 6, 7] (Table 3).

Considering the obtained results, we decided to improve the accuracy of risk prediction by employing a multivariate analysis. Using logistic regression, we were able to identify the relationships between independent and response variables. We also assessed the mutual influence of the variables and the contribution of each variable to the classification. Results of statistical modeling are presented in Table 4.

The constructed model was characterized by a high level of significance. The values of both regression coefficients

Table 4. Characteristics of the regression model for the choice of a temporary dental prosthesis (TDPC)

Parameter	TDPC
Level of significance	$p = 0.001$
Coefficient of determination, Cox & Snell's R^2	0.834
Coefficient of determination, Nagelkerke's R^2	0.758
Hosmer & Lemeshow test, significance	$p = 0.594$
Concordance correlation coefficient	0.8946

Table 5. Standardized regression coefficients included in the model for the choice of TDPC

Variable	Coefficient	Standard error	Wald test
Severity of bone atrophy	–2.13953	0.40234	0.1203
Bone quality	3.58284	0.47428	11.1382
Condition of oral mucosa	–1.85714	0.83806	11.6227
Allergy	3.46292	0.44173	10.968
Poor mouth hygiene	1.55758	0.41697	13.954
Smoking	0.056017	0.070499	0.6314
Constant	–8.64908	85.2702	0.01029

Table 6. Operational characteristics of the model for the choice of TDPC

Parameter	TDPC
Area under curve (AUC)	0.921
Mean squared error[a]	0.0524
–95% CI (AUC)	0.873
+95% CI (AUC)	0.963
z-score	9.645
Significance, *p* (area = 0.5)	0.001
Youden J	0.8284
Optimal cut-off value	≤ 1.43
Sensitivity	94.37
–95% CI (Se)	76.2
+95% CI (Se)	98.7
Specificity	92.56
–95% CI (Sp)	79.8
+95% CI (Sp)	97.6
+Likelihood ratio (+LR)	7.31
–95% CI (+LR)	2.5
+95% CI (+LR)	21.4
–Likelihood ratio (–LR)	0.18
–95% CI (–LR)	0.08
+95% CI (–LR)	0.4
+Prognostic value (+PV)	89.9
–95% CI (+PV)	75.3
+95% CI (+PV)	96.3
–Prognostic value (–PV)	82.2
–95% CI (–PV)	67.2
+95% CI (–PV)	91.3

of determination (R^2) were quite high, suggesting a relatively high stability of our prediction model. The obtained value of the concordance correlation coefficient spoke in favor of this conclusion. Using the Hosmer-Lemeshow test, we assessed the goodness of fit by comparing the observed and expected frequencies. In our case, the fit was good, with over 5% statistical significance Standardazied regression coefficients included in the model and presented in Table 5 reflected all stages of the algorithm.

The following logistic regression equation was proposed based on the results of multivariate modeling:

$$F = c + k_1x_1 + k_2x_2 + \ldots + k_nx_n,$$

where F is a dependent variable; c is a constant; k_i is a coefficient of the regression function; x_i is a predictor (a variable).

Logistic regression and the use of the abovementioned equation for determining individual F values included ROC-curve analysis. The following parameters were calculated: an area under curve (AUC), the Youden index, an optimal cut-off value, sensitivity and specificity, positive and negative likelihood ratios (LR), positive and negative predictive values (PV), and 95% CI for each parameter (Table 6).

DISCUSSION

Unsurprisingly, the density of cortical and cancellous bone (classes III and IV according to Lekholm and Zarb's classification) was the leading risk factor for complications associated with temporary dental prostheses, because the success of denture placement is largely determined by bone density. The second

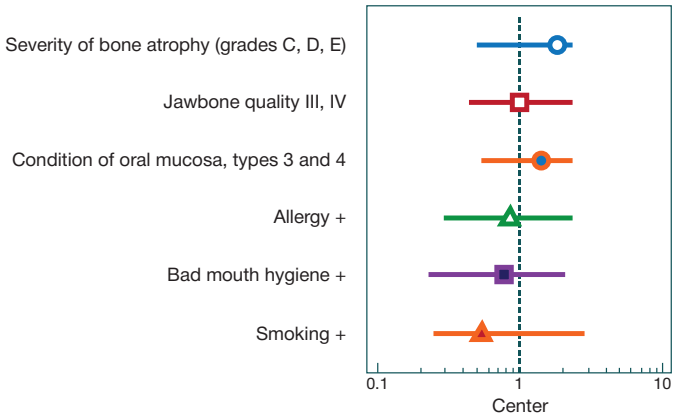

Fig. 1. A forest plot showing risk factors for the complications associated with temporary dental prostheses

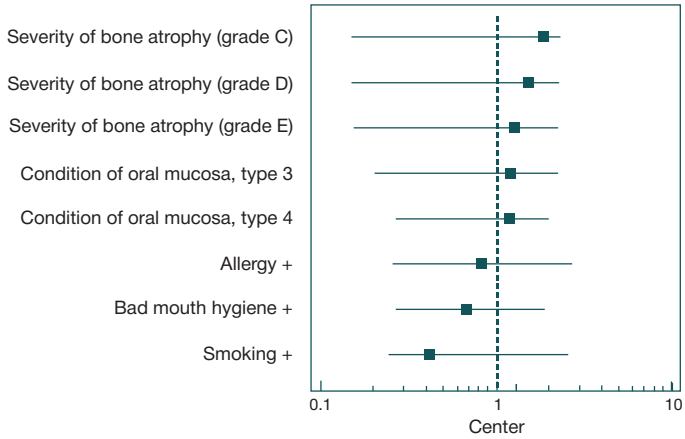

Fig. 2. A forest plot showing the odds ratios of the risk factors for the complications associated with temporary dental prostheses

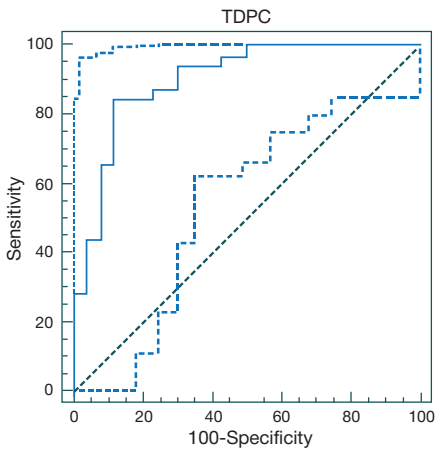

Fig. 3. A ROC curve for the prediction model facilitating the choice of TDPC

most significant risk factor was allergy to the plastic monomer components of the denture. The severity of bone atrophy (Lekholm and Zarb's classification) and the condition of oral mucosa (types 3 and 4) ranked third and fourth in importance, respectively. Poor mouth hygiene and health-compromising habits (smoking) also contributed to the development of complications [2, 4]. Fig. 1 shows a forest plot for the listed risk factors.

The odds of the observed complications associated with temporary dentures worn by edentulous patients in the osseointegration period can be presented in the following descending order: type 4 condition of oral mucosa (Supple's classification), allergy to denture material, type 3 condition of oral mucosa, bone atrophy (grades E and D), bad mouth hygiene, bone atrophy (grade C), and smoking. Fig. 2 shows a forest plot for the odds ratios.

Considering the values of operational characteristic of the model, we think the proposed computerized algorithm is a feasible tool that assists selection of a proper temporary dental prosthesis. Sensitivity and specificity (95% CI) of the proposed algorithm are high; the same is true for the absolute values. The positive likelihood ratio is 7 times higher than the negative likelihood ratio; the positive prognostic value exceeds the negative almost sevenfold. These facts suggest stability of our prediction model confirmed by the AUC value of 0.921 shown in Fig. 3 [8, 9].

CONCLUSIONS

1. The severity of jawbone atrophy and the density of cortical and cancellous bone are the most important factors that should be considered when selecting a temporary removable or fixed denture for edentulous patients in the osseointegration period. 2. It is critical to assess the condition of oral mucosa in order to avoid complications. 3. If the patient is a smoker or has bad hygiene habits, he/she should be offered a removable denture. 4. If the patient is not allergic to plastic and maintains good hygiene, he/she can be offered temporary dentures made of any kind of plastic. 5. Based on the proposed algorithm, we are planning to develop a software that would help the dentist to make a more objective decision when selecting the denture type and material.

References

1. McRory ME, Cagna DR. A technique for fabricating single screw-retained implant-supported interim crowns in conjunction with implant surgery. J Prosthet Dent. 2014 Jun; 111 (6): 455–9. PubMed PMID: 24461941. DOI: 10.1016/j.prosdent.2013.11.005.
2. Aghaloo T, Pi-Anfruns J, Moshaverinia A, et al. The Effects of Systemic Diseases and Medications on Implant Osseointegration: A Systematic Review. Int J Oral Maxillofac Implants. 2019 Suppl; (34): 35–49. PubMed PMID: 31116832. DOI: 10.11607/jomi.19suppl.g3.
3. Parvini P, Saminsky M, Stanner J, et al. Discomfort/pain due to periodontal and peri-implant probing with/without platform switching. Clin Oral Implants Res. 2019 Jul 20. PubMed PMID: 31325382. DOI: 10.1111/clr.13513.
4. Radzewski R, Osmola K. Osseointegration of Dental Implants in Organ Transplant Patients Undergoing Chronic Immunosuppressive Therapy. Implant Dent. 2019 Jul 12. PubMed PMID: 31306295DOI: 10.1097/ID.0000000000000916.
5. Lekholm U, Zarb G. Tissue-Integrated Prostheses Osseointegration in Clinical Dentistry. Chicago: Quintessence publishing, 1985; 199–210.
6. Hu Z, Wang X, Xia W, et al. Nano-Structure Designing Promotion Osseointegration of Hydroxyapatite Coated Ti-6Al-4V Alloy Implants in Diabetic Model. J Biomed Nanotechnol. 2019 Aug 1; 15 (8): 1701–13. PubMed PMID: 31219019. DOI: 10.1166/jbn.2019.2812.
7. Mangano FG, Iezzi G, Shibli JA, et al. Early bone formation around immediately loaded implants with nanostructured calcium-incorporated and machined surface: a randomized, controlled histologic and histomorphometric study in the human posterior maxilla. Clin Oral Investig. 2017 Nov; 21 (8): 2603–11. PubMed PMID: 28154996. DOI: 10.1007/s00784-017-2061-y.
8. Shirokov IYu. Jeksperimental'noe obosnovanie primenenija vremennyh nes#emnyh zubnyh protezov pri dental'noj implantacii [dissertacija]. M., 2013.
9. Robakidze NS, Lobanovskaya AA, Pekarchik DM. Primenenie vremennyh proteznyh konstrukcij v period osteointegracii vnutrikostnyh implantatov. Institut stomatologii. 2016; (2): 78–9.

Литература

1. McRory ME, Cagna DR. A technique for fabricating single screw-retained implant-supported interim crowns in conjunction with implant surgery. J Prosthet Dent. 2014 Jun; 111 (6): 455–9. PubMed PMID: 24461941. DOI: 10.1016/j.prosdent.2013.11.005.
2. Aghaloo T, Pi-Anfruns J, Moshaverinia A, et al. The Effects of Systemic Diseases and Medications on Implant Osseointegration: A Systematic Review. Int J Oral Maxillofac Implants. 2019 Suppl; (34): 35–49. PubMed PMID: 31116832. DOI: 10.11607/jomi.19suppl.g3.
3. Parvini P, Saminsky M, Stanner J, et al. Discomfort/pain due to periodontal and peri-implant probing with/without platform switching. Clin Oral Implants Res. 2019 Jul 20. PubMed PMID: 31325382. DOI: 10.1111/clr.13513.
4. Radzewski R, Osmola K. Osseointegration of Dental Implants in Organ Transplant Patients Undergoing Chronic Immunosuppressive Therapy. Implant Dent. 2019 Jul 12. PubMed PMID: 31306295DOI: 10.1097/ID.0000000000000916.
5. Lekholm U, Zarb G. Tissue-Integrated Prostheses Osseointegration in Clinical Dentistry. Chicago: Quintessence publishing, 1985; 199–210.
6. Hu Z, Wang X, Xia W, et al. Nano-Structure Designing Promotion Osseointegration of Hydroxyapatite Coated Ti-6Al-4V Alloy Implants in Diabetic Model. J Biomed Nanotechnol. 2019 Aug 1; 15 (8): 1701–13. PubMed PMID: 31219019. DOI: 10.1166/jbn.2019.2812.
7. Mangano FG, Iezzi G, Shibli JA, et al. Early bone formation around immediately loaded implants with nanostructured calcium-incorporated and machined surface: a randomized, controlled histologic and histomorphometric study in the human posterior maxilla. Clin Oral Investig. 2017 Nov; 21 (8): 2603–11. PubMed PMID: 28154996. DOI: 10.1007/s00784-017-2061-y.
8. Широков И. Ю. Экспериментальное обоснование применения временных несъемных зубных протезов при дентальной имплантации [диссертация]. М., 2013.
9. Робакидзе Н. С., Лобановская А. А., Пекарчик Д. М. Применение временных протезных конструкций в период остеоинтеграции внутрикостных имплантатов. Институт стоматологии. 2016; (2): 78–9.

SYNCHROTRON IR-MICROSPECTROSCOPY-BASED VISUALIZATION OF MOLECULAR AND CHEMICAL INTERACTIONS BETWEEN DENTAL CEMENT, BIOMIMETIC COMPOSITE AND NATIVE DENTAL TISSUE

Goloshchapov DL[1], Kashkarov VM[1], Ippolitov YuA[2], Ippolitov IYu[2], Jitraporn Vongsvivut[3], Seredin PV[1] ✉

[1] Voronezh State University, Voronezh, Russia

[2] Burdenko Voronezh State Medical University, Voronezh, Russia

[3] Australian Synchrotron, Melbourne, Australia

The low affinity of composite materials for the hard tissue of human teeth poses a challenge to restorative dentists. This study was undertaken to explore molecular and chemical characteristics of the interface between the dental cement, the buffer layer formed from a next generation biomimetic material that mimics the organic mineral composition of human enamel and dentin, and the intact native hard dental tissue. Seven plane-parallel dental slices were analyzed using synchrotron IR microspectroscopy. The obtained absorption spectra of functional molecular groups were organized into cluster maps. This allowed us to identify the intact tissue, the adhesive agent and the biomimetic layer at their interface and to localize and measure concentrations of functional groups involved in the integration of the biomimetic composite into the hard tissue of the human tooth. The proposed biomimetic material is based on nanocrystal carbonate-substituted calcium hydroxyapatite synthesized from a biogenic calcium source and a complex of basic polar amino acids copying the composition of the human tooth and can form a functional bond with hard dental tissue.

Keywords: biomimetic materials, native human tooth hard tissue, IR microspectroscopy, synchrotron radiation

Funding: the study was supported by the Russian Science Foundation (Grant 16-15-00003).

Acknowledgment: IR microspectroscopy was conducted at the Australian Synchrotron.

Author contribution: Goloshchapov DL planned the study, analyzed the literature, collected and interpreted the obtained data; Kashkarov VM collected, analyzed and interpreted the obtained data; Ippolitov YuA planned the study, prepared the samples, collected and analyzed the data; Ippolitov IYu prepared the samples; Jitraporn Vongsvivut conducted IR microspectroscopy; Seredin PV planned the study, analyzed the literature, collected, analyzed and interpreted the obtained data, and conducted IR microspectroscopy.

Compliance with ethical standards: the study was approved by the Ethics Committee of Voronezh State University (Protocol № 2019/3/1 dated March 4, 2019).

✉ **Correspondence should be addressed:** Pavel V. Seredin
Universitetskaya pl.1, Voronezh, 394018; paul@phys.vsu.ru

Received: 18.07.2019 **Accepted:** 31.07.2019 **Published online:** 01.08.2019

DOI: 10.24075/brsmu.2019.047

ВИЗУАЛИЗАЦИЯ МОЛЕКУЛЯРНО-ХИМИЧЕСКОГО ВЗАИМОДЕЙСТВИЯ МАТЕРИАЛА, БИОКОМПОЗИТА И ТКАНИ ЗУБА НА ОСНОВЕ СИНХРОТРОННОЙ ИК-МИКРОСПЕКТРОСКОПИИ

Д. Л. Голощапов[1], В. М. Кашкаров[1], Ю. А. Ипполитов[2], И. Ю. Ипполитов[2], Jitraporn Vongsvivut[3], П. В. Середин[1] ✉

[1] Воронежский государственный университет, Воронеж, Россия

[2] Воронежский государственный медицинский университет имени Н. Н. Бурденко, Россия

[3] Австралийский синхротрон, Мельбурн, Австралия

В реставрационной стоматологии остается актуальной проблема низкого сродства композиционных материалов с нативной твердой тканью зуба. Целью работы было исследовать молекулярно-химические особенности формирования интерфейса стоматологический материал — биомиметический буферный слой — твердая ткань зуба человека. С применением метода молекулярной многомерной ИК-визуализации на 7 плоскопараллельных сегментах образцов был выполнен анализ участка интерфейса здоровая твердая ткань (эмаль/дентин) — биомиметический переходной слой — стоматологический материал/адгезивный, созданный с использованием нового поколения биомиметических материалов, воспроизводящих минералорганический комплекс эмали и дентина зубов человека, с нативными твердыми тканями зуба человека и стоматологическим цементом. Данные спектральной молекулярной визуализации, полученные на основе синхротронного ИК-картирования интенсивности функциональных молекулярных групп, позволили нам обнаружить и визуализировать различия между здоровой тканью, стоматологическим материалом и биомиметическим переходным слоем в межфазных областях (интерфейсах), а также определить локализацию и концентрацию функциональных групп, отвечающих процессам интеграции биомиметического композита и нативной твердой ткани зубов человека. Показано, что разработанная нами биомиметическая система на основе нанокристаллического карбонат-замещенного гидроксиапатита кальция, полученного из биогенного источника кальция и комплекса основных полярных аминокислот, соответствующих органоминеральному комплексу зубов человека, способна образовывать функциональную связь с твердой тканью зуба человека.

Ключевые слова: биомиметические материалы, нативная твердая ткань зуба человека, ИК-микроспектроскопия, синхротронное излучение

Финансирование: исследование выполнено при поддержке гранта Российского Научного Фонда № 16-15-00003.

Благодарности: часть этого исследования была проведена с использованием канала Инфракрасной микроскопии (IRM) на Австралийском синхротроне.

Информация о вкладе авторов: Д. Л. Голощапов — планирование исследования, анализ литературы; сбор, анализ и интерпретация данных; В. М. Кашкаров — сбор, анализ, интерпретация данных; Ю. А. Ипполитов — планирование исследования, подготовка образцов, сбор и анализ данных; И. Ю. Ипполитов — подготовка образцов; Jitraporn Vongsvivut — проведение эксперимента; П. В. Середин — планирование исследования, анализ литературы, сбор, анализ, интерпретация данных, проведение эксперимента.

Соблюдение этических стандартов: исследование одобрено этической комиссией Воронежского государственного университета (протокол № 2019/3/1 от 04 марта 2019 г.).

✉ **Для корреспонденции:** Павел Владимирович Середин
Университетская пл., 1, г. Воронеж, 394018; paul@phys.vsu.ru

Статья получена: 18.07.2019 **Статья принята к печати:** 31.07.2019 **Опубликована онлайн:** 01.08.2019

DOI: 10.24075/vrgmu.2019.047

Although modern composite materials and bonding resins used in restorative dentistry are durable and have a good adhesive capacity, their chemical and structural resemblance to native hard dental tissue is low [1, 2]. The difference in physical and chemical characteristics between synthetic materials and the natural enamel and dentin of human teeth necessitates development of novel restorative composites [2, 3]. Extensive research effort is being channeled into improving the tooth-material interface by employing innovative bonding systems and hybrid buffer layers that increase the durability of dental restorations and enhance the bonding strength between the filling material and hard dental tissue [3–5]. One of the most important questions that should be addressed by researchers is reliable chemical bonding between dental composite fillers/bonding agents and the natural tissue of human teeth [6].

So far, biomimetic materials, whose composition and (nano)structure mimic those of hard dental tissue, have offered the best solution to the problem of interface quality between natural enamel/dentin and synthetic adhesives [7–9]. It is a well-known fact that nanocrystalline hydroxyapatite (HA), which is identical in composition and morphology to enamel apatite found in human teeth, facilitates better integration of restorative materials with the tooth [5, 10]. Besides, enrichment of biomimetic agents with polar amino acids occurring in the natural enamel matrix [11–14] creates a possibility for high-quality repair of damaged enamel or dentin layers and improves mechanical properties of the restoration [12, 15].

There are a few methods used to assess integration of the bonding resin with natural dental tissue and the quality of resin-enamel or resin-dentin interfaces. Fourier-transform infrared spectroscopy (FTIR) is a non-destructive technique that provides information about the molecular structure and fine structural properties of biological objects based on the analysis of their fingerprint vibrational IR spectra [16]. FTIR can be applied to study mechanisms of molecular transformations in biomimetic materials [17, 18] and dental adhesive agents [19], analyze the molecular composition of human teeth [6], and register new mineral phases [20]. Microscopes and sources of synchrotron radiation for IR spectroscopy are instrumental in acquiring large arrays of spectra from a microscopic area of a studied biological sample [17]. Based on the acquired IR spectra, chemical images of the sample can be generated, offering a wealth of information about molecular bonds and their spatial distribution.

The aim of this work was to study molecular and chemical properties of an interface between a dental cement, a biomimetic buffer layer and hard dental tissue based on multidimensional visualization of synchrotron IR spectroscopy data.

METHODS

Synthesis of biomimetic material and sample preparation

The biomimetic composite material was fabricated similar to the bonding system described in [21]. The composite contained hyaluronic acid (0.01–0.05 wt. %), L-histidine (0.01–0.2 wt. %), L-lysine hydrochloride (0.05–0.4 wt. %), L-arginine hydrochloride (0.2–1.6 wt. %), ethylene glycol monomethyl ether (30–85 wt. %), diglycidyl dimethacrylate (1–15 wt. %), urethane dimethacrylate (1–15 wt. %), ethanol (2–20 wt. %), and water (the rest). The analysis of optical absorption and emission properties found that the synthesized material, which contained the listed amino acids, was similar in its properties to natural tooth enamel and dentin [22]. Synthetic carbonate-substituted hydroxyapatite (CSHA) was added to the biomimetic buffer (0.01 g of CSHA per 1 ml of the mixture) to improve the similarity of the biocomposite to natural dental tissue [20].

To ensure adhesion of the biomimetic composite to the tooth, we used a universal adhesive agent that effectively bound to the synthesized materials [23]. The adhesive agent was enriched with CSHA (1 ml of the adhesive per 0.01 g CSCA). Hydroxyapatite was combined with the biomimetic buffer and the adhesive agent, and the mixture was subsequently homogenized for 30 seconds using a QSonica Q55 sonicator (QSonica; USA).

Integration of the synthesized biocomposite material with hard dental tissue was tested on the dental specimens obtained from the patients aged 18 to 45 years who had indications for tooth extraction. The specimens were prepared for filling as described below.

First, enamel was removed using an air-driven micromotor hand piece with a round-head tungsten vanadium steel bur operated at 4,000 rpm and a water-cooling system necessary to avoid overheating of the dental matrix. Dentin was spared. Cavity preparation was finished using a low-speed hand piece. The cavity was washed and dried with compressed air

Second, enamel was etched for 60 s with a 37% phosphoric acid etching gel, rinsed with water and air-dried. Then, a dentin conditioner [21] was applied to the dentin surface for 20–30 s. The conditioner contained hyaluronic acid (0.01–0.05 wt. %), L-histidine (0.01–0.2 wt. %), L-lysine hydrochloride (0.05–0.4 wt. %), and L-arginine hydrochloride (0.2–1.6 wt. %). After that, the cavity was dried.

Third, the biomimetic buffer was evenly applied to the walls of the prepared cavity and dried with compressed air 20 seconds later. The biomimetic layer was coated with a universal CSHA-containing light-curing adhesive agent that was photopolymerized for 20 seconds.

Finally, 1 min after the previous step, the biomimetic buffer layer was coated with a commercial restorative dental compomer containing adhesive components.

Considering the requirements for the geometry of samples subject to IR microspectroscopy, we prepared 7 plane-parallel sections of the restored teeth immediately before the study as described in our previous work [24].

Method of sample analysis

The molecular composition of the samples and the interface between the restorative dental compomer, the biomimetic buffer layer and the native hard tissue of the human tooth was analyzed using attenuated total reflection (ATR) Fourier transform synchrotron infrared microspectroscopy. Measurements were conducted at the Australian Synchrotron Infrared Microspectroscopy Beamline (Melbourne, Australia) equipped with a Hyperion 3000 FTIR microscope (Bruker; USA) and an ATR-FTIR accessory with a germanium prism (Melbourne, Australia) [17]. Figures 1A and B are show the studied segment (marked with the rectangle) that yielded IR absorption spectra at 3800–700 cm–1 wavelength (Fig. 1C).

Using the IR microscope and OPUS 7.5 software (Bruker; USA), we acquired a cluster of IR spectra from a small sample area of 100×100 μm in size (Fig. 1B) with a 2 μm sampling interval and constructed one-dimensional IR images (maps) based on the color codes for the intensity of IR absorption bands (Fig. 1D). The lowest absorbance intensity is shown in red, whereas the highest, in blue. The map demonstrates the distribution of absorbance intensity of a molecular group and, therefore, reveals its concentration in a specified sample area.

RESULTS

By applying IR spectroscopy to the interface between the light-curing adhesive agent, the biomimetic composite material and natural dental enamel/dentin (Fig. 1B), we were able to identify the major vibrational modes active in the IR spectrum (Fig. 1C) that can be used as spectral fingerprints for the compounds present in the studied sample area.

The absorption band at 1163–981 cm^{-1} had the highest intensity and represented the PO_4 mineral component of enamel/dentin apatite [22]. The range between 1700 and 1100 cm^{-1} wavelength represented the protein constituents of organic enamel/dentin and the components of the biomimetic buffer (see *Synthesis of biomimetic material and sample preparation*). Here, the most active vibrational modes were observed for the CH_2–CH_3 collagen group at 1457 cm^{-1} and for Amide absorption bands (Amide I at 1650 cm^{-1}, C=O stretching; Amide II at 1550 cm^{-1}, N–H bending, and Amide III at 1245 cm^{-1}, CN stretching) [18, 19, 22]. We also recorded vibrations at 1725 cm^{-1} wavelength produced by the methyl ester group (–$COOCH_3$), the component of the restorative Bis-GMA dental compomer [19].

Fig. 2A features the IR map of PO_4 distribution across the studied interface segment (Fig. 1B). The IR spectrum specific for this group (Fig. 2B) was acquired from the area of enamel-biomimetic layer integration. The spectrum contained vibrations of the PO_4 group at 1163–981 cm^{-1} wavelength occurring in natural enamel /dentin apatite [19, 20] and the biomimetic agent. We concluded that the part of the interface occupied by the restorative compomer did not contain phosphate groups. The zone bordering on tooth enamel where spectral vibrations were observed at 1163–981 cm^{-1} was ~30 μm in size (Fig. 3A, *the dotted line*).

For further information about the studied interface, an IR image was generated (Fig. 3A). This IR map shows the distribution of absorbance intensity for CN, NH, C=O, and CH_2/CH_3 in the range between 1718 and 1358 cm^{-1} wavelength (Fig. 3B). The listed molecular groups are components of collagen, Amide I and Amide II (the organic constituents of tooth enamel/dentin added to the biomimetic buffer).

The results of the IR map analysis (Fig. 3A) suggest that the distribution of organic components in the biomimetic layer was more homogenous than the distribution of phosphate groups. These findings are consistent with the fact that the proportion of hydroxyapatite in the biomimetic layer was lower than the proportion of organic components.

The IR spectrum presented in Fig. 1C contains an absorption band at 1725 cm^{-1}. It is well known that such vibration is typical for dental cements based on Bis-GMA and polymethyl methacrylate and suggests the presence of the ester group (–$COOCH_3$) [19]. Moreover, this spectral band (Fig. 4B) does not overlap with other vibrations, which allowed us to visually represent it as an IR image (Fig. 4A).

The IR map demonstrates spatial distribution of the restorative dental compomer in the analyzed sample segment (Fig. 4A). The figure shows that the distribution of absorbance intensity of the ester group (–$COOCH_3$) coincides with the spatial distribution of the dental compomer on the map (Fig. 1B).

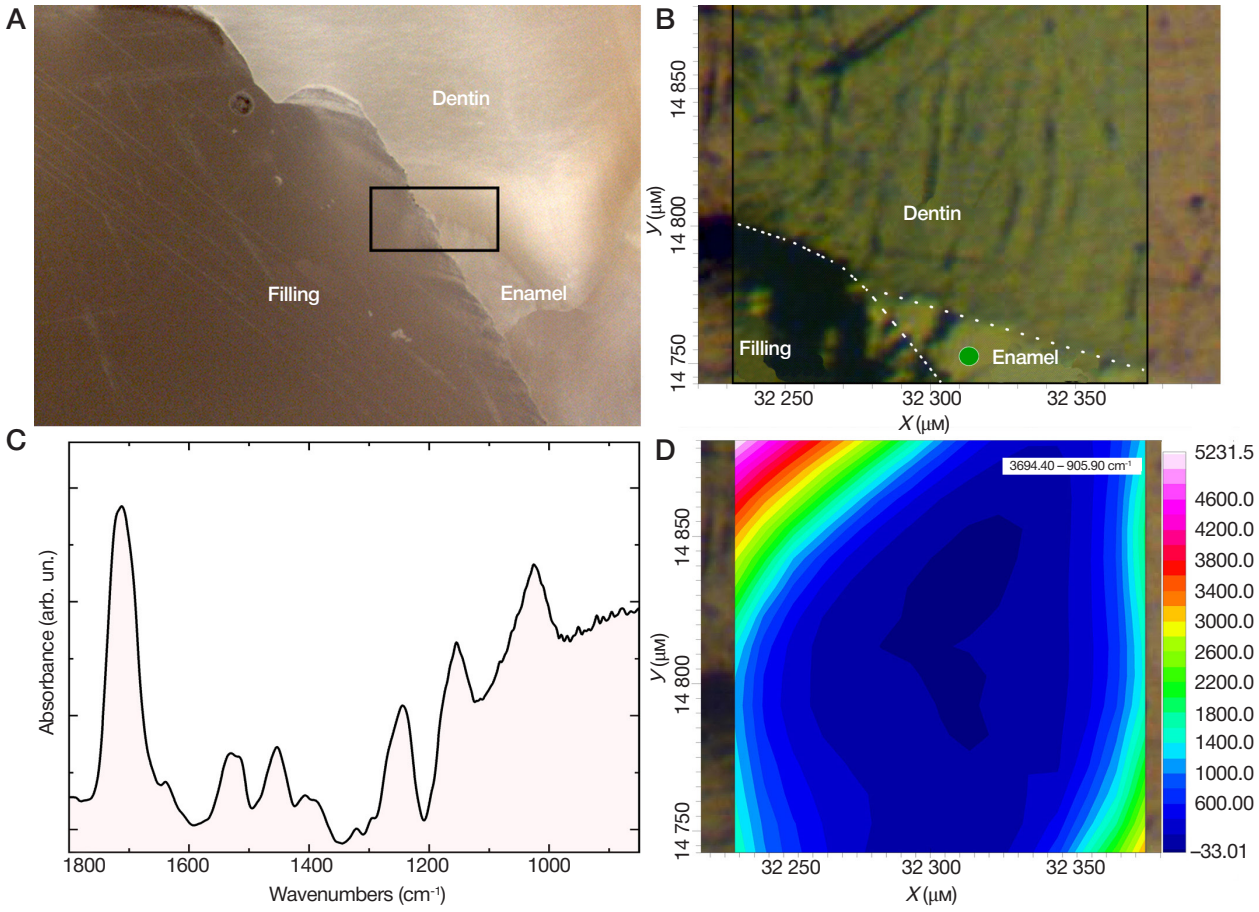

Fig. 1. The optical image of a plane-parallel dental segment from the interface between the dental cement, the biomimetic composite material, enamel and dentin (**A**) sized 100×200 μm; the 20× optical image of the studied interface (**B**); the typical IR absorption spectrum from the studied interface (**C**); the IR map of total absorbance compiled from the IR microspectroscopy data array (**D**)

The analysis of the acquired spectra (Fig. 1B) allowed us to identify an intensive absorption band for Amide III at 1269–1224 cm^{-1} and construct a separate IR map for the biomimetic layer (Fig. 5A). Of note, its vibration (Fig. 5B) did not overlap with the absorption spectra of other functional groups, meaning that it can be used as a marker of a biomimetic composite.

Comparison of the optical data (Fig. 1B) and the IR map (Fig. 5A) clearly shows that the molecular group at 1269–1224 cm^{-1} can be localized to only a narrow segment of the interface between the light-curing material, the biomimetic layer and the enamel/dentin of the human tooth.

DISCUSSION

IR spectroscopy of dental materials [19], biomimetic composites [20], and natural tissue of human teeth [6] characterizes the molecular composition of the studied samples as a single whole. In contrast to the research studies cited in this article, one-dimensional images (IR maps) based on the color codes of absorbance intensity of 4 main spectral ranges (1752–1704 cm^{-1}, 1718–1358 cm^{-1}, 1269–1224 cm^{-1}, and 1163–981 cm^{-1}) became a good visual representation of the spatial distribution of molecular groups across the studied sample and of molecular-chemical interactions occurring at the interface between the light-curing material, the biomimetic layer and the enamel/dentin of the human tooth.

The IR map of the phosphate group (Fig. 2A) revealed the presence of an area with absorbance intensity varying from 1.0 to 7.0. This was part of the biomimetic buffer layer that contained synthetic carbonate-substituted calcium hydroxyapatite introduced into the biomimetic material in order to increase its molecular and chemical resemblance to natural tooth structures [20]. The presence of CSHA in the biomimetic material allowed us to clearly discriminate between the biomimetic layer and the restorative compomer on the IR map (Fig. 2A), where color changes were determined by the intensity of vibrational modes representing the PO_4 group of CSHA. The margin between the natural dental tissue and the biomimetic composite material was blurred, which proves the high similarity of the composite to natural enamel and dentin.

It should be noted, though, that alone, the IR map of phosphate groups is not enough to study the integration of dental cements with the dental enamel/dentin mediated by the biomimetic buffer layer. At 1163–981 cm^{-1} the absorption spectra of phosphate groups (Fig. 2B) can overlap with the vibrational modes of aluminum silicates or silica that are common components of restorative dental materials [19, 25]. However, the analysis of the interface margin (Fig. 1A and 2A) did not reveal significant amounts of such compounds in the analyzed spectral range (Fig. 2B), which can suggest their low concentration in the studied sample area.

While the IR map shows the distribution of the phosphate group, the IR image of vibrations at 1718–1358 cm^{-1} corresponding to the organic components of the sample (Fig. 3A) helps to accurately identify the margin between enamel and dentin. In Fig. 3A, the dentin area (shown in red) has a higher organic content than enamel (shown in green), which is consistent with the available reports [20].

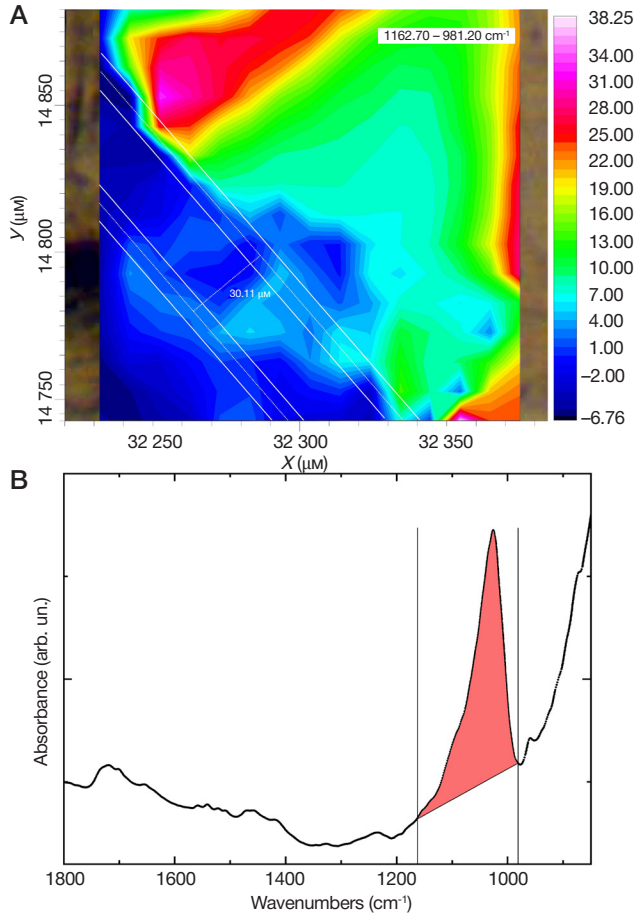

Fig. 2. A. The IR absorbance map based on the color codes for absorbance intensity at 1163–981 cm^{-1}. **B**. The IR absorption spectrum of the enamel area containing a characteristic phosphate vibrational mode at 1163–981 cm^{-1}

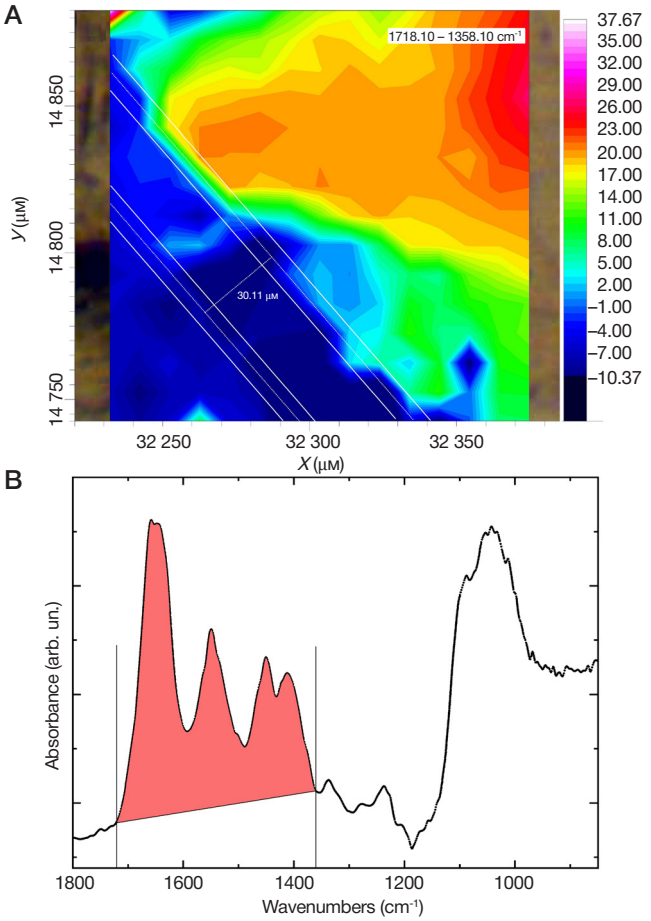

Fig. 3. A. The IR absorbance map based on the color codes for absorbance intensity at 1718–1358 cm^{-1}. **B**. The IR absorption spectrum containing vibrational modes of CN, NH, C=O, and CH_2/CH_3 groups at 1718–1358 cm^{-1}

At the same time, when studying the interactions between the dental compomer/the biomimetic layer and hard dental tissue, one should bear in mind that the spectral range between 1718 and 1358 cm^{-1} contains a few overlapping bands [18]. This complicates result interpretation and makes it difficult to draw unambiguous conclusions about the type of interactions at the compomer/buffer/hard tissue interface.

The IR spectra of the ester group (–$COOCH_3$) (Fig. 4A) and Amide III (Fig. 5A) do not overlap with other vibrational modes. Therefore, the analysis of their IR maps allows us to make the following conclusions. First, it can be clearly seen that the area of integration between the restorative compomer and natural tooth enamel, where absorbance intensity for –$COOCH_3$ varies from its peak to the lowest value, covers a spot ~14 μm in width and overlaps with the area dominated by organic components (Fig. 4A, 5A). Second, the analysis of the distribution of absorbance intensity for Amide III (Fig. 5A) present in the biomimetic layer suggests that this layer separates hard dental tissue from the dental cement.

All IR images (Fig. 2A, 3A, 4A, 5A) offer a good visual representation of the buffer layer, whereas other imaging techniques provide information about the morphology of the tooth-material interface only [2, 4, 15]. This means that buffer layers caught in the integration area and close to each other in composition are hard to analyze.

It is not always possible to visualize interactions occurring at the heterogonous interface between structurally similar materials using a series of one-dimensional IR images [6]. This is a limitation of a one-dimensional approach to the identification of spectral changes for the materials only slightly different in their chemical structure. However, this limitation can be overcome by using multidimensional clusterization methods that can effectively systematize vast arrays of multicomponent IR spectra [26]. Using this approach, we were able to analyze the features of a complex dental compomer/biomimetic layer/enamel/dentin interface. The comprehensive cluster analysis of the spectral ranges 1752–1704 cm^{-1}, 1718–1358 cm^{-1}, 1269–1224 cm^{-1}, and 1163–981 cm^{-1} discovered that interactions between the material and native tooth tissue were mediated by the buffer layer (Fig. 6, *the dotted line*).

The spatial distribution of molecular and chemical phosphate, protein, Amide and ester groups (Fig. 6) shows that the biomimetic layer between enamel and the dental compomer binds to the partially demineralized enamel matrix via a mediator sublayer, which may indicate an organic and mineral interaction in the analyzed region. At the same time, the data analysis (Fig. 6) shows that the buffer layer between the biomimetic material and dentin is wider due to a more porous structure of dentin, as compared to enamel [1, 2]. Clusterization of IR spectra helps to see that organic and mineral components of the biomimetic buffer layer tend to permeate the light-curing adhesive agent, forming a mediator interface.

Considering our findings, one can assume that the real size of a mediator sublayer that facilitates integration between the biomimetic composite material, the restorative compomer and hard dental tissue is 3–4 μm, which is consistent with current state of scientific knowledge [27].

The data yielded by the analysis of all IR images (Fig. 2–6) can be used to reliably discriminate between the functional groups of all materials present at the biomimetic system-hard

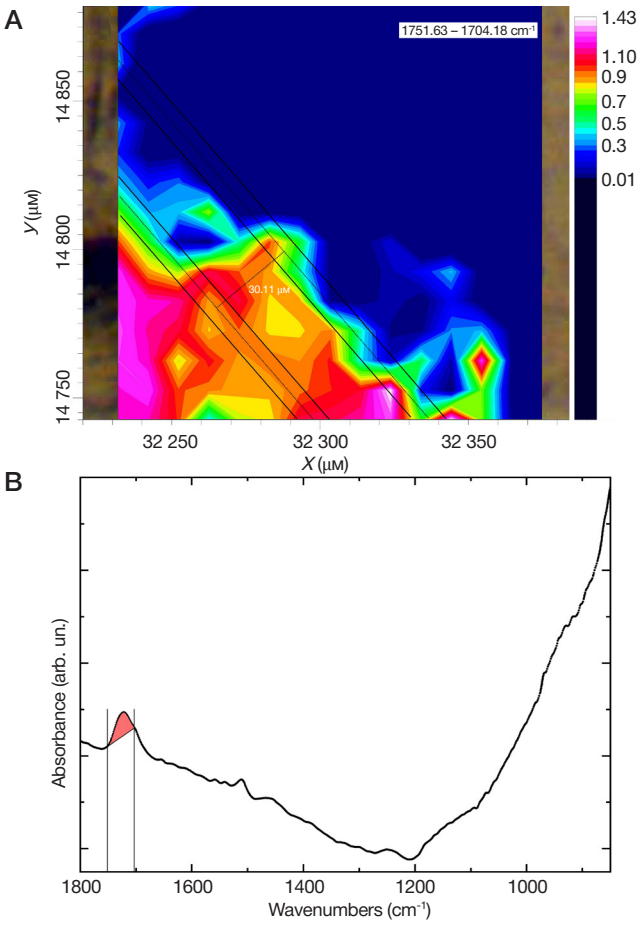

Fig. 4. A. The IR absorbance map based on the color codes for absorbance intensity at 1752–1704 cm^{-1}. **B**. The IR absorption spectrum containing a vibrational mode of the ester group (–$COOCH_3$) at 1752–1704 cm^{-1}

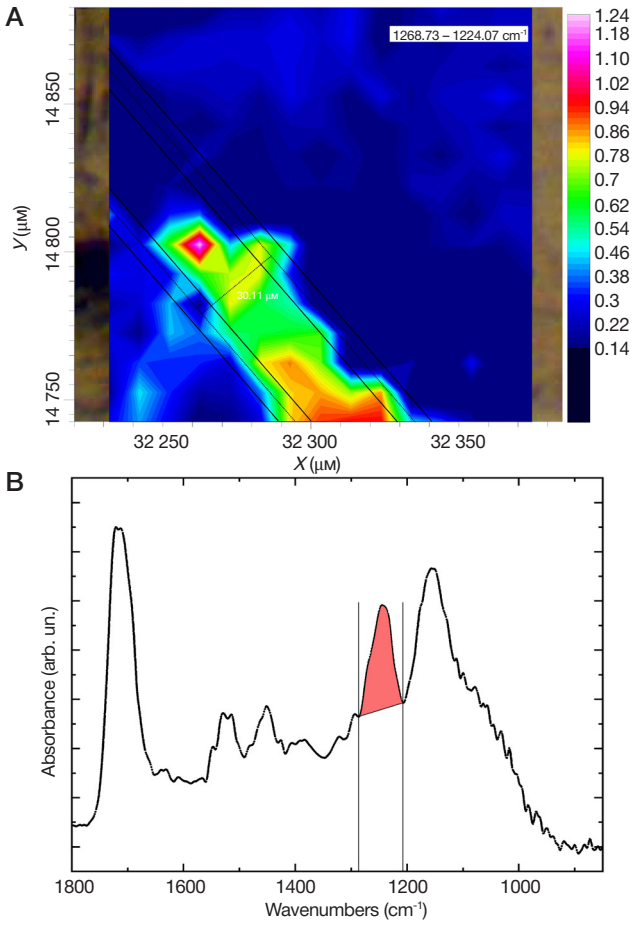

Fig. 5. A. The IR absorbance map based on the color codes for Amide III absorbance intensity at 1269–1224 cm^{-1}. **B**. The IR absorption spectrum of the enamel area containing a characteristic phosphate vibrational mode at 1269–1224 cm^{-1}

native dental tissue interface and confirm the efficacy of the chosen approach to the analysis of integration processes between dental cements and next-generation biomimetic composites.

It should be noted that our findings are true for totally etched samples. However, they may be also true for the samples prepared using other techniques (self-etch or self-adhesive systems) that exploit materials similar in their chemical activity or composition to those used in our study.

CONCLUSIONS

We have demonstrated the feasibility of using multidimensional IR imaging to study the integration of next-generation biomimetic materials mimicking the mineral and organic composition of natural enamel with hard tissue of the human tooth. Using synchrotron radiation and IR maps of absorbance intensity constructed for each functional molecular group, we detected and graphically presented differences between healthy tissue, the dental cement, and the biomimetic buffer layer at their interface and determined the position and concentration of functional groups that indicate integration of the biomimetic composite with hard dental tissue. We have shown that the proposed biomimetic system consisting of nanocrystalline CSHA from a biogenic calcium source and a complex of polar amino acids found in human teeth can form a functional bond with hard tissue of human teeth. The obtained miscrospectroscopy data confirm the chemical differentiation of the materials and the presence of organic and mineral interaction at the interface between the biomimetic system and hard dental tissue.

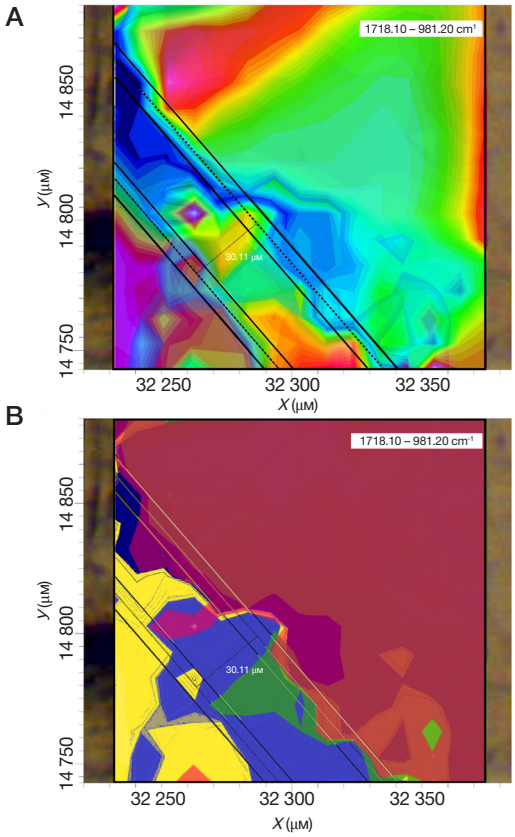

Fig. 6. Cluster analysis of absorption bands at 1760–1690 cm^{-1} and 1520–1360 cm^{-1} delineating the biomimetic composite area

References

1. Peutzfeldt A, Sahafi A, Flury S. Bonding of restorative materials to dentin with various luting agents. Oper Dent. 2011 Jun; 36 (3): 266–73.
2. Temel UB, Van Ende A, Van Meerbeek B, Ermis RB. Bond strength and cement-tooth interfacial characterization of self-adhesive composite cements. Am J Dent. 2017 Aug; 30 (4): 205–11.
3. Rohr N, Fischer J. Tooth surface treatment strategies for adhesive cementation. J Adv Prosthodont. 2017 Apr; 9 (2): 85–92.
4. Pontes DG, Araujo CTP, Prieto LT, de Oliveira DCRS, Coppini EK, Dias CTS, Paulillo LAMS. Nanoleakage of fiber posts luted with different adhesive strategies and the effect of chlorhexidine on the interface of dentin and self-adhesive cements. Gen Dent. 2015 Jun; 63 (3): 31–7.
5. Barandehfard F, Kianpour Rad M, Hosseinnia A, Khoshroo K, Tahriri M, Jazayeri HE, Moharamzadeh K, Tayebi L. The addition of synthesized hydroxyapatite and fluorapatite nanoparticles to a glass-ionomer cement for dental restoration and its effects on mechanical properties. Ceramics International. 2016 Nov 15; 42 (15): 17866–75.
6. Simon JC, A. Lucas S, Lee RC, Darling CL, Staninec M, Vaderhobli R, Pelzner R, Fried D. Near-infrared imaging of secondary caries lesions around composite restorations at wavelengths from 1300–1700-nm. Dental Materials. 2016 Apr 1; 32 (4): 587–95.
7. Uskoković V. Biomineralization and biomimicry of tooth enamel. In: Non-Metallic Biomaterials for Tooth Repair and Replacement [Internet]. Elsevier; 2013 [cited 2014 Sep 10]: 20–44. Available from: http://linkinghub.elsevier.com/retrieve/pii/B9780857092441500021.
8. Niu L, Zhang W, Pashley DH, Breschi L, Mao J, Chen J, Tay FR. Biomimetic remineralization of dentin. Dental Materials. 2014; 30 (1): 77–96.
9. Cao C, Mei M, Li Q, Lo E, Chu C. Methods for Biomimetic Mineralisation of Human Enamel: A Systematic Review. Materials. 2015 May 26; 8 (6): 2873–86.
10. Dorozhkin SV. Hydroxyapatite and Other Calcium Orthophosphates: Bioceramics, Coatings and Dental Applications [Internet]. Nova Science Publishers, Inc New York; 2017 [cited 2017 Aug 23]. 462 p. Available from: https://istina.msu.ru/publications/book/58538935/
11. El Rhilassi A, Mourabet M, Bennani-Ziatni M, El Hamri R, Taitai A. Interaction of some essential amino acids with synthesized poorly crystalline hydroxyapatite. Journal of Saudi Chemical Society. 2016; 20 (Suppl 1): 632–40.
12. Li H, Gong M, Yang A, Ma J, Li X, Yan Y. Degradable biocomposite of nano calcium-deficient hydroxyapatite-multi(amino acid) copolymer. Int J Nanomedicine. 2012; (7): 1287–95.
13. Aljabo A, Abou Neel EA, Knowles JC, Young AM. Development of dental composites with reactive fillers that promote precipitation of antibacterial-hydroxyapatite layers. Materials Science and Engineering: C. 2016; (60): 285–92.
14. Tavafoghi M, Cerruti M. The role of amino acids in hydroxyapatite mineralization. Journal of The Royal Society Interface. 2016 Oct 1; 13 (123): 20160462.
15. Ruan Q, Zhang Y, Yang X, Nutt S, Moradian-Oldak J. An amelogenin–chitosan matrix promotes assembly of an enamel-like layer with a dense interface. Acta Biomaterialia. 2013 Jul; 9 (7): 7289–97.
16. Baker MJ, Trevisan J, Bassan P, Bhargava R, Butler HJ, Dorling KM, et al. Using Fourier transform IR spectroscopy to analyze biological materials. Nat Protocols. 2014; 9 (8): 1771–91.
17. Vongsvivut J, Pérez-Guaita D, Wood BR, Heraud P, Khambatta K, Hartnell D, et al. Synchrotron macro ATR-FTIR microspectroscopy for high-resolution chemical mapping of single cells. Analyst. 2019 Mar 14; 144 (10): 3226–38.

18. Seredin P, Goloshchapov D, Ippolitov Y, Vongsvivut P. Pathology-specific molecular profiles of saliva in patients with multiple dental caries — potential application for predictive, preventive and personalised medical services. EPMA Journal. 2018 Jun 1; 9 (2): 195–203.
19. Hędzelek W, Marcinkowska A, Domka L, Wachowiak R. Infrared Spectroscopic Identification of Chosen Dental Materials and Natural Teeth. Acta Physica Polonica A. 2008 Aug; 114 (2): 471–84.
20. Seredin PV, Goloshchapov DL, Prutskij T, Ippolitov YuA. Fabrication and characterisation of composites materials similar optically and in composition to native dental tissues. Results in Physics. 2017; (7): 1086–94.
21. Erusalimov FA, Ippolitov YuA, Kunin AA. Bioactive bonding system [Internet]. RU2423966C2, 2011 [cited 2019 Jul 18]. Available from: https://patents.google.com/patent/RU2423966C2/en
22. Seredin PV, Goloshchapov DL, Gushchin MS, Ippolitov YA, Prutskij T. The importance of the biomimetic composites components for recreating the optical properties and molecular composition of intact dental tissues. J Phys: Conf Ser. 2017; 917 (4): 042019.
23. Ippolitov YuA. The possibility of bond system biological compatibility improvement for adhesion of hard dental tissues to filling material. Volgogradskij nauchno-medicinskij zhurnal. 2010; 4 (28): 31–4.
24. Seredin PV, Goloshchapov DL, Prutskij T, Ippolitov YuA. A Simultaneous Analysis of Microregions of Carious Dentin by the Methods of Laser-Induced Fluorescence and Raman Spectromicroscopy. Opt Spectrosc. 2018 Nov 1; 125 (5): 803–9.
25. Khan AS, Khalid H, Sarfraz Z, Khan M, Iqbal J, Muhammad N, et al. Vibrational spectroscopy of selective dental restorative materials. Applied Spectroscopy Reviews. 2017 Jul 3; 52 (6): 507–40.
26. Kobrina Y, Rieppo L, Saarakkala S, Pulkkinen HJ, Tiitu V, Valonen P, et al. Cluster analysis of infrared spectra can differentiate intact and repaired articular cartilage. Osteoarthritis and Cartilage. 2013 Mar 1; 21 (3): 462–9.
27. Atmeh AR, Chong EZ, Richard G, Festy F, Watson TF. Dentin-cement Interfacial Interaction: Calcium Silicates and Polyalkenoates. Journal of Dental Research [Internet]. 2012 Mar 20 [cited 2018 Apr 13]; Available from: http://journals.sagepub.com/doi/abs/10.1177/0022034512443068

Литература

1. Peutzfeldt A, Sahafi A, Flury S. Bonding of restorative materials to dentin with various luting agents. Oper Dent. 2011 Jun; 36 (3): 266–73.
2. Temel UB, Van Ende A, Van Meerbeek B, Ermis RB. Bond strength and cement-tooth interfacial characterization of self-adhesive composite cements. Am J Dent. 2017 Aug; 30 (4): 205–11.
3. Rohr N, Fischer J. Tooth surface treatment strategies for adhesive cementation. J Adv Prosthodont. 2017 Apr; 9 (2): 85–92.
4. Pontes DG, Araujo CTP, Prieto LT, de Oliveira DCRS, Coppini EK, Dias CTS, Paulillo LAMS. Nanoleakage of fiber posts luted with different adhesive strategies and the effect of chlorhexidine on the interface of dentin and self-adhesive cements. Gen Dent. 2015 Jun; 63 (3): 31–7.
5. Barandehfard F, Kianpour Rad M, Hosseinnia A, Khoshroo K, Tahriri M, Jazayeri HE, Moharamzadeh K, Tayebi L. The addition of synthesized hydroxyapatite and fluorapatite nanoparticles to a glass-ionomer cement for dental restoration and its effects on mechanical properties. Ceramics International. 2016 Nov 15; 42 (15): 17866–75.
6. Simon JC, A. Lucas S, Lee RC, Darling CL, Staninec M, Vaderhobli R, Pelzner R, Fried D. Near-infrared imaging of secondary caries lesions around composite restorations at wavelengths from 1300–1700-nm. Dental Materials. 2016 Apr 1; 32 (4): 587–95.
7. Uskoković V. Biomineralization and biomimicry of tooth enamel. In: Non-Metallic Biomaterials for Tooth Repair and Replacement [Internet]. Elsevier; 2013 [cited 2014 Sep 10]: 20–44. Available from: http://linkinghub.elsevier.com/retrieve/pii/B9780857092441500021.
8. Niu L, Zhang W, Pashley DH, Breschi L, Mao J, Chen J, Tay FR. Biomimetic remineralization of dentin. Dental Materials. 2014; 30 (1): 77–96.
9. Cao C, Mei M, Li Q, Lo E, Chu C. Methods for Biomimetic Mineralisation of Human Enamel: A Systematic Review. Materials. 2015 May 26; 8 (6): 2873–86.
10. Dorozhkin SV. Hydroxyapatite and Other Calcium Orthophosphates: Bioceramics, Coatings and Dental Applications [Internet]. Nova Science Publishers, Inc New York; 2017 [cited 2017 Aug 23]. 462 p. Available from: https://istina.msu.ru/publications/book/58538935/
11. El Rhilassi A, Mourabet M, Bennani-Ziatni M, El Hamri R, Taitai A. Interaction of some essential amino acids with synthesized poorly crystalline hydroxyapatite. Journal of Saudi Chemical Society. 2016; 20 (Suppl 1): 632–40.
12. Li H, Gong M, Yang A, Ma J, Li X, Yan Y. Degradable biocomposite of nano calcium-deficient hydroxyapatite-multi (amino acid) copolymer. Int J Nanomedicine. 2012; (7): 1287–95.
13. Aljabo A, Abou Neel EA, Knowles JC, Young AM. Development of dental composites with reactive fillers that promote precipitation of antibacterial-hydroxyapatite layers. Materials Science and Engineering: C. 2016; (60): 285–92.
14. Tavafoghi M, Cerruti M. The role of amino acids in hydroxyapatite mineralization. Journal of The Royal Society Interface. 2016 Oct 1; 13 (123): 20160462.
15. Ruan Q, Zhang Y, Yang X, Nutt S, Moradian-Oldak J. An amelogenin–chitosan matrix promotes assembly of an enamel-like layer with a dense interface. Acta Biomaterialia. 2013 Jul; 9 (7): 7289–97.
16. Baker MJ, Trevisan J, Bassan P, Bhargava R, Butler HJ, Dorling KM, et al. Using Fourier transform IR spectroscopy to analyze biological materials. Nat Protocols. 2014; 9 (8): 1771–91.
17. Vongsvivut J, Pérez-Guaita D, Wood BR, Heraud P, Khambatta K, Hartnell D, et al. Synchrotron macro ATR-FTIR microspectroscopy for high-resolution chemical mapping of single cells. Analyst. 2019 Mar 14; 144 (10): 3226–38.
18. Seredin P, Goloshchapov D, Ippolitov Y, Vongsvivut P. Pathology-specific molecular profiles of saliva in patients with multiple dental caries — potential application for predictive, preventive and personalised medical services. EPMA Journal. 2018 Jun 1; 9 (2): 195–203.
19. Hędzelek W, Marcinkowska A, Domka L, Wachowiak R. Infrared Spectroscopic Identification of Chosen Dental Materials and Natural Teeth. Acta Physica Polonica A. 2008 Aug; 114 (2): 471–84.
20. Seredin PV, Goloshchapov DL, Prutskij T, Ippolitov YuA. Fabrication and characterisation of composites materials similar optically and in composition to native dental tissues. Results in Physics. 2017; (7): 1086–94.
21. Ерусалимов Ф. А., Ипполитов Ю. А., Кунин А. А. Биоактивная бондинговая система [интернет]. RU2423966C2, 2011 [cited 2019 May 20]. Доступно по ссылке: https://patents.google.com/patent/RU2423966C2/ru.
22. Seredin PV, Goloshchapov DL, Gushchin MS, Ippolitov YA, Prutskij T. The importance of the biomimetic composites components for recreating the optical properties and molecular composition of intact dental tissues. J Phys: Conf Ser. 2017; 917 (4): 042019.
23. Ипполитов Ю. А. Возможность повышения биологической тропности светоотверждаемой бондинговой системы для адгезии твердых тканей зуба к пломбировочному материалу. Волгоградский научно-медицинский журнал. 2010; 4 (28): 31–4.
24. Середин П. В., Голощапов Д. Л., Prutskij T., Ипполитов Ю. А. Единовременный анализ микрообластей кариозного дентина методами лазерно-индуцированной флуоресценции и рамановской спектромикроскопии. Оптика и спектроскопия. 2018; 125 (11): 708.
25. Khan AS, Khalid H, Sarfraz Z, Khan M, Iqbal J, Muhammad N, et al. Vibrational spectroscopy of selective dental restorative materials. Applied Spectroscopy Reviews. 2017 Jul 3; 52 (6): 507–40.
26. Kobrina Y, Rieppo L, Saarakkala S, Pulkkinen HJ, Tiitu V, Valonen P,

et al. Cluster analysis of infrared spectra can differentiate intact and repaired articular cartilage. Osteoarthritis and Cartilage. 2013 Mar 1; 21 (3): 462–9.

27. Atmeh AR, Chong EZ, Richard G, Festy F, Watson TF. Dentin-cement Interfacial Interaction: Calcium Silicates and Polyalkenoates. Journal of Dental Research [Internet]. 2012 Mar 20 [cited 2018 Apr 13]; Available from: http://journals.sagepub.com/doi/abs/10.1177/0022034512443068.

HIRUDOTHERAPY IN TREATMENT OF CHRONIC GENERALISED PERIODONTITIS

Sashkina TI[1], Abdullaeva AI[1]✉, Runova GS[2], Saldusova IV[2], Zajchenko OV[2], Faskhutdinov DK[2], Sokolova SI[2], Pustovaya EP[3]

[1] Pirogov Russian National Research Medical University, Moscow, Russia

[2] AI Yevdokimov Moscow State University of Medicine and Dentistry, Moscow, Russia

[3] Peoples Friendship University of Russia, Moscow, Russia

Chronic generalized periodontitis (CGP) is a disease associated with low susceptibility to the therapeutic protocols applied; practitioners tend to characterize it as a disease presenting certain difficulties. Therefore, the search for drugs and methods capable of increasing the efficacy of CGP therapy is an ongoing process. Additional problems, which have to do with either with antibiotic resistance or increased sensitivity to drugs, also occur quite often. This study aimed to assess the possibility of applying hirudotherapy in the context of conservative treatment of CGP. 50 patients with CGP without somatic pathology were examined and treated. The participants were divided into two groups (n = 25), all group members of about the same age. At the first stage, the treatment followed the accepted standard: professional oral hygiene procedures, antimicrobial and anti-inflammatory drugs, demonstration of proper personal oral hygiene routines. Then, first group went through a monthlong hirudotherapy course that consisted of 6 to 8 individual procedures. Second group was observed throughout this period with the aim to control the level of their compliance with the oral hygiene routines they were trained. Having analyzed the results, we found that hirudotherapy was more effective than what was prescribed to the second (control) group. The papillary marginal alveolar index (PMA), which reflects the severity of inflammation and gum bleeding, decreased significantly in the first group, where medicinal leeches were used: in the patients with severe CGP it went down by 6%, in those with moderately severe CGP the index decreased by 24% and the participants whose CGP was only light had the PMA go down by 2%. Thus, we have demonstrated the efficacy of hirudotherapy in the context of conservative CGP treatment, which allows recommending this method for inclusion into clinical practice.

Keywords: chronic generalized periodontitis, hirudotherapy, periodontal indices

Author contribution: Sashkina TI, Abdullaeva AI — research planning, data processing, manuscript editing; Zaychenko OV and Pustovaya EP — data processing, statistical data processing, manuscript editing; Sokolova SI, Saldusova IV — data processing, manuscript editing; Faskhutdinov DK, Runova GS — data collection, manuscript drafting.

Compliance with ethical standards: the study was approved by the Ethics Committee of Pirogov Russian National Research Medical University (protocol № 981 of June 24, 2019).

✉ **Correspondence should be addressed:** Aytan I. Abdullaeva
Ostrovityanova 1, Moscow, 117997; aitanka@list.ru

Received: 25.06.2019 **Accepted:** 25.07.2019 **Published online:** 18.08.2019

DOI: 10.24075/brsmu.2019.052

ГИРУДОТЕРАПИЯ В ЛЕЧЕНИИ ХРОНИЧЕСКОГО ГЕНЕРАЛИЗОВАННОГО ПАРОДОНТИТА

Т. И. Сашкина[1], А. И. Абдуллаева[1]✉, Г. С. Рунова[2], И. В. Салдусова[2], О. В. Зайченко[2], Д. К. Фасхутдинов[2], С. И. Соколова[2], Е. П. Пустовая[3]

[1] Российский национальный исследовательский медицинский университет имени Н. И. Пирогова, Москва, Россия

[2] Московский государственный медико-стоматологический университет имени А. И. Евдокимова, Москва, Россия

[3] Российский университет дружбы народов, Москва, Россия

Хронический генерализованный пародонтит (ХГП) — заболевание, которое представляет определенные трудности для специалистов, поскольку характеризуется устойчивостью к применяемой терапии. Поэтому постоянно идет поиск препаратов и методов, позволяющих повысить эффективность лечения ХГП. Нередко возникают дополнительные проблемы, которые связаны либо с антибиотикорезистентностью, либо с повышенной чувствительностью к препаратам. Целью исследования было определить возможность использования гирудотерапии при консервативном лечении пациентов с ХГП. Было обследовано и пролечено 50 пациентов с ХГП, не имеющих соматической патологии. Они были разделены на две группы по 25 человек, примерно одного возраста. В каждой из групп сначала проводили лечение в соответствии с принятым стандартом: назначали профессиональные гигиенические процедуры, антимикробные и противовоспалительные препараты, обучали индивидуальной гигиене. Затем пациентам первой группы проводили курс гирудотерапии, состоящий из 6–8 процедур в течение месяца. При этом пациенты второй группы находились на диспансерном учете с целью контроля гигиены полости рта. Анализ полученных результатов показал более высокую эффективность гирудотерапии по отношению к группе сравнения. В группе, в которой использовали медицинские пиявки, происходило достоверное снижение папиллярно-маргинально-альвеолярного индекса (PMA), характеризующего интенсивность воспалительного процесса и кровоточивость тканей десны: на 32% при легкой степени тяжести, на 24% при средней степени тяжести, на 6% при тяжелой степени тяжести ХГП. Таким образом, показана эффективность гирудотерапии в консервативном лечении пациентов с ХГП, что позволяет рекомендовать этот метод в клиническую практику.

Ключевые слова: хронический генерализованный пародонтит, гирудотерапия, пародонтальные индексы

Информация о вкладе авторов: Т. И. Сашкина, А. И. Абдуллаева — планирование исследования, обработка полученных данных, редактирование рукописи; О. В. Зайченко и Е. П. Пустовая — обработка полученных данных, статистическая обработка данных, редактирование рукописи; С. И. Соколова, И. В. Салдусова — обработка полученных данных, редактирование рукописи; Д. К. Фасхутдинов, Г. С. Рунова — сбор данных, написание черновика рукописи.

Соблюдение этических стандартов: исследование было одобрено этическим комитетом РНИМУ имени Н. И. Пирогова (протокол № 981 от 24 июня 2019 г.).

✉ **Для корреспонденции:** Айтан Измировна Абдуллаева
ул. Островитянова, д. 1, г. Москва, 117997; aitanka@list.ru

Статья получена: 25.06.2019 **Статья принята к печати:** 25.07.2019 **Опубликована онлайн:** 18.08.2019

DOI: 10.24075/vrgmu.2019.052

According to the WHO, over 90% of the world's population suffer from chronic inflammatory periodontal diseases that run for a long period of time and resist treatment, leading to tooth loss, development of chronic diseases of the gastrointestinal tract, cardiovascular and other systems, which negatively affect health and quality of life of such people [1, 2]. Therefore, periodontitis is more than a medical problem, it is also a social one since it affects the lives of people. Successful periodontitis therapies are standing problem for dental professionals. There are various approaches to the treatment of periodontitis. Surgical, physiotherapeutic and alternative treatment methods, like naturopathy, often complete the courses of mandatory antimicrobial therapy and professional oral hygiene procedures. According to the published literature, hirudotherapy is one of the methods applied to counter various inflammatory diseases. Leech saliva is a bacteriostatic agent, which means it reduces the bacterial load on periodontal tissues and normalizes hemostasis [3–6]. This fact encouraged us to study hirudotherapy as a treatment modality that can be a part of the conservative CGP therapy [4, 5].

The goal of this research effort was to learn the efficacy of hirudotherapy in the complex conservative treatment of CGP patients.

METHODS

The study involved 50 patients, 21 male and 29 female, aged 32 to 52 years, suffering from light, moderately severe and severe CGP. Inclusion criteria: signed informed consent; the presence of CGP absence of concomitant somatic pathology at the age of 32 to 52 years; taken training in wound care; preliminary therapy in accordance with the standard approved by the Ministry of Health of the Russian Federation; Exclusion criteria: the presence of concomitant somatic pathology; age younger than 32 and older than 52 years; non-compliance with the medical requirements and non-compliance with oral hygiene; lack of prior therapy in accordance with the standard approved by the Minister of Health of the Russian Federation. They were divided into two groups so as to have the clinical and functional characteristics. 25 patients formed the treatment group: 9 (36%) had light CGP, 9 (36%) other — moderately severe CGP and in 7 (28%) patients the disease developed into the severe stage. The distribution of CGP stages in the control stages was the same (Fig. 1). No participant had a somatic pathology aggravating the disease in question. We used the objective indices to assess the efficacy of treatment: PMA and the Green-Vermillion index, which allow monitoring the degree of inflammation.

For the treatment group patients, a week's course included the standard antimicrobial, anti-inflammatory therapy, professional oral hygiene procedures, which were followed by hirudotherapy, i. e. attaching leeches to the inflamed periodontal tissues (Fig. 2). We used the standard size (0.6–1 g) medicinal leeches. The course, which ran for a month, consisted of 6–8 procedures conducted twice a week. The leeches were attached 2 hours after eating; the patients were warned that their oral cavities should be free from specific odors, such as those of onion, garlic, mouth rinse, coffee, cardamom. Also, the patients were forbidden to smoke and to use perfumes 5–6 hours before their visits to the dentist.

The patients in the control group received standard treatment. Instead of hirudotherapy, they were observed with the aim to control how they follow the prescribed personal oral hygiene routines.

We applied the Student's test in statistical processing of the obtained results; the confidence level was set at 95% ($p < 0.05$). STATISTICA 10 software (Round Rock; USA) was used to perform the processing.

RESULTS

Having analyzed the data collected, we learned that medicinal leeches augmented the effect of standard therapy in the treatment group, and the indices describing state of periodontal tissue showed a continuing downward trend. After treatment, the PMA index was at the lowest point in light CGP cases: from 21.89 ± 2.03 to 14.89 ± 2.14 ($p < 0.05$). In patients with moderately severe CGP the PMA decrease was less obvious: from 33.74 ± 3.57 to 25.74 ± 3.21. In the cases where the disease has progressed to severe stage, PMA went down slightly, but the decrease could not be called significant: from 67.85 ± 1.28 to 64.24 ± 1.26 ($p \geq 0.05$) (Fig. 3). Compared to the treatment group, the results registered in the control group were less pronounced. The PMA index decreased from 24.91 ± 2.73 to 19.91 ± 2.08 ($p < 0.05$) in light CGP cases, which is significant but not as great as what was seen in the treatment group. In patients with moderately severe CGP the index changed from 33.61 ± 3.14 to 28.36 ± 3.44, and in severe CGP cases — from 67.15 ± 1.28 to 66.85 ± 1.18 (Fig. 4), both the former and the latter change being non-significant ($p \geq 0.05$). Comparing the

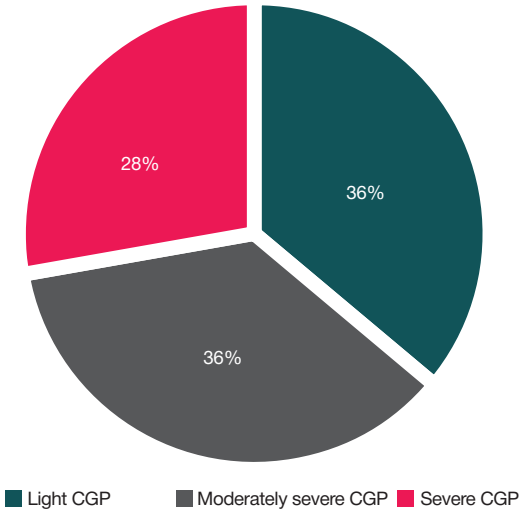

Fig. 1. Distribution of CGP patients in groups depending on the severity of the disease ($n = 25$)

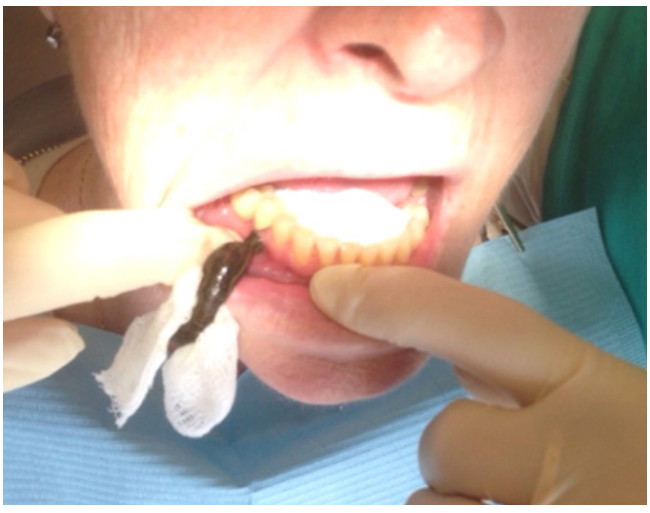

Fig. 2. Applying medicinal leeches to a CGP patient. A standard-sized medicinal leech is attached to the inflamed periodontal tissues

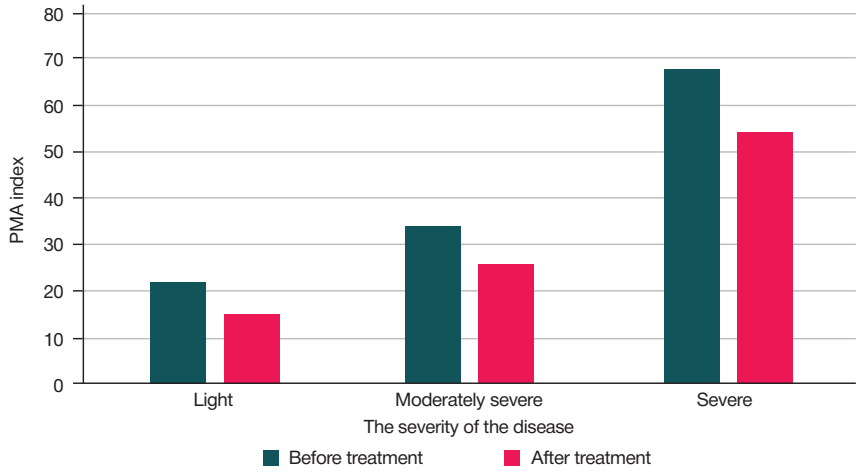

Fig. 3. PMA index dynamics, treatment group (*n* = 25)

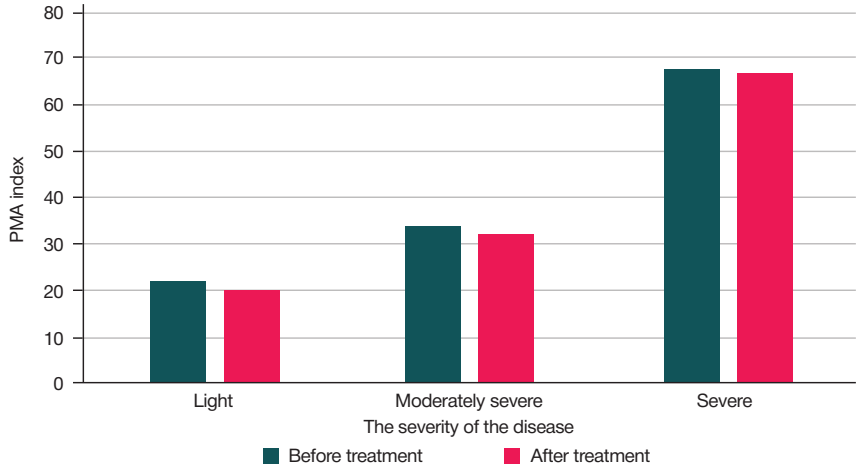

Fig. 4. PMA index dynamics, control group (*n* = 25)

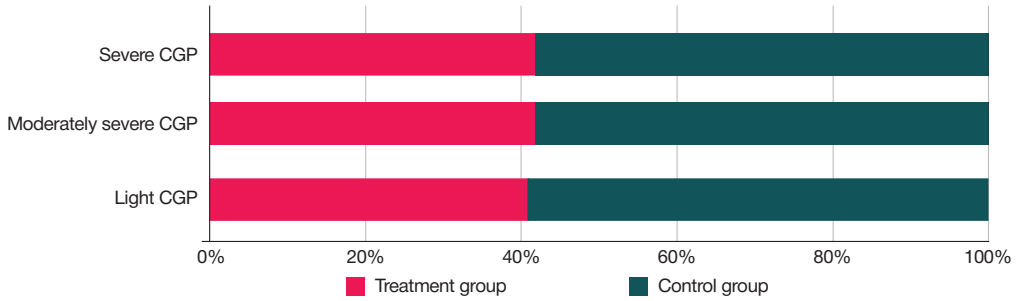

Fig. 5. PMA index comparison after treatment, control and treatment groups

data collected in both groups, we discovered that the protocol applied in the treatment group delivered a stronger clinical effect in light and moderately severe CGP cases (Fig. 5).

DISCUSSION

To a certain extent, the findings of our study are consistent with those of a paper published in 2014 that described introduction of hirudotherapy and Lipin (liposomal drug) to the periodontitis treatment protocol. The authors of that paper wrote about the suggested complex approach being more effective than the standard one, but did not measure the contribution of each component to the final result of the treatment [6]. We showed that medicinal leeches, applied separately, help arrest inflammation in CGP patients, reduce edema, arterial hyperemia and gum bleeding. Application of medicinal leeches made the effect from standard treatment more pronounced and lasting (compared to the control group), which increased duration of the remission. The dynamics of change of the indices monitored was positive; the change to the better was registered after 2–4 hirudotherapy procedures. The effect was stronger in light and moderately severe CGP cases.

CONCLUSIONS

The study demonstrated a positive effect hirudotherapy offers as part of the CGP treatment protocol. This treatment tactic significantly increases the efficacy of standard therapeutic measures and significantly reduces the inflammatory potential of periodontal tissues: pain, itching, bleeding gums. Given the growing antibiotic resistance and high sensitivity of population to antibacterial drugs in particular, hirudotherapy may be the method of choice, and sometimes one of the few treatment modalities applicable to certain groups of population.

References

1. Sashkina TI, Poryadin GV, Runova GS, Dubrovin DS, Faskhutdinov DK, Markina ML, et al. The application of an immunomodulator for the correction of the inflammatory process in periodontal tissues of the patients presenting with chronic generalized periodontitis. Rossiiskaya stomatologia. 2016; 9 (3): 38–41. In Russian.
2. Grudyanov AI, Tkacheva ON, Avraamova TV, Khvatova NT. The relationship between inflammatory periodontal diseases and cardiovascular diseases. Rossiiskaya stomatologia. 2015; 94 (3): 50–5. In Russian.
3. Danilevskij NF. Zabolevaniya slizistoj obolochki polosti rta. M.: GEOTAR-Media, 2001. In Russian.
4. Tsepov LM, Tsepova EL, Tsepov AL. Marginal periodontitis: local focus of serious problems. Parodontologia. 2014; 3 (72): 3–10.
5. Trevilatto PC, de Brito RBJr, Scarel-Caminaga RM, de Souza AP, Sallum AW, Line SRP. Polymorphism in the tumor necrosis factor-alpha gene (TNFA–308 G/A) is not associated with susceptibility to chronic periodontitis in a Brazilian population. Dentistry 3000. 2015; (3): 1.
6. Abduvaliev AA, Daurekhanov AM, Hirudotherapy as a complex treatment of patients with reactive arthritis. Bulletin of KazNMU. 2017; (1): 249–52.

Литература

1. Сашкина Т. И., Порядин Г. В., Рунова Г. С., Дубровин Д. С., Фасхутдинов Д. К., Маркина М. Л., и др. Применение иммуномодулятора для коррекции воспалительного процесса в тканях пародонта у больных с хроническим генерализованным пародонтитом. Российская стоматология. 2016; 9 (3): 38–41.
2. Грудянов А. И., Ткачева О. Н., Авраамова Т. В., Хватова Н. Т. Вопросы взаимосвязи воспалительных заболеваний пародонта и сердечно-сосудистой патологии. Стоматология. 2015; 94 (3): 50–5.
3. Данилевский Н. Ф. Заболевания слизистой оболочки полости рта. М.: ГЭОТАР-Медиа, 2001.
4. Цепов Л. М., Цепова Е. Л., Цепов А. Л. Пародонтит: локальный очаг серьезных проблем. Пародонтология. 2014; 3 (72): 3–10.
5. Trevilatto PC, de Brito RBJr, Scarel-Caminaga RM, de Souza AP, Sallum AW, Line SRP. Polymorphism in the tumor necrosis factor-alpha gene (TNFA–308 G/A) is not associated with susceptibility to chronic periodontitis in a Brazilian population. Dentistry 3000. 2015; (3): 1.
6. Абдувалиев А. А., Дауреханов А. М. Гирудотерапия в комплексном лечении больных реактивным артритом. Вестник КазНМУ. 2017; (1): 249–52.

THE IMPACT OF ELECTRONIC DEVICES ON THE PHYSICAL GROWTH AND DEVELOPMENT OF THE MODERN YOUTH AND RECOMMENDATIONS ON THEIR SAFE USE

Milushkina OYu[1], Skoblina NA[1], Markelova SV[1], Tatarinchik AA[1], Melikhova EP[2] ✉, Libina II[2], Popov MV[2]

[1] Pirogov Russian National Research Medical University, Moscow, Russia

[2] Burdenko Voronezh State Medical University, Voronezh, Russia

The impact of excessive exposure to electronic devices (ED) on youth health remains understudied. There is a pressing need to develop recommendations for the safe use of stationary and mobile ED aimed at minimizing health risks. In this work, we assess the effect of ED on the physical growth and development of high-school and university students and provide recommendations for preventing the negative impact of prolonged screen time on health. The study recruited 460 high-school and 598 university students. Standard anthropometric measurements were taken. The psychological and emotional state of the participants was evaluated using the Test Anxiety Inventory by Spielberg (modified by Khanin). To estimate daily and weekly exposure to ED the participants were asked to fill out standardized questionnaires. In high school students, the average screen time was 7 h a day; in university students, 8.5 to 10 h a day. Only 60% of the participants, regardless of their place of residence or the type of educational institution they were attending, were physically healthy. We conclude that prolonged and frequent exposure to ED is one of the factors that can interfere with normal physical growth and development in youth. Regular daily use of stationary ED increases the risk of developing body weight deficit by 24% and gaining excess body weight by 10%. We recommend that students should eliminate computers, laptops and stationary ED from their daily activities for at least one day at the weekend and reduce total screen time to 3 hours a day.

Keywords: health, electronic devices, information and communication technologies, physical growth and development, psycho-emotional state, high-school students, university students

Author contribution: Milushkina OYu and Skoblina NA supervised the study, processed the collected data and wrote the manuscript; Markelova SV, Libina II and Popov MV collected and processed the data; Tatarinchik AA analyzed the literature, collected and processed the data; Melikhova EP collected and processed the data and edited the manuscript.

Compliance with ethical standards: the study was approved by the Ethics Committee of Pirogov Russian National Medical Research University (Protocol 159 dated November 21, 2016). Informed consent was obtained from all study participants.

✉ **Correspondence should be addressed:** Ekaterina P. Melikhova
Studencheskaya 10, Voronezh, 394036; katerina.2109@mail.ru

Received: 04.07.2019 **Accepted:** 18.07.2019 **Published online:** 23.07.2019

DOI: 10.24075/brsmu.2019.046

ВЛИЯНИЕ ЭЛЕКТРОННЫХ УСТРОЙСТВ НА ФИЗИЧЕСКОЕ РАЗВИТИЕ СОВРЕМЕННОЙ МОЛОДЕЖИ И РЕКОМЕНДАЦИИ ПО РЕГЛАМЕНТУ ИХ ИСПОЛЬЗОВАНИЯ

О. Ю. Милушкина[1], Н. А. Скоблина[1], С. В. Маркелова[1], А. А. Татаринчик[1], Е. П. Мелихова[2] ✉, И. И. Либина[2], М. В. Попов[2]

[1] Российский национальный исследовательский медицинский университет имени Н. И. Пирогова, Москва, Россия

[2] Воронежский государственный медицинский университет имени Н. Н. Бурденко, Воронеж, Россия

Влияние частого и длительного использования электронных устройств (ЭУ) на состояние здоровья молодежи до сих пор недостаточно изучено. Исследования по регламентации использования стационарных и мобильных ЭУ для обеспечения оптимального физического развития молодежи становятся особо актуальными. Целью работы было установить характер и степень влияния использования ЭУ на физическое развитие молодых людей и рекомендовать режим использования ЭУ в течение дня для профилактики возникновения отклонений в физическом развитии. Для определения физического развития 460 старшеклассников и 598 студентов использовали гигиенический, инструментальный, социологический, статистический методы исследования: стандартную антропометрическую методику; для оценки психоэмоционального состояния — тест Спилберга–Ханина; для учета использования ЭУ проводили анкетирование с применением стандартизированных опросников. При среднем суммарном ежедневном времени использования ЭУ у старших школьников, составляющем 7 ч, и у студентов, равном 8,5–10 ч, нормальное физическое развитие выявлено в среднем только у 60% обследованных, причем это не связано с регионом проживания или типом образовательного учреждения. Показано, что частое и длительное использование ЭУ молодежью служит одним из факторов, способных вызвать отклонения в физическом развитии. Установлено, что ежедневное использование стационарных ЭУ увеличивает риск возникновения у подрастающего поколения нарушений в физическом развитии за счет дефицита массы тела на 24% и его избытка на 10%. В качестве профилактических мероприятий рекомендованы отказ от использования стационарных ЭУ, компьютера и ноутбука на 1 день в неделю (в выходной день) и ограничение суммарного времени использования всех видов ЭУ до 3 ч в день.

Ключевые слова: здоровье, электронные устройства, физическое развитие, информационно-коммуникационные технологии, психоэмоциональное состояние, школьники, студенты

Информация о вкладе авторов: О. Ю. Милушкина и Н. А. Скоблина — научное руководство, обработка материала, написание статьи; С. В. Маркелова, И. И. Либина и М. В. Попов — сбор и обработка материала; А. А. Татаринчик — анализ литературных данных, сбор и обработка материала; Е. П. Мелихова — сбор и обработка материала, редактирование статьи.

Соблюдение этических стандартов: исследование одобрено этическим комитетом ФГБОУ ВО РНИМУ имени Н. И. Пирогова Минздрава России (протокол № 159 от 21 ноября 2016 г.); для каждого обследованного было получено добровольное информирование согласие.

✉ **Для корреспонденции:** Екатерина Петровна Мелихова
ул. Студенческая, д. 10, г. Воронеж, 394036; katerina.2109@mail.ru

Статья получена: 04.07.2019 **Статья принята к печати:** 18.07.2019 **Опубликована онлайн:** 23.07.2019

DOI: 10.24075/vrgmu.2019.046

In recent years, information and communication technologies (ICT) and in particular electronic devices (ED) have been increasingly recognized as a significant environmental factor affecting young people's health [1–8].

Over the last two decades, ED have been actively used both inside and outside the classroom. In 2008, only 3 quarters of adolescents and young adults aged 12 to 24 years had access to Internet; by 2018, the figures had soared to 96.9%. There are now significantly more Web users who go online every day among young people than among adults. The growing size of young Internet audience can be linked to the availability of mobile ED capable of connecting to the Web, such as mobile phones in the first place [9, 10].

The use of ICT in the classroom is beneficial for both the teacher and the student. Although ICT deployment may not be cheap, the ultimate education costs will be lower in comparison with "traditional" education. The curriculum can be adjusted to an individual student's rate of learning based on his/her academic progress. There are no strict requirements on the learning/teaching space. ICT provide effective tools for monitoring a student's progress. In turn, any student can easily access any snippet of information taught during the course. These ICT advantages provide a possibility for inclusive learning. Still, some authors hold the opinion that expansion of computerized education significantly increases health risks for the students learning in a digital environment [11].

Overuse of ED has a number of negative effects, including escapism from the real world into the Web, deterioration of physical and mental health, etc. [12–15]. For example, research conducted in the educational institutions of Irkutsk demonstrated that intensive computerized learning negatively affected intellectual performance, increased anxiety and stimulated hyperactivity in children [16].

The use of electronic devices by children in preschool facilities and schools is regulated by a number of special guidelines, including Sanitary Rules and Regulations (SanPiN) 2.2.2/2.4 1340-03 (*Requirements for personal computers and learning spaces*), SanPiN 2.4.1.3049-13 (*Safety and health requirements for the design, maintenance and operation of preschool educational facilities*), SanPiN 2.4.2.2821-10 (*Safety and health requirements for the learning environment in schools*), recommendations on the *Safety assessment of e-book readers and their use in educational institutions*, etc. The majority of these guidelines regulate the use of stationary ED in educational institutions (but not outside the classroom), leaving mobile devices out of the equation. This shapes the need for developing total screen time recommendations for children and teenagers.

In 2015, the Government of the Russian Federation adopted the Children's Information Security Concept. The document highlights the importance of creating a safe information environment that would promote social adaptation, foster personal, cognitive, intellectual and physical development, protect and sustain mental health and wellbeing and stimulate a positive view of life [17]. A lot of effort has been channeled into researching the effects of ED on the mental and physical health of young people and into elaborating safety regulations on the use of ED. However, to this day the impact of ED on children's growth and physical development has not been studied. Therefore, it is important to propose screen time recommendations for young people in order to ensure their harmonious physical development, as prescribed by the Concept.

In the study presented below, we assess the effect of ED on the growth and physical development of high-school and university students and give screen time recommendations.

METHODS

The study conducted in 2017–2018 recruited 460 high-school students from Moscow region and 598 university students from Moscow, Voronezh and Arkhangelsk. The study included high-school/university students of both sexes who gave informed consent to participate. The mean age of the participants was 16 years for high-school and 20 years for university students. At this age young people can choose for themselves how much they will use ED during the day or at nighttime. Older and younger individuals were excluded from the study. Because it takes a certain time for the body size and composition to change, the impact of ED should be assessed in the context of its total duration. The age groups included in the study had a sufficiently long experience (over 10 years) of using ED.

Our multicenter study included schools with standard and advanced curricula, as well as gymnasiums (schools preparing students for university), and higher educational institutions specializing in 1) public healthcare and medical sciences, 2) mathematics and mechanics. The educational institutions were located in different climate zones.

First, we assessed the growth and physical development of high-school and university students using a conventional anthropometric method and instrumentation. Body height (cm) was measured with 0.5 cm precision with a standard anthropometer measuring set. Body weight was measured with 100 g precision using an InBody 230 analyzer (Biospace; South Korea). The obtained values were compared with regression scales available for the regions involved in the study.

Considering that body weight and height may not provide sufficient information about the effect of the studied factor on the growth and physical development of the participants, we additionally analyzed the body composition using an InBody 230 analyzer (Biospace; South Korea). This allowed us to estimate muscle mass (kg), fat mass (kg), and body mass index (kg/m^2) and to provide weight management recommendations (the amount of weight the subject was recommended to gain or lose). Reference values returned by the analyzer corresponded to the normal ranges adopted in the Western clinical practice. BMI was compared to the values recommended by WHO (18.5–24.9).

Because different body builds are considered to be prone to developing different weight statuses, we determined the body build for each participant using a classification proposed by Shtefko and Ostrovsky and modified by Darskaya [18]. Characteristics of body types are presented in Table 1.

Table 1. Characteristics of body types

Type	Characteristics	Prone to developing body weight deficit	Prone to gaining excess body weight
Asthenic, weak	Slender, flat-chested, lean, with weak musculature; epigastric angle < 90°	Yes	No
Thoracic, weak	Slender with elliptical chest, average muscle development, low fat mass; epigastric angle < 90°	Yes/no	No
Muscular, strong	Broad in shoulders, with symmetrical elliptical chest, average or well-developed musculature, average or increased fat mass; epigastric angle = 90°,	No	Yes/no
Abdominal, strong	Broad, with short cone-shaped chest, average muscular development, prone to fat deposition; epigastric angle ≥90°	No	Yes

Psychological and emotional states of the participants were assessed using the Spielberg-Khanin anxiety inventory [19].

In the second part of our study, we asked the participants to fill out standardized questionnaires designed at the Research Institute of Hygiene and Health Protection of Children and Adolescents (National Medical Research Center for Children's Health) [20]. The questionnaires allowed us to assess the frequency of exposure to ED, its total daily and weekly duration.

Lastly, the obtained data were processed using Statistica 10.0 (StatSoft; USA). We tested a hypothesis about the impact of frequency and duration exposure to ED on the physical health in young people. Arithmetic means, the standard error of the mean and the standard deviation were calculated. Student's t-test was applied to assess significance of differences. For continuous quantitative variables, Pearson's correlation coefficient was calculated. For discrete qualitative variables, contingency tables were built; relationship between the variables were assessed using Pearson's correlation coefficient.

Relative risks (RR) were calculated to estimate the probability of a certain outcome in the groups. Four-field contingency tables were constructed and analyzed using the online statistical calculator [21]. The 95% CI was also computed.

RESULTS

In the first part of our study, we measured the main growth parameters: body weight and height, which had typical age and sex-related peculiarities. No regional differences were observed between university students in terms of weight and height (Table 2). Using regional regression scales, we established that only 60.6 ± 1.2% of high-school boys, 56.8 ± 2.4% of male university students, 61.2 ± 2.7% of high-school girls, and 63.3 ± 1.5% of female university students were developing harmoniously.

BMI was 21.1 ± 3.2 kg/m^2 and 20.1 ± 3.3 kg/m^2 for high-school boys and girls, respectively. In the group of university students, BMI was 23.04 ± 3.7 kg/m^2 and 21.28 ± 3.5 kg/m^2 for males and females, respectively. According to WHO recommendations, the normal BMI range for the studied age group is between 18.5 and 24.9 kg/m^2. However, as many as 20.3% of male and 15.6% of female university students participating in the study had BMI over 25 kg/m^2.

Body weight deficit was observed in 24.2 ± 1.5% of high-school boys, 30.6 ± 2.1% of high-school girls, 10.5 ± 1.2% of male and 21.8 ± 2.3% of female university students. Excess weight was observed in 12.2 ± 2.1% of high-school boys, 6.2 ± 1.1% of high-school girls, 24.6 ± 1.2% of male and 12.0 ± 1.5% of female university students. The rest of the participants were obese. On the whole, high-school students were prone to developing body weight deficit whereas university students, to gaining excess weight.

The analysis of body composition revealed that unlike height, fat mass was increasing with age ($p < 0.05$) in both boys and girls. Importantly, the children were not building muscle mass, regardless of their sex. This is an alarming trend: children with body weight deficit do not develop sufficient muscle mass and, therefore, do not join the ranks of their normally growing peers. Although the total body weight was increasing with age in our participants, it was largely due to fat accumulation. Young people with excess body weight continued to accumulate more fat. Based on the analysis of body composition, high-school and university students were recommended to increase their muscle mass by an average of 2 to 4 kg; additionally, university students were recommended to reduce their fat mass by an average of 2.5 kg (Table 2).

Additionally, we determined body build types of the young people included in the study. Relatively weak types (asthenic and thoracic) accounted for 40.0% of the participants, whereas relatively strong types (muscular and abdominal) made up 25.0% of the participants; the rest of the high-school students did not represent any particular build. Such distribution is normal for the general population. We found a correlation between the deviations from normal growth caused by weight deficit and the abdominal body build (Pearson's correlation coefficient was 0.72; $p < 0.005$).

The alarming number of high-school and university students with abnormal body weight raises a question of their underlying causes and prompts investigation of ED contribution to body weight deficit and obesity.

In the second part of the study, the participants reported that they used different types of ED every day, including mobile phones, laptops, tablets, computers (ranked here in the descending order). Only 0.5% of the surveyed did not use ED. In this respect, no significant differences were observed between boys and girls, male and female university students, high-school and university students or the participants from different regions. This suggests that ED are enjoying wide popularity among young people in the general population.

Table 2. Growth parameters and body composition in high-school and university students presented as mean values (M ± *m*)

Growth parameters	High-school		University	
	boys	girls	males	females
Height, cm	175.5 ± 0.4	165.4 ± 0.5*	176.9 ± 0.5	165.9 ± 0.3
Body weight, kg	65.0 ± 1.0	55.2 ± 1.1*	72.4 ± 0.9**	58.7 ± 0.7**
Fat mass, kg	10.1 ± 0.2	13.0 ± 0.1*	13.9 ± 0.2**	15.9 ± 0.3**
Recommended fat mass reduction/increase, kg	0.2 ± 0.01	0.2 ± 0.01	–2.5 ± 0.05	–2.4 ± 0.04
Muscle mass, kg	30.1 ± 0.7	22.9 ± 0.8*	33.0 ± 0.5	23.3 ± 0.7
Recommended muscle mass reduction/increase	3.7 ± 0.7	3.9 ± 0.6	1.8 ± 0.4	3.6 ± 0.5

Note: * $p < 0.05$ — between high-school boys and girls; ** $p < 0.05$ between high-school and university students.

Table 3. Relative risks of deviations from normal growth patterns in high-school and university students based on the frequency of exposure to stationary ED

Outcomes	Factor	RR (relative risk)	EF, % (etiologic fraction)	Se (sensitivity of the method)	Sp (specificity of the method)
Body weight deficit	Frequency of exposure to stationary ED (every day)	2.13	23.6	0.29	0.88
Excess body weight	Frequency of exposure to stationary ED (every day)	1.59	9.8	0.67	0.47

The participants used at least 2 different types of ED every day, such as a mobile phone and a stationary computer or a laptop, in the first place (Pearson's correlation coefficient was 0.5; $p < 0.001$).

The participants switched from their mobile phones to ED and back throughout the day, which means that total daily screen time was prolonged. For high-school students, total daily screen time (inside and outside the classroom) was 7 h. For male university students, it was 8.5 h and for female students, 10 h. The observed trends did not differ between the regions.

Lastly, we investigated the impact of frequent (daily) and prolonged (in terms of hours) use of ED on the physical growth of the participants and its contribution to developing weight deficit or excess weight.

The risks were analyzed. Knowing the risk factors and their significance will help in developing methods for risk mitigation and prevention of adverse effects on young people's health (Table 3).

For body weight deficit, RR was 2.13 (DI: 2,01–2,21), i.e., daily exposure to stationary ED increases the risk of body weight deficit and contributes to negative outcomes. The etiologic fraction was as high as almost 24%; apparently, other factors made their contribution, too.

For excess body weight, RR was 1.59 (DI: 1.11–3.15); the etiologic fraction was 9.8%.

With mobile ED and a different frequency of weekly exposure to ED, no risks were identified. Perhaps, exposure to stationary ED leads to the reduction of physically active behaviors, thereby affecting the growth and development of a child.

However, the analysis of correlations between fat mass and the duration of exposure to either stationary or mobile ED expressed in hours reveals statistically significant ($p < 0.05$) correlations between fat mass and the duration of exposure to a computer or a laptop (0.45) and a mobile phone (0.55). Perhaps, the opportunity to use mobile phones in a sitting position in wi-fi zones in public transport, shopping malls, and parks turns the phone into a stationary device.

We also determined the total daily exposure time to stationary and mobile ED that did not have a negative impact of young people's health (Fig. 1–2).

The analysis reveals that safe daily screen time is below 3 hours a day. Considering that there are always children, adolescents and young people in a population whose physical development is not harmonious, a 5.0% body weight gain (relative to the reference values) ensuing from 4 hours of daily exposure to ED would be acceptable if 4 hours of screen time a day were not correlated with a sharp increase in body weight deficit (up to 21.0%).

We also analyzed the correlations between the abnormalities in physical growth of high-school students with different body

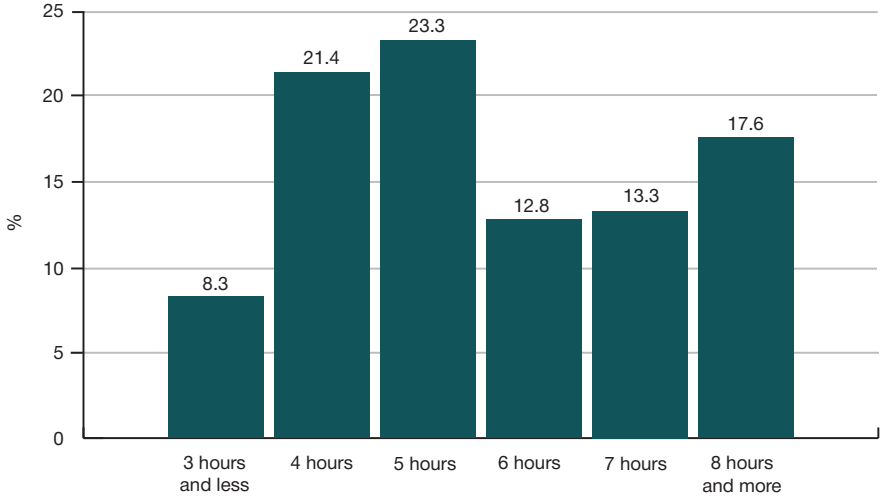

Fig. 1. Body weight deficit in high-school and university students exposed to different amounts of screen time a day

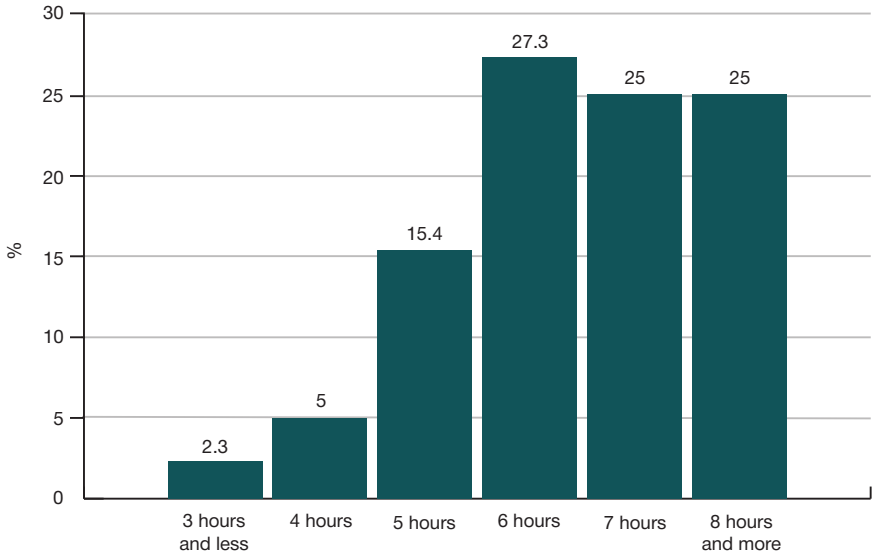

Fig. 2. Excess body weight in high-school and university students exposed to different amounts of screen time a day

builds and the frequency of weekly exposure to stationary ED (a computer or a laptop).

Body weight deficit was observed only in asthenic children (100%) from the subgroup of individuals who used ED once or twice a week. Exposure to ED 3 to 4 times a week was associated with body weight deficit in both asthenic (80%) and muscular (20%) types. Regular daily exposure to ED affected asthenic (60%), muscular (20%) and thoracic (20%) types. We conclude that it is not only "weak" types who can develop body weight deficit, which they are prone to, but also "strong" muscular types, who usually do not have this propensity.

Excess weight was observed in the children with abdominal body build (100%) who used ED once or twice a week. Exposure to ED 3 to 4 times a week was associated with excess weight in abdominal (75%) and thoracic (25%) types. Regular daily exposure to ED affected abdominal (50%), thoracic (25%) and muscular (25%) types. We conclude that the "weak" thoracic type usually not prone to accumulating fat can develop excess body weight associated with exposure to ED.

Besides, after frequent and prolonged exposure to a combination of stationary and mobile ED, high-school and university students complained of fatigue (26% and 58%, respectively). Prolonged screen time also triggered anxiety. University students who used ED over 5 hours a day had a high level of anxiety (48.2 ± 2.6 points on the anxiety scale); students who used ED 3 to 5 hours a day scored 42.1 ± 1.6 points (moderate anxiety) and those who used ED 1 to 3 hours a day scored 36.1 ± 1.2 points (moderate anxiety). The analysis revealed statistically significant correlations between anxiety and the duration of exposure to ED expressed in hours ($r = 0.66$; $p < 0.05$).

DISCUSSION

In a population, there are always children, adolescents and young people whose physical development is not harmonious. In the last decade, the number of Moscow residents with excess weight and weight deficit in the age group of 8 to 17 years has risen to 11.5% and 22.3%, respectively, which is consistent with the reports of other researchers [22, 23].

Our findings demonstrate that this trend is gaining momentum. Only 60% of the participants could boast harmonious physical development. This was not determined by their place of residence or the type of educational institution they were attending. According to the population studies conducted before ED became omnipresent, at that time 68% of the population were developing normally [22]. The negative trend we observed prompts investigation of ED contribution to body weight deficit and excess weight in young people.

Frequent and prolonged exposure to ED significantly changes the lifestyle of modern students, stealing time allocated for sleep and physical activities [24, 25].

Overuse of ED and obsession with modern ICT has a profound impact on the wellbeing of children and university students, increasing anxiety, causing sleep problems and other health problems [26, 27].

In this study, we were able to assess the impact of ED on the physical development of young people. The study demonstrates that daily exposure to stationary ED increases the risk of inharmonious physical development caused by weight deficit or excess weight gain by 24% and 10%, respectively. Because no risks were identified associated with a different frequency of exposure to stationary ED, we believe that introducing at least one ED-free day into a weekly schedule is a good safety measure that will also give a student more spare time for physical activities.

The fact that the use of stationary ED once or twice a week promotes body weight deficit only in asthenic children and excess weight gain only in the abdominal type speaks in favor of our proposal. At the same time, regular daily use of stationary ED can cause health problems in any body build type.

The study demonstrates that the impact of ED on high-school and university students should be assessed in the context of its total duration, meaning that we should account for both classroom and recreational screen time and the use of both stationary and mobile ED. Reducing total screen time to 3 hours a day would be an effective measure for preventing body weight deficit or excess weight gain. However, one should bear in mind that young people tend to respond negatively to strict measures, so positive health promotion should also be included in to the equation [28–30].

Because it takes a certain time for the body size and composition to change, we additionally assessed the impact of ED on more labile psychoemotional parameters. We found that university students who use stationary and mobile ED below 3 hours a day have a lower level of anxiety.

Sedentary behaviors associated with ED result in the lack of physical activities, which is key to understanding the results yielded by the study. Its deficit prevents muscle mass from developing and promotes fat deposition. The effects of frequent and prolonged use of ED can be presented as the following chain of events: frequent and prolonged exposure to ED → prevailing sedentary behaviors → reduction in physical activity → reduced muscle mass and growing fat mass → deviation from normal physical development and growth.

Our study does not cover the whole range of possible consequences of frequent and prolonged exposure to ED. For example, we have not investigated the effect of ED on muscle strength and lung capacity in young people.

CONCLUSIONS

Frequent and prolonged use of ED by young people is one of the factors that could interfere with their normal growth and physical development. This factor however, can be controlled. Safety measures include total elimination of a computer or laptop from daily activities at least once a week (at the weekend) and reduction of total screen time to 3 hours a day. It is also important to promote healthy lifestyles, educate young people about the consequences of ED overuse and their role in health problems, including obesity.

References

1. Buhtijarov IV, Denisov JI, Eremin AL. Osnovy informacionnoj gigieny: koncepcii i problemy innovacij. Gigiena i sanitarija. 2014; 93 (4): 5–9. Russian.
2. Kuchma VR, Suhareva LM, Hramcov PI. Gigienicheskaja bezopasnost' zhiznedejatel'nosti detej v cifrovoj srede. Zdorov'e naselenija i sreda obitanija. 2016; 8 (281): 4–7. Russian.
3. Ushakov IB, Popov VI, Popova OA. Nekotorye aspekty jekologicheskoj bezopasnosti cheloveka v uslovijah hronicheskogo

vozdejstvija impul'sov jelektromagnitnyh polej. Jekologija cheloveka. 2018; (1): 3–7. Russian.
4. Denisov JI. Informacionnaja gigiena i regulirovanie informacii dlja ujazvimyh grupp naselenija. Gigiena i sanitarija. 2014; 93 (5): 43–9. Russian.
5. Vjatleva OA, Kurganskij AM. Mobil'nye telefony i zdorov'e detej 6–10 let: znachenie vremennyh rezhimov i intensivnost' izluchenija. Zdorov'e naselenija i sreda obitanija. 2017; 8 (293): 27–30. Russian.
6. Popov VI, Melihova EP. Izuchenie i metodologija issledovanija kachestva zhizni studentov. Gigiena i sanitarija. 2016; 95 (9): 879–84. Russian.
7. Vershinin AE, Avdonina LA. Vlijanie sotovyh telefonov na zdorov'e cheloveka. Vestnik Penzenskogo gosudarstvennogo universiteta. 2015; 3 (11): 175–7. Russian.
8. Vasileva TI, Sarokvasha OJ. Vlijanie jelektromagnitnogo polja sotovogo telefona na organizm cheloveka v zavisimosti ot vozrasta. Vestnik Samarskogo gosudarstvennogo universiteta. 2012; 3/2 (94): 29–36. Russian.
9. Kazarjan KR, Plugotarenko SA, Vorob'eva EN, Davydov SG, Levova IJu, Ishunkina IV, i dr. Internet v Rossii v 2017. Sostojanie, tendencii i perspektivy razvitija. Otraslevoj doklad. M.: Tipografija «Forvard Print», 2018; 96 s. Russian.
10. Vyatleva OA. Mobil'nye telefony i zdorov'e detej 6–10 let: znachenie vremennyh rezhimov i intensivnost' izluchenija. Zdorov'e naselenija i sreda obitanija. 2017; 8 (293): 27–30. Russian.
11. Kuchma VR, Suhareva LM, Hramcov PI. Covremennye podhody k obespecheniju gigienicheskoj bezopasnosti zhiznedejatel'nosti detej v giperinformacionnom obshhestve. Voprosy shkol'noj i universitetskoj mediciny i zdorov'ja. 2015; (3): 22–7. Russian.
12. Sokolova NV, Popov VI, Alferova SI, Artjuhova IG, Kvarachelija AG. Kompleksnyj podhod k gigienicheskoj ocenke kachestva zhizni studencheskoj molodezhi. Bjulleten' Vostochno-Sibirskogo nauchnogo centra Sibirskogo otdelenija Rossijskoj akademii medicinskih nauk. 2013; 3–2 (91): 130–4. Russian.
13. Wimalasundera S. Computer vision syndrome. Galle Medical. 2006; 11 (1): 201–4.
14. Lepp A, Barcley JE, Karpinski AC. The relationship between cell phone use, academic performance, anxiety, and Satisfaction with Life in college students. Computers in Human Behavior. 2014; (31): 343–50.
15. Lanaj K, Johnson RE, Barnes CM Beginning the workday yet already depleted? Consequences of late-night smartphone use and sleep. Organizational Behavior and Human Decision Processes. 2014; 124 (1): 11–23.
16. Kuchma VR, Tkachuk EA, Tarmaeva IJu. Psihofiziologicheskoe sostojanie detej v uslovijah informatizacii ih zhiznedejatel'nosti i intensifikacii obrazovanija. Gigiena i sanitarija. 2016; 95 (12): 1183–8. Russian.
17. Koncepciya informacionnoj bezopasnosti detej. Rasporjazhenie pravitel'stva RF № 2471-r (02 dekabrja 2015). Russian.
18. Baranov AA, Kuchma VR, Skoblina NA. Fizicheskoe razvitie detej na rubezhe tysjacheletij. M.: NCZD RAMN, 2008; 216 s. Russian.
19. Kuchma VR, Ushakov IB, Sokolova NV, Rapoport IK, Esaulenko IJe, Gubina OI, i dr. Metody ocenki kachestva zhizni shkol'nikov. Voronezh: Istoki, 2006; 112 s. Russian.
20. Kuchma VR, Suhareva LM, Hramcov PI, Rapoport IK, Zvezdina IV, Sokolova SB, i dr. Rukovodstvo po gigiene detej i podrostkov, medicinskomu obespecheniju obuchajushhihsja v obrazovatel'nyh organizacijah. M.: Izd-vo NCZD RAMN, 2016; 610 s. Russian.
21. Medicinskaya statistika: onlajn kal'kuljatory dlja rascheta statisticheskih kriteriev. Dostupno po ssylke: https://medstatistic.ru/calculators.html.
22. Milushkina OJ. Markelova SV, Skoblina NA, Tatarinchik AA, Fedotov DM, Korolik VV, i dr. Osobennosti obraza zhizni sovremennoj studencheskoj molodezhi. Zdorov'e naselenija i sreda obitanija. 2018; 11 (308): 5–8. Russian.
23. Kordenko AN, Kovylova VI, Popov VI, Tarasenko PA. Kriticheskie faktory kachestva zhizni podrostkov. Gigiena i sanitarija. 2015; 94 (9): 20–1. Russian.
24. Bokareva NA. Vedushhie faktory, formirujushhie fizicheskoe razvitie sovremennyh detej megapolisa Moskvy [dissertacija]. M., 2014. Russian.
25. Kuchma VR, Suhareva LM, Rapoport IK. Populjacionnoe zdorov'e detskogo naselenija, riski zdorov'ju i sanitarno-jepidemiologicheskoe blagopoluchie obuchajushhihsja: problemy, puti reshenija, tehnologii dejatel'nosti. Gigiena i sanitarija. 2017; 96 (10): 990–5. Russian.
26. Ushakov IB, Popov VI, Petrova TN, Esaulenko IJ. Izuchenie zdorov'ja studentov kak rezul'tat vzaimodejstvija mediko-biologicheskih, jekologicheskih i social'no-gigienicheskih faktorov riska. Medicina truda i promyshlennaja jekologija. 2017; (4): 33–6. Russian.
27. Libina II, Mazurenko NJ. Ispol'zovanie sovremennyh informacionnyh tehnologij v gigienicheskom obuchenii studentov medicinskogo vuza. Prikladnye informacionnye aspekty mediciny. 2016; 19 (4): 39–42. Russian.
28. Kuchma VR, Milushkina OJ, Bokareva NA, Skoblina NA. Sovremennye napravlenija profilakticheskoj raboty v obrazovatel'nyh organizacijah. Gigiena i sanitarija. 2014; 93 (6): 107–11. Russian.
29. Baranov AA, Kuchma VR, Anufrieva EV, Sokolova SB, Skoblina NA, Virabova AR. i dr. Ocenka kachestva okazanija medicinskoj pomoshhi obuchajushhimsja v obrazovatel'nyh organizacijah. Vestnik Rossijskoj akademii medicinskih nauk. 2017; 72 (3): 180–94. Russian.
30. Sokolova NV, Popov VI, Kartysheva SI, Koroleva AO. Nekotorye aspekty profilakticheskoj dejatel'nosti uchitelja, napravlennoj na uluchshenie sostojanija zdorov'ja shkol'nikov. Gigiena i sanitarija. 2014; 93 (1): 90–1. Russian.

Литература

1. Бухтияров И. В., Денисов Э. И., Еремин А. Л. Основы информационной гигиены: концепции и проблемы инноваций. Гигиена и санитария. 2014; 93 (4): 5–9.
2. Кучма В. Р., Сухарева Л. М., Храмцов П. И. Гигиеническая безопасность жизнедеятельности детей в цифровой среде. Здоровье населения и среда обитания. 2016; 8 (281): 4–7.
3. Ушаков И. Б., Попов В. И., Попова О. А. Некоторые аспекты экологической безопасности человека в условиях хронического воздействия импульсов электромагнитных полей. Экология человека. 2018; (1): 3–7.
4. Денисов Э. И. Информационная гигиена и регулирование информации для уязвимых групп населения. Гигиена и санитария. 2014; 93 (5): 43–9.
5. Вятлева О. А., Курганский А. М. Мобильные телефоны и здоровье детей 6–10 лет: значение временных режимов и интенсивность излучения. Здоровье населения и среда обитания. 2017; 8 (293): 27–30.
6. Попов В. И., Мелихова Е. П. Изучение и методология исследования качества жизни студентов. Гигиена и санитария. 2016; 95 (9): 879–84.
7. Вершинин А. Е., Авдонина Л. А. Влияние сотовых телефонов на здоровье человека. Вестник Пензенского государственного университета. 2015; 3 (11): 175–7.
8. Васильева Т. И., Сарокваша О. Ю. Влияние электромагнитного поля сотового телефона на организм человека в зависимости от возраста. Вестник Самарского государственного университета. 2012; 3/2 (94): 29–36.
9. Казарян К. Р., Плуготаренко С. А., Воробьева Е. Н., Давыдов С. Г., Левова И. Ю., Ишунькина И. В. и др. Интернет в России в 2017. Состояние, тенденции и перспективы развития. Отраслевой доклад. М.: Типография «Форвард Принт», 2018; 96 с.
10. Вятлева, О. А. Мобильные телефоны и здоровье детей 6–10 лет: значение временных режимов и интенсивность излучения. Здоровье населения и среда обитания. 2017; 8 (293): 27–30.
11. Кучма В. Р., Сухарева Л. М., Храмцов П. И. Современные подходы к обеспечению гигиенической безопасности жизнедеятельности детей в гиперинформационном обществе.

Вопросы школьной и университетской медицины и здоровья. 2015; (3): 22–7.
12. Соколова Н. В., Попов В. И., Алферова С. И., Артюхова И. Г., Кварацхелия А. Г. Комплексный подход к гигиенической оценке качества жизни студенческой молодежи. Бюллетень Восточно-Сибирского научного центра Сибирского отделения Российской академии медицинских наук. 2013; 3–2 (91): 130–4.
13. Wimalasundera S. Computer vision syndrome. Galle Medical. 2006; 11 (1): 201–4.
14. Lepp A, Barcley JE, Karpinski AC. The relationship between cell phone use, academic performance, anxiety, and Satisfaction with Life in college students. Computers in Human Behavior. 2014; (31): 343–50.
15. Lanaj K, Johnson RE, Barnes CM Beginning the workday yet already depleted? Consequences of late-night smartphone use and sleep. Organizational Behavior and Human Decision Processes. 2014; 124 (1): 11–23.
16. Кучма В. Р., Ткачук Е. А., Тармаева И. Ю. Психофизиологическое состояние детей в условиях информатизации их жизнедеятельности и интенсификации образования. Гигиена и санитария. 2016; 95 (12): 1183–8.
17. Концепция информационной безопасности детей. Распоряжение правительства РФ № 2471-р (02 декабря 2015). Доступно по ссылке: http://www.consultant.ru/document/cons_doc_LAW_190009/.
18. Баранов А. А., Кучма В. Р., Скоблина Н. А. Физическое развитие детей на рубеже тысячелетий. М.: НЦЗД РАМН, 2008; 216 с.
19. Кучма В. Р., Ушаков И. Б. и др. Методы оценки качества жизни школьников. Воронеж: Истоки, 2006; 112 с.
20. Кучма В. Р., Сухарева Л. М., Храмцов П. И., Рапопорт И. К., Звездина И. В., Соколова С. Б. и др. Руководство по гигиене детей и подростков, медицинскому обеспечению обучающихся в образовательных организациях. М.: Изд-во НЦЗД РАМН, 2016; 610 с.
21. Медицинская статистика: онлайн-калькуляторы для расчета статистических критериев. Доступно по ссылке: https://medstatistic.ru/calculators.html.
22. Бокарева Н. А. Ведущие факторы, формирующие физическое развитие современных детей мегаполиса Москвы [диссертация]. М., 2014.
23. Кучма В. Р., Сухарева Л. М., Рапопорт И. К. Популяционное здоровье детского населения, риски здоровью и санитарно-эпидемиологическое благополучие обучающихся: проблемы, пути решения, технологии деятельности. Гигиена и санитария. 2017; 96 (10): 990–5.
24. Милушкина О. Ю. Маркелова С. В., Скоблина Н. А., Татаринчик А. А., Федотов Д. М., Королик В. В. и др. Особенности образа жизни современной студенческой молодежи. Здоровье населения и среда обитания. 2018; 11 (308): 5–8.
25. Корденко А. Н., Ковылова В. И., Попов В. И., Тарасенко П. А. Критические факторы качества жизни подростков. Гигиена и санитария. 2015; 94 (9): 20–1.
26. Ушаков И. Б., Попов В. И., Петрова Т. Н., Есауленко И. Э. Изучение здоровья студентов как результат взаимодействия медико-биологических, экологических и социально-гигиенических факторов риска. Медицина труда и промышленная экология. 2017; (4): 33–6.
27. Либина И. И., Мазуренко Н. Ю. Использование современных информационных технологий в гигиеническом обучении студентов медицинского вуза. Прикладные информационные аспекты медицины. 2016; 19 (4): 39–42.
28. Кучма В. Р., Милушкина О. Ю., Бокарева Н. А., Скоблина Н. А. Современные направления профилактической работы в образовательных организациях. Гигиена и санитария. 2014; 93 (6): 107–11.
29. Баранов А. А., Кучма В. Р., Ануфриева Е. В., Соколова С. Б., Скоблина Н. А., Вирабова А. Р. и др. Оценка качества оказания медицинской помощи обучающимся в образовательных организациях. Вестник Российской академии медицинских наук. 2017; 72 (3): 180–94.
30. Соколова Н. В., Попов В. И., Картышева С. И., Королева А. О. Некоторые аспекты профилактической деятельности учителя, направленной на улучшение состояния здоровья школьников. Гигиена и санитария. 2014; 93 (1): 90–1.

A MEDICAL CAREER: BARRIERS TO PROFESSIONAL IDENTITY

Mettini E[1], Yasko BA[2] ✉, Kazarin BV[2], Ostroushko MG[3]

[1] Pirogov Russian National Research Medical University, Moscow, Russia

[2] Kuban State Medical University, Krasnodar, Russia

[3] Regional Clinical Hospital № 2, Krasnodar, Russia

Sometimes, a minor scientific event leaves a much more memorable trace than a large conference. On May 30–31, 2019, Pirogov Russian National Research Medical University hosted a symposium on medical identities in various communities. Reports, reviews and discussions presented at the symposium focused on the problem of identity, a unique phenomenon that results from self-reflecting on a complex dynamic process of personal development. Professional identity is particularly important for a medical doctor. This article inspired by the reports of our colleagues summarizes the results of the symposium.

Keywords: physician, identity, self-concept, professional identity, barriers, professional crisis, professiogenesis

Acknowledgement: the authors thank all participants of the symposium on *Medical identities in different communities* held on May 30–31, 2019 at Pirogov Russian National Research Medical University) whose reports inspired us to write this article.

Author contribution: Mettini E conceived the article and supervised its preparation; Yasko BA planned the article, systematized the concepts of identity and identity crisis used in the studies of healthcare workers; Kazarin BV suggested analyzing the role of postgraduate education in overcoming the barriers to professional identity in medical doctors; Ostroushko MG provided and analyzed empirical data.

✉ **Correspondence should be addressed:** Bela F. Yasko
Sedina 4, Krasnodar, 350063; shabela@yandex.ru

Received: 06.08.2019 **Accepted:** 21.08.2019 **Published online:** 26.08.2019

DOI: 10.24075/brsmu.2019.055

ПРОФЕССИОНАЛЬНЫЙ ПУТЬ ВРАЧА: «БАРЬЕРЫ» ИДЕНТИЧНОСТИ

Э. Меттини[1], Б. А. Ясько[2] ✉, Б. В. Казарин[2], М. Г. Остроушко[3]

[1] Российский национальный исследовательский медицинский университет имени Н. И. Пирогова, Москва, Россия

[2] Кубанский государственный медицинский университет, Краснодар, Россия

[3] Краевая клиническая больница № 2, Краснодар, Россия

Незначительное по масштабам научное событие нередко оставляет след более выразительный, чем иная крупная конференция. В Российском национальном исследовательском медицинском университете имени Н. И. Пирогова 30–31 мая 2019 г. прошел симпозиум «Медицинские идентичности в разных обществах». Сделанные здесь доклады, обзоры, прошедшие в их контекстах дискуссии были посвящены проблеме идентичности — уникальному явлению, формирующемуся как результат отрефлексированности субъектом сложного многогранного динамичного процесса личностного становления. Особую значимость, на наш взгляд, идентичность имеет в профессиональной жизни врача, что обусловило несомненную актуальность докладов и диалогов, составивших содержательность проведенного симпозиума, и целесообразность обобщения его результатов в виде предлагаемого читателю мнения.

Ключевые слова: врач, идентичность, Я-концепция, профессиональная идентичность, профессиональные барьеры, профессиональные кризисы, профессиогенез

Благодарности: авторы выражают благодарность всем участникам симпозиума «Медицинские идентичности в разных обществах» (РНИМУ имени Н. И. Пирогова, 30–31 мая 2019 г.), материалы выступлений которых позволили обобщить некоторые результаты научного взаимодействия в виде представленного мнения.

Информация о вкладе авторов: Э. Меттини — идея публикации; общее руководство подготовкой публикации; Б. А. Ясько — план публикации, систематизация понятий «идентичность», «кризисы идентичности» в исследованиях субъектов медицинского труда; Б. В. Казарин — идея анализа роли последипломного образования в преодолении барьеров становления профессиональной идентичности врача-руководителя; М. Г. Остроушко — предоставление эмпирического материала, первичный анализ эмпирических данных.

✉ **Для корреспонденции:** Бэла Аслановна Ясько
М. Седина, д. 4, г. Краснодар, 350063; shabela@yandex.ru

Статья получена: 06.08.2019 **Статья принята к печати:** 21.08.2019 **Опубликована онлайн:** 26.08.2019

DOI: 10.24075/vrgmu.2019.055

Identity as a subject of human and social sciences

For more than half a century, identity has been in the focus of human and social studies that deal with various aspects of human existence, personal development, self-actualization, responding to challenges and crises, and building life-style resources. Classic psychoanalytic works approached identification as a psychological defense mechanism [1, 2]; in contrast, E. Erikson in his epigenetic theory defined the search for identity as a developmental stage in adolescence [3]. As a phenomenon, identity is explored by philosophy, linguistics, culture and social studies of human beings and their social nature. Recent linguistic research has demonstrated that an increasing use of semiotic resources in shaping and expressing identity is one of key characteristics of this complex phenomenon [4]. In psychology, the concept of identity is also enjoying a surge of interest. Terms like personal, gender, group, ethnic, professional and organizational identities have entered the lexicon of psychologists and are widely used in psychotherapy and psychological consulting. The program of the 16th European Congress of Psychology held in Moscow in July 2019 included the symposium on *Personal identity in the conditions of multi-vector changes in the society*. This signals a profound interest in the phenomena of identity and identification across the scientific community. The participants of the discussion pointed out that multivector changes

sweeping through the globe are complicating the process of personal identification affected by new social and technological challenges brought about by the advent of the digital era. The speakers talked about a new phenomenon of online identity [5] and about national identity that comes into being as a group of individuals reflects on its historical experience [6]. Risks for social failure are increasing, as seen from the rising number of cases of unconfirmed identity [7] and gender identity crisis [8].

Professional identity of a medical doctor: the mystery of formation

To understand what a doctor's professional identity really is, one has to identify a stage of medical training it starts to shape at, the factors involved and the intensity of the process. For a long time, little effort has been channeled into this field of research. On the whole, our foreign colleagues have paid more attention to this problem. Specifically, there have been persistent attempts to shed light on the nature and mechanisms of professional identity formation in the early stages of professional development. In medical students, professional identity is seen as a result of resolving difficult ethical dilemmas [9] and as an intrinsic part of a student's personality [10]. Some Russian authors have studied professional identity in the context of daily routine of young Russian physicians working in different environments (cities, towns or villages) [11]. Those authors discriminate between 3 types of professional identity, depending on which view on the profession dominates the mindset of a young physician: being a helper (a doctor is a helping profession), being an expert (a doctor is an expert in a medical field), or being a researcher (a doctor is a researcher focusing on academic science).

The concept of professional identity holds a central place in the contemporary labor psychology and is loaded with a wide range of meanings [12]. One of them is particularly important for grasping the essence of professional development: professional identity is an indicator of how well an individual, their expertise and professional achievements meet the healthcare demands posed by society, professional community and its corporate culture [12] Seeing professional identity as an ability to self-identify in a profession can be used as a methodological landmark in research studies exploring the complexity of psychological aspects pertaining to the development of professional identity in healthcare workers [12]. Just like motivation, professional identity determines professionalism.

We face a lot of barriers in different stages of our career that put our professional identity at risk for shattering. Overcoming these barriers helps us to self-identify professionally at younger age and facilitates self-actualization later in life [13]. The barriers make one's professional path nonlinear and thereby create a prerequisite for redefining the vectors of the chosen carrier, prevent one from professional stagnation, and enhance their professional identity. Some of the barriers are purely individual experience; however, others are common to the entire medical profession. The latter include professional crises that need to be overcome in order to self-actualize [14].

The first barrier is the problem of choice: a young individual torn by a conflict of motives and preferences creates a professional self-image and eventually decides in favor of a medical carrier. This crisis is a powerful stimulus: the decision to become a doctor means one has to accept responsibility, mobilize their internal resources and set off on a long and difficult journey of professional education. Achieved professional identity is a reward for overcoming this first barrier.

Other crises that will follow help an individual to build their confidence as a professional and to transform their self-image into a profession-related self-concept. Normative crises occurring in a medical carrier include crises in year 1 and 3 of medical training, a crisis related to the choice of specialty, a crisis at the start of a professional carrier, a crisis related to maintaining and improving qualifications, and a crisis of retirement.

The professional path of a medical doctor is also filled with obstacles that cause a risk for destroying his/her professional identity that include the so-called supernormative and extraordinary crises. An example of such a barrier is a crisis experienced when a doctor has to change their specialty or job. In this case, a typically normative crisis a person has to go through when starting a new job becomes supernormative or even acquires features of the extraordinary crisis that puts the doctor under a lot of stress. Such crises strike when a physician is offered a senior management position in a healthcare institution [15]. It is accompanied by frustration of a professional self-concept dissonant with a new identity (I as a senior executive). Studies have shown that in terms of confidence, "I in the present" becomes weaker than "I in the past", the person feels the lack of competencies required for a new position, engages in negative coping strategies, etc. [15, 16]. Introducing the psychology of management into the curriculum taught to healthcare workers who study organization of healthcare and public health could help to overcome this barrier. Lectures and workshops on the psychology of management help students to develop standard competences that a senior executive is expected to demonstrate in their new position [17]. The essays and reports prepared by the graduates of the Department of Public Health and Healthcare (the Faculty of Continuous Professional Education, Kuban State Medical University) reveal a positive shift from frustration to realizing the points of integration between two professional identities: I as a physician and I as a senior executive.

CONCLUSIONS

Professional identity is the core of a person's self-image. This core not a monolith. It is subject to various interventions arising from changes, challenges and demands from both within and without. In order to succeed in medical profession and to overcome the barriers occurring in all stages of their professional career and throughout life, one has to understanding the meaning of those barriers. The significance of the problem discussed at the symposium necessitates research into the mechanisms, factors involved and patterns of professional identity formation in medical doctors living in contemporary society.

References

1. Freud Z. Psihologija mass i analiz chelovecheskogo «Ja». SPb.: Azbuka-Attikus, 2013; 192 s. Russian.
2. Lacan J. Iznanka psihoanaliza. M.: Logos, 2008. 272 s. Russian.
3. Hjelle L, Ziegler D. Teorii lichnosti. SPb.: Piter, 2017; 608 s.
4. Molodichenko ER Identity and discourse: from social theory to practice linguistic analysis. Scientific and technical statements of St. Petersburg state Polytechnic University. Humanities and social sciences. 2017; 8 (3): 122–30.
5. Ryabikina Z, Bogomolova K. Personal identity in the conditions existence virtualization. Book of Abstracts: XVI European

Congress of Psychology (ECP 2019) (2–5 July, 2019. Lomonosov Moscow State University, Moscow). Moscow: Moscow University Press, 2019; 20.
6. Berberyan A, Tuchina O. Historical experience and national identity in the era of globalization. Book of Abstracts: XVI European Congress of Psychology (ECP 2019) (2–5 July, 2019. Lomonosov Moscow State University, Moscow). Moscow: Moscow University Press, 2019; 22–3.
7. Ryabikina Z, Makarevskaya Y. Unconfirmed identity as an indicator of social failure of personality. Book of Abstracts: XVI European Congress of Psychology (ECP 2019) (2–5 July, 2019. Lomonosov Moscow State University, Moscow). Moscow: Moscow University Press, 2019; 24.
8. Ozhigova L. Crisis of a person's gender-based identity. Personal identity in the conditions existence virtualization. Book of Abstracts: XVI European Congress of Psychology (ECP 2019) (2–5 July, 2019. Lomonosov Moscow State University, Moscow). Moscow: Moscow University Press, 2019; 26.
9. Binyamin G. Growing from Dilemmas: Developing a Professional Identity Through Collaborating Reflections on Relational Dilemmas. Advances in Health Sciences Education. 2018; 23 (1): 43–60.
10. Broadhead RS. The Private Lives and Professional Identity of Medical Students. London: Routledge, 2017; 140 p.
11. Galkin KA. Generational succession of medical students in the context of formation the professional identity. Socio-economic researches, humanities and law: theory and practice. 2017; (13): 62–6.
12. Ermolaeva EP. The relationship of identity, relevance and marginalization of the professional in modern society. In: A. A. Oboznov, A. L. Zhuravlev, editors. Actual problems of labor psychology, engineering psychology and ergonomics. Issue 7. M.: Institute of psychology RAS, 2015; 11– 22.
13. Cimanuk EE, Devyatovskaya IV. Continuous education as a resource of overcoming of psychological barriers in the process of professional development. Education and science. 2015; (1): 80–92.
14. Yasko BA. Organizational psychology of health care: personnel, leadership, culture. Monograph. Krasnodar: Kuban. State. Un-t, 2013; 260 p.
15. Tkhagalegova LV. Treatment of time and psychology of life and existential crises. Book of Abstracts: XXII International Symposium "Psychological problems of meaning of life and Acme". Moscow: PI RAO, 2017; 294–5.
16. Yasko BA, Kasarin BV, Rimmavi MH. Basics of administrative competence of a doctor-head as a subject in a post graduate education system. International Journal of Experimental Education. 2011; (1): 15–7.
17. Ob utverzhdenii professional'nogo standarta «Specialist v oblasti organizacii zdravoohraneniya i obshhestvennogo zdorov'ja». Prikaz Ministerstva truda i social'noj zashhity RF ot 7 noyabrya 2017 g. # 768n. Dostupno po ssylke: https://www.garant.ru/products/ipo/prime/doc/71722794/. Russian.

Литература

1. Фрейд З. Психология масс и анализ человеческого «Я». СПб.: Азбука-Аттикус, 2013; 192 с.
2. Лакан Ж. Изнанка психоанализа. М.: Логос, 2008; 272 с.
3. Хьелл Л., Зиглер Д. Теории личности. СПб.: Питер, 2017; 608 с.
4. Молодыченко Е. Р. Идентичность и дискурс: от социальной теории к практике лингвистического анализа. Научно-технические ведомости Санкт-петербургского государственного политехнического университета. Гуманитарные и общественные науки. 2017; 8 (3); 122–30.
5. Ryabikina Z, Bogomolova K. Personal identity in the conditions existence virtualization. Book of Abstracts: XVI European Congress of Psychology (ECP 2019) (2–5 July, 2019. Lomonosov Moscow State University, Moscow). Moscow: Moscow University Press, 2019; 20.
6. Berberyan A, Tuchina O. Historical experience and national identity in the era of globalization. Book of Abstracts: XVI European Congress of Psychology (ECP 2019) (2–5 July, 2019. Lomonosov Moscow State University, Moscow). Moscow: Moscow University Press, 2019; 22–3.
7. Ryabikina Z, Makarevskaya Y. Unconfirmed identity as an indicator of social failure of personality. Book of Abstracts: XVI European Congress of Psychology (ECP 2019) (2–5 July, 2019. Lomonosov Moscow State University, Moscow). Moscow: Moscow University Press, 2019; 24.
8. Ozhigova L. Crisis of a person's gender-based identity. Personal identity in the conditions existence virtualization. Book of Abstracts: XVI European Congress of Psychology (ECP 2019) (2–5 July, 2019. Lomonosov Moscow State University, Moscow). Moscow: Moscow University Press, 2019; 26.
9. Binyamin G. Growing from Dilemmas: Developing a Professional Identity Through Collaborating Reflections on Relational Dilemmas. Advances in Health Sciences Education. 2018; 23 (1): 43–60.
10. Broadhead RS. The Private Lives and Professional Identity of Medical Students. London: Routledge, 2017; 140 p.
11. Галкин К. А. Поколенческая преемственность студентов врачей в контексте формирования профессиональной идентичности. Социально-экономические исследования, гуманитарные науки и юриспруденция: теория и практика. 2017; (13): 62–6.
12. Ермолаева Е. П. Взаимосвязь идентичности, востребованности и маргинализма профессионала в современном обществе. В книге: Обознов А. А., Журавлев А. Л., редакторы. Актуальные проблемы психологии труда, инженерной психологии и эргономики. Выпуск 7. М.: Институт психологии РАН, 2015; с. 11– 22.
13. Сыманюк Э. Э., Девятовская И. В. Непрерывное образование как ресурс преодоления психологических барьеров в процессе профессионального развития. Образование и наука. 2015; (1): 80–92.
14. Ясько Б. А. Организационная психология здравоохранения: персонал, лидерство, культура. Монография. Краснодар: Кубан. гос. ун-т, 2013; 260 с.
15. Тхагалижокова Л. В. Отношение ко времени и психология жизненных и экзистенциальных кризисов. Материалы XXII Международного симпозиума «Психологические проблемы смысла жизни и акме». Москва: ПИ РАО, 2017.
16. Yasko BA, Kasarin BV, Rimmavi MH. Basics of administrative competence of a doctor-head as a subject in a post graduate education system. International Journal of Experimental Education. 2011; (1): 15–17.
17. Об утверждении профессионального стандарта «Специалист в области организации здравоохранения и общественного здоровья». Приказ Министерства труда и социальной защиты РФ от 7 ноября 2017 г. № 768н. Доступно по ссылке: https://www.garant.ru/products/ipo/prime/doc/71722794/.